UNIVERSITY OF CALGARY

Creep Behaviour and Creep Mechanisms of Normal and Healing Ligaments

by

Gail Marilyn Thornton

A THESIS

SUBMITTED TO THE FACULTY OF GRADUATE STUDIES

IN PARTIAL FULFILMENT OF THE REQUIREMENTS FOR THE

DEGREE OF DOCTOR OF PHILOSOPHY

DEPARTMENT OF CIVIL ENGINEERING

CALGARY, ALBERTA

APRIL, 2000

ABSTRACT

Patients with knee ligament injuries often undergo ligament reconstructions to restore joint stability and, potentially, abate osteoarthritis. Careful literature review suggests that in 10% to 40% of these patients the graft tissue "stretches out". Some graft elongation is likely due to creep (increased elongation of tissue under repeated or sustained load). Quantifying creep behaviour and identifying creep mechanisms in both normal and healing ligaments is important for finding clinically relevant means to prevent creep.

Ligament creep was accurately predicted using a novel yet simple structural model that incorporated both collagen fibre recruitment and fibre creep. Using the inverse stress relaxation function to model fibre creep in conjunction with fibre recruitment produced a superior prediction of ligament creep than that obtained from the inverse stress relaxation function alone. This implied mechanistic role of fibre recruitment during creep was supported using a new approach to quantify crimp patterns at stresses in the toe region (increasing stiffness) and linear region (constant stiffness) of the stress-strain curve. Ligament creep was relatively insensitive to increases in stress in the toe region; however, creep strain increased significantly when tested at the linear region stress. Concomitantly, fibre recruitment was evident at the toe region stresses; however, recruitment was limited at the linear region stress. Elevating the water content of normal ligament using phosphate buffered saline increased the creep response.

Therefore, both water content and fibre recruitment are important mechanistic factors involved in creep of normal ligaments.

Ligament scars had inferior creep behaviour compared to normal ligaments even after 14 weeks. In addition to inferior collagen properties affecting fibre recruitment and increased water content, increased glycosaminoglycan content and flaws in scar tissue were implicated as potential mechanisms of scar creep. Similarly, ligament autografts had persistently abnormal creep behaviour and creep recovery after 2 years likely due to infiltration by scar tissue. Short-term immobilization of autografts had long-term detrimental consequences perhaps due to re-injury of the graft at remobilization.

Treatments that restore normal properties to these mechanistic factors in order to control creep would improve joint healing by restoring joint kinematics and maintaining normal joint loading.

ACKNOWLEDGEMENTS

I gratefully acknowledge the studentship support received from the Medical Research Council of Canada and the McCaig Fund. Additional financial support for this work was provided by the Canadian Arthritis Society and the Alberta Heritage Foundation for Medical Research.

I wish to thank Dr. N.G. Shrive and Dr. C.B. Frank for their thoughtful support and careful guidance over the course of this thesis work and throughout the years. I want to express my gratitude to Dr. J.L. Ronsky for her helpful advice during my thesis work. Also, I want to thank Dr. R. Gill and Dr. A. Amis for examining this thesis.

I want to extend thanks to Dr. R.S. Boorman for collaboration in the experimental work on long-term autografts. Additionally, I would like to recognize the technical and surgical assistance provided by Gail Leask, Linda Marchuk, Leona Barclay, Craig Sutherland, Kent Paulson and Dr. T. Majima.

Finally, a word of thanks to my insightful colleagues and supportive friends: especially, Carla Sciarretta, Brett and Helen McGuinness, Greg and Sandra Wohl and, with my highest regard, Raymond Boykiw.

The *Journal of Orthopaedic Research* granted permission for use of previously published material in this thesis, specifically from Thornton et al. (1997) (reference 143) and Thornton et al. (1999) (reference 144).

DEDICATION

To My Family

TABLE OF CONTENTS

LIST OF TABLES

LIST OF FIGURES

LIST OF ABBREVIATIONS AND SYMBOLS

Abbreviations

ACL = anterior cruciate ligament

MCL = medial collateral ligament

GAGs = glycosaminoglycans

QLV = Quasi-Linear Viscoelastic

MTS = MTS Systems Corporation, Minneapolis, Minnesota, U.S.A.

CT = compression-tension

RH = relative humidity

PBS = phosphate buffered saline

s.d. = standard deviation

SUC = sucrose

"lig0" = "ligament zero"

"old lig0" = "ligament zero" prior to soaking

"new lig0" = "ligament zero" after soaking

contra = contralateral

immob = immobilized

remob = remobilized

Symbols

σ = stress

ε = strain

t or τ = time (or time step)

$\sigma(\varepsilon,t)$ = stress response as a function strain and time

g(t) = time varying stress relaxation function where g(0) = 1

$\sigma^e(\varepsilon)$ = time-independent elastic response

$\sigma(t)$ = stress function for static stress relaxation test

σ_o = initial stress for stress relaxation test

$\varepsilon(t)$ = strain function for static creep test

j(t) = time varying creep function where j(0) = 1

ε_o = initial strain for creep test

$\bar{g}(s)$ = Laplace Transformation of g(t)

$\bar{j}(s)$ = Laplace Transformation of j(t)

A_n = constants for g(t)

B_n = constants for j(t)

$\hat{j}(t)$ = predicted creep function from fitted stress relaxation function or inverse stress relaxation function

$\hat{g}(t)$ = predicted stress relaxation function from fitted creep function or inverse creep function

T = uniform MCL thickness

b = MCL breadth

L_o = MCL initial length

λ_L = stretch required to uncrimp the fibres at the left side of the ligament

λ_R = stretch required to uncrimp the fibres at the right side of the ligament

$(\lambda_R-\lambda_L)$ = variation in crimp

w = width location into ligament breadth (taken from left side of ligament)

λ = stretch at width location w

w(0) = width of recruited fibres at time equals zero

$\lambda(0)$ = stretch of fibres associated with w(0)

$\varepsilon(w,t)$ = strain in the ligament at a particular width and time step

$\varepsilon(w,0)$ = strain in the ligament at a particular width and time equals zero

$\sigma(w,t)$ = stress in the ligament at a particular width and time step

$\sigma(w,0)$ = stress in the ligament at a particular width and time equals 0

J(t) = creep compliance of MCL predicted from inverse stress relaxation function and fibre modulus

E_F = fibre modulus

F = applied static creep test force

$w(\Delta t)$ = width of recruited fibres at time step Δt

$\lambda(\Delta t)$ = stretch of fibres associated with $w(\Delta t)$

$\varepsilon(w, \Delta t)$ = strain in the ligament at a particular width and time step Δt

$\varepsilon_C(\Delta t)$ = increment of creep strain

r^2 = coefficient of determination (square of correlation coefficient)

C1 = peak strain of the first cycle in the cyclic creep

C30 = peak strain of the thirtieth cycle in the cyclic creep

Si = strain at the beginning of the constant stress application in the static creep

Sf = strain at the end of the twenty minute constant stress application in the static creep

C# = cycle number

Cf = strain at the end of the static creep test

Ci = peak strain of the first cycle in the cyclic creep test

Ri = strain at the beginning of the recovery period

Rf = strain at the end of the recovery period

LIST OF RELEVANT ANATOMIC NOMENCLATURE

Body Planes

Frontal = plane dividing body into front and back parts
(defining anterior and posterior directions)

Median = plane at the midline dividing body into equal right and left halves

Sagittal = plane parallel to the median plane dividing body into right and left parts
(defining medial and lateral directions)

Transverse = plane dividing body into upper and lower parts
(defining superior and inferior directions)

Anatomic directions

Anterior = directed forward or towards the front part

Posterior = directed backward or towards the back part

Medial = directed towards the median plane

Lateral = directed away from the median plane

Superior = directed upwards or towards the upper part

Inferior = directed downwards or towards the lower part

In reference to limbs or structures of a limb:

Proximal = situated closer to the median plane or the root of the limb

Distal = situated further from the median plane or the root of the limb

Movements

abduction = draw away from the median plane (in frontal plane)

adduction = draw towards the median plane (in frontal plane)

flexion = movement bringing limbs into a more bent position (sometimes but not exclusively in the sagittal plane)

extension = movement bringing limbs into a straighter position (sometimes but not exclusively in the sagittal plane)

internal rotation = anterior aspect rotates towards the median plane (in transverse plane)

external rotation = anterior aspect rotates away from median plane (in transverse plane)

Positional Descriptors

varus = distal bone bent towards median plane with respect to proximal bone (in frontal plane) and, for the knee, varus means O-shaped

valgus = distal bone bent away from median plane with respect to proximal bone (in frontal plane) and, for the knee, valgus means X-shaped

Compiled from references 44, 61 and 88.

CHAPTER 1

INTRODUCTION

1.1 Current State of Knowledge

1.1.1 Clinical Problem

Skeletal ligaments are discrete bands of dense connective tissue which connect bones across a joint. Ligaments resist tensile forces and function to guide joint motion and maintain joint stability (75). Joint sprains involving partial or total ligament tears comprise a large proportion of all musculoskeletal injuries (58). Per annum, joint sprains may affect about 5% to 10% of the population under the age of 65; in other words, 30 to 40 million ligament injuries in North America (58). Injuries to the knee predominate (75) and the anterior cruciate ligament (ACL) is the most commonly injured ligament (141). For example, injury to the ACL occurs in 1 in every 3000 Americans annually (62). In fact, injuries to the ACL and medial collateral ligament (MCL) comprise 90% of the knee ligament injures in young, active people (166). Unfortunately, the ligaments of some percentage of patients do not heal effectively (having persistent joint laxity), particularly when the ACL and/or the MCL are involved. These patients are susceptible to disabling symptoms of joint instability and to possible development of osteoarthritis (39).

The ACL is an intra-articular structure that acts to restrict primarily anterior tibial displacement and secondarily internal tibial rotation (61) (Figure 1.1). The MCL is an extra-articular structure that restricts primarily valgus angulation and external tibial

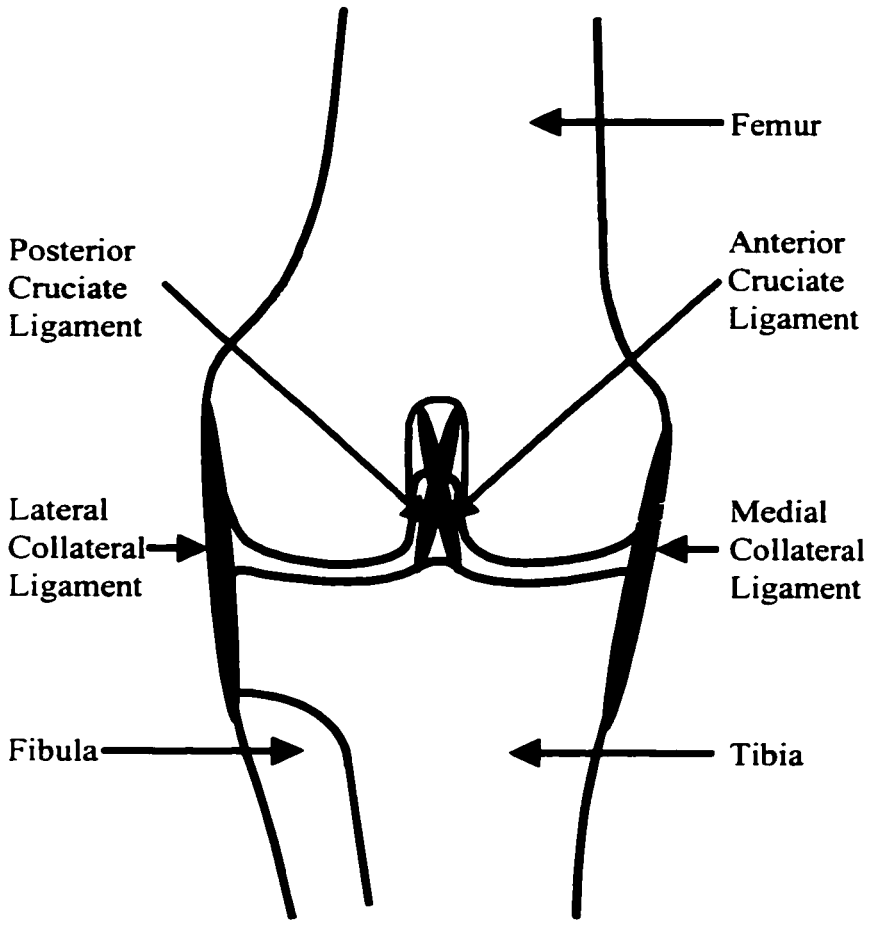

Figure 1.1: Schematic of Right Knee – Anterior View

rotation and secondarily anterior tibial displacement (61). Isolated injury to the MCL heals effectively without surgical intervention (141). The MCL heals with scar tissue that bridges the gap between the torn ligament ends (75). Unfortunately, a small number of patients may have persistent joint instability (119). Injury to the ACL is typically repaired with surgical intervention using a graft tissue (75). The graft tissue most frequently used is an autogenous tendon graft from around the knee, although allografts (tendon and fascial) and synthetic grafts (ligament augmentation devices) are also used (57,114). Most patients have a clinical improvement with ACL reconstruction.

Careful review of the literature suggests that some percentage of these grafts likely fail due to elongation of the graft tissue or "stretching out" of the graft. This is evident in clinical studies (1,2,16,22,26,38,48,68,81,87,102,114,133,147) and in experimental work in animal models (17,21,76,85,113,146,171). Elongation of a graft complex results in increased joint laxity; that is, abnormally increased passive or active displacement of the bones relative to each other. Such laxity apparently occurs quite rapidly in animal models. In goats, for example, Holden et al. (1988) documented an average 500% increase in joint laxity only 2 weeks after surgery and this persisted for 8 weeks. Ng et al. (1995) also used a goat model and found increased laxity persisted out to one year. They speculated that early uncontrolled rehabilitation could account for graft lengthening in their study. They also found reduced laxity in a few joints at 1 and 3 years after reconstruction that may have been related to osteoarthritic changes in the joints. Graft elongation does not appear to be model specific. In a dog model, 200% elongation

was seen 3 months post-surgery (171) and, in a rabbit model, 200% elongation was found at 52 weeks (17).

Clinically, joint laxity is assessed measuring anterior-posterior displacement of the knee with an arthometer; for example, the KT-1000. Arthometers are typically used to compare the left knee to the right knee. A side-to-side difference between knees of less than 3 mm is considered normal and greater than 3 mm is considered pathologic (37). Reviewing the literature suggest that 10% to 40% of reconstructed knee joints have greater than 3 mm side to side difference (1,2,16,26,38,48,68,81,87,102,133,147), and that 5% to 15% have greater than 5 mm side to side difference (1,2,16,38,68,102,133,147) over various post-surgical follow-up times. Noyes and Barber (1992) found a small percentage (13%) of the patients had a stretched graft as early as 4 weeks post-surgery. Lerat et al. (1997) documented that laxity increased over the first 6 months and leveled off thereafter. These changes in laxity and resulting effects on joint kinematics (21,22) may be a factor in the degenerative changes related to osteoarthritis seen in some joints despite reconstruction (1,39,48,81).

The "stretching out" of grafts may have occurred because the tissue was exposed to stresses sufficient to cause creep of the tissue. Creep is the increase in elongation (strain) of a tissue under repeated or sustained load (stress). In other words, grafts may undergo an increase in elongation due to their loading environment. Once the loading stops and the tissue is allowed a period of rest, the tissue may return to its original length before loading occurred. If this does not happen, the tissue would have a permanent elongation or unrecovered creep.

Measurement of ligament loading is a complex undertaking. The approaches can be categorized as direct and indirect. Direct measurement generally requires a force transducer to contact the structure being measured. Holden et al. (1994) used an implantable transducer to measure the *in vivo* force in the ACL of goats during different activities. Forces were measured in the ACL during standing, walking and trotting. Interestingly, the force in the ACL increased with increasing level of activity. Butler et al. (1998) measure the *in vivo* changes in force to the flexor digitorum profundus tendon of rabbits and also found increased activity level increased peak forces. Yamamoto and Takauchi (1998) measured the peak forces in rat patellar tendon during running and used the peak force of 50 cycles to represent the average peak force in the patellar tendon. Although these studies did not comment on the magnitude of load in repeated cycles and whether or not it changed, some revealing evidence of creep was found using direct measurement of strain in ACL grafts in humans. Using a Hall-effect transducer *in vivo*, Beynnon et al. (1994a) documented increases in graft length in the first 20 cycles of passive motion post-reconstruction and identified this as a creep response. They commented that creep would produce graft elongation resulting in increased anterior displacement of the tibia relative to the femur. Using an *in vitro* test on bilateral cadaveric knees 8 months post-surgery, Beynnon et al. (1997) found that the strain in the graft was less than the strain in the native ACL suggesting that although the graft had the same role of controlling joint biomechanics as the ACL, it was permanently stretched by this demand. The permanent stretch of the graft was also detected by increased laxity of

the reconstructed joint. More recently, force transducers are being designed that can be implanted into grafts in order to understand how grafts are loaded *in vivo* (50,149).

Indirect methods of assessing ligament forces involve the measurement of kinematic data (bone positions and accelerations) and kinetic data (joint forces and moments). The challenge is then to find a way to translate the joint force and moment data into the loads on the various structures of the joint (ligaments, tendons and contact surfaces). One such approach uses a robotic/universal force-moment sensor testing system to record the kinematic data of a cadaveric intact knee joint (167). By reproducing the kinematics of the intact joint, the *in situ* ligament forces are calculated by comparing the force vector differences before and after transection of the ligament of interest. Likewise, forces in a tissue used to reconstruct an injured ligament can also be determined. Another approach has been measuring gait biomechanics and then using mathematical modeling to solve the dynamically indeterminate problem of muscle force, ligament force and bony contact force balance. A recent review by O'Connor and Zavatsky (1993) indicated that, of the extensive work in gait biomechanics, very few studies have addressed this latter step in order to calculate ligament forces. In one of these studies, Collins and O'Connor (1991) examined forces on ligament during normal walking. Electromyography data indicated that only one of the major flexor or extensor muscle groups (quadriceps, hamstrings, gastrocnemius) was active over most of the gait cycle. Under such conditions, they determined that knee ligaments must be loaded (33,115). In fact, they found that the ACL had a potential role in 65% to 100% of the gait cycle. Although neither of these indirect measurement methods have expressly assessed

creep, the gait analysis information gives a perspective on ligament load *in vivo*. In addition, recent attention has focused on measuring differences in gait biomechanics comparing patients with ACL reconstruction to control groups (42,105,145). Similar studies could provide data to confirm that loading of the graft *in vivo* makes it vulnerable to unrecovered creep.

Under normal conditions, joint structures act to maintain equilibrium and the loading on ligaments would be within a functional, physiologic range. Consider that the same step cadence repeated in walking requires the same accelerations and decelerations of the limbs and, thus, would produce the same joint force and moments in each step. If one considers the case of only one active muscle group at a particular stage of the gait cycle, in order to achieve a balance of the forces and moments, ligaments must be carrying the same load at that same time in each step. If the ligaments did not carry the same loading in each step, the forces and moments would not be balanced; thus, as a consequence the kinematics would change. Therefore, under the conditions of repeated kinematic behaviour (walking, for example), ligaments would likely be subjected to similar repeated loads. Ligaments would respond to this environment through creep.

Creep is likely also important in other situations. First, muscle-tendon units carry high loads and dynamically balance forces at the joint. If muscles fatigue and if control systems are imperfect, joint ligaments will be subjected to increased tensile loads. Second, Panjabi et al. (1996) indicate that under the dynamic conditions of daily living, muscle forces may not be large enough, correctly directed or appropriately timed to compensate for the altered viscoelastic behaviour of an injured ligament. This situation

would permit increased ligament loading and would also parallel the situation where a graft (with different viscoelastic properties) is replacing a native ligament. Clearly, muscle fatigue in this case might permit even greater loading of the graft. Third, if one ligament of the knee was "stretched out" (unrecovered creep), this may alter how forces are balanced at the knee. In addition to potentially increasing joint loading, this may result in other ligaments being subjected to increased creep loading. Finally, the clinical evidence that grafts fail by "stretching out" suggests that grafts are exposed to repeated loads that cause creep. It is unlikely that exposing a graft to repeated extension between a minimum and maximum deformation would create the permanent elongation indicative of the "stretched out" graft.

The principal evidence that creep is an important soft tissue behaviour is the substantial clinical evidence that some ACL grafts can "stretch out". Since excessive ligament creep could result in joint laxity and altered gait biomechanics after injury or after reconstructive surgery, the accurate description of creep is of considerable significance. The mechanisms of creep are also of significance to be able to determine clinically relevant means of preventing creep. A mechanism of creep within the scope of this thesis is a factor that when manipulated influences creep behaviour. For example, if changing a particular property (biochemical or morphological) resulted in an increased creep response that property would be classified as a mechanism of creep. Minimizing graft creep is likely an important component in the joint healing process, ensuring that the graft controls joint kinematics in the same way as the original structure and that the joint is loaded within the same range of physiologically acceptable forces.

1.1.2 Experimental Investigations on Normal Ligaments

Ligaments serve important roles in maintaining joint stability and guiding joint motion (along with bone geometry, muscular action and other soft tissues) (68). In order to understand the structure and function of the ligaments, previous experimental studies have investigated the biochemistry, morphology and biomechanics (failure and stress relaxation properties) of normal ligaments.

1.1.2.1 Biochemistry

Skeletal ligaments are bands of dense collagenous tissue which connect one bone to another at joints in the body (see rabbit MCL in Figure 1.2). Ligament tissue is composed of cells and extracellular matrix into which fibrillar structures are embedded in a ground substance (154). Ligament cells are called fibroblasts. Although relatively scarce, fibroblasts are responsible for synthesis and degradation of the ligament matrix (61).

The ligament matrix consists of numerous components in varying amounts. First, water is the most abundant component of ligament, comprising around two-thirds of the tissue wet weight (61). Water may have a variety of interactions with other matrix components: primarily, freely associated with the interfibrillar gel or bound to polar side chains and, possibly, bound to other matrix components (61). Water likely functions to influence ligament viscoelastic behaviour, interacting with proteogylcans to provide lubrication for sliding of collagen fascicles and to assist cellular functions (delivery of nutrients and removal of wastes) (61).

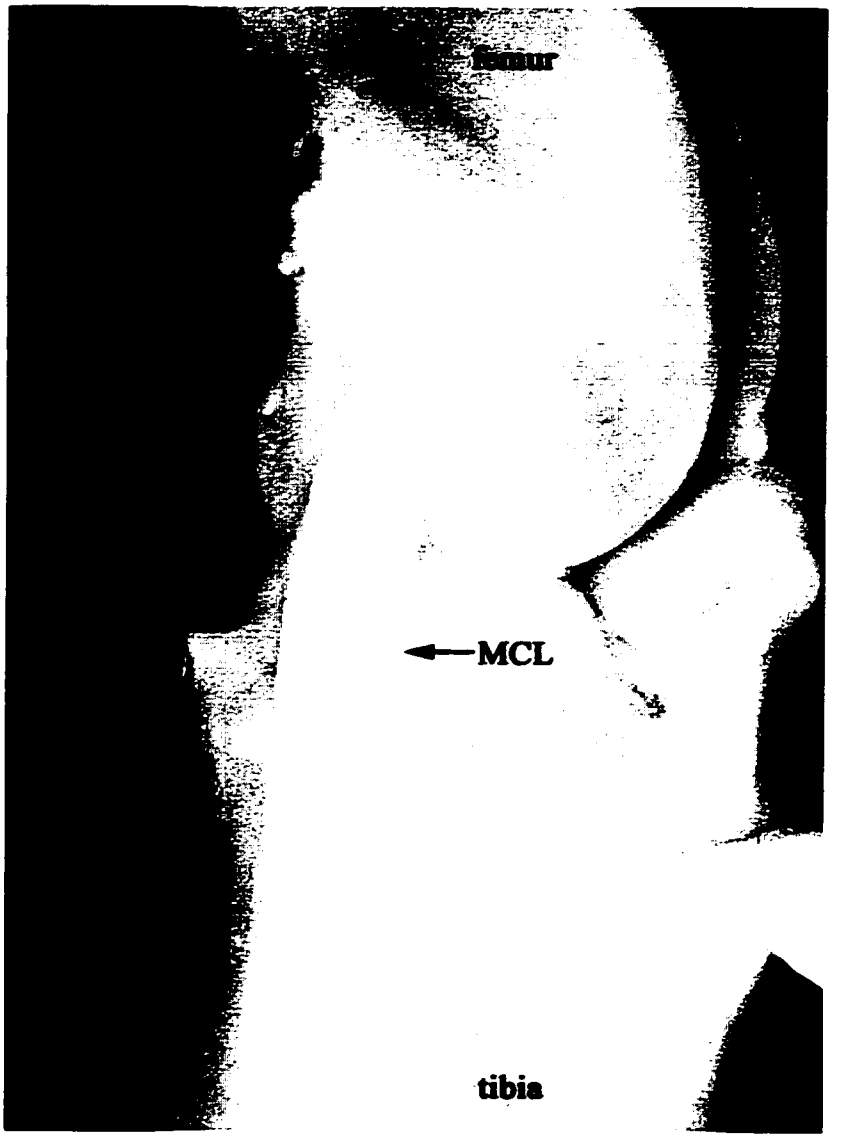

Figure 1.2: Rabbit Medial Collateral Ligament (MCL)

Second, the major component of the dry weight is fibrillar collagen which is arranged in fibrous form extending from one bone to another. Collagen comprises about 25% of the wet weight or about 75% of the dry weight (59). Type I collagen is the principal collagen type in ligament accounting for around 20% of the weight. Other collagens comprise 3-5% of the weight (59) and they include mostly Type III plus small quantities of other types (V, VI, X and XII) (61). Collagen carries tensile stress and this will be described further in relation to ligament morphology.

Third, proteoglycans comprise less than 1% of the ligament weight (61) and are part of the so-called "ground substance" (154). Proteoglycans contain different types and numbers of carbohydrate side chains called glycosaminoglycans (GAGs) covalently bound to a protein core (10,23). GAGs possess a high negative charge and large numbers of hydroxyl groups and, therefore, highly attract water (hydrophilic) (10). Thus, proteoglycans likely have a role in the amount and movement of water in the ligament (61). Together GAGs and water are key factors in collagen fibre-ground substance interaction, providing spacing and lubrication for fibre sliding and viscoelastic behaviour (10,56). Fourth, elastin, another fibrillar component, comprises 1-2% of the ligament weight (59). Elastin stretches out from a coiled configuration when stressed and likely has a role in low-load tension and recovery mechanical responses (61). Finally, fibronectins and other glycoproteins account for 1-2% of the ligament weight (59). Fibronectin is found in small amounts, typically associated with other matrix components (at borders of fibres and ground substance) (61,154).

1.1.2.2 Morphology

Ligament collagen has a hierarchical structure assembling tropocollagen into microfibrils, then subfibrils, then fibrils that are finally aggregated into collagen fibres. Fibrils are generally 50 to 500 nm in diameter (61). Fibrils have a periodicity of 67 nm (D-spacing) characteristic of fibre forming collagens (154). Fibrils aggregate to form collagen fibres. Fibres are generally 50 to 300 μm in diameter (61). In the rabbit MCL, fibroblasts align in rows between fibre bundles and are elongated with application of tensile stress (61). Fibres and fibre bundles can aggregate into fascicles and these fascicles are not obvious in all structures; for example, the MCL (61).

Ligaments and tendons have a regular undulating wave-form revealed using polarized light microscopy that was described as crimp by Diamant et al. (1972). This collagen fibre waviness occurs along the long axis of the structure. To date, there is no consensus on whether the wave-form is sharp kinked bands or smooth sinusoid-like undulations (143) or combined helical and planar waviness (168). Nevertheless, it is clear that the crimp wave-form is affected by tissue elongation and joint position. Viidik and Ekholm (1968) found that crimp vanished gradually when the fibres of tendon were elongated and the straightening out of crimp occurred unevenly across the sectioned tendon. In addition, Matyas et al. (1988) showed changes in the crimp patterns over the cross-section of the rabbit MCL with changes in joint position. The anterior fibres were more taut in flexion and the posterior fibres were more taut in extension (104). Therefore, at the structural level, considerable variation in crimp exists over the cross-section of the MCL. Essentially, the uncrimped lengths of different fibres in the same tissue are

different. In any joint position there will exist a group of fibres that are more taut than the rest. As the joint position changes new fibres are recruited to the taut group while others are released (61). Similar "functional subunits" that tighten and loosen in different joint positions have also been observed in the human MCL and ACL (13,61,83).

The stress-strain curve of ligaments and tendons is nonlinear, comprised of a toe region at the lower stresses represented by increased stiffness with increasing stress (Figure 1.3). The next phase is a linear region where constant stiffness (modulus) is attained; the linear region continues until failure occurs. Features of the stress-strain curve have been related to crimp. Rigby et al. (1959) used isolated tendons from rat tail and observed that the toe region correlated to the disappearance of crimp and that crimp was absent when the linear part of the curve was reached. Viidik and Ekholm (1968) used rabbit Achilles tendon sectioned to a uniform thickness with parallel sides and described similar findings to Rigby et al. (1959). Viidik (1972) used rabbit Achilles and other hind limb tendons cut to parallel-sided pieces of uniform thickness in a study that simultaneously documented mechanical and morphological behaviour. Again, the toe region was found to relate to the straightening out of crimp. Thus, crimp is an index of collagen fibre recruitment. Viidik (1972) also showed images that related to specific points on the stress-strain curve. Crimped fibres in the toe region and straightened fibres in the linear region were shown. There was no image of the crimp pattern at the transition between the toe and linear region. It is generally accepted that the toe region involves the straightening out of crimp as fibres are recruited and the linear region is the

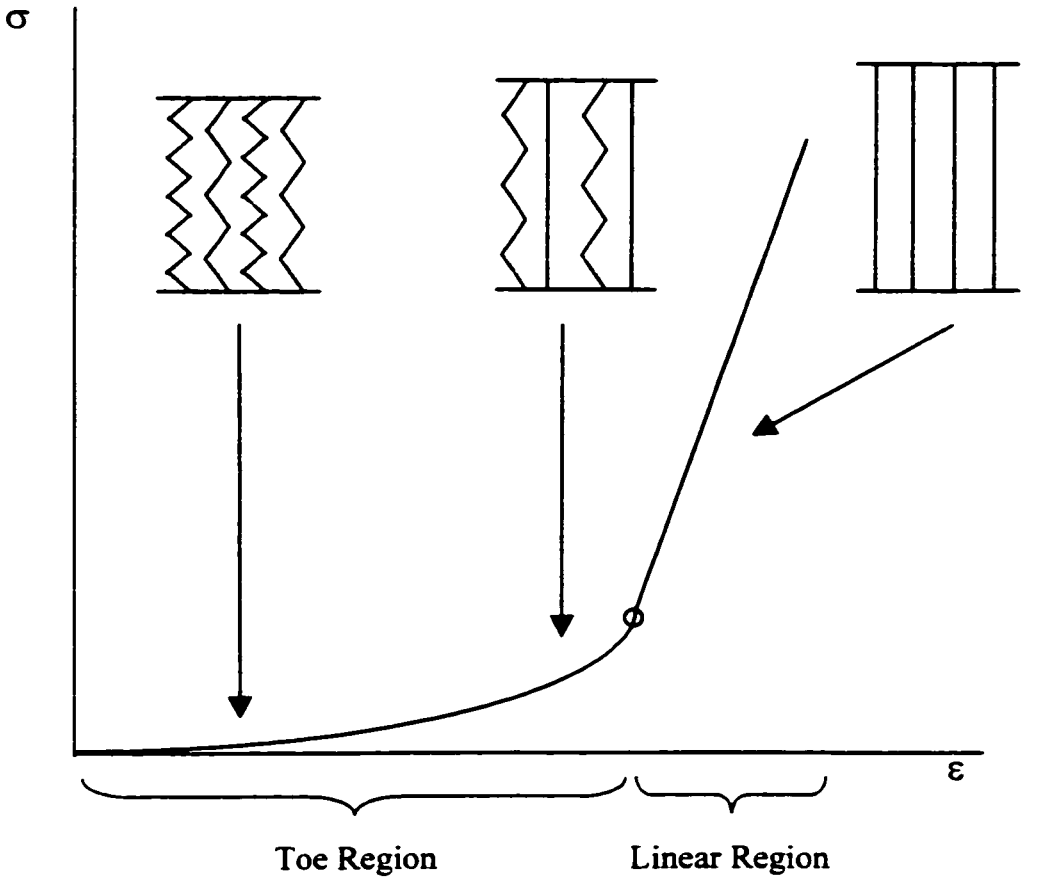

Figure 1.3: Schematic of Stress-Strain Curve and Corresponding Crimp

"σ" is stress and "ε" is strain

result of fibres being recruited and straightened. Recently, Viidik (1990) cautioned that the transition between these regions is gradual.

1.1.2.3 Biomechanics

The majority of previous experimental studies of ligament and tendon behaviour have focused on high-load failure characteristics. A few studies have examined ligament viscoelastic properties, and these have been limited essentially to either measuring (25,52,113) or modeling (92,101,159,160) stress relaxation. Stress relaxation is the decrease in stress in the tissue under repeated or constant strain.

Another characteristic viscoelastic property is creep: the increase in strain in the tissue under repeated or constant stress. In what is likely the first reporting of creep in soft tissues, Roy (1880) observed that animal tissues, when stretched with hanging weights, elongated rapidly and subsequently had a continuing elongation to an equilibrium point. Historically, creep of soft tissues other than cartilage (15,109,110,136) has received little attention.

A few studies in the 1960s addressed the creep of ligaments and tendons. Viidik (1966) investigated the viscoelastic properties of the rabbit ACL. In this study, creep was defined as the behaviour of the ligament under both constant stress and constant strain. However, only constant strain tests were performed. Later, Viidik (1968) identified these tests correctly as load relaxation tests. Interestingly, over the course of these load relaxation tests, the load was adjusted occasionally (at set time intervals) back to the initial load value and elongation was observed to increase. If the frequency of these load

adjustments was increased to approximate a constant load more closely (although this is difficult with a screw-fed test system), these data would certainly be consistent with creep. Two other studies from this decade investigated the creep of murine tail tendons. Morchio and Ciferri (1969) used dehydrated rat tail tendon to document the creep that followed chemical contraction in KSCN solution under a weight of 1 gram mass (hanging on one end of the tendon). Stromberg and Wiederhielm (1969) documented the creep of mouse tail tendons under constant load applied using hanging weights. The tendons were dehydrated to permit grip fixation at tendon ends. Present experimental technologies allow better control of test conditions (environment chambers with controlled temperature and humidity) and load application (customized closed-loop servo-hydraulic test systems).

Of the limited studies on creep of tendon and ligament, the majority have been performed on tendon. A few creep studies have focused on the viscoelastic properties of the tendons of the human hand. Cohen et al. (1976) determined the activation energy for viscoelastic creep of normal human digital tendon using temperature change (T-jump) analysis. T-jump analysis exposes the tissue to small rapid changes in temperature during a creep test. Goldstein et al. (1987) investigated the cumulative increase in strain that results when flexor digitorum profundus tendon and tendon sheaths were exposed to physiologic loading representative of a repetitive task. Monleon Pradas and Diaz Calleja (1990) modeled the creep of the human flexor tendon based on a quasilinear assumption similar to the Quasi-Linear Viscoelastic theory that Fung developed in 1972 (63).

Recent attention has been paid to the creep properties of human patellar tendon, which is used for ACL replacement. Kerboull et al. (1991) documented the low-load cyclic creep (80 cycles at 1 Hz from 0 N to 50 N) of central thirds of previously frozen human patellar tendon exposed to freeze-drying (lyophilization) and gamma irradiation (2.5 Mrad). These investigators found that both freeze-drying and gamma irradiation increased the tendon creep response and the largest increase occurred when the procedures were used in combination. Rasmussen et al. (1994) assessed the creep of lateral and medial halves of previously frozen human patellar tendon treated with gamma irradiation (4 Mrad). A static creep test representative of a pre-tensioning procedure (90 N sustained for 10 minutes) and a cyclic creep test representative of 1 hour of walking (3600 cycles at 1 Hz from 50 N to 200 N) were performed. The authors found no difference in the cyclic and static creep behaviour between the control and irradiated specimens. In another study, Howard et al. (1996) found that central third patellar tendon grafts crept during a pre-tensioning procedure both *in vivo* at the time of surgery (89 N sustained for 4 minutes) and *in vitro* (89 N sustained for 15 minutes). In addition, Schatzmann et al. (1998) documented pre-conditioning of central thirds of patellar tendons using cyclic creep between 75 N and 800 N at 0.5 Hz. They found that high-load cyclic creep improved the failure characteristics compared tendons that were not preconditioned. Although these studies used treatments to prepare the graft tissue for implantation, the creep behaviour was measured before implantation. Documenting the creep behavior of grafts after implantation and subsequent healing in the vascular,

cellular, living environment could aid our understanding of why some grafts "stretch out" *in vivo*.

A few studies have investigated the creep of dental and knee ligaments. Daly et al. (1974) documented the *in vivo* static creep of the peridontal ligament in response to torsional loading (60 second duration). They found that the peridontal ligament had a reasonably close approximation to linear viscoelastic behaviour at low torques and non-linear behaviour at higher torques. Two other studies from the 1990s investigated the creep of knee ligaments. Viidik (1990) documented the creep and stress relaxation of rabbit ACL at one load (100 N) with different test times. No determination of the relationship between creep and stress relaxation was made. Duquette et al. (1996) examined the creep behaviour of collateral ligaments of spontaneously diabetic rats, insulin-treated diabetic rates and non-diabetic rats. Cyclic sinusoidal creep tests were performed at one low stress. The components of complex compliance (storage and loss) as well as logarithmic creep rate were determined. Diabetes affected the loss compliance but not the storage compliance. No clear relationship between the diabetic effects and creep were established.

Despite these investigations, what remains unknown is the creep behaviour of normal knee ligaments over a range of stresses that are in the toe and linear regions of the ligament stress-strain curve. Establishing such a baseline of normal ligament creep behaviour is an essential first step in understanding the changes in knee ligament creep with injury or disease.

Given the concentration of previous investigations on stress-relaxation properties, no one has yet determined if creep can be predicted from previously documented stress relaxation for ligament. Models of soft tissue behaviour can be classified into three types: continuum, phenomenological and structural (97). Continuum models involve specialization of general material theories for biological tissues. Phenomenological models use mathematical expressions the fit specific modes of behaviour. Structural models develop constitutive relations based in the tissue structure. Structural models have the advantage of relating tissue microstructure to mechanical behaviour; whereas, the advantage of phenomenological models is the description of generalized tissue behaviour (165). The Quasi-Linear Viscoelastic (QLV) theory developed in 1972 by Fung (1993) is a phenomenological approach that models the nonlinear viscoelastic behaviour of soft tissues within the framework of a linear theory (71). QLV theory is the most widely accepted model of viscoelastic properties of tendon and ligament (72,86,159,160,165), with relaxation being the parameter modelled. Creep can also be modelled by QLV and the linear framework allows creep to be predicted from the relaxation using Laplace Transformations. Time varying functions can be used to describe experimental stress relaxation and creep. Nevertheless, Fung (1993) questioned if the microstructural processes taking place during creep and stress relaxation were different. If ligament creep cannot be predicted by stress relaxation using QLV and Laplace Transformations, the behavioural difference may reveal an important mechanism of creep. If this is the case, a structural model that incorporates parameters for the ligament microstructure would help to identify the microstructural processes that are

different between creep and relaxation. A modified phenomenological model might be predictive but would not reveal the structural mechanism of creep.

Collagen properties likely have an important mechanistic role in creep. Cohen et al. (1976) speculated that the activation energy of tendon creep (T-jump analysis) was between the high activation energy for fibrillar creep and the low activation energy for interfibrillar sliding and shear of the interfibrillar gel that results from the straightening out of the wavy fibres. In later studies (78,79), these investigators modelled this behaviour combining the activation energy for the toe region (straightening out of wavy fibres) and the linear region (fibril creep) based on different amounts of collagen fibre crimp. However, no morphological documentation of fibre crimp was made. Interestingly, however, fibril morphology has been documented during creep. Purslow et al. (1998) observed no changes in D-spacing of rat skin during a low-load creep test (uniaxial tension). However, Mosler et al. (1985) found changes in the D-spacing of rat tail tendon and human flexor tendon during creep tests at higher loads (5% elongation typically in the linear region). D-spacing changes were correlated to the linear region of the stress-strain curve by Viidik and Ekholm (1968). Despite some attention to fibril morphology, what remains unknown is how the collagen fibre morphology changes during creep.

1.1.2.4 Summary of Gaps in Knowledge Regarding Normal Ligaments

What is not known is how crimp is related to creep behaviour of ligament. The role of collagen fibre recruitment in ligament could be investigated by not only describing

but also quantifying the amount of crimp in the ligament immediately before and immediately after creep testing. Fibre recruitment during creep of an intact ligament should be measured at stresses in the toe and linear region and at the transition between the toe and linear region measured from the stress-strain curve to explore the effect of potential differences in fibre recruitment on creep. Creep testing over a range of stresses would also provide a normal ligament creep behaviour baseline to which studies of healing ligament creep could be compared. In addition to morphological measurements, structural modeling of ligament creep behaviour could be used to examine the potential mechanistic role of fibre recruitment during creep.

Biochemical changes during creep may also have important mechanistic implications. Hannafin and Arnoczky (1994) documented that cyclic and static creep caused a significant (yet small) water loss in canine flexor digitorum profundus tendon. Others have shown the effect of altered water content on stress relaxation. Chimich et al. (1992) showed that immature rabbit MCLs immersed in 25% sucrose to reduce water content (50% initial water content) had less cyclic relaxation than MCLs immersed in phosphate buffered saline to increase water content (74% initial water content). Similarly, Haut and Haut (1997) found that human patellar tendons had slower static relaxation in hypertonic solutions (25% sucrose) than in hypotonic solutions (distilled water). What remains unknown is how changes in ligament initial water content before creep testing will affect subsequent creep behaviour which may reveal an important mechanistic role of water in creep. Also of interest would be to gain an understanding of how increases in creep test stress would affect the amount of water moving out of the

ligament during creep. Establishing a baseline of normal creep behaviour and creep mechanisms is essential for baseline comparison with ligament injury and healing.

1.1.3 Experimental Investigations on Healing Ligaments

Since creep of healing ligaments may have important implications for joint instability and altered kinematics, quantifying creep and understanding its mechanisms may be useful for finding clinically relevant means of preventing creep.

1.1.3.1 Biochemistry, Morphology and Biomechanics of Ligament Scars

A cascade of events occurs following ligament injury: bleeding and inflammation, production of matrix, and matrix remodeling (59). Biochemical and morphological changes in the rabbit medial collateral gap model of ligament healing have been documented previously by this laboratory. The biochemical profile of MCL gap scar was altered compared to normal MCL (74). Water content was higher than that of controls in the early stages of healing (51,52). Cellularity (DNA concentration) and GAG (hexosamine) content remained elevated over 14 weeks of healing (51,52). Scar collagen (hydoxyproline) concentration returned to normal values by 14 weeks; however, collagen crosslink (hydroxylysylpyridinoline) densities reached only 55% of normal values by 14 weeks (56). Collagen fibre realignment towards the long axis of the ligament equaled normal values by 14 weeks (54). However, collagen fibril diameters were significantly smaller than in control MCLs at all healing intervals (55).

The mechanical failure properties of MCL scars have also been shown to be inferior to normal ligament (52). Combined ligament injury to the MCL and ACL creates an increased stress environment on the healing MCL. In several models (25,70,164), these stress-inducing conditions caused increased laxity. Excessive creep of healing ligaments could contribute to joint dysfunction by allowing either temporary or permanent abnormalities in joint kinematics.

No one has yet documented the creep behaviour of early ligament scars in isolated MCL injuries. Ligament scars have changing morphological and biochemical properties over time. Because of the changes in these properties over the healing intervals, rabbit MCL gap scar was an effective model in which to investigate the correlations between creep behaviour and several different biological indices, potentially revealing some of the mechanisms of scar creep.

1.1.3.2 Biochemistry, Morphology and Biomechanics of Ligament Autografts

Knee joints with ligament injury and chronic laxity are often reconstructed using soft tissue autografts. These autografts produce a clinical improvement and yet recent evidence has shown that some of these autografts can "stretch out" (creep) over time.

Graft tissue is infiltrated with scar tissue post-implantation (9,127). The cellularity of the graft is increased in early stages of healing (9,127). It appears that these cells are from extrinsic sources (57). An orthotopic rabbit MCL autograft model was used by Sabiston et al. (1990a). Collagen content was not different than contralaterals over the 48 weeks of healing but GAG content (hexosamine) was significantly elevated

over this same time period. Cellularity (DNA concentration) returned to normal values by 24 weeks. These early changes in MCL autografts (127) parallel the changes observed in the proliferative phase of MCL scars in early healing (52). Analysis of biopsied patellar tendon autografts used for clinical ACL reconstruction have also revealed a predominance of small diameter fibrils and less parallel arrangement of fibrils (116). Similar morphological changes were observed in MCL scars (54,55).

Few studies have documented the experimental creep and creep recovery of autografts at different healing intervals with any type of rehabilitation. Boorman et al. (1998) recently documented the increased creep response and increased unrecovered creep of rabbit MCL autografts compared to normal MCLs after short-term healing (3 and 8 weeks). Interestingly, Sabiston et al. (1990b) showed that the failure stress-strain characteristics and stress relaxation behaviour of this same model of grafts returned to contralateral behaviour by 48 weeks.

What remains unknown is whether the creep behaviour of these MCL autografts returns to normal after long-term healing. Furthermore, no study has yet examined the ability of these grafts to recover from exposure to creep stresses.

1.1.3.3 Immobilization Effects on Biochemistry, Morphology and Biomechanics

In the past, injured ligaments had been treated with immobilization to prevent the healing tissue from experiencing damaging stresses (163). However, there appears to be a spectrum of positive joint loading with detrimental extremes of immobility, at the one end, and instability, at the other. Immobilization of healing ligaments resulted in

decreased failure strength compared to healing ligaments than were not immobilized (162) and control ligaments (67,162). Similarly, others have documented decreased failure loads of immobilized healing ligaments compared to non-immobilized healing ligaments (70) and control ligaments (70,148).

In the rabbit MCL gap model of scar, collagen alignment in immobilized scar was within normal values at all healing intervals, even though collagen fibre alignment in non-immobilized scar required 14 weeks to achieve normal alignment (54). Valias et al. (1981) found that immobilization of healing rat MCLs caused increased cellularity and permitted more collagen degradation than synthesis.

The creep behaviour of ligaments scars subjected to immobilization has not been documented previously. Likewise, only limited attention has been paid to the immobilization of ligament autografts. Rabbit MCL autografts that remained immobilized for an entire (but short-term) healing interval had greater creep than comparable non-immobilized grafts (24). Short-term immobilization, however, may not have a detrimental effect on graft creep and recovery if the grafts are permitted a long-term healing interval.

1.1.3.4 Summary of Gaps in Knowledge Regarding Healing Ligaments

What is not known is how the creep behaviour of ligament scars compares to normal ligament creep behaviour. Correlating scar creep behaviour with potential mechanisms of scar creep may aid in identifying clinically relevant means of preventing creep. The creep and recovery behaviour of long-term healing grafts is presently

unknown. Previous creep studies of graft tissues used for ligament replacement (patellar tendon) did not include actual implantation of the graft and thus excluded the effects of subsequent healing. Finally, immobilization may be a potentially effective intervention to minimize creep of healing ligament. Short-term immobilization of both short-term and long-term healing ligaments could be used to investigate the effect of immobilization on creep.

1.2 Significance and Rationale

Knee joints with ligament injury are prone to instability and potential development of osteoarthritis. Injury to the ACL with or without injury to the MCL is common. Generally, the injury to the ACL is treated with a reconstruction using graft tissue. Careful analysis of the clinical literature suggest that 10% to 40% of patients with reconstructed knee joints experience a "stretching out" of the graft tissue. This graft elongation is likely due to a creep response of the graft tissue. Creep is the increase in elongation (or strain) of a material under repeated or sustained load (or stress). Although creep has been investigated in other engineering materials and biological materials such as bone and cartilage, little attention has been paid to the effect of creep on normal ligament and healing ligament. Chronic joint looseness may develop from the "stretching out", or creep, of the tissues that replace the injured tissues including graft tissues used in ACL reconstructions and the scar tissue produced in MCL repair.

Creep behaviour will be investigated in three models: rabbit normal MCL, rabbit MCL gap scar and rabbit MCL orthotopic autograft. These three models have well-

characterized morphological and biochemical properties which is advantageous for the goal of investigating the mechanisms of creep. Potential mechanisms of creep may involve the recruitment of collagen fibres, creep of collagen fibres, movement of water out of the ligament and initial content of water in the ligament. If creep is not accurately predicted from inverse stress relaxation behaviour, a mechanism of creep may be revealed. A structural model of ligament behaviour will be able to attribute differences in creep and stress relaxation to a particular microstructural property. As well, clinically relevant means of preventing creep may be determined as a result of studying creep of ligament scars and ligament autografts and how both are affected by immobilization. Minimization of creep in the clinical setting could prevent persistent joint laxity and altered joint kinematics and, potentially, prevent the development of debilitating osteoarthritis.

Although creep may only be small in magnitude and may only produce small changes in joint mechanics, it may have large implications for joint function. Radin et al. (1991) found that patients with knee pain had very subtle differences in gait parameters at heel strike compared to asymptomatic patients. This so-called "microklutziness" created repetitive impulse loading at the joint (physiologic but rapid loading), thought to provoke osteoarthrotic changes. Although the underlying reason for this "microklutziness" has been attributed to "micro-incoordination of neuromuscular control", the result at the joint is a change in joint loading. The creep of healing ligaments would also likely result in some change in joint loading. Clearly, small changes in joint mechanics have important

implications because they may create loading conditions that potentially lead to development of osteoarthritis.

1.3 Hypotheses and Aims

The investigations in this thesis are framed as a series of questions in a critical path process. The first important question was: "Can creep behaviour be predicted by stress relaxation behaviour that was documented previously?" Using Quasi-Linear Viscoelastic theory, the inverse stress relaxation function was used to predicted creep behaviour. The hypothesis was that this would not produce an accurate prediction principally because the behaviour of the ligament in the two test conditions was different. Based on what has been described previously about the recruitment of fibres during loading, the stress relaxation test which is performed at a prescribed deformation would recruit only a specific number of fibres. That number of fibres will not change over the course of the relaxation test because the deformation does not change. Creep, on the other hand, is performed at a constant stress and permits deformation over the course of the test so it is likely that some fibres would be recruited initially upon loading and others would be recruited progressively over the course of the test as the deformation increases. The second key question was: "Can fibre recruitment account for the difference between creep and stress relaxation?" The investigation of the above hypothesis was two-fold. The first approach was to develop a structural model that incorporated both fibre recruitment and fibre creep. The inverse stress relaxation function was used to predict fibre creep because it was the behaviour of a specific group of fibres. Fibre recruitment

was modeled using a linear distribution of crimp in an idealized ligament. This was used to support the concept that recruitment can account for the difference between experimental creep behaviour and the creep behaviour predicted from stress relaxation behaviour. The second approach was to quantify experimentally the changes in ligament fibre recruitment during creep and during stress relaxation using crimp pattern as an index of recruitment. This was evaluated by creep testing normal MCLs at stresses in both the toe and linear regions of the stress-strain curve to determine how creep and fibre recruitment might be affected by stress level. This was also used to further support the notion that fibre recruitment can account for the difference between creep and relaxation.

In addition to fibre recruitment, water content may be an important factor in viscoelastic behaviour of normal ligament. Therefore, the third important question was: "How are creep and water content related (both water content initial conditions and water content changes during creep)?" The changes in water content of normal ligament due to creep testing at various stress levels was measured. The hypothesis was that water content would decrease as a result of creep testing and the amount of the decrease would be a function of the stress applied. The efficiency of water return to the ligament after creep testing was also assessed. Further, to investigate how altered water content after activity (or injury) would affect creep, the initial conditions of water content in normal ligament were varied by soaking the MCL in phosphate buffered saline (swelling) or sucrose (osmotic removal of water). The expected result was that increased water content would increase creep and decreased water content would decrease creep. The goal of

these studies on normal ligaments was to identify if fibre recruitment and water content were indeed mechanisms of creep.

The study of healing ligaments was of paramount importance for understanding the clinical implications of creep. The fourth question to be addressed was therefore: "Are ligament scars more susceptible to creep than normal ligaments?" The creep response of ligament scars was assessed at 3, 6 and 14 weeks of healing. The hypothesis was that MCL scars would creep more than normal ligaments tested at the same stress. If true, the question arises as to which biochemical and morphological changes in scar could account for such behaviour. Potential mechanisms of scar creep were identified when the changes to a particular biochemical or morphological property matched the changes that occurred in scar creep over the 14 weeks of healing. The final question was: "Does immobilization of ligament scars and ligament grafts minimize or exacerbate creep?" The creep behaviour of autografts without immobilization also merited attention; thus, the creep behaviour of autografts with one and two years of healing was quantified. The structural scaffold of the graft, although infiltrated by scar, was hypothesized to have better creep resistance than scar and to have improved creep resistance with time post-operatively. An additional group of one year healing autografts had 6 weeks of early post-operative immobilization followed by remobilization for the remainder of the year. The investigations using autografts provided information on whether the short-term vulnerability to creep was reversed with time and whether short-term immobilization was a further benefit to enhancing creep resistance. The goal of the investigations on healing ligaments were to identify mechanisms of scar creep (including fibre recruitment and

water content) and to determine the efficacy of ligament grafting and immobilization for minimizing creep.

CHAPTER 2

PREDICTING CREEP BEHAVIOUR FROM STRESS RELAXATION BEHAVIOUR

2.1 Introduction

2.1.1 Creep and Stress Relaxation

The Quasi-Linear Viscoelastic (QLV) theory developed by Fung in 1972 (63) models the nonlinear viscoelastic behaviour of soft tissues within the framework of a linear theory (71). There are two viscoelastic properties of interest: (a) stress relaxation, which is the decrease in stress with a tissue under repeated or constant strain; and (b) creep, which is the increase in strain of a tissue under repeated or constant stress (Figure 2.1). QLV theory is the most widely accepted model of viscoelastic properties of tendon and ligament (72,86,159,160,165), with relaxation being the parameter modelled. In experimental studies, relaxation is also the more commonly measured property (25,52,113).

Ligaments, however, may function in normal daily activity under the action of repeated low loads (77). The same step, for example, repeated in walking requires the same acceleration and deceleration of the limbs and thus the same loads at the joint. Ligaments would likely respond to this environment through creep rather than relaxation. Since excessive ligament creep could result in joint laxity after injury or after

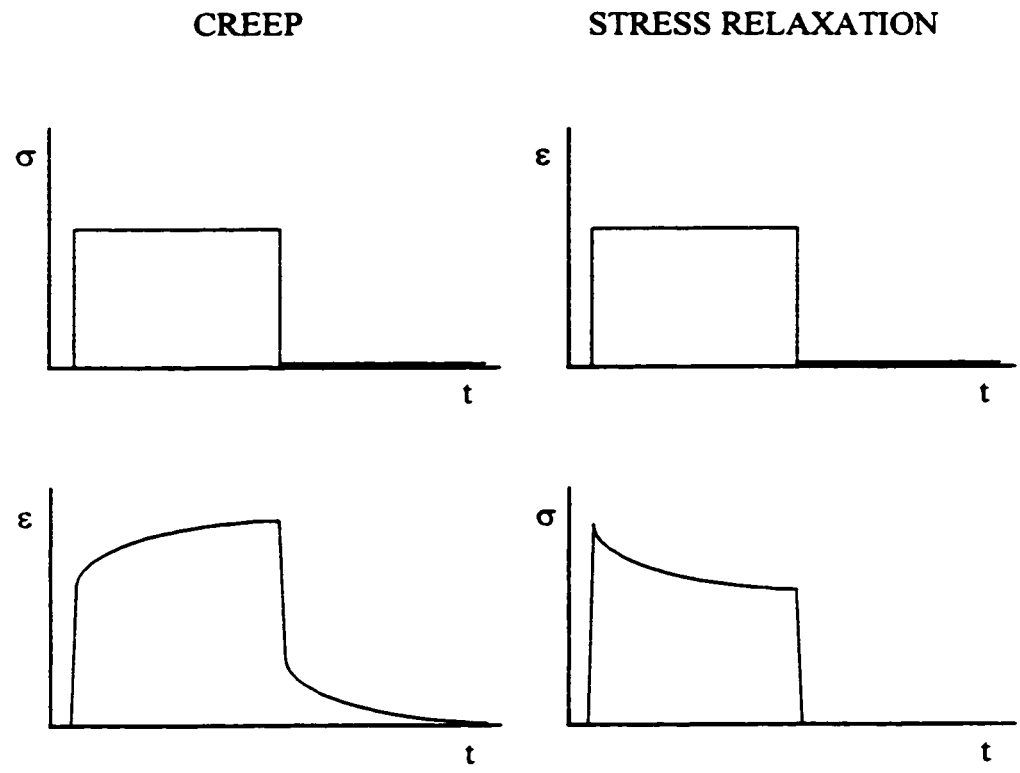

Figure 2.1: Schematic of Creep and Stress Relaxation Tests

"σ" indicates stress, "ε" indicates strain, and "t" indicates time

reconstructive surgery, the accurate description of creep could be of considerable significance.

It is unknown, however, whether or how creep relates to stress relaxation for ligament; that is, can inferences be made about creep behaviour based on previously documented stress relaxation behaviour? The goal was to determine if static creep can be predicted from static stress relaxation at low (functional) stresses (143). QLV theory (63) was employed to model the behaviour of the rabbit MCL. The theory states that stress, σ, developed in a soft tissue subjected to uniaxial tension is a function of time, t, and strain, ε.

$$\sigma(\varepsilon,t) = g(t)\,\sigma^e(\varepsilon) \qquad [1];$$

where g(t) is the relaxation function where g(0)=1 and $\sigma^e(\varepsilon)$ is the time-independent elastic response. QLV combines the time-dependent and elastic components of the mechanical response using a hereditary integral formulation assuming infinitesimal step changes in strain applied to the tissue in a state of strain ε at an instant of time τ.

$$\sigma(t) = \int_0^t g(t-\tau)\frac{\partial\sigma^e}{\partial\varepsilon}\frac{\partial\varepsilon}{\partial\tau}d\tau \qquad [2]$$

The meaning of this expression is the stress response is the sum of contributions of all the past changes each of which is governed by the same relaxation function. The hereditary integral formulation is similar to the formulation for linear viscoelasticity except that the elastic response, $\sigma^e(\varepsilon)$, in QLV has assumed the role of strain, ε, in the conventional

linear viscoelastic theory (49). Thus, the convenience of QLV is that methods used in linear viscoelasticity can be applied.

In this study, the special cases of constant-strain relaxation tests and constant-stress creep tests were investigated. In a static stress relaxation test, the strain is held constant and the stress reduces to a function of time alone: $\sigma(t) = g(t)\,\sigma_o$ [3], where g(t) is the time varying relaxation function with $g(0) = 1$ and σ_o is the initial stress. Similarly, in a static creep test where the stress is held constant, the developed strain reduces to a function of time alone: $\varepsilon(t) = j(t)\,\varepsilon_o$ [4], where j(t) is the time varying creep function with $j(0) = 1$ and ε_o is the initial strain.

Linear viscoelastic theory, which is applicable within the linear framework of the QLV theory, indicates that the time varying stress relaxation function, g(t), and creep function, j(t), should be predictable from one another as follows:

$$g(0) = \frac{1}{j(0)} \quad [5] \qquad \text{and} \qquad g(\infty) = \frac{1}{j(\infty)} \quad [6] \qquad \text{or} \qquad \bar{g}(s)\bar{j}(s) = \frac{1}{s^2} \quad [7]$$

where $\bar{g}(s)$ and $\bar{j}(s)$ are the Laplace Transformations of g(t) and j(t), respectively. Equation [5] must be satisfied based on QLV requirements. Therefore, the hypothesis was that the relationships stated in equations [6] and [7] would hold; that is, the time varying function which describes the experimental ligament static creep would be inversely proportional to the function which describes experimental static stress relaxation evaluated at time infinity and would be equivalent to the time domain function

for creep predicted from the experimental stress relaxation function using Laplace transformations and equation [7].

Aim 1. To quantify the stress relaxation and creep properties of normal rabbit MCL at low stresses (14 MPa and 4.1 MPa) and to determine if the creep function of ligament can be predicted from the stress relaxation function as suggested by theory.

2.1.2 Model

The experimental creep function may not be equivalent to the time domain function for creep predicted from the experimental stress relaxation function using Laplace Transformations and Quasi-Linear Viscoelastic theory. This discrepancy may be due to the behaviour of the fibre structure of the ligament in these two types of tests. The collagen fibres of ligament have a characteristic crimp pattern (8,10). The disappearance of crimp in tendon fibres has been correlated to the stress-strain curve (152); thus, crimp is an index of collagen fibre recruitment. When subjected to tensile loading, the response of ligaments (or tendons) is a nonlinear stress-strain curve composed of a toe region at the lower stresses represented by increasing stiffness with increasing stress (Figure 2.2). The next phase is a linear region where constant stiffness is attained. The linear region continues until failure begins. The ligament stress-strain curve has been explained previously using crimp (152): the toe region is the straightening out of crimp as collagen fibres are recruited. This process is complete in the linear region of the stress-strain curve.

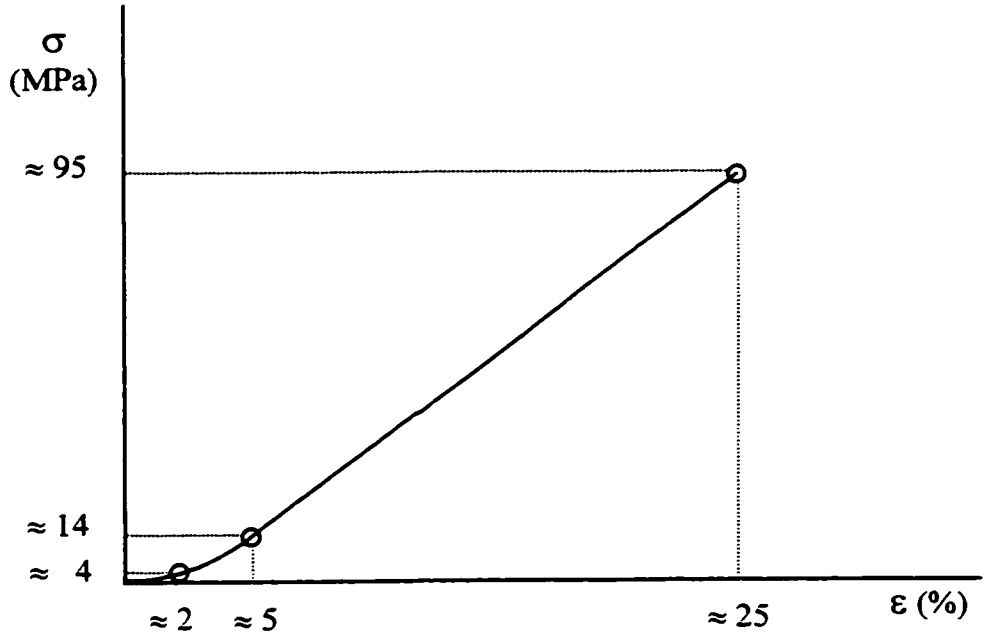

Figure 2.2: Typical Rabbit MCL Stress-Strain Curve

"σ" indicates stress and "ε" indicates strain

4.1 MPa is in the toe region of the stress-strain curve.

14 MPa is at the transition between the toe and linear regions.

Based on these morphological findings, the fibres are likely recruited differently in creep test than in a stress relaxation test. In a static stress relaxation test, the ligament is stretched to a prescribed strain and maintained at that constant strain. This would recruit a discrete group of fibres initially. The resulting behaviour of these discrete fibres is recorded over the course of the static test. In a static creep test, the ligament is loaded to a prescribed stress and maintained at that constant stress. Since strain is not controlled, the behaviour measured is that of the fibres loaded initially and those fibres recruited progressively over the course of the static test. The experimental creep behaviour may not be predicted by the inverse stress relaxation function because of fibre recruitment during static creep. Hence, the proposed model incorporates the recruitment of fibres and the creep of previously recruited fibres.

A structural model has parameters related to the structure of the tissue, unlike a phenomenological model, like QLV, where mathematical expressions are fit to specific modes of behaviour. A structural model is appropriate to demonstrate that stress relaxation behaviour can be used to predict creep behaviour if fibre recruitment is included. Previous structural models have expressed fibre recruitment in ligament and tendon using collagen fibres with different initial lengths distributed according to a probability density function (40,41,82,96,97,100). The different initial lengths of collagen fibres allow for progressive recruitment of fibres. As the ligament is stretched, the initially crimped fibres become sequentially straightened and loaded (89). Fibres only contribute mechanically once they are straightened. The straightened fibres are then

governed by constitutive equations; for example, linear viscoelasticity. The proposed model will use a simplified fibre recruitment pattern but will follow the assumption that fibres only creep once straightened and are governed by linear viscoelasticity.

Aim 2. If creep cannot be predicted from stress relaxation, to develop a structural model to account for the difference by including fibre recruitment and fibre creep.

2.2 Methods

2.2.1 Creep and Stress Relaxation

Eleven skeletally mature (one-year-old) female New Zealand White rabbits (Riemans Fur Ranch, St. Agatha, Ontario, Canada) were used in this study which was approved by the University of Calgary Animal Care Committee. The MCL from one knee joint from each animal was used to measure stress relaxation and the MCL of the opposite knee was used to measure creep (right and left knees were alternated). The creep and stress relaxation were evaluated at two low stresses: 14 MPa (n=8) and 4.1 MPa (n=3). 4.1 MPa is in the toe region of the normal MCL stress-strain curve (Figure 2.2 and Appendix 1). 14 MPa is at the transition between the toe and linear regions of the stress-strain curve. At these stresses, there should not be complete collagen fibre recruitment (152), but active recruitment potentially within a functional (but pre-damage) range. The recruitment of collagen fibres during creep testing is investigated in Chapter 3. Also, each ligament tested at 14 MPa was elongated to failure at 20 mm/min,

providing further confirmation that the prescribed stress corresponded to the transition between the toe region and the linear region of the stress-strain curve.

For tests conducted at 14 MPa, specimens were tested in an MTS system (MTS Systems Corporation, Minneapolis, Minnesota, U.S.A) following the protocol shown in Figure 2.3. Animals were sacrificed with an overdose of pentobarbital (Euthanyl, 1.5 mL/animal, MTC Pharmaceuticals, Cambridge, Ontario, Canada). The hindlimbs were disarticulated at the hip and ankle. All soft tissues including muscle and fascia were removed rapidly from the femur and tibia, leaving the menisci, collateral and cruciate ligaments. Bones were transected 3 cm from the MCL insertions. Tissues were kept moist by wrapping the joint with phosphate buffered saline (PBS) soaked gauze.

The tibia was cemented into the upper grip of our test system with polymethylmethacrylate. The upper grip was attached to the 500 N load cell (Model 661.12A-05) of the hydraulic actuator (Model 242.02 with servovalve Model 252.21C-01) of the MTS system and positioned for alignment of the MCL with the load axis of the actuator. Load was zeroed to account for specimen weight. The femur was cemented into the lower grip with the knee at approximately 70° flexion, and displacement was zeroed. The customized grip system was designed for easy and accurate alignment of the long axis of the MCL with the load axis to prevent eccentric loading (94). Tissues were then kept moist by intermittent application (every 30 to 60 seconds) of PBS.

The joint experienced two cycles of 5 N compression and 2 N tension at 1 mm/min. Menisci, cruciate and lateral collateral ligaments were dissected away leaving

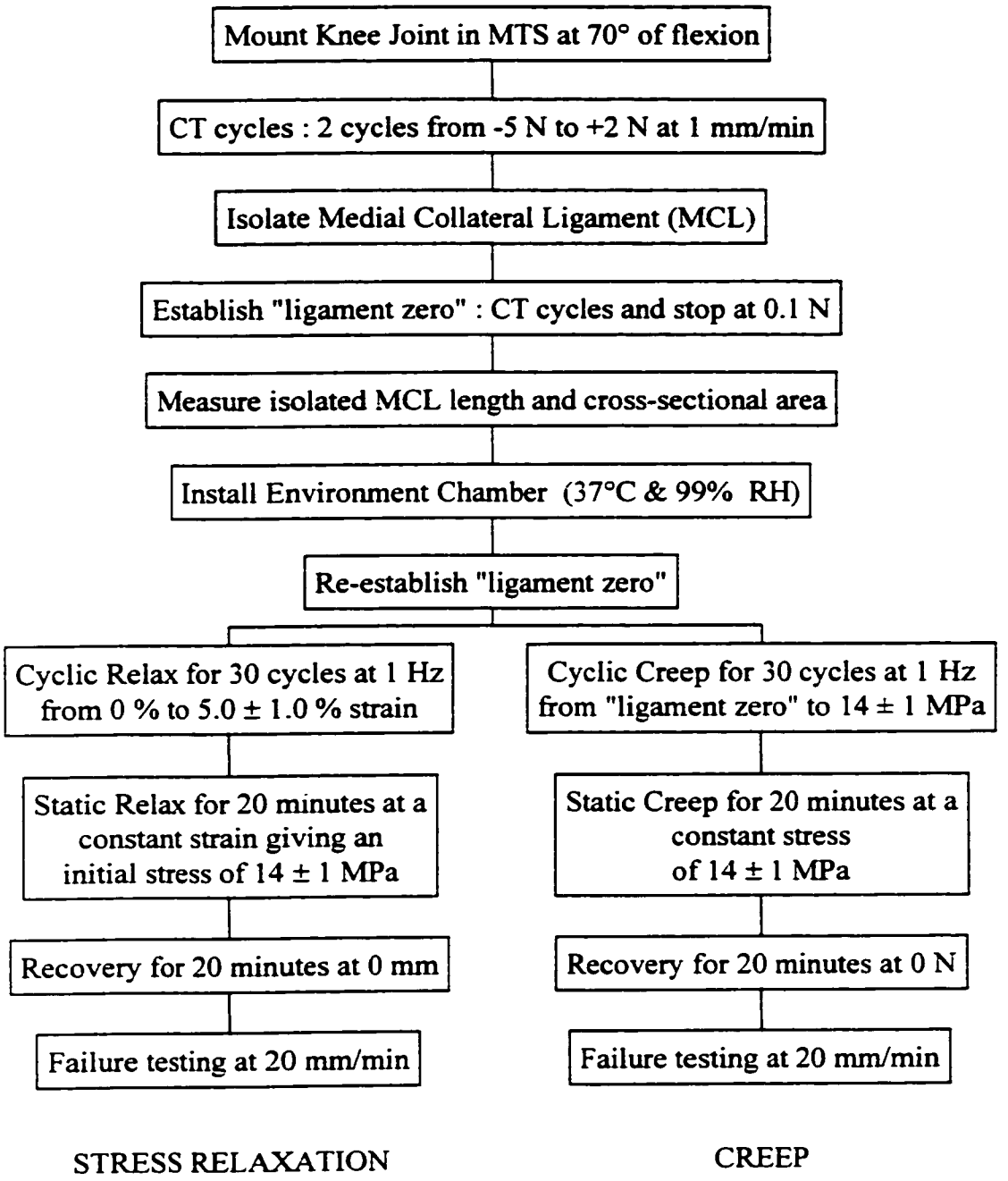

Figure 2.3: Creep and Stress Relaxation Test Protocol for MCLs Tested at 14 MPa

n=8 in both groups (stress relaxation and creep)

"CT" is compression-tension and "RH" is relative humidity

the isolated MCL. Additional compression-tension cycles were then performed. The second cycle ended at 0.1 N tension to establish "ligament zero". The MCL length was measured at the transition between periosteal and palpable ligamentous tissue at both femoral and tibial insertions using Vernier calipers. Vernier calipers were accurate to 0.01 mm; visual estimates of transition areas were accurate to roughly 0.1 mm. In order to accommodate the area caliper, a small portion of the medial femoral condyle was removed lateral to the MCL and distal to the femoral MCL insertion. Then, 5 N tension was applied and maintained during the measurement of the cross-sectional area of the midsubstance of the MCL using an area caliper (accurate to 0.01 mm^2) as previously described (134). A custom built environment chamber (37°C and 99% relative humidity) was installed around each test specimen (158), and compression-tension cycles were performed to re-establish "ligament zero".

Subsequent to "ligament zero" being established, relaxation specimens were subjected to a strain-based test whereas creep specimens were subjected to a stress-based test over a similar time period. In each cyclic creep test, the MCL was loaded for 30 cycles at 1 Hz from "ligament zero" to 14 ± 1 MPa. For the subsequent static creep test, each MCL was then loaded immediately to 14 ± 1 MPa and held in load control for 20 minutes. That ligament was next allowed to recover at 0 N for 20 minutes while its length was recorded by the MTS. The MCL was finally elongated to failure at 20 mm/min. In each cyclic relaxation test, the MCL was elongated to 30 cycles at 1 Hz from 0 % strain to 5.0 ± 1.0 % strain. For the static relaxation test, each MCL was then elongated to

5.0 ± 1.0 % strain (an initial stress of 14 ± 1 MPa) and held in length control for 20 minutes. That ligament recovered at 0 mm for 20 minutes and, finally, was elongated to failure at 20 mm/min.

In order to examine the creep and relaxation at another toe region stress and to provide samples for crimp analysis, tests at 4.1MPa (n=3) had a modified protocol (Figure 2.4). Subsequent to "ligament zero" being established, both relaxation and creep specimens were subjected to cyclic creep (30 cycles at 1 Hz from "ligament zero" to 4.1 ± 0.2 MPa). The relaxation specimens then underwent static relaxation at a constant strain corresponding to an initial stress of 4.1 ± 0.2 MPa. The creep specimens, on the other hand, underwent static creep at a constant stress of 4.1 ± 0.2 MPa. Three samples (in addition to the 8 already described) were tested at 14 MPa to confirm that the static stress relaxation functions obtained after cyclic creep (instead of cyclic relaxation) were within the range of the static relaxation functions determined when cyclic relaxation was used. Measuring static relaxation after cyclic creep allowed these samples (n=3 at 4.1 MPa and n=3 at 14 MPa) to be included in the groups for histological analysis of ligament crimp patterns (Chapter 3).

The stress relaxation, g(t), and creep, j(t), functions were determined by least squares curve fitting to the normalized static experimental stress relaxation and creep data. At 14 MPa, curve fits were performed on the data from eight stress relaxation tests and seven creep tests (one creep specimen was excluded because of a fault in the test

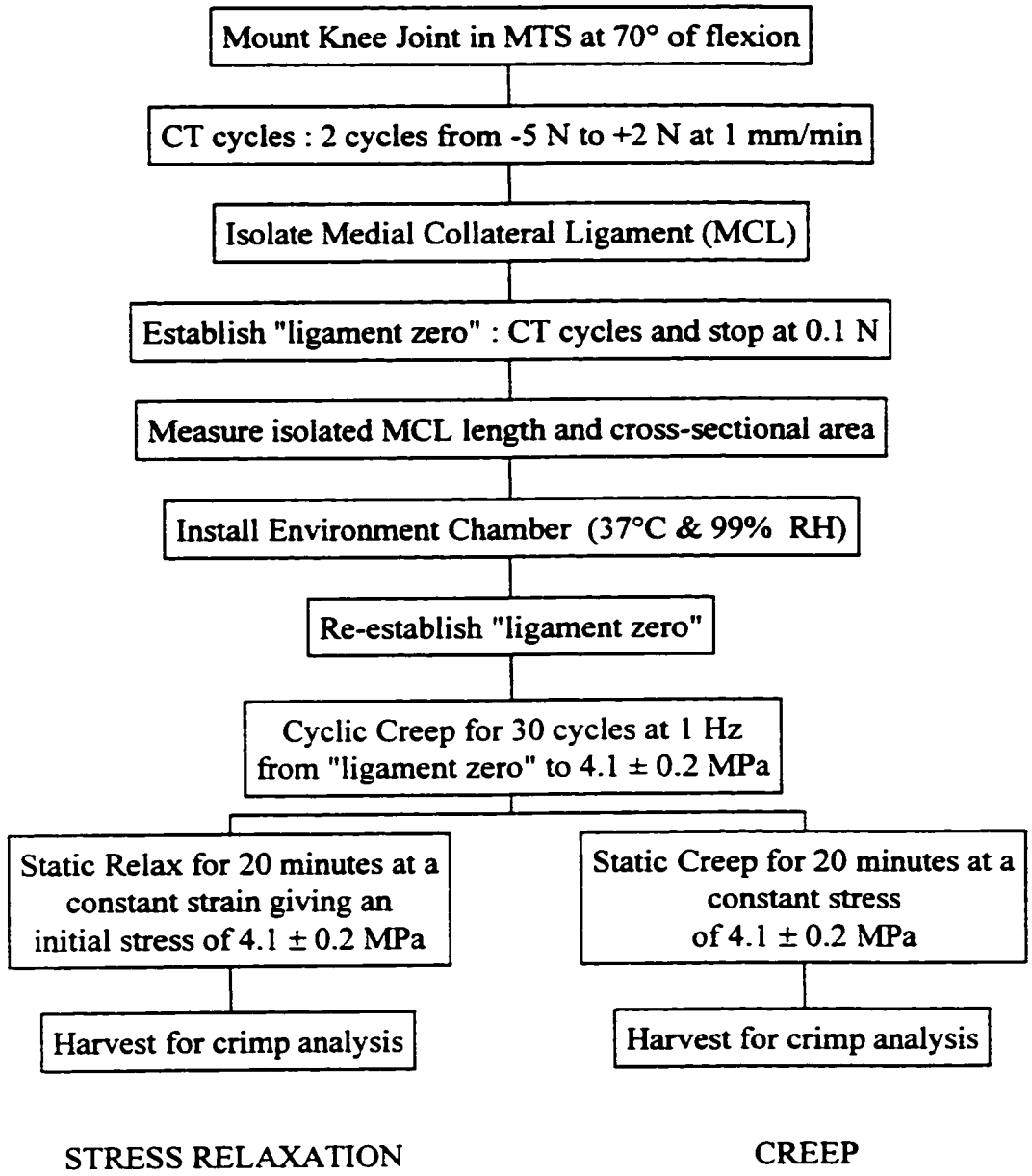

Figure 2.4: Creep and Stress Relaxation Test Protocol for MCLs Tested at 4.1 MPa

n=3 in both groups (stress relaxation and creep)

"CT" is compression-tension and "RH" is relative humidity

procedure). At 4.1 MPa, curve fits were performed on all three pairs of specimens. Generalized standard linear solid modelling was used (63):

$$g(t) = A_1 e^{-A_2 t} + A_3 e^{-A_4 t} + A_5 \quad [8]$$

$$j(t) = B_1 e^{-B_2 t} + B_3 e^{-B_4 t} + B_5 \quad [9]$$

The fitted stress relaxation function [8] was then inverted using Laplace transformations and equation [7] to determine the predicted creep function, $\hat{j}(t)$, which was of the same form (two exponential terms and one constant term). The same procedure was performed on the fitted creep function [9] to find the predicted stress relaxation function, $\hat{g}(t)$. The actual and predicted function values at infinity were compared using Student's t-tests (significance at $p=0.05$). Strain, ε, was defined as the deformation of the MCL divided by the undeformed MCL length, and stress, σ, was defined as the recorded force divided by the total MCL cross-sectional area. The actual and predicted stresses and strains were compared using Student's t-tests (significance at $p=0.05$).

2.2.2 Model

The simple model that includes fibre recruitment and fibre creep is based on several assumptions. The "ligament" has rectangular cross-section: uniform thickness, T, and breadth, b (Figure 2.5). Properties are constant across the thickness of the ligament and crimp is assumed to increase linearly from a minimum at one side of the breadth (λ_L) to a maximum at the other (λ_R). Fibres only carry load after they have been straightened; thus, fibres take up load as the ligament is stretched, starting from the side of minimum

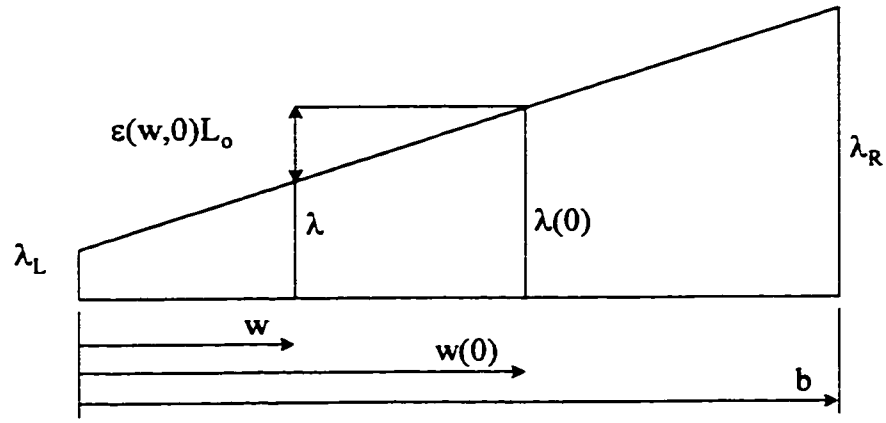

Figure 2.5: Schematic of Model Ligament at time equals zero

"b" is breadth, "w" is width, "λ" is stretch, "L_o" is initial length and "ε" is strain

crimp. A load is applied to the model which recruits only some of the fibres across the breadth.

At time equal to zero (t = 0), the stretch, $\lambda(0)$, and the width of recruited fibres, w(0), are related using geometry.

$$\frac{\lambda(0)-\lambda_L}{w(0)}=\frac{\lambda_R-\lambda_L}{b} \qquad [10]$$

$$\lambda(0)-\lambda_L=\left(\frac{\lambda_R-\lambda_L}{b}\right)w(0) \qquad [10']$$

The strain in the width of recruited fibres is found relating the stretch, λ and the width, w, (L_o = MCL initial length).

$$\frac{\varepsilon(w,0)L_o}{w(0)-w}=\frac{\lambda(0)-\lambda_L}{w(0)} \qquad [11]$$

$$\varepsilon(w,0)=\frac{\lambda_R-\lambda_L}{bL_o}(w(0)-w) \qquad [11']$$

The strain in the fibres is related to the stress using linear viscoelasticity. Fibres only begin to creep after they are straightened (uncrimped) (Figure 2.6). The fibre creep compliance, J(t), is modeled by the inverse of the stress relaxation function from experiment, $\hat{j}(t)$, and the estimated fibre modulus, E_F. Thus, the stress relaxation is taken to be the behaviour of a discrete group of fibres recruited at the applied strain.

$$\sigma(w,0)=\frac{\varepsilon(w,0)}{J(0)} \quad \text{where} \quad J(t)=\frac{\hat{j}(t)}{E_F} \qquad [12] \text{ and } [13]$$

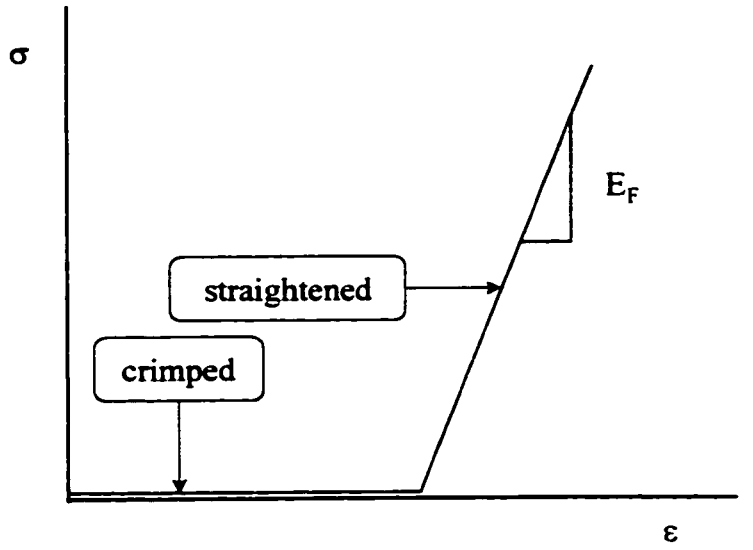

Figure 2.6: Idealized Fibre Stress-Strain Curve

"σ" indicates stress, "ε" indicates strain, and "E_F" indicates fibre modulus

The force is related to the stress by integrating over the applicable cross-section.

$$F = \int_0^{w(0)} \sigma(w,0) T dw = \int_0^{w(0)} \frac{\varepsilon(w,0)}{J(0)} T dw \qquad [14]$$

$$F = \int_0^{w(0)} \frac{(\lambda_R - \lambda_L)T}{bL_o} \left(\frac{w(0) - w}{J(0)} \right) dw \qquad [14']$$

Equation [14''] can be solved for w(0) because the applied force was constant throughout the static creep test. The force and geometry parameters were constant and the creep compliance function [13] was evaluated at the appropriate time.

$$F = \frac{(\lambda_R - \lambda_L)T}{bL_o} \left[\frac{w(0)^2}{2J(0)} \right] \qquad [14'']$$

In the small time step which occurs immediately after loading (from t = 0 to t = Δt), the fibres initially loaded creep, an increase in extension occurs and thus more fibres are recruited to load-bearing. Stress is redistributed among all the fibres now bearing load. The overall load does not change from beginning to end of the time step. At the end of the first time step, t = Δt, the initial and creep strain are as follows (Figure 2.7).

$$\varepsilon(w, \Delta t) = \varepsilon(w,0) + \varepsilon_C(\Delta t) \qquad [15]$$

$$\varepsilon(w, \Delta t) = \frac{\lambda_R - \lambda_L}{bL_o} (w(\Delta t) - w) \qquad [15']$$

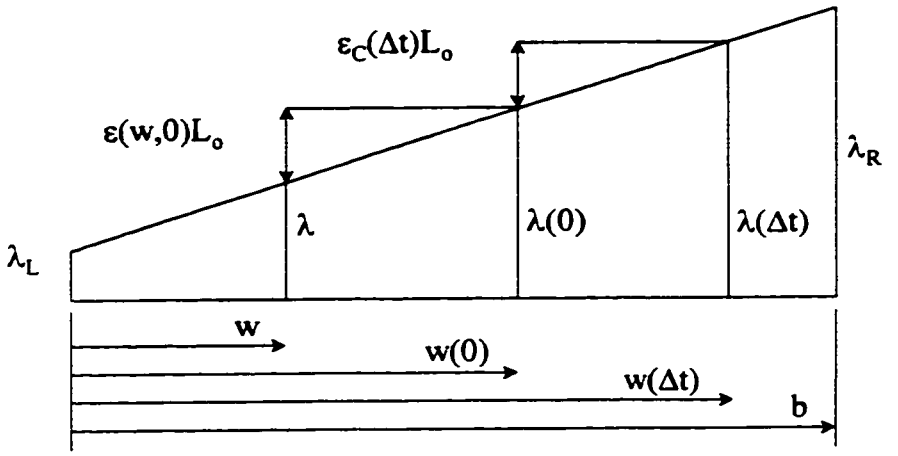

Figure 2.7: Schematic of Model Ligament at time equals Δt

"b" is breadth, "w" is width, "λ" is stretch, "L_o" is initial length and "ε" is strain

The group of fibres initially loaded, from 0 to w(0), creep with J(Δt); whereas, those recruited during the time step, from w(0) to w(Δt), are governed by J(0).

$$\text{For } 0 \rightarrow w(0) \qquad \sigma(w,\Delta t) = \frac{\varepsilon(w,\Delta t)}{J(\Delta t)} \qquad [16]$$

$$\text{For } w(0) \rightarrow w(\Delta t) \qquad \sigma(w,\Delta t) = \frac{\varepsilon(w,\Delta t)}{J(0)} \qquad [17]$$

The force is again calculated with integration and direct solution for w(Δt) is possible.

$$F = \int_0^{w(0)} \frac{(\lambda(\Delta t) - \lambda_L)\Pi}{J(\Delta t)L_o}\left(\frac{w(\Delta t) - w}{w(\Delta t)}\right)dw + \int_{w(0)}^{w(\Delta t)} \frac{(\lambda(\Delta t) - \lambda_L)\Pi}{J(0)L_o}\left(\frac{w(\Delta t) - w}{w(\Delta t)}\right)dw \qquad [18]$$

$$F = \int_0^{w(0)} \frac{(\lambda_R - \lambda_L)\Pi}{bL_o}\left(\frac{w(\Delta t) - w}{J(\Delta t)}\right)dw + \int_{w(0)}^{w(\Delta t)} \frac{(\lambda_R - \lambda_L)\Pi}{bL_o}\left(\frac{w(\Delta t) - w}{J(0)}\right)dw \qquad [18']$$

$$F = \frac{(\lambda_R - \lambda_L)\Pi}{bL_o}\left[\left(\frac{1}{2J(0)}\right)w(\Delta t)^2 + \left(-\frac{w(0)}{J(0)} + \frac{w(0)}{J(\Delta t)}\right)w(\Delta t) + \left(\frac{w(0)^2}{2J(0)} - \frac{w(0)^2}{2J(\Delta t)}\right)\right] \qquad [18'']$$

The increment of creep strain may now be calculated (Figure 2.7).

$$\varepsilon_C(\Delta t) = \frac{(\lambda_R - \lambda_L)}{bL_o}(w(\Delta t) - w(0)) \qquad [19]$$

In fact, the force expression can be parameterized for every nΔt, where n=1 at the end of the first time step. Equation [20] can be solved for w(nΔt), given the constant force during the static creep test.

$$F = \frac{(\lambda_R - \lambda_L)T}{bL_o}\left\{\left[\frac{1}{2J(0)}\right]w(n\Delta t)^2 + \left[\sum_{i=1}^{n} -\frac{w((n-i)\Delta t)}{J((i-1)\Delta t)} + \frac{w((n-i)\Delta t)}{J(i\Delta t)}\right]w(\Delta t) + \left[\sum_{i=1}^{n} + \frac{w((n-i)\Delta t)^2}{2J((i-1)\Delta t)} - \frac{w((n-i)\Delta t)^2}{2J(i\Delta t)}\right]\right\} \quad [20]$$

The increment of creep strain is calculated from sequential time steps.

$$\varepsilon_C(n\Delta t) = \frac{(\lambda_R - \lambda_L)}{bL_o}[w(n\Delta t) - w((n-1)\Delta t)] \quad [21]$$

2.3 Results

2.3.1 Creep and Stress Relaxation

The results for a representative pair of specimens tested at 14 MPa are shown in Figure 2.8. As with all specimens (Appendix 2, Table A2.1), the functions for g(t) and j(t) were fitted to the data with coefficients of determination, r^2, greater than 0.99. None the less, the predicted functions, $\hat{j}(t)$ and $\hat{g}(t)$, were vastly different from the experimental behaviour.

Subsequently, the unknown constants from equations [8] and [9] (A_1 to A_5 and B_1 to B_5) were averaged to produce overall stress relaxation and creep functions at 14 MPa.

$$g_{14}(t) = (0.19 \pm 0.04)e^{(-0.039\pm0.006)t} + (0.16 \pm 0.03)e^{(-0.002\pm0.001)t} + (0.65 \pm 0.06) \quad [22]$$

$$j_{14}(t) = (-0.08 \pm 0.01)e^{(-0.031\pm0.006)t} + (-0.08 \pm 0.01)e^{(-0.003\pm0.001)t} + (1.16 \pm 0.02) \quad [23]$$

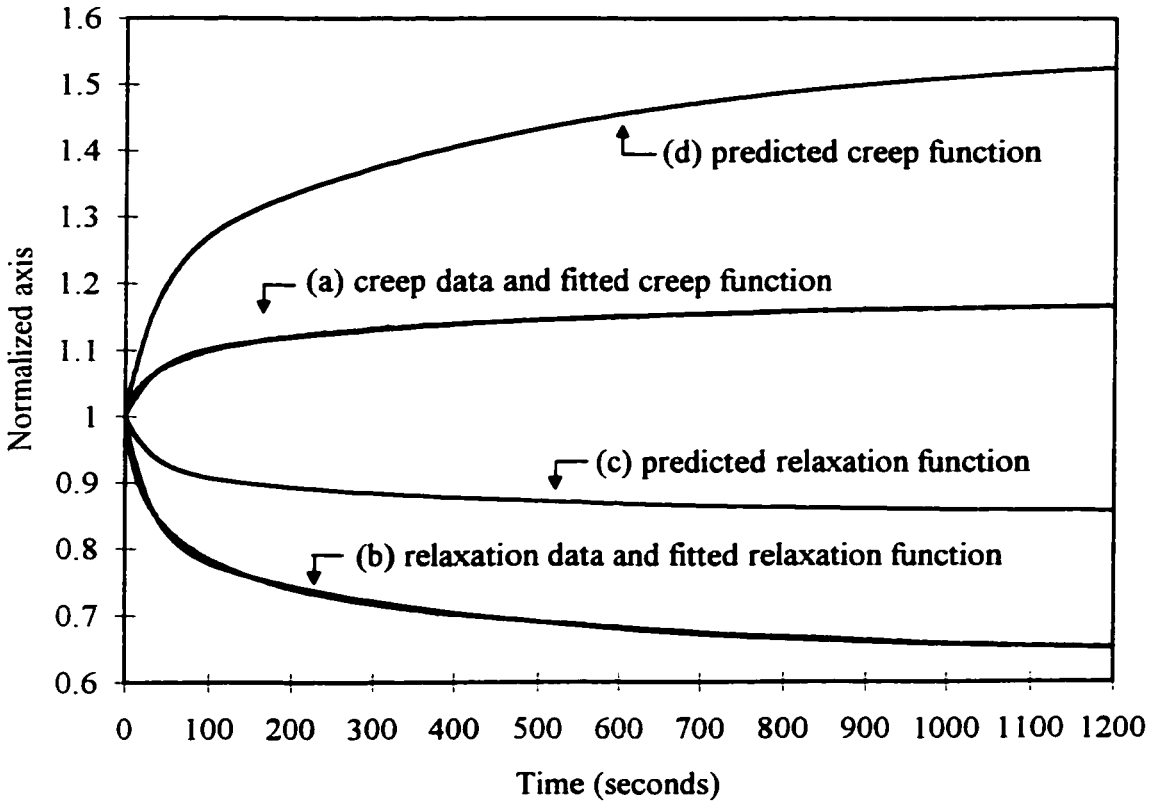

Figure 2.8: Experimental Data, Fitted Functions and Predicted Functions for the Creep and Stress Relaxation of a Representative Pair at 14 MPa

(a) fitted creep function $j_{14}(t) = -0.09e^{-0.031t} - 0.08e^{-0.002t} + 1.17$, r^2=0.997

(b) fitted relaxation function $g_{14}(t) = 0.19e^{-0.034t} + 0.17e^{-0.002t} + 0.64$, r^2=0.997

(c) predicted relaxation function $\hat{g}_{14}(t) = 0.08e^{-0.033t} + 0.06e^{-0.003t} + 0.86$

(d) predicted creep function $\hat{j}_{14}(t) = -0.23e^{-0.028t} - 0.33e^{-0.002t} + 1.56$

As well, the constants of the predicted functions were averaged to produce overall functions.

$$\hat{g}_{14}(t) = (0.08 \pm 0.01)e^{(-0.034 \pm 0.007)t} + (0.06 \pm 0.01)e^{(-0.003 \pm 0.001)t} + (0.86 \pm 0.02) \quad [24]$$

$$\hat{j}_{14}(t) = (-0.23 \pm 0.05)e^{(-0.031 \pm 0.004)t} + (-0.33 \pm 0.09)e^{(-0.002 \pm 0.001)t} + (1.56 \pm 0.14) \quad [25]$$

The stress relaxation data predicted that the creep strain at infinity should be increased 56% from the initial strain, whereas the experimental increase was significantly less at only 16% of the initial, ($p=0.0001$) ($\hat{j}(\infty) = 1.56 \pm 0.14$: $j(\infty) = 1.16 \pm 0.02$; Table 2.1). The corresponding strains at infinity were calculated using QLV (equation [4]). The actual strain, 5.0 ± 0.4 %, was significantly less than the predicted strain, 6.7 ± 1.3 % ($p=0.005$).

The over-prediction of creep using the inverse relaxation function occurred at 4.1MPa. The creep and stress relaxation of a representative pair are shown in Figure 2.9 and all functions are listed in Appendix 2 (Table A2.2). Again, function constants were averaged to determine overall functions.

$$g_{4.1}(t) = (0.35 \pm 0.03)e^{(-0.027 \pm 0.001)t} + (0.31 \pm 0.01)e^{(-0.003 \pm 0.001)t} + (0.34 \pm 0.03) \quad [26]$$

$$j_{4.1}(t) = (-0.20 \pm 0.01)e^{(-0.018 \pm 0.002)t} + (-0.25 \pm 0.02)e^{(-0.002 \pm 0.001)t} + (1.45 \pm 0.02) \quad [27]$$

$$\hat{g}_{4.1}(t) = (0.18 \pm 0.01)e^{(-0.022 \pm 0.003)t} + (0.13 \pm 0.01)e^{(-0.002 \pm 0.001)t} + (0.69 \pm 0.01) \quad [28]$$

$$\hat{j}_{4.1}(t) = (-0.46 \pm 0.05)e^{(-0.018 \pm 0.001)t} + (-1.55 \pm 0.23)e^{(-0.001 \pm 0.001)t} + (3.01 \pm 0.27) \quad [29]$$

The inverse stress relaxation function at 4.1 MPa predicted a three-fold increase in strain; whereas, the experimental creep function indicated an increase of only 0.45 times

Table 2.1: Comparison of Stress Relaxation and Creep Function Values at Time Infinity and Corresponding Stresses and Strains for 14 MPa Tests

PARAMETER	Creep	Stress Relaxation
Experimental		
σ_o	14.9 ± 0.3 MPa	13.3 ± 0.2 MPa [a]
ε_o	4.3 ± 0.4 %	4.3 ± 0.5 %
$j(\infty)$	1.16 ± 0.02	
$\varepsilon(\infty)$	5.0 ± 0.4 %	
$g(\infty)$		0.65 ± 0.06
$\sigma(\infty)$		8.6 ± 0.9 MPa
Predicted		
$\hat{j}(\infty)$		1.56 ± 0.14 [b]
$\hat{\varepsilon}(\infty)$		6.7 ± 1.3 % [b]
$\hat{g}(\infty)$	0.86 ± 0.02 [b]	
$\hat{\sigma}(\infty)$	12.8 ± 0.4 MPa [b]	

Data are shown as mean ± standard deviation.

"a" indicates significantly different than creep ($p<0.0001$)

"b" indicates significantly different than corresponding experimental value ($p<0.005$)

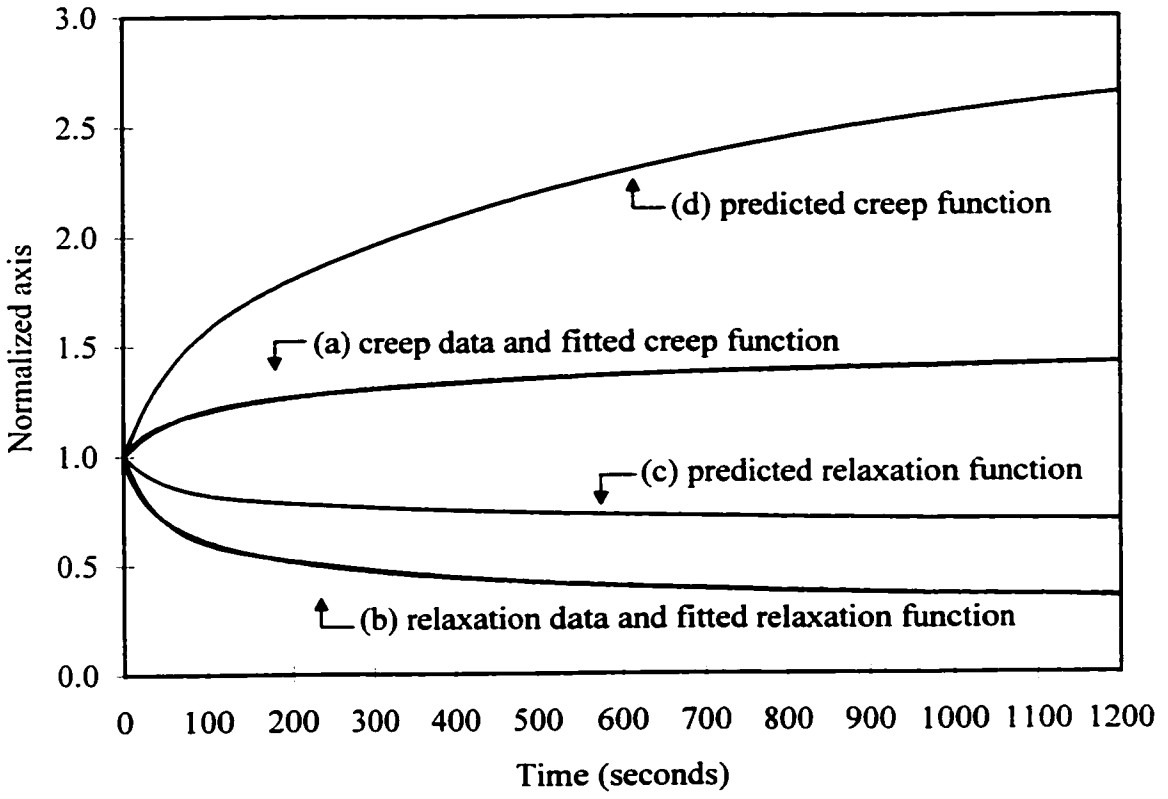

Figure 2.9: Experimental Data, Fitted Functions and Predicted Functions for the Creep and Stress Relaxation of a Representative Pair at 4.1 MPa

(a) fitted creep function $j_{4.1}(t) = -0.20e^{-0.018t} - 0.25e^{-0.002t} + 1.45$, r^2=0.998

(b) fitted relaxation function $g_{4.1}(t) = 0.35e^{-0.027t} + 0.31e^{-0.003t} + 0.34$, r^2=0.998

(c) predicted relaxation function $\hat{g}_{4.1}(t) = 0.17e^{-0.022t} + 0.14e^{-0.002t} + 0.69$

(d) predicted creep function $\hat{j}_{4.1}(t) = -0.46e^{-0.018t} - 1.46e^{-0.001t} + 2.92$

at time infinity ($p=0.0006$) ($\hat{j}(\infty) = 3.01 \pm 0.27$: $j(\infty) = 1.45 \pm 0.02$; Table 2.2). The actual strain, 2.5 ± 0.2 %, was significantly less than the predicted strain, 6.0 ± 0.6 % ($p=0.0005$).

In order to compare the results of the creep and stress relaxation tests, an attempt to produce the same initial point on the static curves was made (Tables 2.1 and 2.2). At 14 MPa, the initial static strains were not significantly different, but the stresses were significantly different (creep being 1.6 MPa higher; $p=0.0001$). This discrepancy was the result of a limitation of our test protocol which, despite our attempts, allowed a slight overshoot of the creep initial stress. If anything this would have biased the experimental results towards a larger creep strain that was closer to the predicted value. At 4.1 MPa, the static initial stresses were not different but the static initial strains were different (creep being 0.3% lower; $p=0.02$). It is unlikely that this small difference in strain would have accounted for the over two-fold difference in between the experimental and predicted values.

2.3.2 Model

Given the false prediction of creep behaviour by the inverse stress relaxation functions as compared with the experimentally measured creep behaviour for both the 14 and 4.1 MPa cases, a model that incorporated fibre recruitment was used to determine if a better prediction was possible. Model performance was tested at 14 and 4.1 MPa using

Table 2.2: Comparison of Stress Relaxation and Creep Function Values at Time Infinity and Corresponding Stresses and Strains for 4.1 MPa Tests

PARAMETER	Creep	Stress Relaxation
Experimental		
σ_o	3.9 ± 0.1 MPa	3.9 ± 0.1 MPa
ε_o	1.7 ± 0.1 %	2.0 ± 0.1 % [a]
$j(\infty)$	1.45 ± 0.02	
$\varepsilon(\infty)$	2.5 ± 0.2 %	
$g(\infty)$		0.33 ± 0.03
$\sigma(\infty)$		1.3 ± 0.1 MPa
Predicted		
$\hat{j}(\infty)$		3.01 ± 0.27 [b]
$\hat{\varepsilon}(\infty)$		6.0 ± 0.6 % [b]
$\hat{g}(\infty)$	0.69 ± 0.01 [b]	
$\hat{\sigma}(\infty)$	2.7 ± 0.1 MPa [b]	

Data are shown as mean ± standard deviation.

"a" indicates significantly different than creep ($p<0.02$)

"b" indicates significantly different than corresponding experimental value ($p<0.0006$)

pairs representative of the overall functions (as shown in Figures 2.8 and 2.9, respectively).

$$j_{14}(t) = -0.09e^{-0.031t} - 0.08e^{-0.002t} + 1.17 \quad [28]$$

$$\hat{j}_{14}(t) = -0.23e^{-0.028t} - 0.33e^{-0.002t} + 1.56 \quad [29]$$

$$j_{4.1}(t) = -0.20e^{-0.018t} - 0.25e^{-0.002t} + 1.45 \quad [30]$$

$$\hat{j}_{4.1}(t) = -0.46e^{-0.018t} - 1.46e^{-0.001t} + 2.92 \quad [31]$$

Constant model parameters are listed in Table 2.3: (a) applied static creep test force, F, (b) MCL initial length, L_o, (c) MCL thickness, T, and (d) MCL breadth, b. The solution must satisfy $w(n\Delta t) < b$; that is, the width of the recruited fibres cannot exceed the breadth of the ligament. Variable parameters were altered to obtain the least-squares fit to the experimental creep data using 10 second time steps to 200 seconds and 100 second time steps to 1200 seconds. The frequency of time steps was increased where the change in strain was the largest. Variation in crimp, $(\lambda_R-\lambda_L)$, was limited to a maximum of 1.73 mm because a nearly extinguished crimp pattern post-creep at 28 MPa has been documented (see Chapter 3). Fibre modulus, E_F, (which was used to calculate fibre creep compliance) had multiple values: (a) initial modulus for creep test, E_F = 609.0 MPa at 14 MPa and E_F = 393.0 MPa at 4.1 MPa, (b) failure modulus of MCL, E_F = 774.2 MPa, and (c) modulus range quoted in literature (100), E_F = 400-1000 MPa (Appendix 3). After E_F was selected, $(\lambda_R-\lambda_L)$ was varied to find the least-squares fit ensuring that $w(1200) < b$.

Table 2.3 : Model Parameter Values for 14 and 4.1 MPa Creep Test Stresses

Model Parameter	**Creep Stress = 14 MPa**	**Creep Stress = 4.1 MPa**
F = static creep test force (N)	59.7	14.2
L_o = MCL initial length (mm)	23.2	23.3
T = MCL thickness (mm)	1.21	1.21
b = MCL breadth (mm)	4.86	4.71
E_F = fibre modulus (MPa)		
(a) initial modulus for creep test	609.9	393.0
(b) MCL failure modulus	774.2	774.2
(c) fibre modulus from literature	400-1000	400-1000

The contribution of fibre recruitment was varied to evaluate model performance at 14 MPa (Figure 2.10). A moderate improvement in the prediction of creep was produced when the fibre modulus was estimated as the initial modulus for the creep test (E_F = 609.9 MPa). The model performance was only moderately improved compared to the inverse stress relaxation function. The creep behaviour was predicted when the fibre modulus was taken to be the failure modulus of the MCL (r^2=0.99 when E_F = 774.2 MPa). The model demonstrates that the width of the recruited fibres increased with each time step (Figure 2.11a). This progressive recruitment redistributed the loading on the fibres; for example, the stress at the location w = 0 decreased with each time step (Figure 2.11b). Similar predictions were found when fibre modulus values were within the range quoted from literature starting at 730 MPa (Table 2.4). The width of the recruited fibres decreased as the fibre modulus increased.

Similar model performance was documented at 4.1 MPa (Figure 2.12). When the fibre modulus was estimated as the initial modulus for the creep test (E_F = 393.0 MPa), the prediction was slightly improved compared to the inverse stress relaxation function. When the fibre modulus equaled the failure modulus of the MCL (E_F = 774.2 MPa), the prediction of creep was greatly improved (r^2=0.98). Over time, the recruited width increased and the stress on the fibres initially recruited decreased (Figure 2.13). Similar best fit model predictions were achieved using fibre moduli within the range from the literature (100) starting at 680 MPa (Table 2.4).

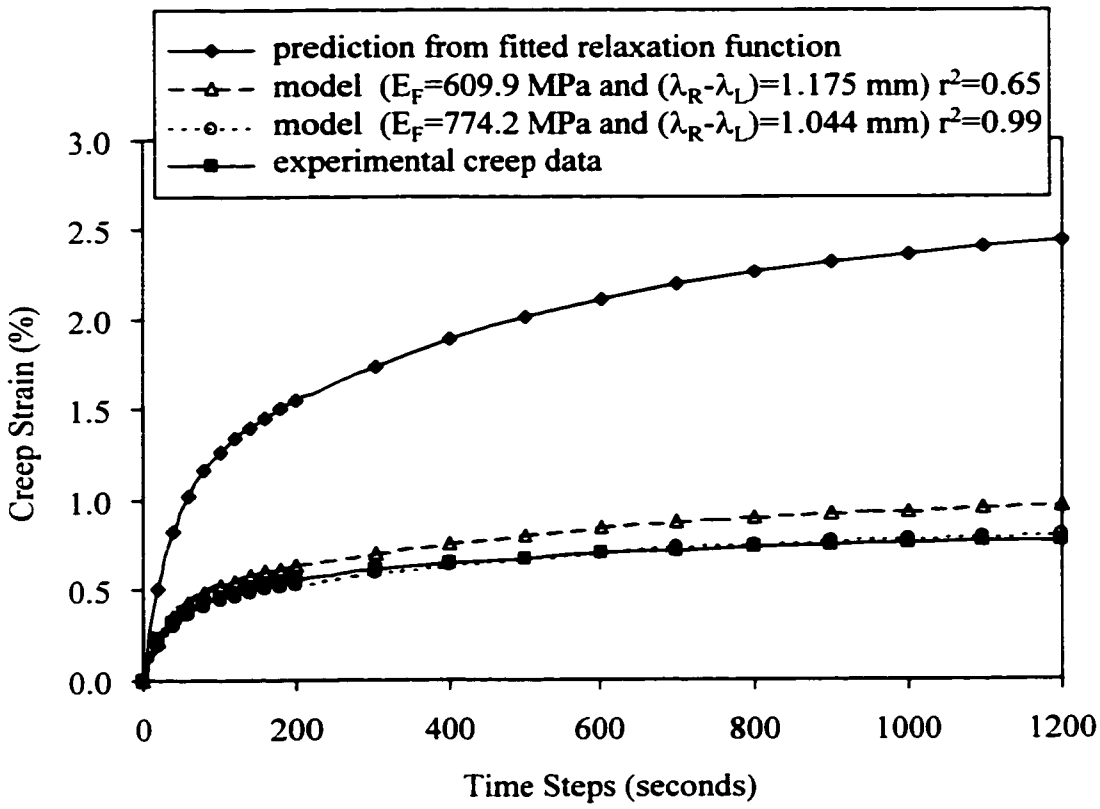

Figure 2.10: Model Predictions for Creep Behaviour at 14 MPa

"E_F" indicates fibre modulus and "(λ_R-λ_L)" indicates variation in crimp

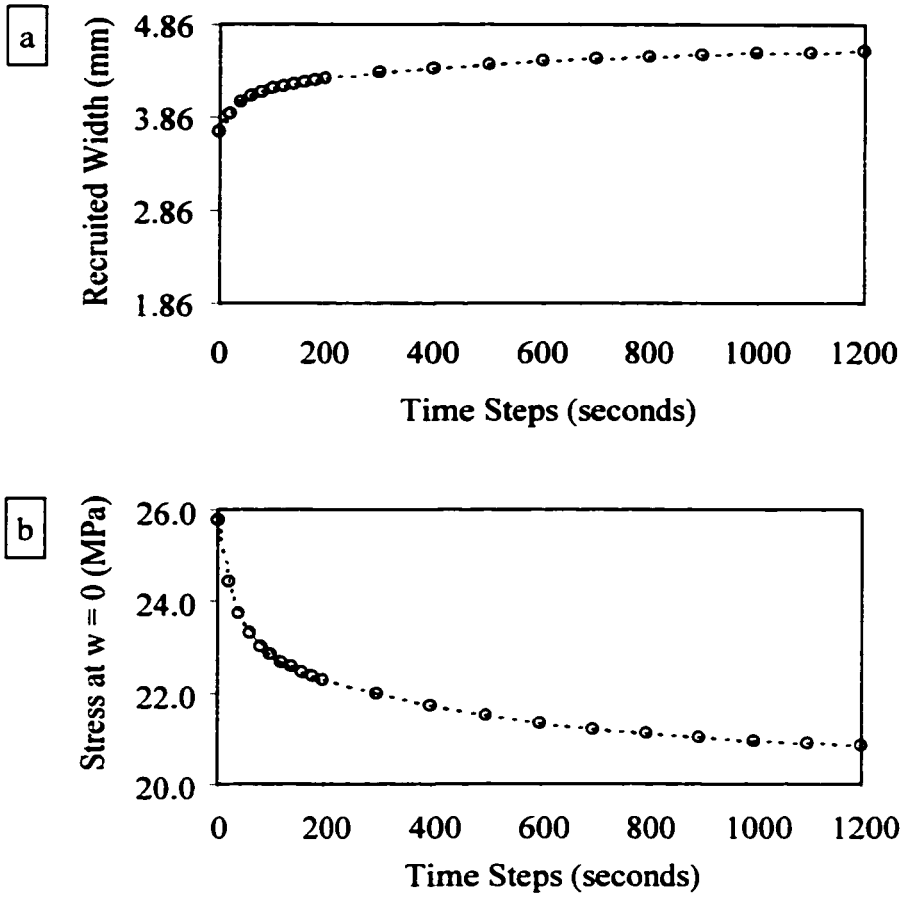

Figure 2.11: Model Properties for Creep Behaviour at 14 MPa with Fibre Modulus, E_F, = 774.2 MPa and Variation in Crimp, (λ_R-λ_L), = 1.044 mm

(a) Increase in Width of Recruited Fibres (b) Decrease in Stress at w = 0

Table 2.4: Best Fit Model Predictions at Different Fibre Modulus Values

Creep Stress (MPa)	**Fibre Modulus [E_F] (MPa)**	**Variation in Crimp [λ_R-λ_L] (mm)**	**Recruited Width [w(1200)] (mm)**	**Ratio of Recruited Width to Breadth [w(1200)/b]**	**r^2**
14	730	0.984	4.86	1.00	0.99
14	**774.2**	**1.044**	**4.58**	**0.94**	**0.99**
14	800	1.078	4.43	0.91	0.99
14	900	1.213	3.94	0.81	0.99
14	1000	1.348	3.54	0.73	0.99
4.1	680	0.445	4.71	1.00	0.98
4.1	700	0.458	4.57	0.97	0.98
4.1	**774.2**	**0.507**	**4.13**	**0.88**	**0.98**
4.1	800	0.524	3.99	0.85	0.98
4.1	900	0.589	3.55	0.75	0.98
4.1	1000	0.655	3.20	0.68	0.98

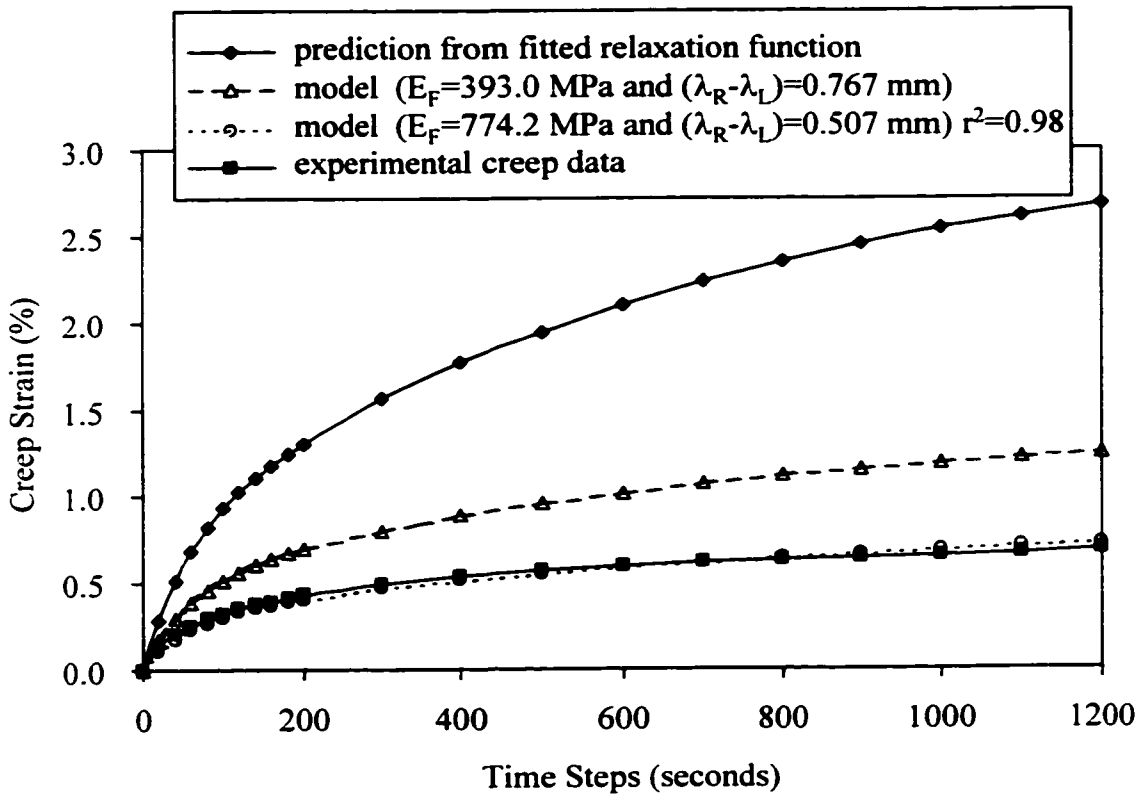

Figure 2.12: Model Predictions for Creep Behaviour at 4.1 MPa

"E_F" indicates fibre modulus and "(λ_R-λ_L)" indicates variation in crimp

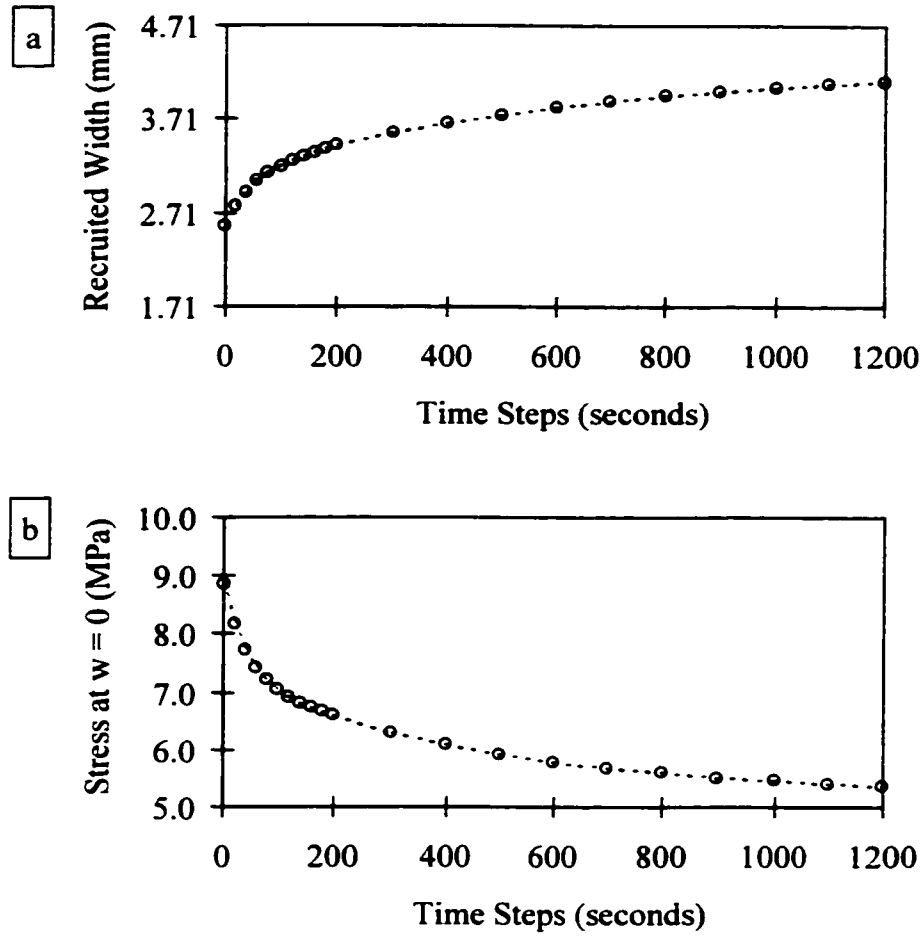

Figure 2.13: Model Properties for Creep Behaviour at 4.1 MPa with Fibre Modulus, E_F, = 774.2 MPa and Variation in Crimp, (λ_R-λ_L), = 0.507 mm

(a) Increase in Width of Recruited Fibres (b) Decrease in Stress at w = 0

2.4 Discussion

2.4.1 Creep and Stress Relaxation

These results are the first to show that the creep and stress relaxation functions of rabbit MCL at low stresses were significantly different. The values of the functions evaluated at time infinity were not inversely proportional. Ligament creep was significantly less than that predicted by stress relaxation. These data suggest that inferences about the creep behaviour of ligaments cannot be made from previously documented stress relaxation behaviour.

Fung (1993) speculated that creep is fundamentally more nonlinear than relaxation, and that the microstructural processes taking place in a material undergoing creep could be quite different from those taking place in a material undergoing relaxation. Based on the known behaviours of tendon and ligament, which have been shown to feature collagen fibre recruitment at increasing loads (152), it can be speculated that progressive recruitment of fibres would occur during creep while such recruitment would be unlikely to occur during stress relaxation. Different collagen fibres in the same tissue have different uncrimped lengths; thus, as the tissue is elongated, fibre bundles will be recruited or stretched out progressively (152,165). Since static stress relaxation is performed at a constant strain, the stress relaxation response may be that of a discrete group of fibres that are recruited at the prescribed constant elongation. However, static creep is performed at constant stress, thus, allowing increasing strain. Hence, the creep response may be that of fibres that are recruited initially and other fibres recruited

progressively. The question therefore arises as to how much the creep of fibres, on the one hand, and the recruitment of fibres, on the other, contribute to the time varying function of a tissue under constant stress?

Interestingly, Chimich et al. (1992) showed that stress relaxation can be affected by water content. In that experiment, a substantial difference in tissue water content, 70% (in PBS) versus 52% (in 25% sucrose), corresponded to a substantial difference in the cyclic relaxation of normal adolescent rabbit MCL, 45% versus 15%, respectively. This result showed that a major alteration in water content can influence viscoelastic behaviour. There is, therefore, the possibility that differences in water content could help explain the current results. However, during viscoelastic tests, it appears that only minor reductions in water content occur. In the cyclic relaxation tests recorded by Chimich et al. (1992) only one of the four cases showed a statistically significant reduction in water content (4%) compared to uncycled controls. Similarly, only a 4% decrease in water content was observed after cyclic followed by static creep testing at 4.1 MPa (compared to pre-test controls; Chapter 3). Furthermore, MCLs from additional animals were tested at 14 MPa to assess water content after static creep testing (57.8 ± 1.9%; n=3) and after static relaxation testing (61.0 ± 0.5%; n=2). The water content after static creep at 14 MPa was only 8% less than pre-test controls and was not significantly different than the water content after static relaxation. Additionally, Hannafin and Arnoczky (1994) documented only a 2% reduction in water content of canine flexor tendons subject to cyclic creep and only a 5% reduction in water content subject to static creep compared to

no-load controls. Thus, the small changes in water content in all the above viscoelastic tests, and the small differences between the creep and relaxation test protocols do not appear to be sufficient to explain the distinct difference noted here between creep and stress relaxation behaviour.

The use of the QLV theory is widely accepted for modelling ligament and tendon behaviour (165). The mathematically simple formulations of creep and stress relaxation used here were well correlated to the data (r^2>0.99) and produced predicted functions with similar terms. However, with simple stress relaxation functions, premature cut-off of the experiment can lead to erroneous limiting values (63). Static testing for only twenty minutes may therefore be a limitation of the study. However, when $\hat{j}(t)$ and $\hat{g}(t)$ were compared to j(t) and g(t), the predicted functions were vastly different from the experimental behaviour (Figure 2.8 and 2.9). This confirms the conclusion that creep and stress relaxation are different phenomena.

2.4.2 Model

This simple model that incorporated fibre recruitment and creep of recruited fibres was able to predict the experimental creep behaviour of the MCL and was a substantial improvement over the prediction from the inverse stress relaxation function alone. Despite the simplicity of the assumptions in the model, this model demonstrates categorically that fibre recruitment is a major factor accounting for the difference between creep measured experimentally and that predicted from relaxation data. In cases of partial

recruitment, the modulus for the fibres actually loaded, rather than a value averaged for the total cross-sectional area is essential for accurate predictions of creep. Additionally, the model demonstrates that stress redistribution occurs, reducing the stress in the fibres loaded by the initial application of force. The progressive recruitment of fibres and the corresponding redistribution of stress over a larger number of fibres served to minimize creep.

On initial loading, across the ligament cross-section some fibres are straightened and others remain crimped. The model assumption was that fibres only creep after they have been straightened. Prediction was poor using the initial modulus for the creep test, which is an underestimate of the actual fibre modulus because it is an averaged value for the total cross-section including both straightened and crimped fibres. The best fit prediction of ligament creep was achieved when the fibre modulus was taken as the MCL failure modulus which is the result of straightening all of the fibres in the cross-section (assuming limited contribution from the matrix). All fibres in the cross-section were assumed to be loaded at "failure", and this modulus applied equally to all fibres. In addition, the best fit was also obtained using other values of fibre modulus that were within the range of the collagen fibre modulus quoted in the literature (100). Adjustments to other model assumptions (e.g. area geometry, initial crimp distribution) could also have helped in the final convergence of model to experiment.

Because the purpose of this model was to demonstrate that creep of progressively recruited fibres could account for the differences between creep and inverse stress

relaxation behaviour, only a simple fibre recruitment pattern was required. The straightening of fibres in the present model was based on a linear distribution of crimp along the breadth of an idealized ligament of rectangular cross-section with uniform properties along the thickness. The straightening of fibres in parallel fibred tissue subjected to uniaxial strain has previously been modeled in a more complex fashion using probability density functions of fibre initial lengths: normal or Gaussian distributions (40,41,97,100) and Weibull distribution (82). In all these models the loading assumption was that fibres only carry load after they are straightened. Different constitutive equations were then used to represent the mechanical behaviour of the straightened fibres. For the case of ligaments and tendons, the constitutive equations were directly assumed linear elastic (40,100) or reduced to linear elastic from generalized strain energy expressions (82,97). In two cases, linear elastic models were changed to viscoelastic models by changing the constitutive equations of fibres to linear viscoelastic expressions (41,96). The present model is similar because fibre creep occurred only when the fibres were straightened and fibre creep behaviour was linear viscoelastic even though the process of fibre recruitment was simplified. This is a nonlinear structural model in which the nonlinearity is created by the progressive recruitment of the fibres. Our data published in Thornton et al. (1997) was used by Lakes and Vanderby (1999) to show that a phenomenological nonlinear model was also predictive.

The advantage of the structural model presented here was that a new understanding of fibre recruitment during creep was gained. This model assumed that

stress relaxation behaviour was that of a discrete group of fibres recruited at the applied deformation. Because deformation does not change over the course of the test, the measured behaviour was that of only these initially recruited fibres. Thus, the inverse of this stress relaxation function was the creep function of a discrete group of fibres with no contribution from progressive recruitment. The crimp patterns of MCL subjected to relaxation tests were similar comparing the percent crimped areas of sections harvested at the start of the static relaxation test and at the end of the static relaxation test for both 4.1 and 14 MPa initial stresses (see Chapter 3). The crimp patterns of MCL subjected to creep testing had significantly different crimp patterns pre-creep and post-creep at both 4.1 and 14 MPa. These data support the assumption that stress relaxation behaviour is that of initially loaded fibres without progressive fibre recruitment.

The model presented here does not include parameters for water exudation out of the matrix during creep. Lanir (1983) and Hurschler et al. (1997) formulated models that included a hydrostatic pressure term for the contribution of a hydrated matrix. The results of Chen et al. (1995) in which pressure in a tendon during deformation was small compared to stress was used to justify a negligible pressure in the uniaxial tension case of the model in Hurschler et al. (1997).

To summarize, this was the first investigation to demonstrate that experimental creep behaviour of ligament was significantly different than the creep behaviour predicted using the inverse function of the experimental stress relaxation behaviour. Using the novel approach of modeling fibre creep with the inverse stress relaxation function and

then incorporating fibre recruitment, the experimental creep behaviour of ligament was accurately predicted. Clearly, fibre recruitment is an important consideration for both experimental and theoretical investigations of the mechanical properties of ligament. This unique approach also revealed that fibre recruitment was important for determining ligament stress because fibre modulus was underestimated if the total cross-sectional area was used (both crimped and straightened fibres together). In addition to all these implications for *in vitro* studies of ligament, fibre recruitment is likely key to understanding how ligaments work *in vivo*. Collagen fibre recruitment may be functionally important in helping ligaments resist creep at functional stresses. The resulting minimization of creep may be useful for preventing fatigue of tissues and loss of joint stability during long term activities.

CHAPTER 3

CREEP BEHAVIOUR AND CREEP MECHANISMS OF NORMAL LIGAMENTS

3.1 Introduction

The creep behaviour of ligament was shown previously to be predicted when the creep of collagen fibres (inverse stress relaxation function) was incorporated with the progressive recruitment of collagen fibres. Fibre recruitment was implicated as a mechanism of creep in normal ligament and this merited further investigation. Collagen fibres of ligament have a characteristic crimp pattern. When examined using polarized light microscopy, a regular undulating wave-form, or crimp, is revealed (43). The stress-strain curve was descriptively related to crimp pattern by Viidik (1972): the toe region represents the straightening out of crimp as the collagen fibres are recruited and the linear region represents the completion of recruitment and straightening (Figure 3.1). Therefore, crimp is an index of collagen fibre recruitment. In the current study, crimp patterns were not only described but also the percent crimped area was quantified as a measurement of fibre recruitment during creep. The hypothesis was that collagen fibres would be recruited during creep and that the percent crimped area would decrease post-creep when compared to pre-creep values. In addition, the percent crimped area

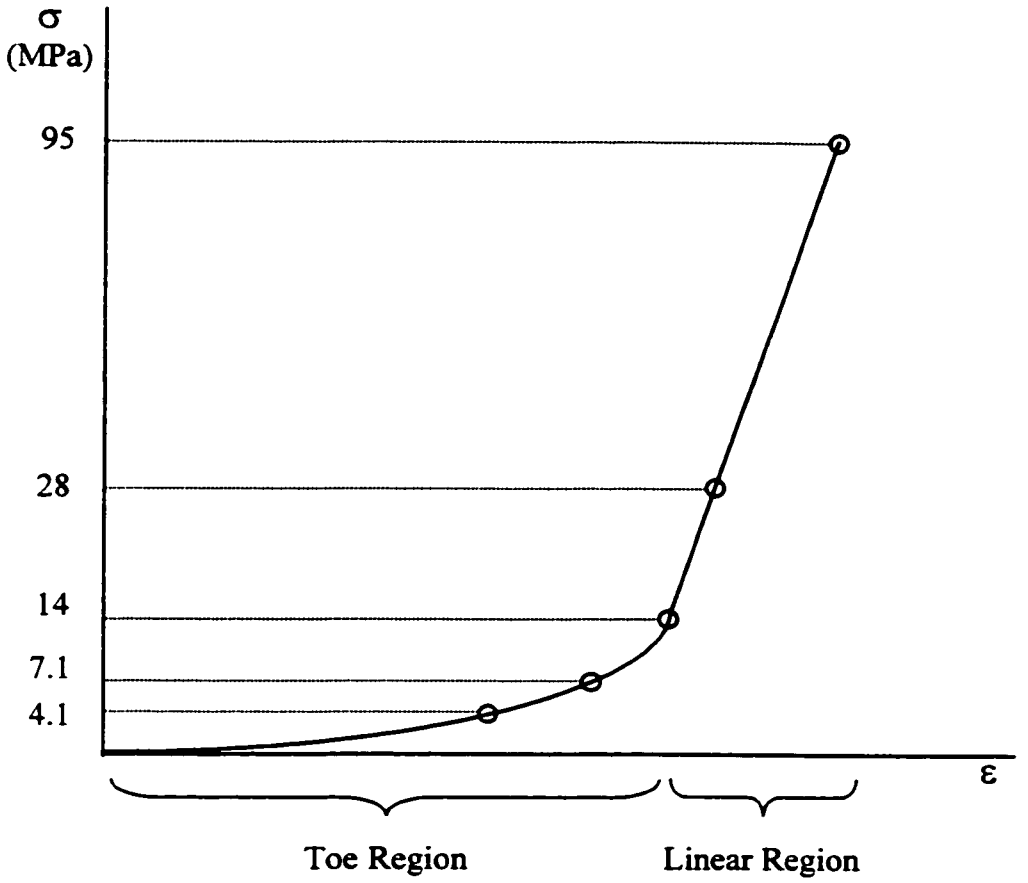

Figure 3.1: Schematic of a Typical Rabbit MCL Stress-Strain Curve

"σ" indicates stress and "ε" indicates strain

4.1 MPa and 7.1 MPa are in the toe region of the stress-strain curve.

14 MPa is at the transition between the toe and linear regions.

28 MPa is in the linear region.

pre-relaxation was expected to be similar to the percent crimped area post-relaxation because strain does not change in a relaxation test.

Before the crimp analysis was performed, baseline creep behaviour of the normal MCL required quantification. Given the previously described relationship between crimp and the stress-strain curve, creep was measured at stresses in the toe and linear regions (Figure 3.1). Additionally, water content of ligament was expected to decrease as a result of creep testing (69). The creep tests involved both cyclic creep and static creep components and assumed that creep test order would not affect the creep strain.

Aim 1. To quantify the creep behaviour and water content changes of normal skeletally mature rabbit MCL over a range of stresses: 4.1 and 7.1 MPa are in the toe region of the stress-strain curve, 14MPa is at the transition between the toe and linear regions, and 28 MPa is well into the linear region.

Aim 2. To determine the differences in cyclic and static creep when the test order is inverted and assess if total creep (cumulative result of serial cyclic and static creep) is equivalent.

Aim 3. To assess the alteration in the crimp pattern pre-creep and post-creep, and pre-relaxation and post-relaxation to investigate the role of fibre recruitment during creep and the absence of fibre recruitment during relaxation.

3.2 Methods

3.2.1 Normal MCL Creep and Water Content

In order to assess the baseline relationship between creep behaviour and creep test stress for normal rabbit MCLs, four different stresses were selected. No one has yet studied the creep behaviour of normal knee ligaments over a range of stresses which may be important considering that ligaments have been shown to be subjected to a range of loads depending on the activity performed (77). The creep test stresses selected were in the toe and linear regions of a typical normal skeletally mature rabbit MCL stress-strain curve (Figure 3.1): 4.1 MPa and 7.1 MPa were in the toe region of the curve, 14 MPa was at the transition between the toe and linear regions and 28 MPa was well into the linear region. The MCLs of 58 normal skeletally mature (one-year-old) female New Zealand White rabbits were assigned to groups according to the schedule listed on Table 3.1. From 45 of these rabbits only one MCL per rabbit was used and the MCL from the contralateral limb was used in a different study. From the other 13 rabbits, both MCLs were used with the intent of avoiding pairing whenever possible; thus, pairing is shown on Table 3.1 whenever more that one pair is in the groups being compared. If one looks at only those specimens included in the creep analysis, the distribution was as follows: 4.1 MPa (n = 7), 7.1 MPa (n = 6), 14 MPa (n = 9) and 28 MPa (n = 6). The 14 MPa samples included the 7 samples from the creep and relaxation study (Chapter 2) and 2 samples for crimp analysis. In the other groups for creep analysis, 6 or 7 samples including those for crimp analysis were assigned to the respective groups and pairing was

Table 3.1: Normal MCLs and Designated Test Groups

Group	Creep Analysis	Water Content	Crimp Analysis
Section 3.2.1			
4.1 MPa	n=7	n=4 post-creep	n=2 post-creep^
7.1 MPa	n=6*	n=6 post-recovery	
14 MPa	n=9		n=2 post-creep
28 MPa	n=6*	n=4 post-recovery	n=2 post-creep
pre-test		n=6 pre-test	
28 MPa discontinuous	n=6		n=2 post-creep
4.1 MPa recovery	n=7	n=5 post-recovery	
14 MPa water		n=3 post-creep	
14 MPa water		n=2 post-recovery	
14 MPa water		n=2 post-relaxation	
Section 3.2.2			
4.1 MPa inverted	n=5	n=5 post-creep	
Section 3.2.3			
crimp control			n=2 control
4.1 MPa crimp			n=2 pre-creep^ (pre-relaxation)
4.1 MPa crimp			n=2 post-relaxation
14 MPa crimp			n=2 pre-creep (pre-relaxation)
14 MPa crimp			n=2 post-relaxation
28 MPa crimp			n=2 pre-creep

"n" indicates ligament numbers, "*" indicates 2 pairs between 7.1 and 28 MPa groups and "^" indicates two pairs between 4.1 MPa pre-creep and post-creep groups

avoided (except for 2 pairs between the 7.1 and 28 MPa groups). After creep testing, tissue water content was assessed either immediately after the creep test (post-creep) or after a recovery period (post-recovery). The pre-test water content of normal MCLs was measured using 6 normal MCLs harvested from 6 rabbits (contralateral limbs used in a different study).

In order to investigate discontinuities at 28 MPa, recovery at 4.1 MPa and water content at 14 MPa, three sub-groups were also included (Table 3.1). First, six MCLs tested at 28 MPa had mechanically detectable discontinuities during the creep test where there was a step increase in deformation with no change in the programmed force. Two of these MCLs with discontinuities underwent crimp analysis. Second, seven MCLs tested at 4.1 MPa were used to measure the recovery behaviour after creep testing; that is, the change in deformation with the ligament held at 0 N for 20 minutes. The group at 4.1 MPa was added to have a group with recovery data for comparison with autografts also tested at this stress (see Chapter 6). There were no significant differences between the creep behaviour in the two 4.1 MPa groups. Third, the MCLs included in the creep analysis at 14 MPa were tested to failure (n=7; Chapter 2) or used in the crimp analysis (n=2). Additional MCLs were tested at 14 MPa to assess water content: post-creep (n=3), post-recovery (n=2) and post-relaxation (n=2). There were no statistical differences in creep behaviour of the samples tested at 14 MPa but these water content samples were not included in the creep analysis in order to keep the group sample numbers similar.

Animals were sacrificed with an overdose of pentobarbital (Euthanyl, 1.5 mL/animal, MTC Pharmaceuticals, Cambridge, Ontario, Canada). The hindlimbs were disarticulated at the hip and ankle. All soft tissues including muscle and fascia were removed rapidly from the femur and tibia, leaving the menisci, collateral and cruciate ligaments. If required for water content analysis, the MCL was excised at this point. If required for creep analysis, bones were transected 3 cm from the MCL insertions. Tissues were kept moist by wrapping the joint with PBS soaked gauze.

The tibia was cemented into the upper grip of our test system with polymethylmethacrylate. The upper grip was attached to the 500 N load cell (Model 661.12A-05) of the hydraulic actuator (Model 242.02) of the MTS system (MTS Systems Corporation, Minneapolis, Minnesota, U.S.A.) (Figure 3.2a). The MCL was aligned with the load axis of the actuator (Figure 3.2b). The load recorded by the system was zeroed to account for specimen weight. The femur was cemented into the lower grip with the knee at approximately 70° flexion. Once the cement had hardened, the displacement and force were set to zero. Tissues were then kept moist by intermittent application (every 30 to 60 seconds) of PBS.

The mechanical testing protocol is shown in Figure 3.3. The knee joint experienced two cycles of 5 N compression and 2 N tension at 1 mm/min. Menisci, cruciate and lateral collateral ligaments were dissected away leaving the isolated MCL. Additional compression-tension cycles were then performed. The second cycle ended at 0.1 N tension to establish "ligament zero". The MCL length was measured at the

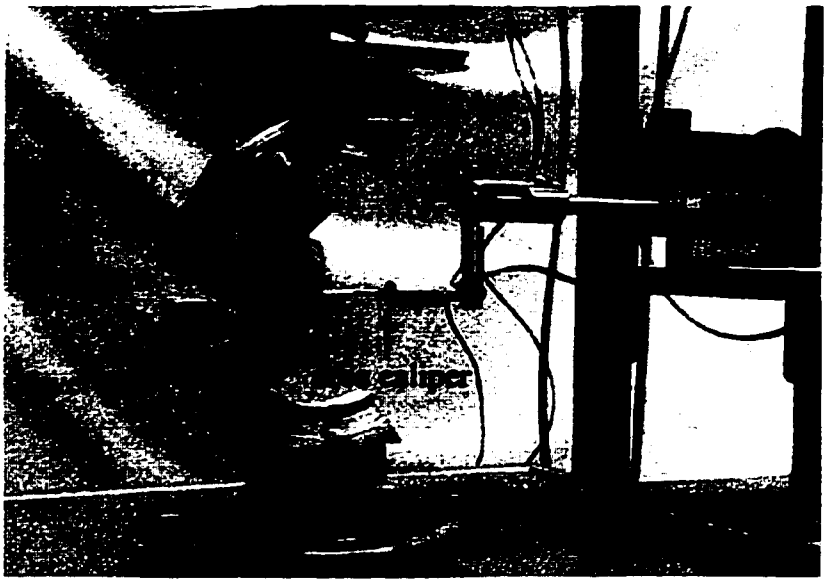

Figure 3.2: **(a) MTS Actuator and Load Cell with Environment Chamber Enclosing the Grips and Knee Joint**

(b) Grips, Knee Joint with Isolated MCL, and Area Caliper

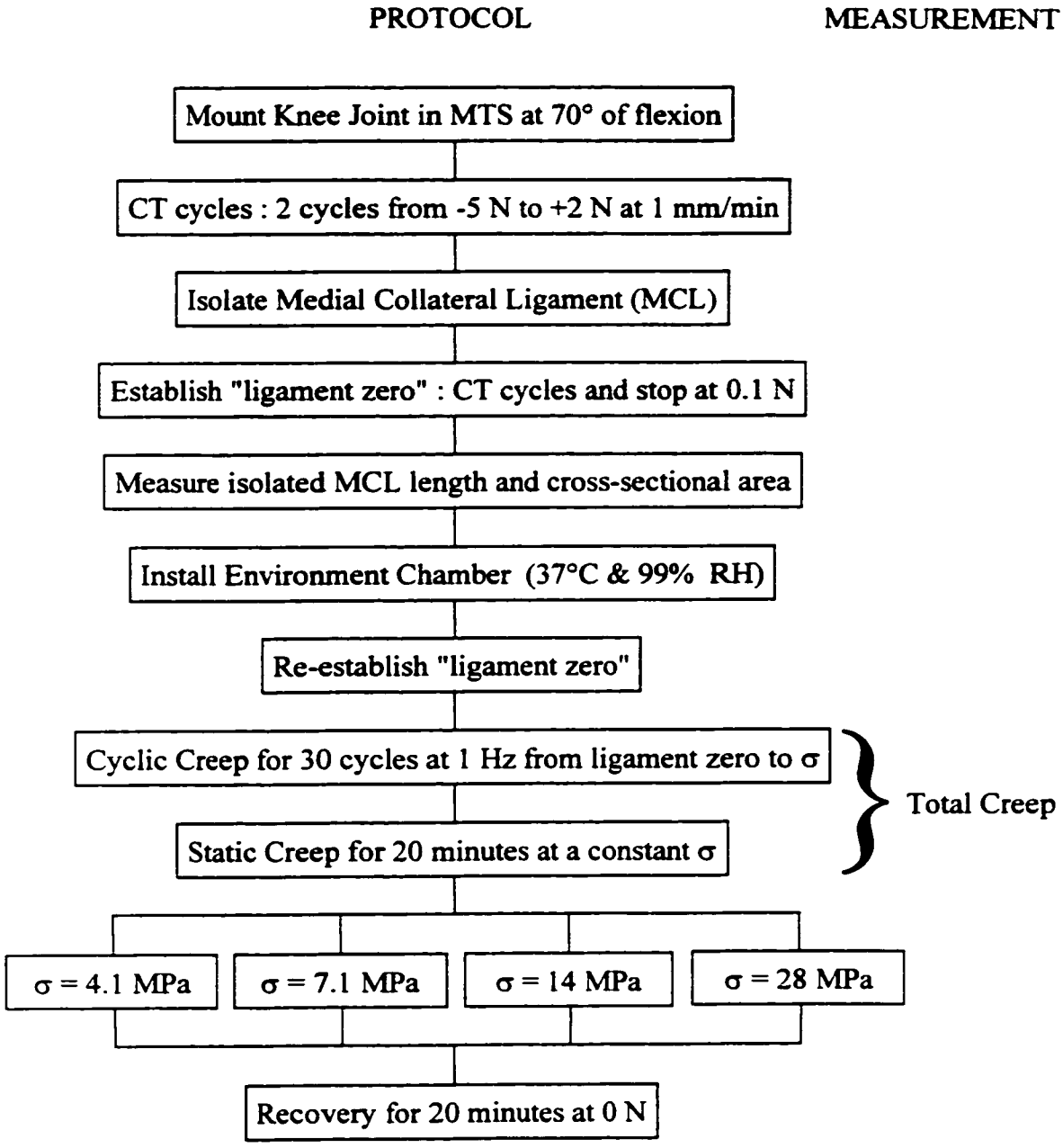

Figure 3.3: Creep Test Protocol for Normal MCLs

"CT" is compression-tension and "RH" is relative humidity

transition between periosteal and ligamentous tissue at both femoral and tibial insertions using Vernier calipers (accurate to 0.01 mm). A small portion of the medial femoral condyle lateral to the MCL and distal to the femoral MCL insertion was removed. The hydraulic actuator was commanded to load to 5 N and maintain load control to facilitate measurement of the cross-sectional area of the midsubstance of the ligament using an area caliper (accurate to 0.01 mm^2) as previously described (134). A custom built environment chamber (37°C and 99% relative humidity) (158) was installed around each test specimen and compression-tension cycles were performed to re-establish "ligament zero".

In each cyclic creep test, the tissue was loaded for 30 cycles at 1 Hz from "ligament zero" to the prescribed stress for that particular test. For a static creep test, each MCL was then loaded immediately to the same stress as in cycling and held in load control for 20 minutes. If intended for post-creep water content, that ligament was harvested. If intended for post-recovery water content, that ligament was allowed to recover at 0 N for 20 minutes and then harvested.

Wet weights were measured immediately on a microbalance (accurate to 0.0001 g). Each sample was then lyophilized until the dry weight ceased to change. Water content was calculated by subtracting the dry weight from the wet weight and dividing by the wet weight to express a percentage water content (53). Water contents of MCLs were assessed at 3 different test time points (Figure 3.4): prior to any mechanical testing (pre-test), immediately after the creep test (post-creep) and after the recovery

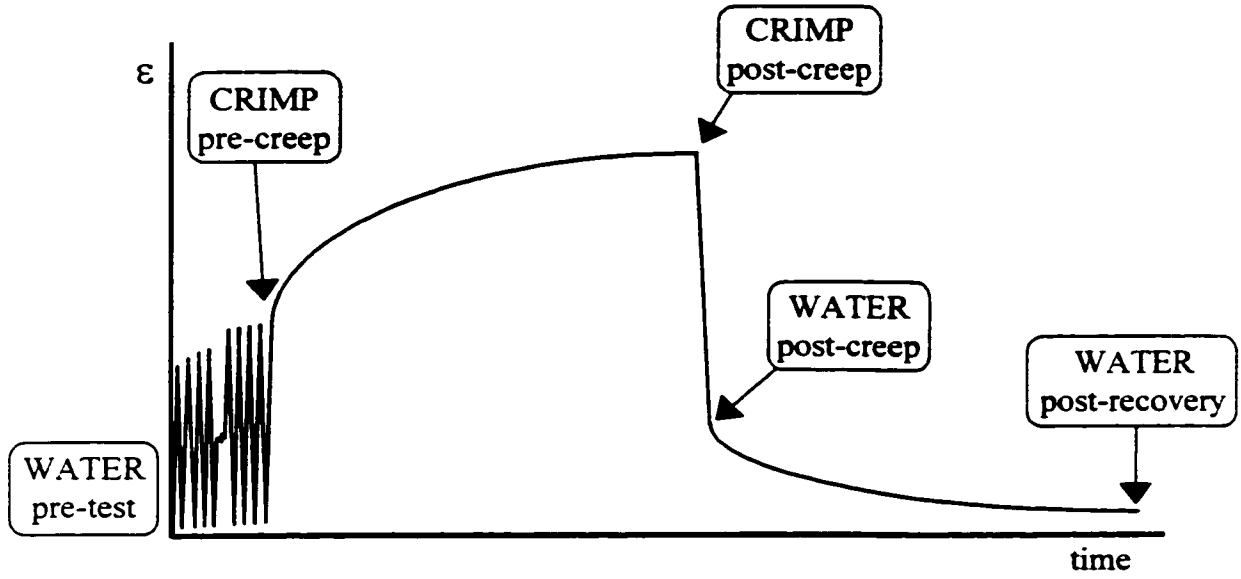

Figure 3.4: Schematic of Test Time Points for Harvesting

Water Content and Crimp Samples

period (post-recovery). Of the MCLs included in the creep analysis, several were included in the water content assessment: 4.1 MPa post-creep (n=4), 7.1 MPa post-recovery (n=6) and 28 MPa post-recovery (n=4). From the additional groups, water content information was also obtained: pre-test (n=6), 4.1 MPa post-recovery (n=5) and 14 MPa post-creep (n=3) and post-recovery (n=2).

Creep stress was controlled for each ligament by applying a load calculated from the midsubstance cross-sectional area for that ligament. Strain was defined as the deformation of the MCL (crosshead displacement) divided by the undeformed MCL length. Total creep strain was the increase in strain from the time load was first applied to immediately prior to when the load was removed completely. For the standard order creep tests (cyclic creep followed by static creep), total creep strain is therefore the increase in strain from the peak of the first loading cycle in the cyclic creep test to the end of the 20 minute static creep test (Figure 3.5a). Cyclic creep strain was defined as the increase in strain from the peak strain of the first cycle to the peak strain of the thirtieth cycle. Static creep strain was defined as the increase in strain from the from the beginning of the constant stress application to the end of the 20 minute constant stress application.

Total creep strain takes into account the complete creep testing protocol because 30 seconds of loading in cyclic creep may be too short to reveal meaningful creep strains, while the cumulative increase in strain (total creep strain) over an additional 1200 seconds of static creep was thought to be more representative of longer term effects.

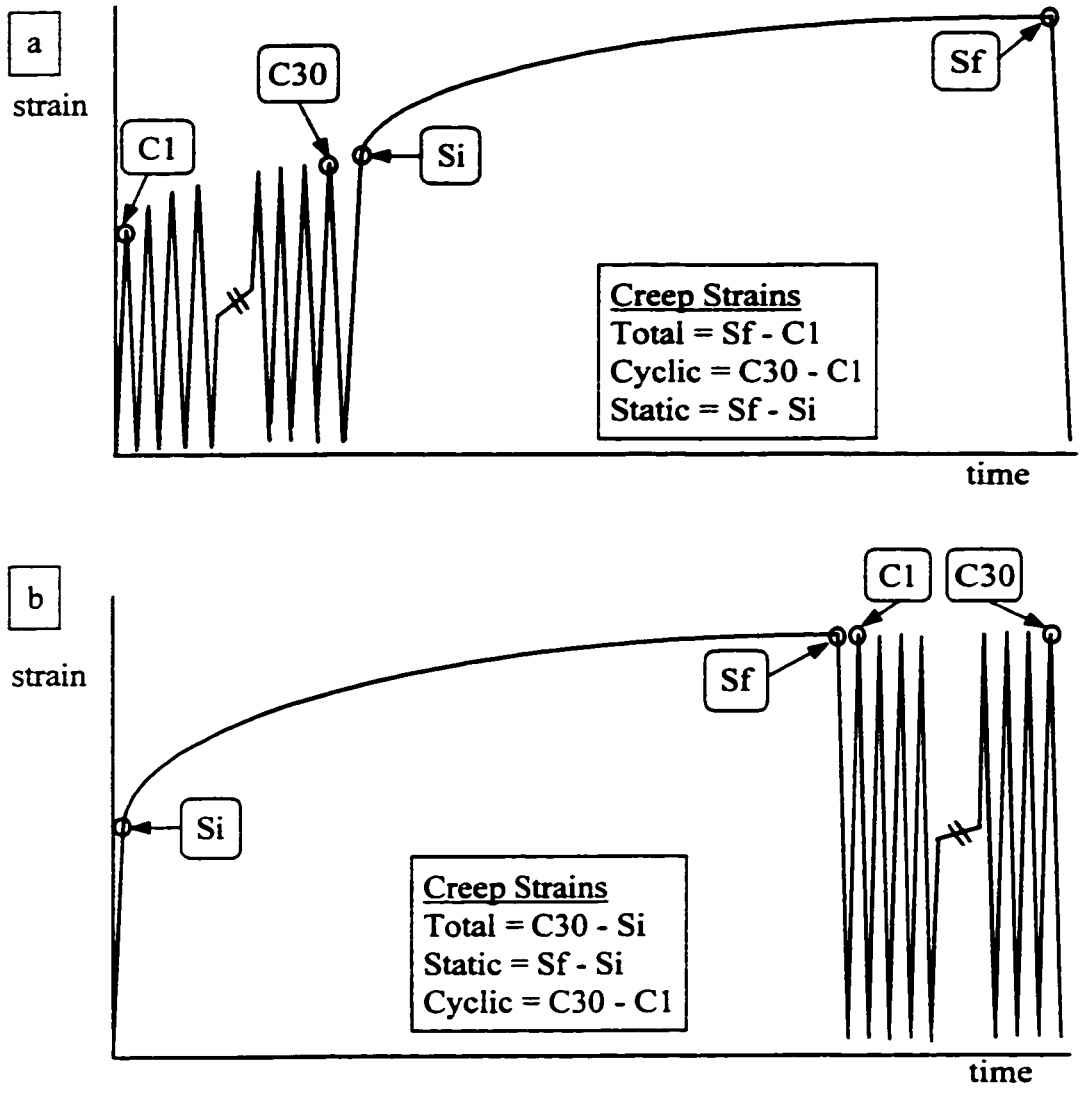

Figure 3.5: (a) Schematic of Standard Order Creep Tests

(b) Schematic of Inverted Order Creep Tests

"C1" is the peak strain of the first cycle in the cyclic creep

"C30" is the peak strain of the thirtieth cycle in the cyclic creep

"Si" is the strain at the beginning of the constant stress application in the static creep

"Sf" is the strain at the end of the 20 minute constant stress application in the static creep

As well, the use of total creep strain facilitates comparison of the standard order and inverted order creep tests (Section 3.2.2). Thirty cycles of cyclic creep were used to ensure that a steady state response was achieved, that is, there was little change in strain between the twenty-nineth and thirtieth cycles, 0.2%. Likewise, after 20 minutes of static creep, there was only a 0.1% change in strain in the last second recorded.

The cyclic creep test was further analyzed determining the cyclic modulus of the first and thirtieth cycle; that is, the slope of the stress-strain plot (the correlation on a plot of load against deformation is stiffness). The tangent modulus of the loading curve was taken over the last 80% of the stress range ensuring the linear regression coefficient of determination, r^2, was greater than 0.99. The increase in modulus from the first to the thirtieth cycle was calculated and assessed with a paired t-test ($p=0.05$).

One-way analysis of variance followed by linear contrast was employed to compare normal groups to each other. Linear contrasts provide an exact p-value for the comparison. Statistical significance was defined at $p<0.05$.

3.2.2 Creep Test Order Variation

The majority of tests were performed in the standard order (cyclic creep followed by static creep; Figure 3.5a). To determine if there was any effect of creep test order, the standard order was inverted (static creep followed by cyclic creep; Figure 3.5b) for an additional group of normal MCLs tested at 4.1 MPa (n=5). After establishment of "ligament zero" in the environment chamber, the MCL was loaded immediately to

4.1 MPa and held in load control for 20 minutes for the static creep test. For the cyclic creep test, the MCL was then loaded immediately for 30 cycles at 1 Hz from "ligament zero" to 4.1 MPa. Normal MCLs were harvested for water content assessment after the creep test (post-creep) (Table 3.1).

For the inverted order creep tests (static creep followed by cyclic creep), total creep strain was the difference in the strains at the end of cyclic creep (the peak strain of the thirtieth cycle) and at the beginning of static creep (the beginning of the constant stress application) (Figure 3.5b). The total creep strain and post-creep water contents of the standard and inverted order tests at 4.1 MPa were compared using Student's t-tests (significance at $p=0.05$).

3.2.3 Crimp Analysis

Crimp analysis was performed on both creep and stress relaxation samples. The creep samples followed the protocol previously described in section 3.2.1 (Figure 3.6). After standardized preparation and establishment of "ligament zero", the MCL was subjected to cyclic creep (loading from "ligament zero" to the prescribed stress level for 30 cycles at 1 Hz) and then static creep (loading to the prescribed stress and held in force control for 20 minutes). Crimp was assessed at two test time points at each of the creep test stresses 4.1, 14, and 28 MPa: at the start of static creep (pre-creep; $n=2$ for each stress) and at the end of static creep (post-creep; $n=2$ for each stress). Crimp was also assessed after establishment of "ligament zero" ($n=2$) as a control. The relaxation

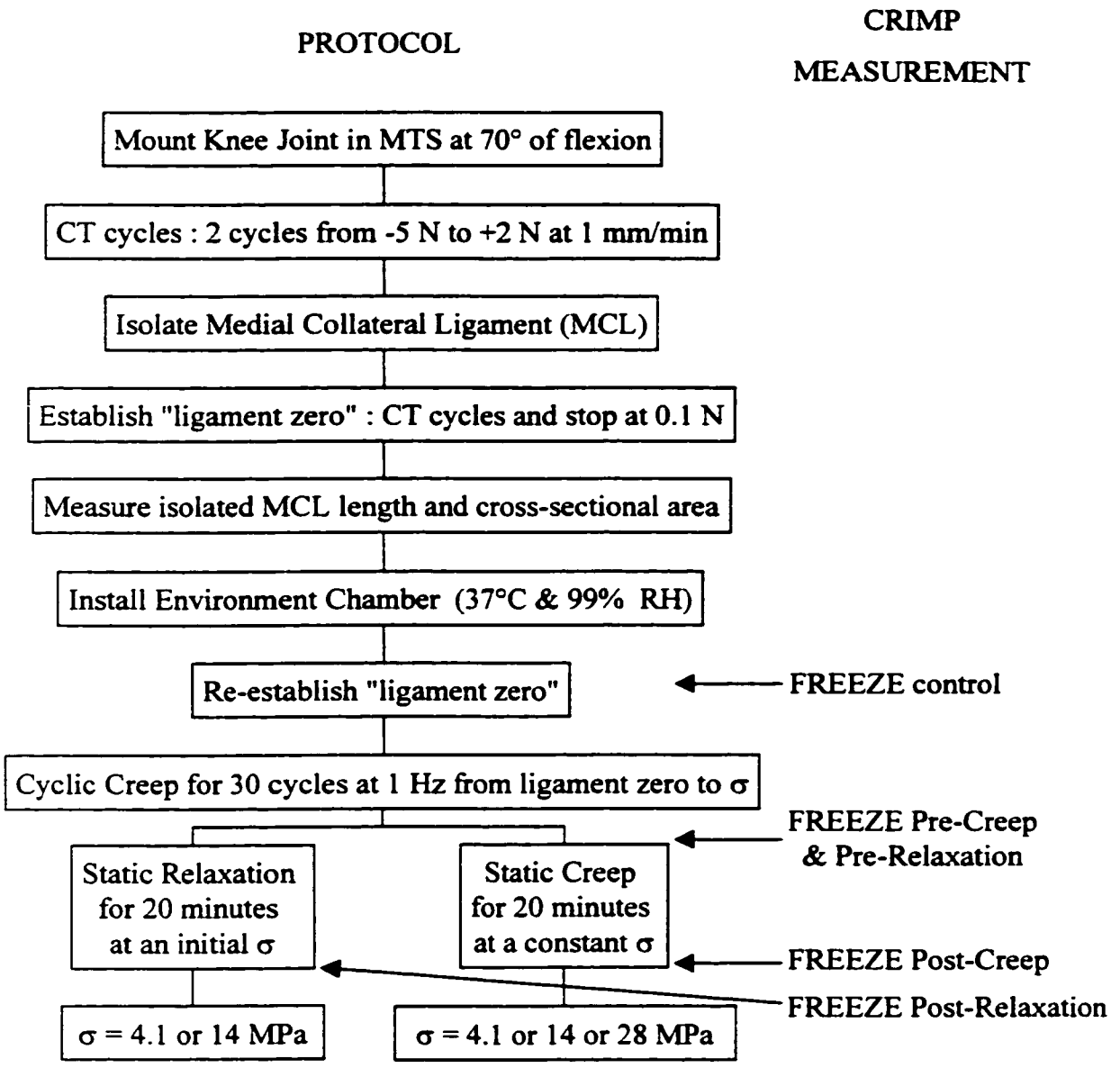

Figure 3.6: Creep Test Protocol for Normal MCL Crimp Analysis

"CT" is compression-tension and "RH" is relative humidity

Pre-Relaxation and Pre-Creep Freezing Points are identical; thus,

Pre-Relaxation and Pre-Creep samples are the same samples.

specimens underwent the standardized protocol until the static step. After undergoing cyclic creep at the prescribed stress, the MCL was loaded to the prescribed initial stress and then held in length control for 20 minutes (Figure 3.6). This allowed the pre-creep and pre-relaxation conditions to be identical and pre-creep data was used as pre-relaxation data. Crimp was assessed at the end of the relaxation test at both 4.1 MPa and 14 MPa (n=2 for each stress).

To quantify crimp, MCLs were washed for 20 seconds with liquid nitrogen while mounted in the MTS at the desired test time-point. The midsubstance of the MCL was removed while frozen and quickly embedded in frozen sectioning media (TissueTek O.C.T. Compound, Sakura Finetek, Torrance, California, U.S.A.). For crimp analysis, tissue was cut in 10 μm thick sagittal sections and stained using hematoxylin and Sirius Red. Sections were examined in a blinded fashion using polarized light microscopy and VIDAS image analysis software (VIDAS 2.1, Kontron Electronik GmbH, Eching, Germany). Percent crimped areas were measured based on three categories (Figure 3.7). Type I Crimp or Substantial Crimp was characterized by a regular banding with a zig-zag waveform. Type II Crimp or Intermediate Crimp had a reduced crimp angle and period. Type III Crimp or Minimal Crimp was characterized by straightened fibres. The striking difference between the categories was adequate to visually distinguish the crimped areas. Nonetheless, Type I and II Crimp were further classified: Type I had a crimp period range of 70-20 μm and crimp angle range of 35°-20° and Type II Crimp had crimp angle less

Type I Crimp

Substantial Crimp

Image size 210 x 140 μm

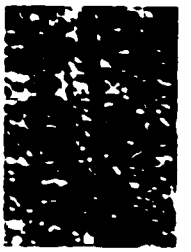

Type II Crimp

Intermediate Crimp

Image size 210 x 140 μm

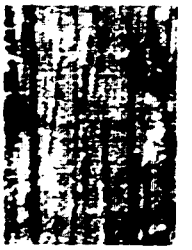

Type III Crimp

Minimal Crimp

Image size 210 x 140 μm

Figure 3.7: Crimp Analysis Categories

than 20° and period less than 30 μm. Percent crimped areas were compared using Student's t-tests (significance at p=0.05).

3.3 Results

3.3.1 Normal MCL Creep and Water Content

The total creep strain of normal MCLs tested at 4.1 and 7.1 MPa (toe region stresses) were not significantly different (Figure 3.8). At 14 MPa, the stress at the transition between the toe and linear regions of the stress-strain curve, the total creep strain was greater than at 4.1 MPa (p=0.04) but not statistically greater than at 7.1MPa (p=0.09) and was significantly less than at 28 MPa (p=0.0001). The cyclic and static components of creep at 14 MPa account for this behaviour. The static creep at 14 MPa is not different than the static creep at 4.1 and 7.1 MPa (Figure 3.9). The cyclic creep strain at 4.1 and 7.1 MPa were not significantly different; however, the cyclic creep strain at 14 MPa was increased over the 2 lower stresses (p<0.001; Figure 3.10). At 28 MPa, the linear region stress, all of the components of creep (total, static and cyclic) were greater than at the 3 lower stresses (p<0.004).

The cyclic modulus increased from cycle 1 to cycle 30 at all creep test stresses (Table 3.2). The increase in modulus was similar at the 3 lower stresses but significantly increased at 28 MPa. Cyclic stress-strain plots of representative samples are shown in Figures 3.11 and 3.12a. In 6 of 12 cases there was a discontinuity in the 28 MPa creep test and 3 of these occurred during cyclic creep. The cyclic discontinuity was

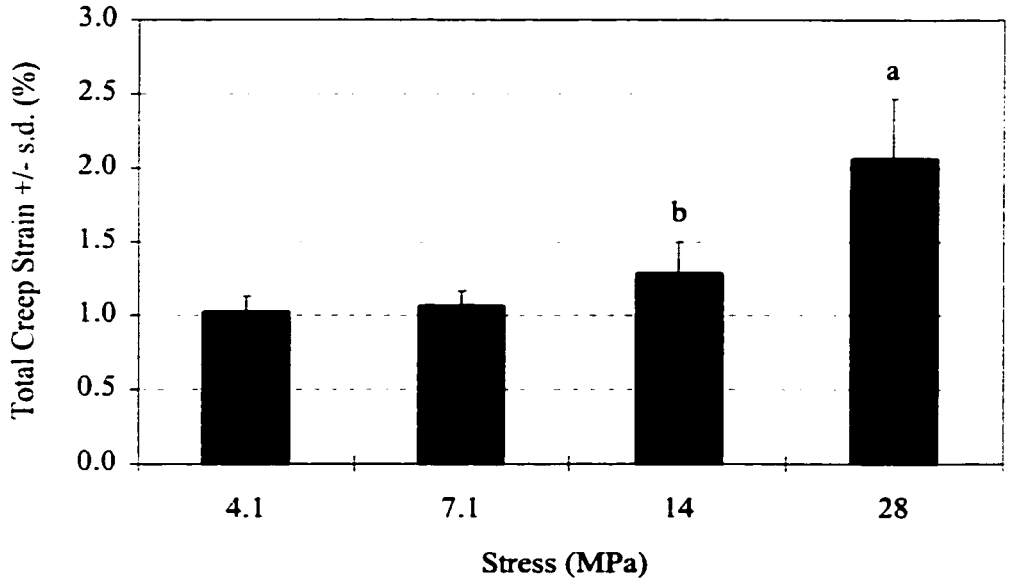

Figure 3.8: Total Creep of Normal MCLs

"s.d." indicates standard deviation

a = significantly greater than the three lower stresses ($p<0.0001$)

b = greater than 4.1 MPa ($p=0.04$) and 7.1 MPa ($p=0.09$)

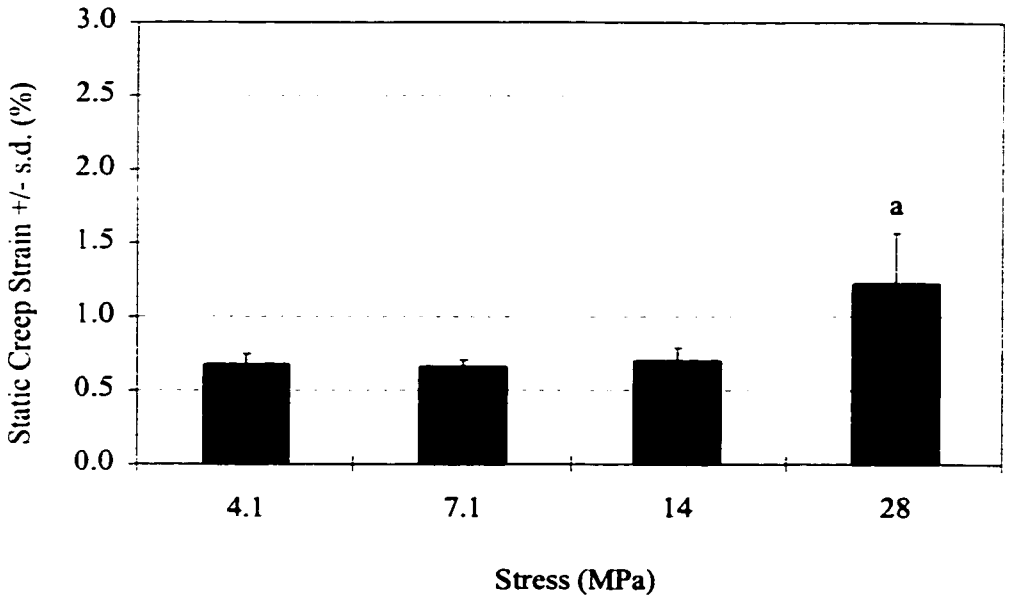

Figure 3.9: Static Creep of Normal MCLs

"s.d." indicates standard deviation

a = significantly greater than the three lower stresses ($p<0.0001$)

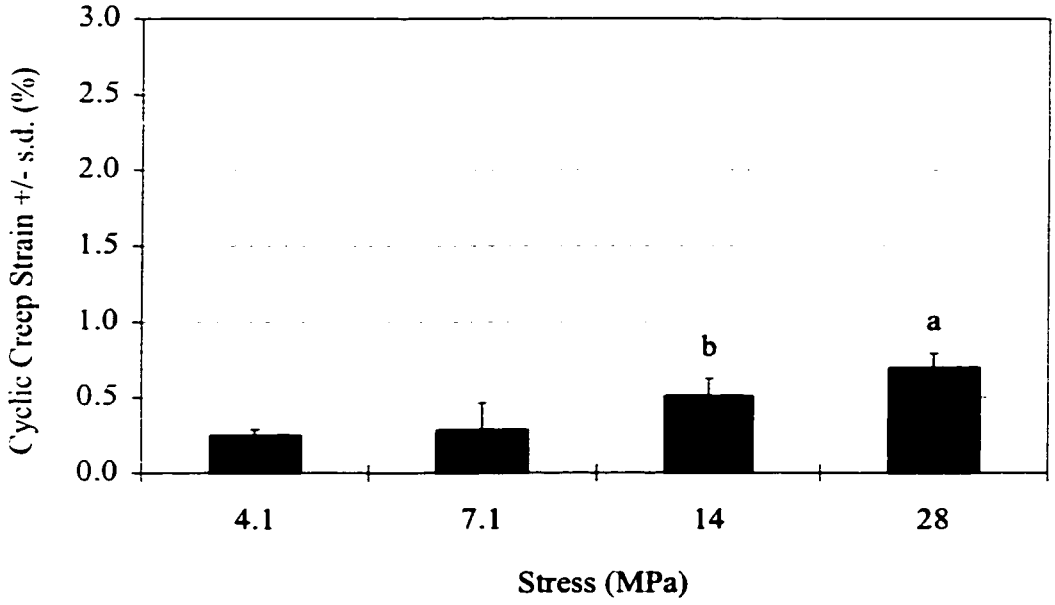

Figure 3.10: Cyclic Creep of Normal MCLs

"s.d." indicates standard deviation

a = significantly greater than the three lower stresses ($p<0.004$)

b = significantly greater than the two lower stresses ($p<0.001$)

Table 3.2: Cyclic Modulus of Normal MCLs at Various Creep Test Stresses

Creep Test Stress (MPa)	Cyclic Modulus Cycle 1 [a] (MPa)	Cyclic Modulus Cycle 30 [a,b] (MPa)	Modulus Increase Cycle 30 - Cycle 1 (MPa)
4.1	362.6 ± 35.3	399.0 ± 37.1	36.4 ± 11.7
7.1	511.5 ± 38.2	550.2 ± 48.6	38.7 ± 11.1
14	579.0 ± 51.2	627.3 ± 52.3	48.3 ± 12.0
28	810.0 ± 88.3	907.0 ± 76.6	97.0 ± 46.8 [c]

"a" indicates that the cyclic modulus was different for all normal groups compared to each other for that particular cycle ($p<0.03$)

"b" indicates that the cyclic modulus at the cycle 30 was greater than at cycle 1 for all groups ($p<0.004$; paired t-test)

"c" indicates that the cyclic modulus increase was greater at 28 MPa than for all the lower stresses ($p<0.0007$)

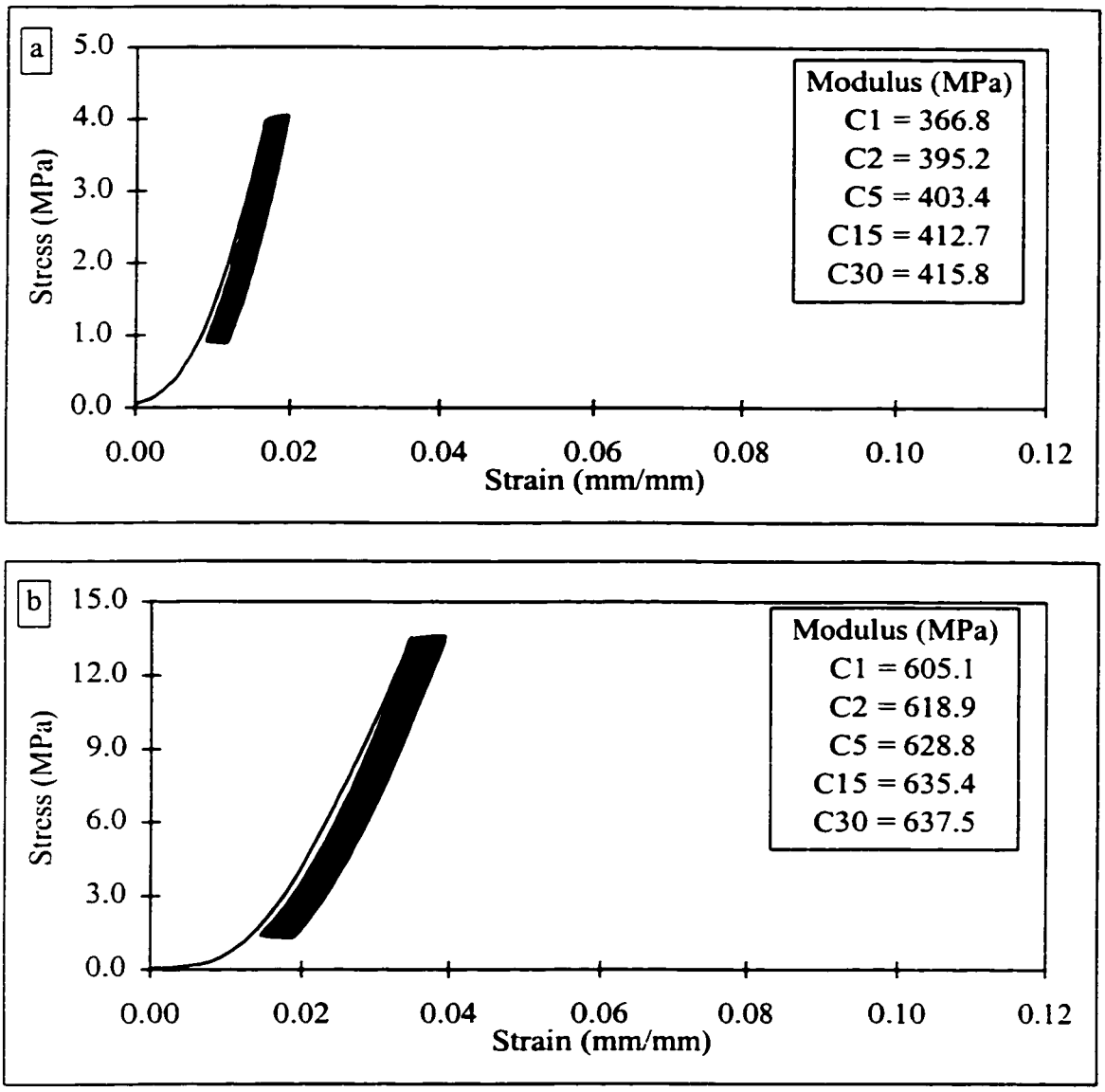

Figure 3.11: (a) Cyclic Plot of a Representative Normal MCL Creep Tested at 4.1 MPa

(b) Cyclic Plot of a Representative Normal MCL Creep Tested at 14 MPa

"C1" indicates Cycle 1

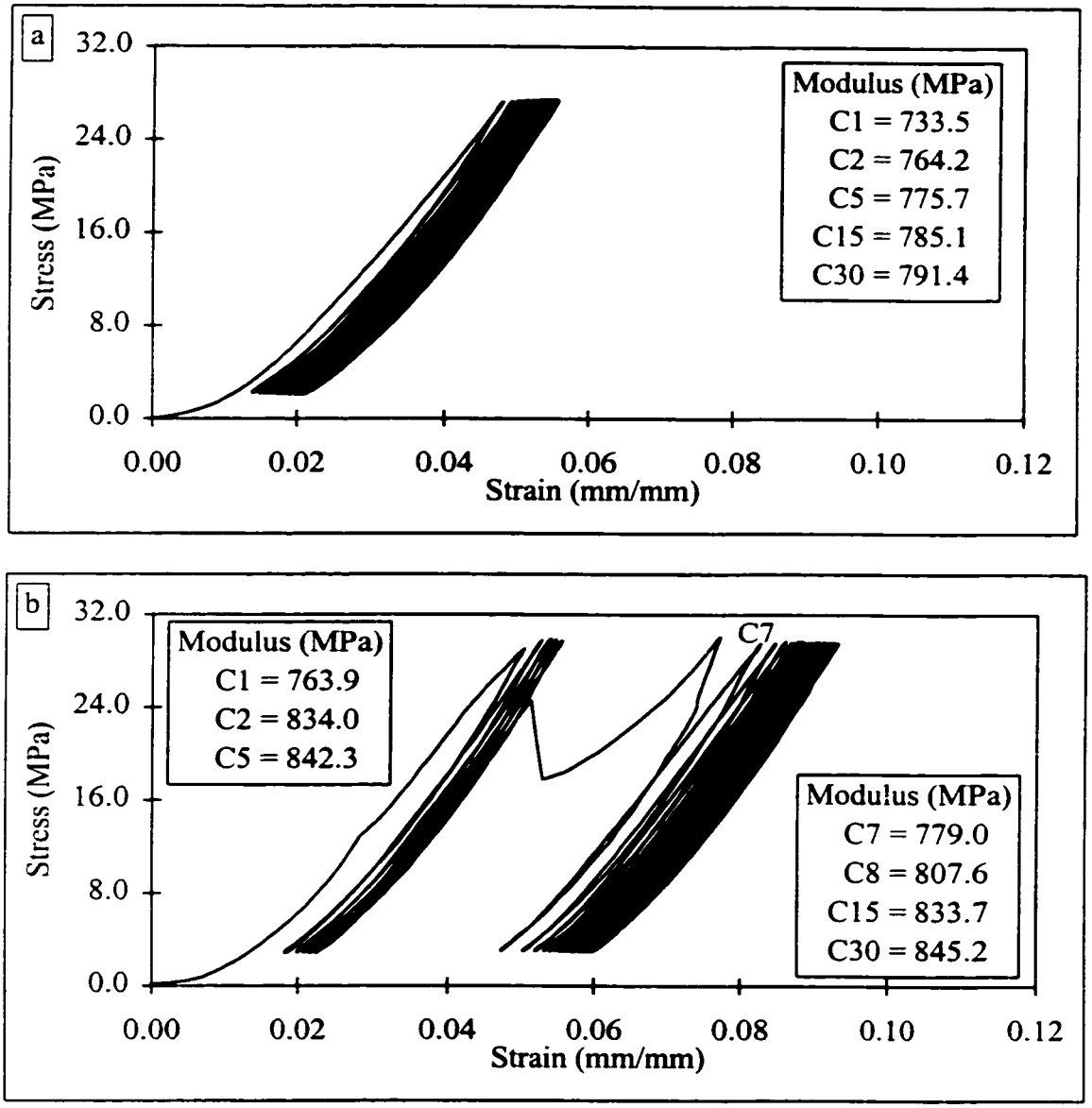

Figure 3.12: (a) Cyclic Plot of a Representative Normal MCL Creep Tested at 28 MPa

(b) Cyclic Plot of Normal MCL Creep Tested at 28 MPa –

Discontinuity at Cycle 6

"C1" indicates Cycle 1

characterized by a decrease in modulus after the discontinuity with an average reduction in modulus of 4.6 ± 3.3% (Figure 3.12b). The discontinuity occurred before cycle 15 and the modulus at cycle 30 was similar to the modulus before the discontinuity occurred; hence, examining only the first and thirtieth cycles would not have revealed the discontinuity.

The water content of normal MCLs had a significant 4% reduction after cyclic and static creep testing at 4.1 MPa compared to pre-test values ($p=0.03$; Figure 3.13). When the MCL was not harvested immediately after creep testing at 4.1 MPa but allowed to remain in the humidified chamber for an additional 20 minute recovery period, the water content returned to pre-test values. The water content of normal MCLs tested at 7.1, 14 and 28 MPa remained less than pre-test values even after the recovery period ($p<0.04$). In fact, there was no change in water content of MCLs tested at 14 MPa comparing the water content after creep testing and after the recovery period. Increasing the creep test stress to 14 MPa caused an increase in water efflux (8% reduction) as compared to 4.1 MPa ($p=0.07$). In addition, post-recovery water content decreased with increasing creep test stress (Figure 3.13).

3.3.2 Creep Test Order Variation

Total creep strain (sum of cyclic and static) was similar regardless of creep test order at 4.1 MPa (Table 3.3). When cyclic creep was tested prior to static creep (standard), the value of cyclic creep was larger than when cyclic creep was tested after

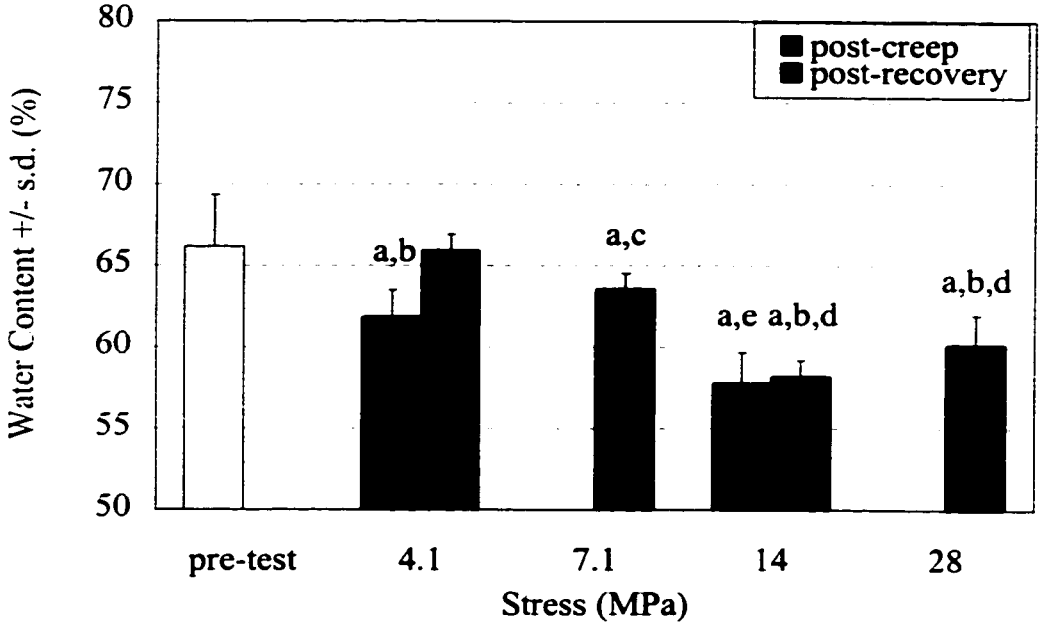

Figure 3.13: Water Content of Normal MCLs

"s.d." indicates standard deviation

significantly different than: a = pre-test ($p<0.04$)

b = 4.1 MPa recovery ($p<0.03$)

c = 4.1 MPa recovery ($p=0.07$)

d = 7.1 MPa recovery ($p<0.05$)

e = 4.1 MPa creep ($p=0.07$)

Table 3.3: **Creep Strains and Water Contents for Standard and Inverted Order Creep Tests of Normal MCLs at 4.1 MPa**

Standard order (4.1 MPa)	Total Creep Sf - C1 (% +/- s.d.)	Cyclic Creep C30 - C1 (% +/- s.d.)	Static Creep Sf - Si (% +/- s.d.)	n	Water Content (%+/- s.d.)	n
normal	1.03±0.11	0.25±0.04 [a]	0.68±0.07 [a]	7	61.9±1.7	4
Inverted order (4.1 MPa)	**Total Creep C30 - Si (% +/- s.d.)**	**Static Creep Sf - Si (% +/- s.d.)**	**Cyclic Creep C30 - C1 (% +/- s.d.)**	**n**	**Water Content (% +/- s.d.)**	**n**
normal	1.13±0.10	1.18±0.10	-0.03±0.02	5	63.4±1.8	5

"C1" is the peak strain of the first cycle in the cyclic creep

"C30" is the peak strain of the thirtieth cycle in the cyclic creep

"Si" is the strain at the beginning of the constant stress application in the static creep

"Sf" is the strain at the end of the 20 minute constant stress application in the static creep

Total creep strain is the cumulative increase in strain over the complete creep test. For example, in the standard order test, total creep strain (Sf-C1) includes cyclic creep strain (C30-C1), static creep strain (Sf-Si) and, as well, the strain difference from the end of cyclic creep to the start of static creep (Si-C30) as shown in Figure 3.5a.

"s.d." indicates standard deviation

"a" indicates significantly different compared to the same parameter measured in the inverted order creep test ($p<0.0001$)

static creep (inverted) ($p=0.0001$). In fact, the cyclic creep strain in the inverted order tests was a small negative amount, caused perhaps by some recovery during the periods of low stress. The static creep strain in the inverted order test (tested first) was larger than the static creep strain in a standard order test (tested second) ($p=0.0001$). The post-test water contents of MCLs tested using the inverted order were not significantly different compared to those tested using the standard order.

3.3.3 Crimp Analysis

Crimp analysis was performed at the start and end of the static creep tests with the MCL held at the creep test stress. Thus, fibre recruitment during creep was quantified comparing crimp distributions pre-creep and post-creep. The crimp pattern of the control MCLs harvested at "ligament zero" (0.1 N tension) had very few, 1.7 ± 1.6 %, straightened fibres (Type III Crimp; Figure 3.14). Interestingly, significant increases in straightened fibres (Type III Crimp) were observed post-creep at both 4.1 MPa (22.5 ± 0.0 %; Figure 3.15) and 14 MPa (75.8 ± 9.0 %; Figure 3.16). At the linear region stress, 28MPa, an almost extinguished crimp pattern was observed, 93.5 ± 0.2 % straightened fibres (Type III Crimp; Figure 3.17). Thus, these groups all had significant decreases in crimped fibres (Type I and Type II Crimp) and significant increases in straightened fibres (Type III Crimp) post-creep ($p<0.06$). Thus, all these groups exhibited fibre recruitment during creep, albeit limited at 28 MPa.

Control at "ligament zero"

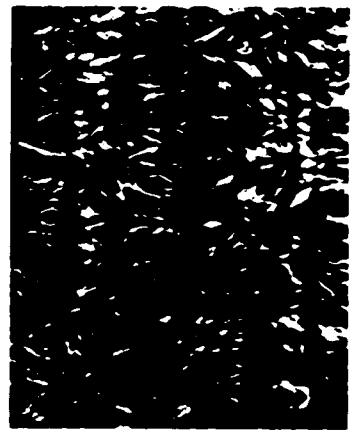

Image Size 370 x 280 μm

TYPE III
1.7 +/- 1.6 %

TYPE I
23.2 +/- 1.7 %

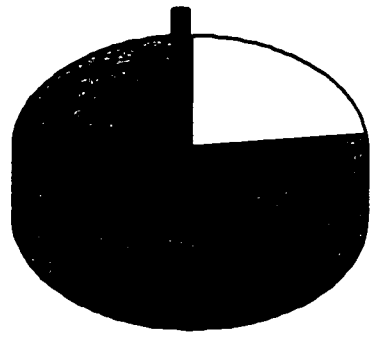

TYPE II
75.1 +/- 3.2 %

Figure 3.14: Crimp Pattern of Control MCLs at "ligament zero"

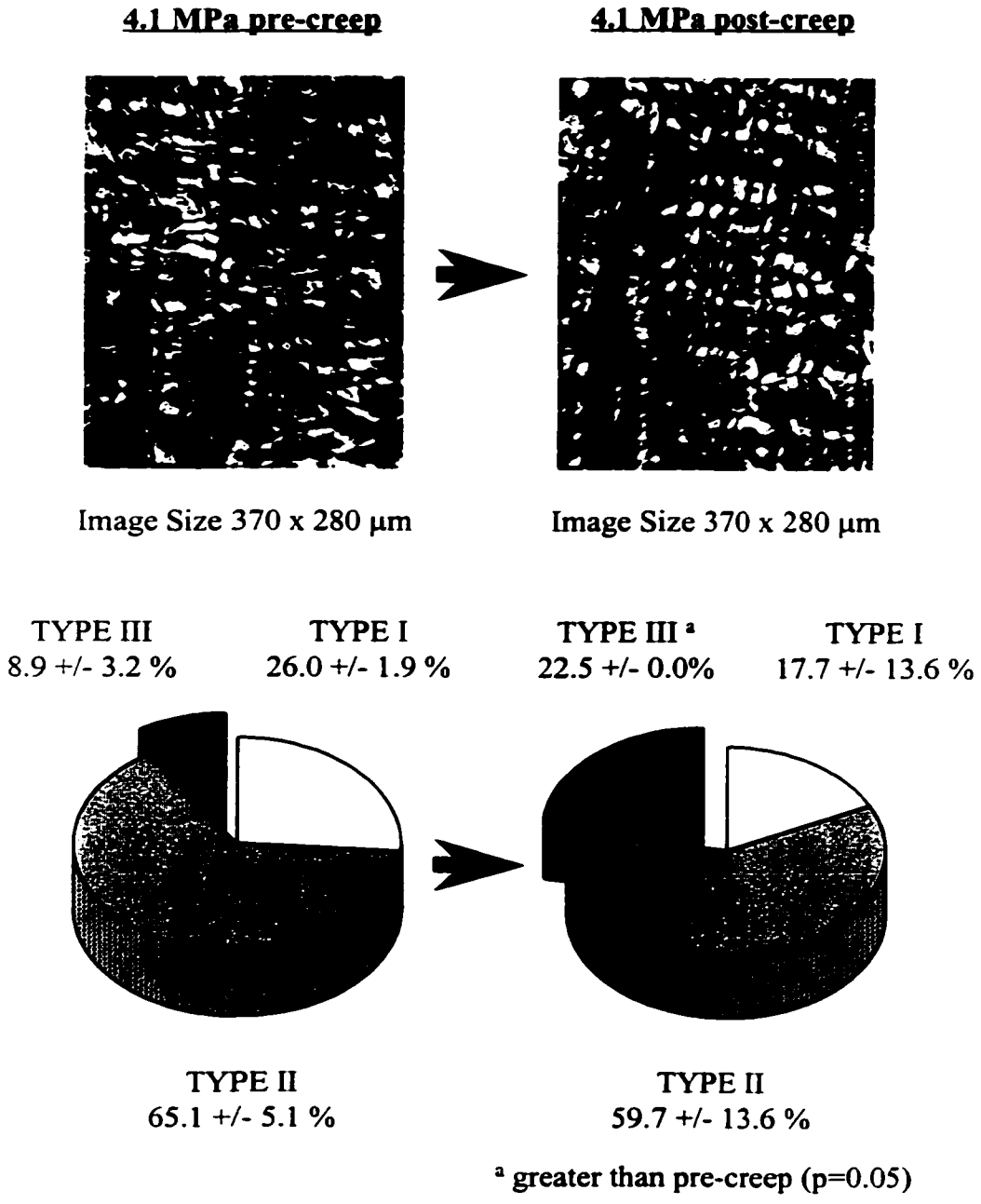

Figure 3.15: Crimp Pattern of MCLs Creep Tested at 4.1 MPa

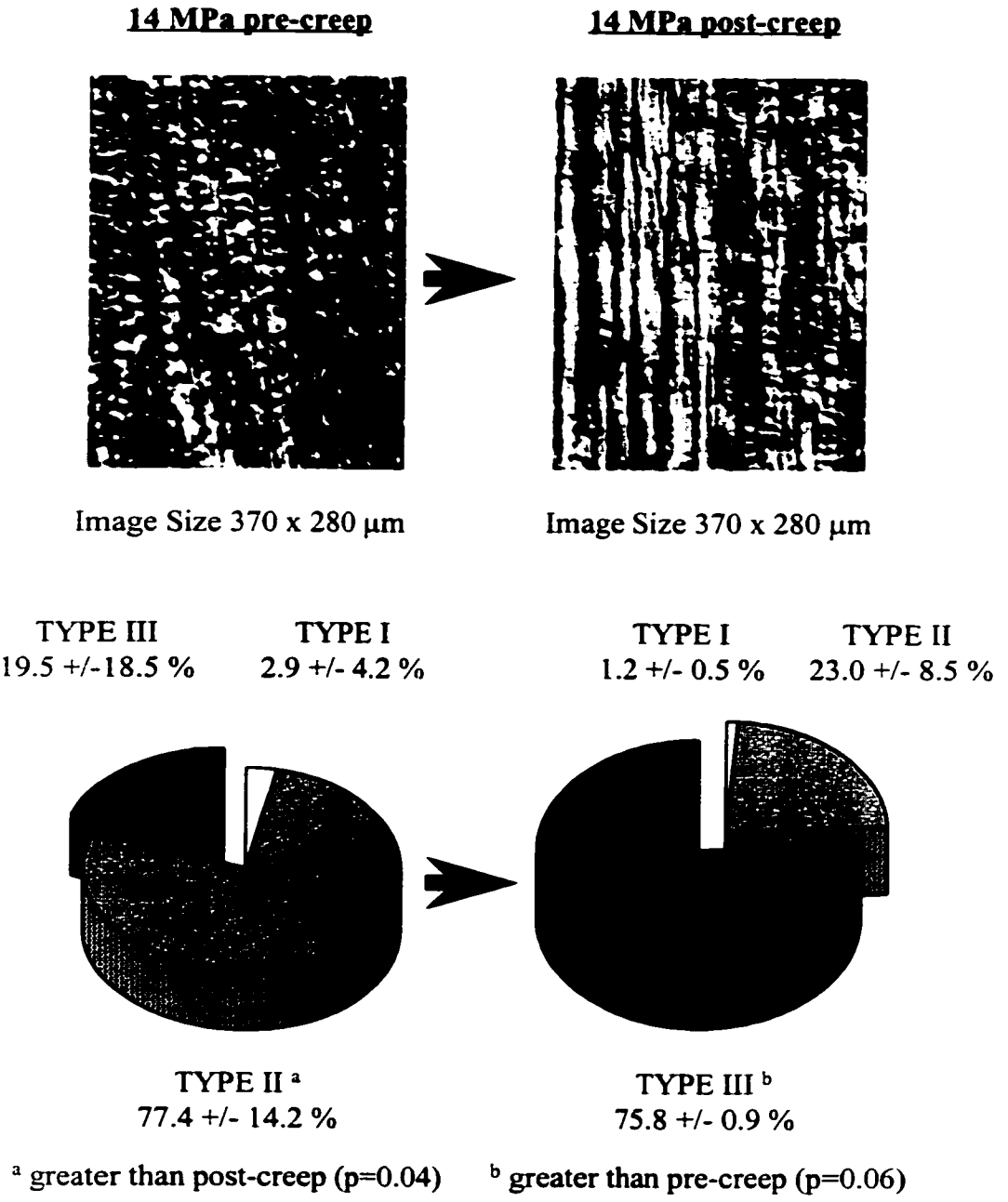

Figure 3.16: Crimp Pattern of MCLs Creep Tested at 14 MPa

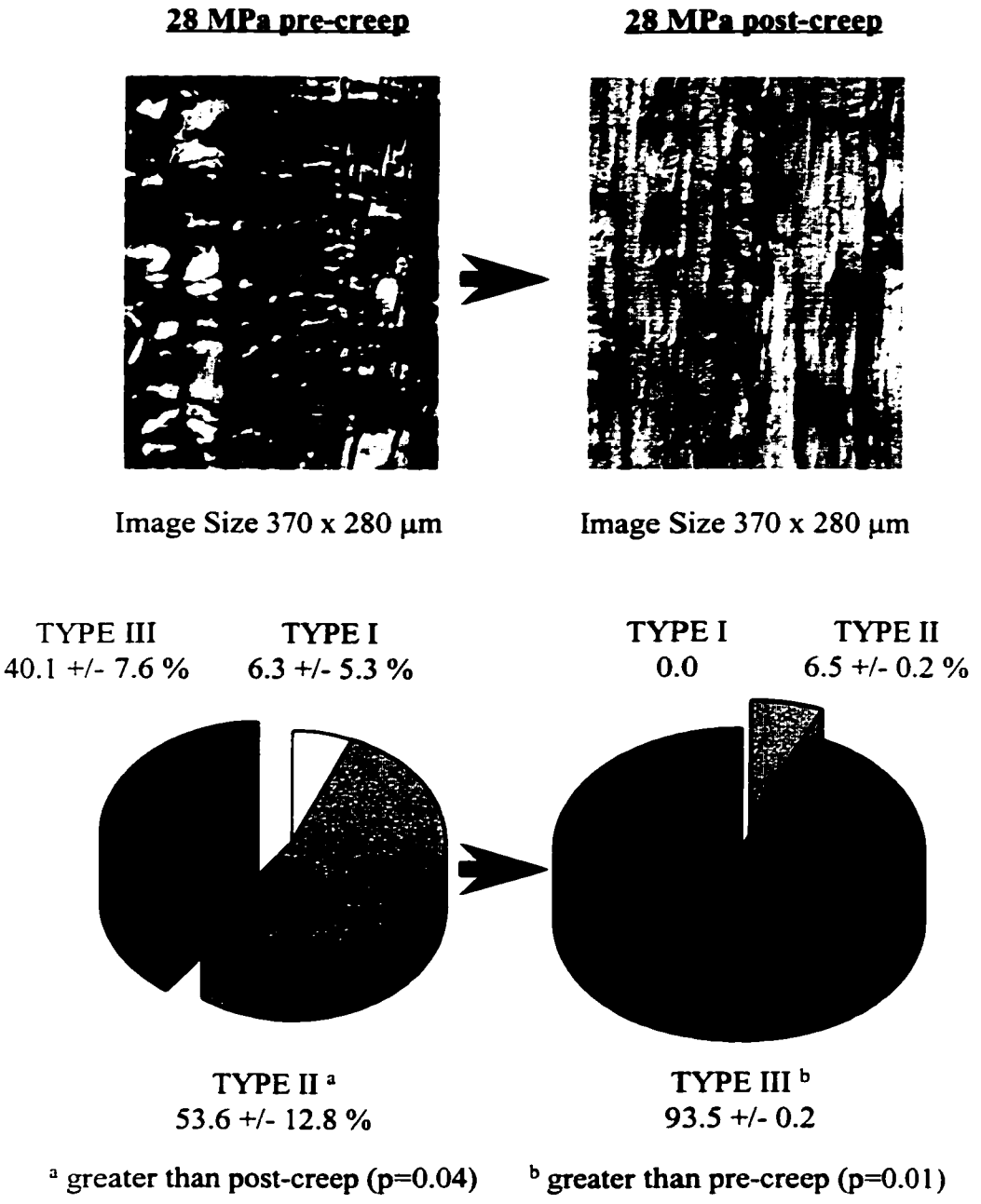

Figure 3.17: Crimp Pattern of MCLs Creep Tested at 28 MPa

At 28 MPa, a step increase in the deformation was noted to occur at an arbitrary time during the creep protocol producing a discontinuous creep test in 6 of 12 specimens. The static creep strains of the 28 MPa discontinuous tests (3.34 ± 1.74 %) was significantly greater than the 28 MPa continuous test (1.22 ± 0.34 %) ($p=0.02$). It is interesting to note that the crimp patterns of the discontinuous samples had more crimped fibres and less straightened fibres than the samples from the tests that had no discontinuities (Figure 3.18), presumably due to a "recoiling" of some fibres after rupture. This interesting phenomenon will be discussed.

The same samples were used for pre-creep and pre-relaxation data because the protocols were identical. There were no significant differences in the crimp patterns measured pre-relaxation and post-relaxation at either 4.1 or 14 MPa (Figures 3.19 and 3.20). There is some variability in the crimp patterns assessed at 14 MPa pre-relaxation and post-relaxation. The tests were programmed to achieve a 14 ± 1 MPa initial stress, which allows for some variability in the strain which is then held constant for the remainder of the test (Table 3.4). These results confirm a relationship between the strain and the crimp patterns in rabbit MCLs with increases in straightened fibres (Type III Crimp) at the higher strains.

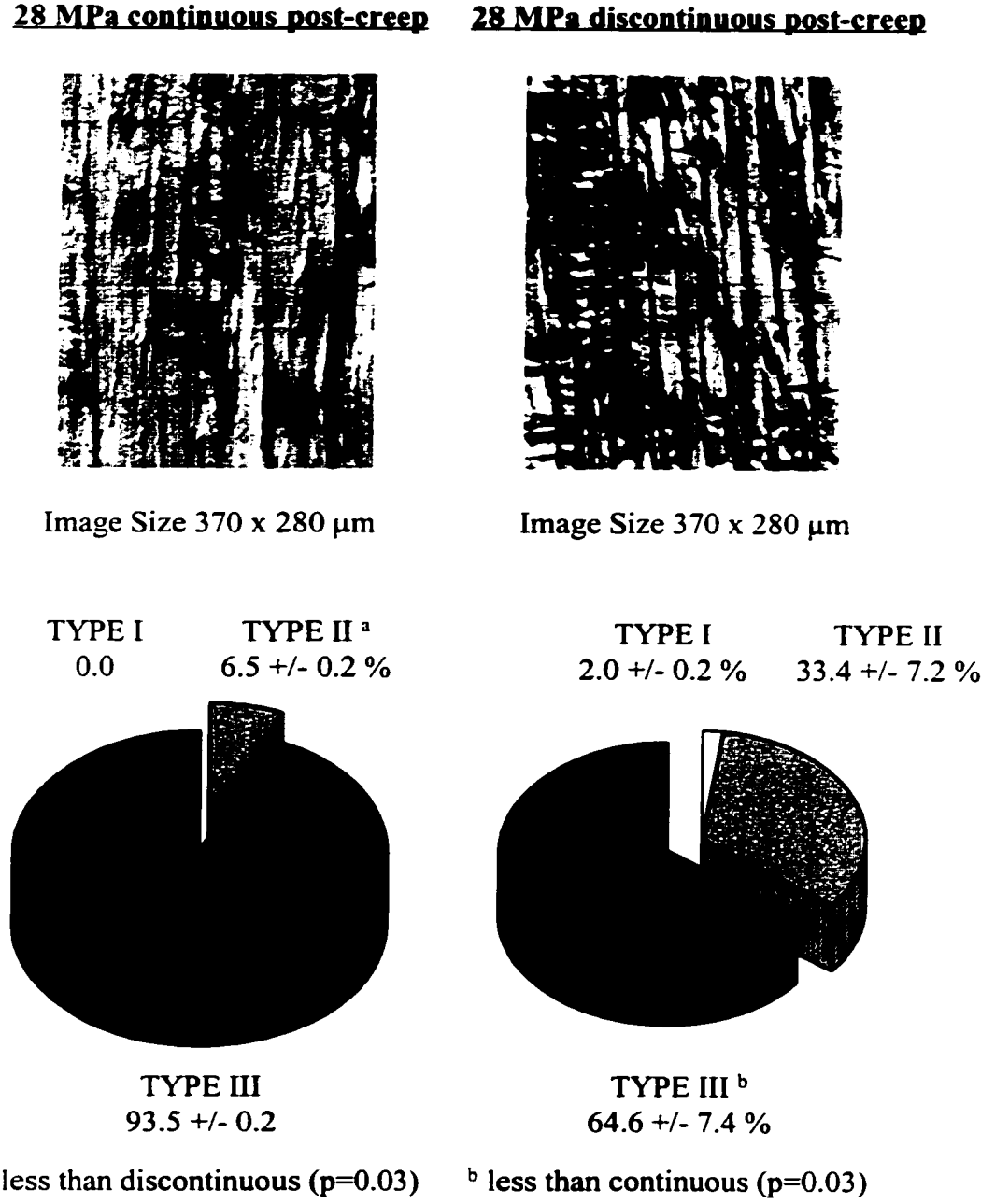

Figure 3.18: Crimp Pattern of 28 MPa continuous and discontinuous MCLs

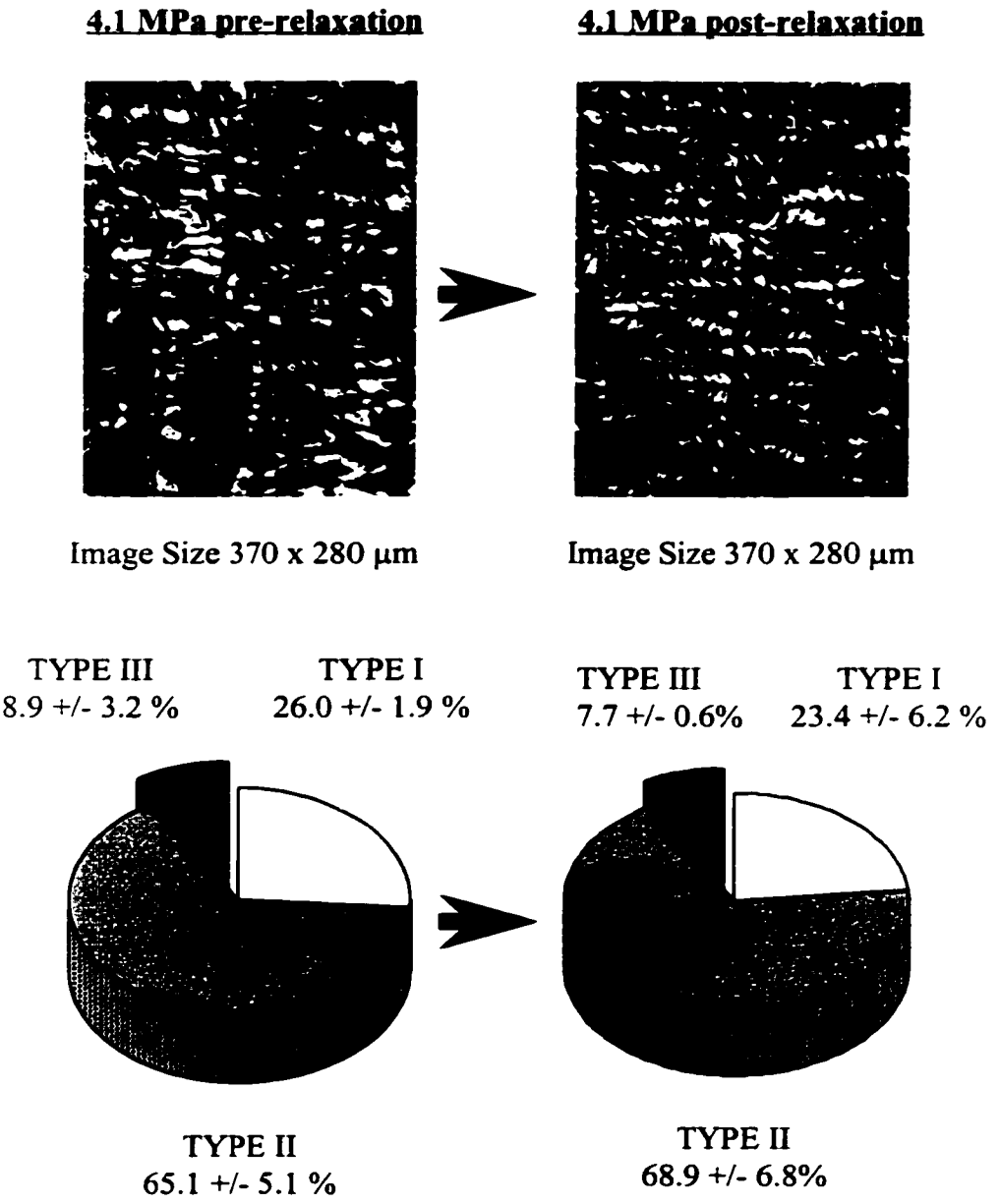

Figure 3.19: Crimp Pattern of MCLs Relaxation Tested at 4.1 MPa

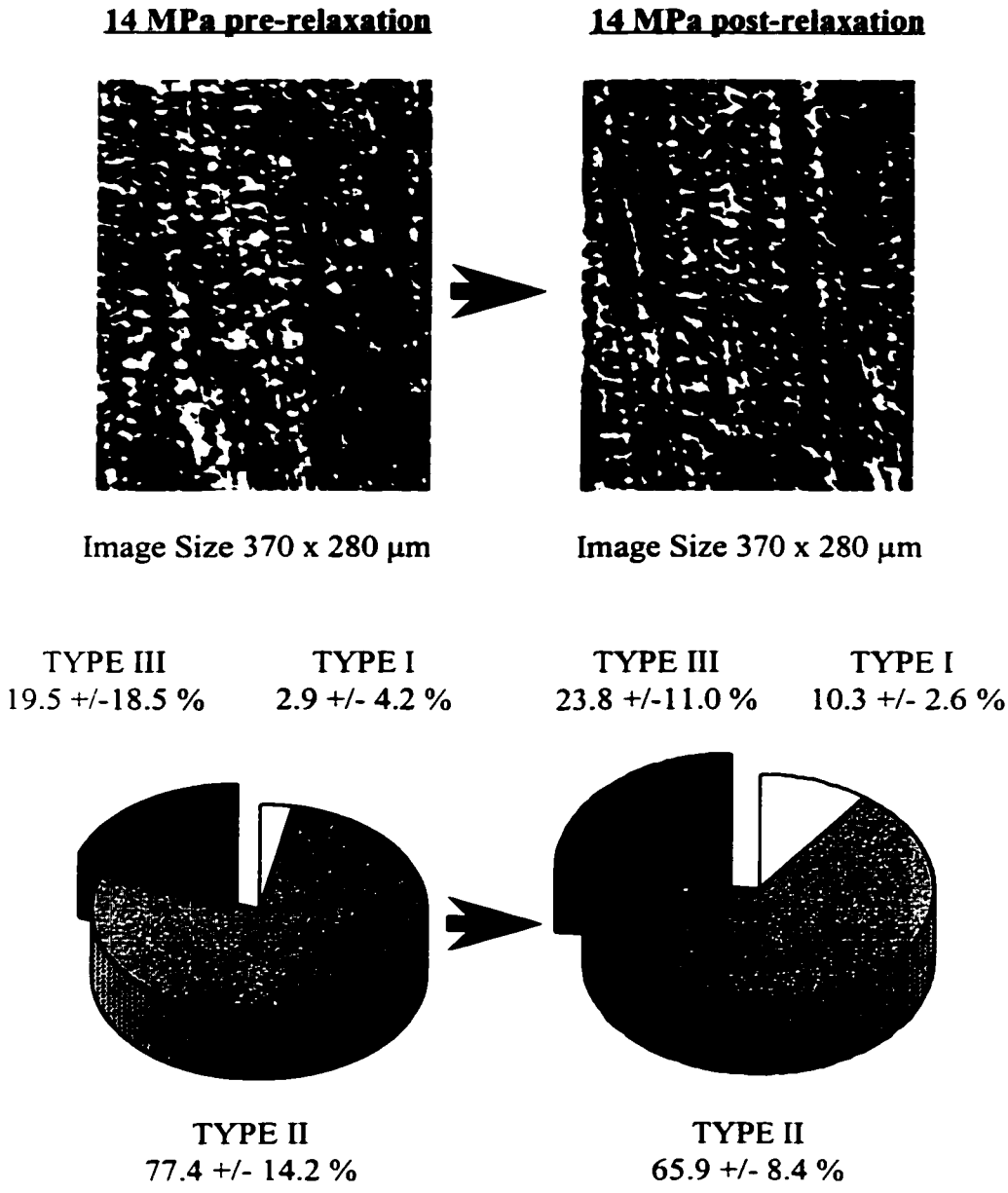

Figure 3.20: Crimp Pattern of MCLs Relaxation Tested at 14 MPa

Table 3.4: Variation in Crimp at 14 MPa due to Different Resulting Strains

Sample	Stress (MPa)	Strain (%)	Type I (% area)	Type II (% area)	Type III (% area)
pre-relaxation 1 left	13.0	3.15	5.9	87.5	6.4
post-relaxation 1 left	13.8	3.58	12.1	71.8	16.1
post-relaxation 2 right	13.4	4.51	8.5	59.9	31.6
pre-relaxation 2 right	13.0	4.80	0.0	67.4	32.6

Pre-relaxation and pre-creep samples are equivalent samples.

3.4 Discussion

These results reveal six important findings. First, these results show that ligaments exhibited creep behaviour with relative insensitivity to creep test stress at stresses in the toe region of the stress-strain curve. Using total ligament cross-sectional area to calculate stress, a three-fold increase in stress had minimal effects on creep behaviour: the increase in cyclic modulus was similar from 4.1 MPa to 14 MPa and the static creep strain was similar over these same stresses. Static creep strain and increase in cyclic modulus were significantly larger at a linear region stress, 28 MPa. This insensitivity to increased creep stress is atypical of viscoelastic materials. One would expect that if the creep test stress was doubled that the creep strain would be doubled for a linear viscoelastic materials (constant ratio between stress and strain at a given time) or at least increased in a nonlinear viscoelastic material. Hence, ligaments have a clever structural response that minimizes creep.

Second, results showed that fibre recruitment (as measured by crimp) had an important role in minimizing creep at toe region stresses. The concurrent crimp analysis provided a potential explanation for the increase in static creep at a stress in the linear region of the stress-strain curve, 28 MPa. At the lower stresses, the crimp analysis showed significant increases in straightened fibres and decreases in crimped fibres post-creep. This observation indicates that collagen fibres were recruited during creep, suggesting that collagen fibre recruitment is a mechanism for minimizing creep at lower (working) stresses. At 28 MPa, there was a predominant increase in straightened fibres

showing an almost extinguished crimp pattern. It is likely that at this stress (in the linear region) there was a limited capability for fibre recruitment to act to minimize creep.

Although the observations from the crimp analysis are boundary condition specific regarding joint angle and the location within the ligament where crimp was analyzed, the principles of recruitment documented here have general implications that apply to different joint positions and different ligaments. In the current study, midsubstance sections were completely analyzed in two dimensions (anterior–posterior and superior-inferior). Generally, only midsubstance sections from the middle of the MCL (moving from medial to lateral) are analyzed in histological protocols from this laboratory because of the consistency of serial sagittal section appearance. Thus, the principle of increased fibre recruitment during creep will also be applicable throughout the ligament in the third dimension (medial-lateral or surface-to-deep). The MCL was tested with the joint at 70° flexion because this joint position was previously defined for the rabbit MCL as an "anatomic" position, the joint position naturally attained before mechanical testing when all muscles were removed and all ligaments and menisci remained intact (94). In addition, the rabbit knee range of motion is from approximately 160° to 30° flexion and, in a sitting posture, the rabbit knee is at 110° flexion. Clearly, the knee joint would achieve 70° flexion during motion and thus can be considered a functionally relevant joint position. The specific crimp pattern observed at an isolated test timepoint (pre-creep or post-creep) may be different in different joint positions. Matyas et al. (1988) documented differences in the crimp pattern of rabbit MCL

midsubstance under no load. In flexion (140°-120° flexion), the anterior region of the MCL had reduced crimp pattern and the posterior region had a regular crimp pattern, suggesting that anterior fibres of the rabbit MCL were more taut in flexion compared to the posterior fibres. In extension (50°-30° flexion), the situation was reversed as posterior fibres were more taut compared to anterior fibres. At 70° flexion used in the present study, no consistent anterior-posterior differences were observed even though the complete midsubstance was analyzed. This joint position may represent an "average" crimp appearance avoiding the extremes of full flexion and extension. Analysis of crimp at one joint angle provides a "snapshot" of the fibre recruitment characteristics at that particular joint angle of interest during a functional activity. Regardless of the boundary conditions of crimp dictated by the joint angle, the general principle that fibres are recruited during creep based on reduced crimp patterns will still apply. In addition to being generalizable to different joint positions, the principles of recruitment during creep are applicable for different ligaments. Crimp is a characteristic feature of both ligaments and tendons (10). Similar to the rabbit MCL, the human MCL and ACL have functional anterior-posterior subdivisions that are taut at different joint angles accommodating the range of motion of the knee (13,56,83). The range of motion of the human knee is about 150° to 0° flexion (51) and a walking cycles takes the knee through approximately 70° to 0° flexion (12). The anterior fibres of the human MCL are taut when the joint is in flexion (83). The anterior fibres of the ACL are also more taut in flexion (13). Clearly, the ACL and MCL of the human knee also have functionally important fibre recruitment.

Although the observations of increased fibre recruitment during creep were made in the rabbit MCL at one specified joint position, this general principle applies to any joint position in any ligament that has fibres that can be recruited as revealed by crimp.

It is likely that the similar static creep strains observed at stresses in the toe region of the stress-strain curve are the result of a combination of collagen fibre creep and collagen fibre recruitment. The incorporation of fibre recruitment and fibre creep was used in the model described in the previous chapter to predict creep from stress relaxation data. Similarly, Cohen et al. (1976) postulated that the activation energy for creep of tendon (T-jump analysis) was between the high activation energy for collagen fibril creep and the low activation energy for interfibrillar sliding due to straightening out of the wavy fibrils. Others studies have also documented the importance of collagen to the viscoelastic properties of ligament. Jenkins and Little (1974) removed the collagenous components of bovine ligamentum nuchae and observed that the viscoelastic properties were dependent on the presence of collagen. Lam et al. (1989) documented age dependent changes to viscoelastic properties of rabbit MCL which may be related to viscoelastic changes of maturing collagen.

Third, these results revealed that water content was reduced during creep testing and was not regained as rapidly as it was lost. Water content was significantly reduced when the MCL was tested at 4.1 MPa and 14 MPa by 4% and 8%, respectively. With increasing stress, there may be a corresponding reduction in the available space between the collagen fibres that the water could occupy. Consistent with this finding, Hannafin

and Arnoczky (1994) previously documented that cyclic and static creep caused a small but significant water loss in canine flexor tendon. The present study also showed that the water content of normal MCLs tested at 4.1 MPa can return to pre-test values after only 20 minutes of recovery in the environment used. That recovery in the humidified environment apparently permits the MCL to take up water that is lost during creep testing. This ability to increase hydration appears to be limited at higher stresses since post-recovery water content at 7.1, 14 and 28 MPa remained less than pre-test values. Perhaps the process of water return during recovery was slower than that of water loss during creep, requiring more than 20 minutes to be complete. In a pilot study on a normal MCL creep tested at 14 MPa, the water content reached 64.8% (similar to pre-test values) after three hours of recovery (with the ligament buckled at -1 mm deformation from "ligament zero"). Water in ligament is either unbound or bound to proteogylcans and other matrix molecules. The gradient for water loss during creep is likely enhanced by the tensile stress and recruitment of fibres. The gradient for water return during recovery could not be enhanced in such a way as the tissue is at zero stress. As well, if loading caused removal of GAGs as seen by Lanir et al. (1988), the gradient for water return would be even further reduced. Additionally, water and proteoglycans may have limited access through the surface area of the ligament due to potential altered permeability in its unloaded state after creep. Proteoglycans in the matrix may be inaccessible due to conformational changes in the fibre organization. Clearly, if an experiment was proposed where consecutive creep tests on the same tissue were to be compared, the length of the

recovery period between each creep test would have to be tailored to ensure equivalence of initial conditions of water content at the start of the next creep test.

Fourth, results showed that damage can occur to rabbit MCLs exposed to repetitive and sustained 28 MPa creep test stress. Of the 12 samples creep tested at 28 MPa, 4 were designated for crimp analysis after static creep testing. Two of these samples had mechanically detectable discontinuities during static creep. Yahia et al. (1990) documented mechanically detectable changes on a stress-strain curve of adolescent rabbit MCLs which were subsequently correlated to rupture of thick collagen fibres using scanning electron microscopy. In the current study, the discontinuous samples tested at 28 MPa had greater percentage of crimp than the continuous samples which may be due to "recoiling" of fibres after rupture. Crimp of fibres after rupture were easily distinguishable from actual functional crimp. First, crimp after fibre rupture was more superficial than functional crimp evident from less distinct banding. Second, this banding had a more irregular pattern with inconsistent and sometimes greater distance between bands. Third, the fibres appear separate from adjacent fibres. Nonetheless, crimp after fibre rupture was classified into the categories previously described for functional crimp using the following modifications: Type II Crimp had irregular and somewhat larger crimp period and Type I Crimp occurred only in a particular fibre separate from its neighbours and not across a group of fibres. For example, crimp analysis of an MCL stretched to failure revealed 51.6% Type I Crimp and 48.4% Type II Crimp using these definitions. Interestingly, Viidik (1972) had previously

documented a slight waviness to tendon collagen fibres that had ruptured at low load levels (one-third of the maximum load); in addition, fibres were noted to glide apart after rupture. Thus, mechanically detectable discontinuities during creep testing are apparently due to damage causing fibre ruptures.

In addition to these discontinuities during static creep, three of the MCLs tested at 28 MPa had mechanically detectable discontinuities in the cyclic creep test after which there was a reduction in modulus. Reduction in modulus was used as an indicator of damage in tendon (156,157) and has been used traditionally in engineering as an indicator for damage especially in composite materials (18). All these findings (mechanical discontinuities, reduction in modulus and damage) suggest that there is some relationship between creep and fatigue at high stresses in this ligament. Traditionally, creep and fatigue have been considered separate phenomena in engineering materials especially when creep occurs under conditions of increased temperature. However, in a viscoelastic material, the phenomena are not so easily separated. In tendon, Wang et al. (1995b) confirmed the two were interrelated. Clearly, the results presented here suggest that future work could seek to better understand the relationship between creep and fatigue in ligament. Further to that point it would be useful to have a morphological marker for damage in ligament and, although it is beyond the scope of this thesis, the characteristics of crimp after fibre rupture described here could be incorporated into the study of creep and fatigue very effectively.

The fifth result of interest was that the creep test stress at which discontinuities occurred was 28 MPa based on area of the total cross-section; however, MCL failure stress from the laboratory database is 95.2 ± 12.4 MPa (failure of the total ligament cross-section). This suggests that different fibres in the cross-section were at different stresses including stresses high enough to cause fibre rupture. Clearly, measurements of area of the total cross-section do not reveal information about stress distribution. The current tests were performed with the joint mounted at 70° flexion. At a different joint position, different fibres in the MCL would be recruited and possibly subjected to different stresses resulting in different areas of damage. Area measurements based on total cross-section oversimplify stress distribution and underestimate the stress on recruited fibres.

Sixth, these resulted showed that, concomitant to confirming that fibres were recruited during creep, there were no differences in the crimp patterns at the start and end of the relaxation tests. This novel finding confirms the speculation made by Fung (1993) that the microstructural processes involved in creep and relaxation were different. Since a static relaxation test requires the strain or deformation to be maintained at a constant value, fibres were not recruited. Thus, during a static stress relaxation test, the recorded behaviour was that of a discrete group of fibres that were recruited initially. The assumption that the creep behaviour of a discrete group of fibres (without recruitment) could be modeled by the inverse relaxation function was confirmed. This was a key assumption in the model of ligament creep described earlier.

Finally, based on the MCL stress-strain curve, 14 MPa was at the transition between the toe and linear region and yet a considerable amount of crimp was evident (only 20% straightened fibres). None the less, after an increase of 0.70% strain, there were 76% straightened fibres. Likewise at 28MPa (a linear region stress), there were 40% straightened fibres pre-creep and, after 1.22% creep strain, there were 94% straightened fibres. There are several possibilities for the fact that crimp is observed at these stresses. First, Viidik (1990) cautioned that the transition between structural events and corresponding regions of the stress-strain curve were gradual. Perhaps, fibre straightening is more gradual in ligament. Since the goal of this study was to compare crimp before and after creep testing, a "snapshot" of crimp immediately upon loading was required. Previous studies might not have captured the crimp pattern upon immediately reaching the stress. Additionally, the fundamental studies that defined the characteristics of crimp and the stress-strain curve used tendon. In fact, the tendon was either isolated tendon units (43,125) or cut to a specified shape with fibre bundles visible on the surface (152,155). In the current study, the full width of the ligament midsubstance was analyzed. The fibre recruitment of the intact ligament would clearly be different to that of an isolated or sectioned tendon. As well, Amiel and Kleiner (1988) documented characteristic differences between the crimp properties of ligaments and tendons of rabbit. Discrepancies may be due to some fundamental difference in recruitment in ligament and tendon. Second, Stouffer et al. (1985), when documenting local crimp of tendon, found that local strain was less than the gross strain measurement. Perhaps, in the

current study, there was a slight undershoot of strain and, as seen in Table 3.4, crimp and strain are highly related in this structure. As described previously, the stress calculation based on gross cross-sectional area underestimated the stress distribution on fibres and this may also be a factor in local fibre behaviour. In the end, the key result is that, at what was defined as the transition between the toe and linear region for the intact ligament, there was still a significant amount of fibre recruitment available to resist creep. However, at what was defined as a linear region stress, fibre recruitment was limited and creep was significantly increased.

In conclusion, this is the first work to quantify creep behaviour of ligaments over a range of stresses. Likewise, it is the first work to quantify crimp distributions in an intact ligament. These new findings taken together show categorically that fibre recruitment is a mechanism for minimizing creep at low, toe region stresses. This is a cleverly designed functional response which serves to prevent joint instability and tissue fatigue during normal activity. Concurrent to quantifying fibre recruitment during creep, fibre recruitment was not found to be a mechanism of stress relaxation. This result is useful for understanding the different structural responses of ligament when subjected to creep and relaxation. Returning to creep behaviour, fibre recruitment and correspondingly resistance to creep was limited at higher stresses. In fact, creep testing at higher stresses revealed that measuring total cross-sectional area to calculate stress oversimplifies the actual stress distribution in the ligament. This unique observation has important implications to the measurement of stress for *in vitro* studies and for the

understanding of how stress is distributed unevenly across the ligament cross-section. In addition to fibre recruitment, water content also appears to have a mechanistic role in creep. A novel finding was that as creep test stress increased, more water was lost during creep testing and less was returned to the ligament during recovery. Looking ahead, since there was variability in the water content after loading, the effect of initial levels of water on creep behaviour still needed to be addressed.

CHAPTER 4

EFFECT OF WATER CONTENT MANIPULATION ON LIGAMENT PRE-STRESS AND CREEP

4.1 Introduction

The mechanical testing described earlier was performed with the ligament enclosed in an environment chamber at 37°C and 99% relative humidity in order to maintain tissue hydration. The results of mechanical tests can be affected by changes in tissue water content. Chimich et al. (1992) documented increased cyclic relaxation in ligaments with increased water content and decreased cyclic relaxation in ligaments with decreased water content. Since water content was shown to affect ligament viscoelasticity measured using stress relaxation, it is likely that creep behaviour will be affected by changes in water content. This may be an important mechanism of creep in normal ligament in addition to the role of fibre recruitment documented earlier.

Inflammation of joints after injury causes swelling of the affected soft tissues (51). Ligaments may be subject to changes in water content as a result of injury (51) or as a result of the treatment of injuries such as ligament reconstruction (127) and joint immobilization (4). Surgical intervention of joints (including ligament grafting) often involves irrigation with salt solutions, possibly altering tissue properties. No one has yet quantified the potentially important effect of increased water content on ligament

pre-stress and resulting creep behaviour. Thus, the expectation was that soaking ligaments in solutions to increase and decrease water content would not change the functional length of ligaments; that is, alter their pre-stress, but would affect their creep behaviour. An increase in water content from normal was expected to cause more creep and a decrease in water content to cause less creep.

Aim 1. To use phosphate buffered saline (PBS; high initial water content) and 25% sucrose solution (SUC; low initial water content) to alter initial water content of ligament and determine the effect of altered water contents on ligament pre-stress and creep behaviour (tested at 4.1 MPa).

Aim 2. To confirm that the manipulation of tissue mechanical properties using these solutions is isolated to water content. For example, to demonstrate that the mechanical properties after soaking in PBS followed by sucrose are the same as the mechanical properties after soaking in sucrose alone. This would indicate that the effects of soaking in PBS were reversed.

4.2 Methods

Normal medial collateral ligaments (MCLs) from female one-year-old New Zealand White rabbits were used in this study. MCL water contents were altered using soaking solutions, either phosphate buffered saline (0.9% PBS; BDH Inc, Toronto, Ontario, Canada) or sucrose (25% SUC; BioRad Laboratories, Richmond, California, U.S.A.). PBS was considered to be close to isotonic and isosmotic for ligament while

sucrose was known to be biologically inert but osmotically active and physiologically compatible with ligament (31). For the single solution tests or soaking in one solution only, the MCL was exposed to that solution for one hour which was previously found to be the time required for equilibrium of water content to develop (31). For the serial solution tests, the MCL was exposed to the first solution for one hour (1:00) and the second solution for one hour and 15 minutes (1:15). Pilot tests were used to determine that the water content of the serial solution tests with this time frame were similar to the single solution tests. The normal MCLs from 34 rabbits were assigned to subgroups according to the schedule shown in Table 4.1. Since all were normal, the ligaments were simply randomized into subgroups. A water bath at 37°C equipped with a container for the solution to soak the limb was used instead of an environment chamber (Figure 4.1).

After standardized dissection, the knee joint was mounted in a materials testing system (MTS Systems Corporation, Minneapolis, Minnesota, U.S.A.). Compression-tension cycles (CT cycles) consisting of two cycles of 5 N compression and 2 N tension were performed prior to isolation of the MCL (Figure 4.2). Additional CT cycles were performed ending at 0.1 N tension to establish "ligament zero". The MCL was loaded to a sustained load of 5 N tension to facilitate measurement of cross-sectional area. Then, CT cycles were performed to re-establish "ligament zero" immediately prior to soaking. After the last cycle ended at 0.1 N tension, the crosshead displacement was set equal to 0 mm. This crosshead displacement is the "ligament zero" prior to soaking or "oldlig0".

Table 4.1: Designated Test Groups for Normal and Soaked MCLs

Unilateral Limb n = ligaments	Creep n	Water n / point	Contralateral Limb n = ligaments	Creep n	Water n / point
normal normal	4 3	4 / post-test (crimp)	normal		4 / pre-test
Sucrose (SUC) 1:00	4	4 / post-test	Sucrose (SUC) 1:00		4 / pre-test
PBS 1:00 no manual 0 *PBS 1:00 no manual 0*	4 *1*	4 / post-test *1 / post-test*	PBS 1:00 no manual 0 *PBS 1:00 manual 0*	 *1*	4 / pre-test *1 / post-test*
PBS 1:00 manual 0 *PBS 1:00 manual 0* *PBS 1:00 manual 0* PBS 1:00 manual 0	3[a] *1* *2*	2 / post-test *1 / post-test* *2 / post-test* 4 / pre-test	serial soak pilot tests *PBS 1:00 no manual 0* *SUC 1:00 & PBS 1:15* serial soak pilot tests	 *1* *2*	 *1 / post-test* *2 / post-test*
SUC 1:00 & PBS 1:15 *SUC 1:00 & PBS 1:15*	 *2*	3 / pre-test *2 / post-test*	PBS 1:00 & SUC 1:15 *PBS 1:00 manual 0*	 *2*	3 / pre-test *2 / post-test*
PBS 1:00 & SUC 1:15 manual 0 PBS 1:00 & SUC 1:15 no manual 0	2 1	2 / post-test 1 / post-test	SUC 1:00 manual 0 serial soak pilot tests	1[b]	1 / post-test

Italicized lines are repeated for clarity, "pre-test" water content was assessed immediately prior to creep testing and "manual 0" indicates that the creep test was started at 0 mm.

"a" water content of one sample not measured and "b" one sample had test program error

Figure 4.1: **(a) Top View of Water Bath for Single and Serial Solution Tests (b) Side View of Grips, Knee Joint with Isolated MCL, and Container for Soaking Solution**

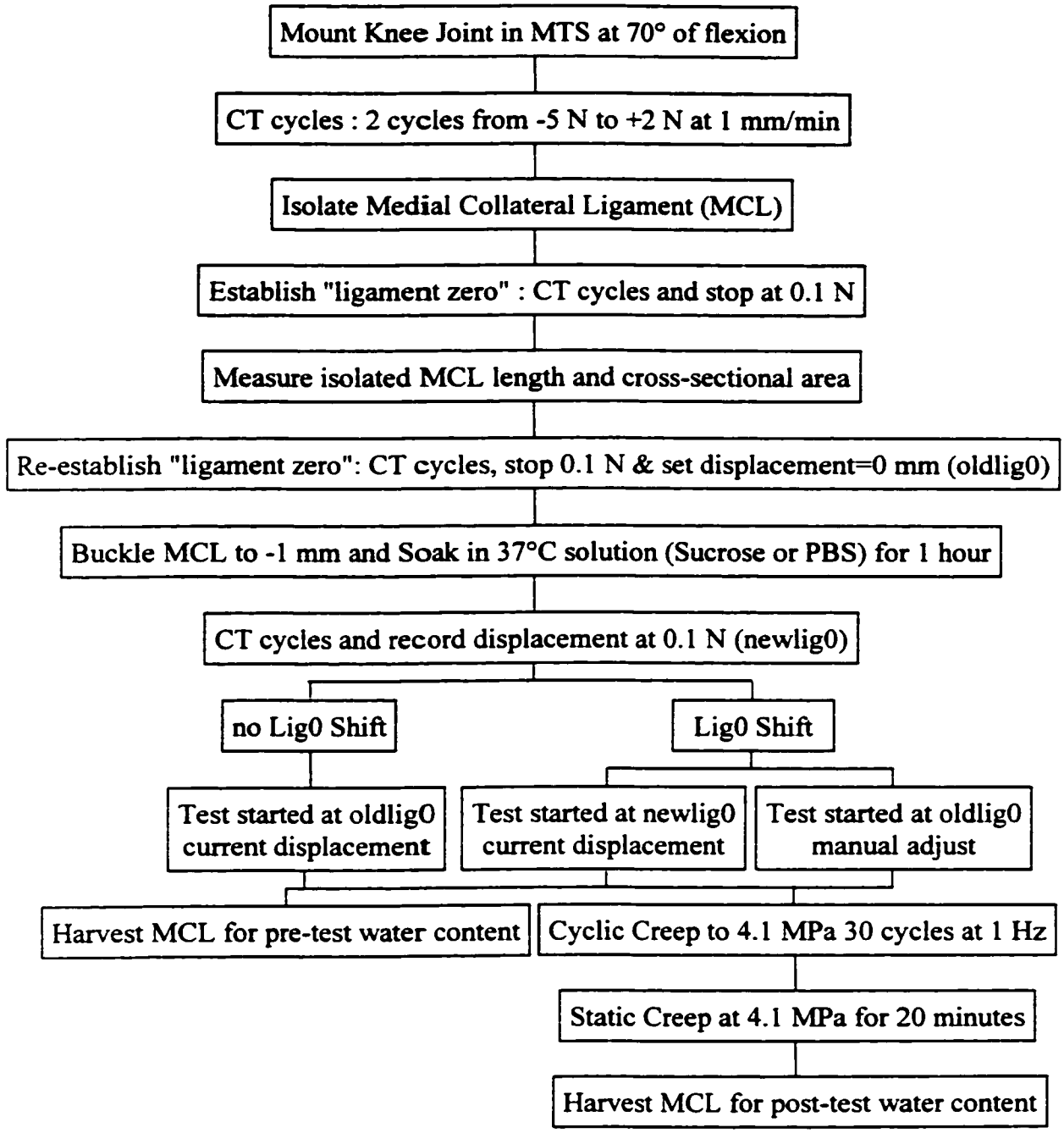

Figure 4.2: Single Solution Test Protocol

"PBS" is phosphate buffered saline and "CT" is compression-tension

"Lig0 Shift" is the shift in "ligament zero" as a result of soaking.

4.2.1 Single Solution Tests

For the single solution tests, the MCL was then surrounded with the soaking solution, buckled to -1 mm and maintained in this state for one hour. Additional CT cycles were then performed and the displacement corresponding to 0.1 N tension was recorded. Thus, the shift in "ligament zero" due to soaking could be determined (Lig0 Shift). If no shift occurred, the creep test was therefore started from the original "ligament zero" or "oldlig0". If a shift occurred, creep tests were started either (a) at the displacement corresponding to 0.1 N tension after soaking (i.e. the current displacement) or "newlig0", or (b) at the original "ligament zero" prior to soaking or "oldlig0". In the second case, the crosshead was manually returned to 0.03 ± 0.03 mm measured from "oldlig0".

A creep test stress of 4.1 MPa was used because it was in the toe region of a normal rabbit MCL failure stress-strain curve and is thus thought to be a functional stress. For all MCLs, the creep test stress was based on the cross-sectional area measured before exposure to the soaking solutions and thus was the same for every subgroup regardless of changes in hydration. Cyclic creep was 30 cycles from the starting point (as described above) to 4.1 MPa at 1 Hz. The ligament was then immediately loaded to 4.1 MPa and held at that stress for 20 minutes for the static creep test. Normal ligaments were creep tested at 4.1 MPa (listed as the 4.1 MPa creep group in Chapter 3).

Stress was applied to the MCL using a force based on the cross-sectional area of the MCL measured before soaking. Strain was defined as the deformation of the MCL

divided by the undeformed MCL length. Total creep strain was defined as the increase in strain from the peak of the first loading cycle in the cyclic creep test to the end of the 20 minute static creep test. Water contents of MCLs were assessed after creep testing (post-test). In addition, the pre-test water content of MCLs were assessed after soaking and at the "ligament zero" appropriate for that test group.

4.2.2 Serial Solution Tests

For the serial solution tests (soaking in one solution followed by the other solution), the protocol was the same up to the end of the first one hour (1:00) soaking step (Figure 4.3). Then, once the CT cycles were performed and the displacement at 0.1 N tension was recorded, no adjustment to the crosshead position was made. The solutions were exchanged and the MCL was buckled to -1 mm to soak in the alternate solution for 1 hour and 15 minutes (1:15). Then, additional CT cycles were performed and the displacement at 0.1 N tension was recorded. Thus, the shift in "ligament zero" after the first soaking and second soaking steps were measured. The difference in these measurements is the shift in "ligament zero" in the second solution. The MCL was then manually returned to "ligament zero" prior to soaking (oldlig0). The remainder of the creep test protocol was identical to the single solution test protocol starting the creep test from "oldlig0". Water content assessment and creep testing were performed in the same manner as for the single solution tests.

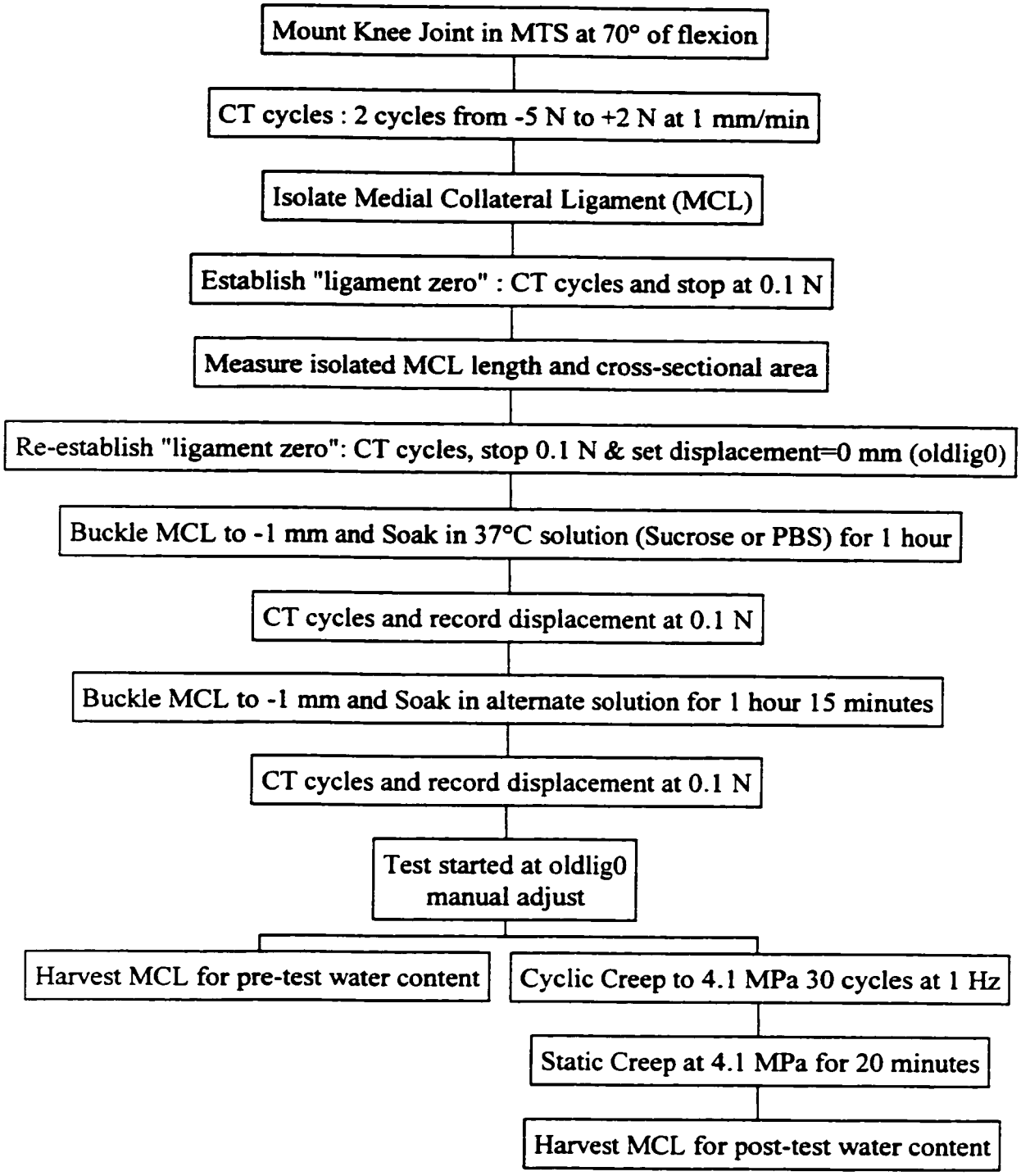

Figure 4.3: Serial Solution Test Protocol

"PBS" is phosphate buffered saline and "CT" is compression-tension

Two pairs of MCLs were used to measure changes in the cross-sectional area due to soaking. Two additional pairs of MCLs were used to examine the effects of adding protease inhibitors to the PBS and the effects of loading frequency on PBS tests started from "newlig0". In cases where paired data was compared, paired t-tests were used (including data in Table 4.1). All other data were analyzed using analysis of variance with statistical significance defined at $p=0.05$.

4.3 Results

4.3.1 Single Solution Tests

Soaking in both sucrose and PBS for 60 minutes when the MCL was buckled altered the water contents of the ligaments prior to mechanical testing. Sucrose decreased and PBS increased the water content of normal MCLs by 15% and 5%, respectively (Figure 4.4). Thus, pre-test water content of both sucrose and PBS groups were significantly different than normal ($p<0.001$). The two PBS groups (see Figure 4.4) were not different from each other pre-test. Post-test water contents of all PBS newlig0, PBS oldlig0, and normal groups were lower than their pre-test values ($p<0.0004$). Water contents of sucrose soaked MCLs were not different pre-test and post-test. The PBS oldlig0 group had post-test water content significantly less than PBS newlig0 ($p=0.02$).

MCLs tested in PBS had a shift in "ligament zero" to -0.08±0.03 mm at 0.1 N and increase in tension to 1.31 ± 0.77 N at 0 mm (Table 4.2). The sucrose soaked MCLs, on the other hand, showed no shift in "ligament zero". The shift in "ligament zero" and the

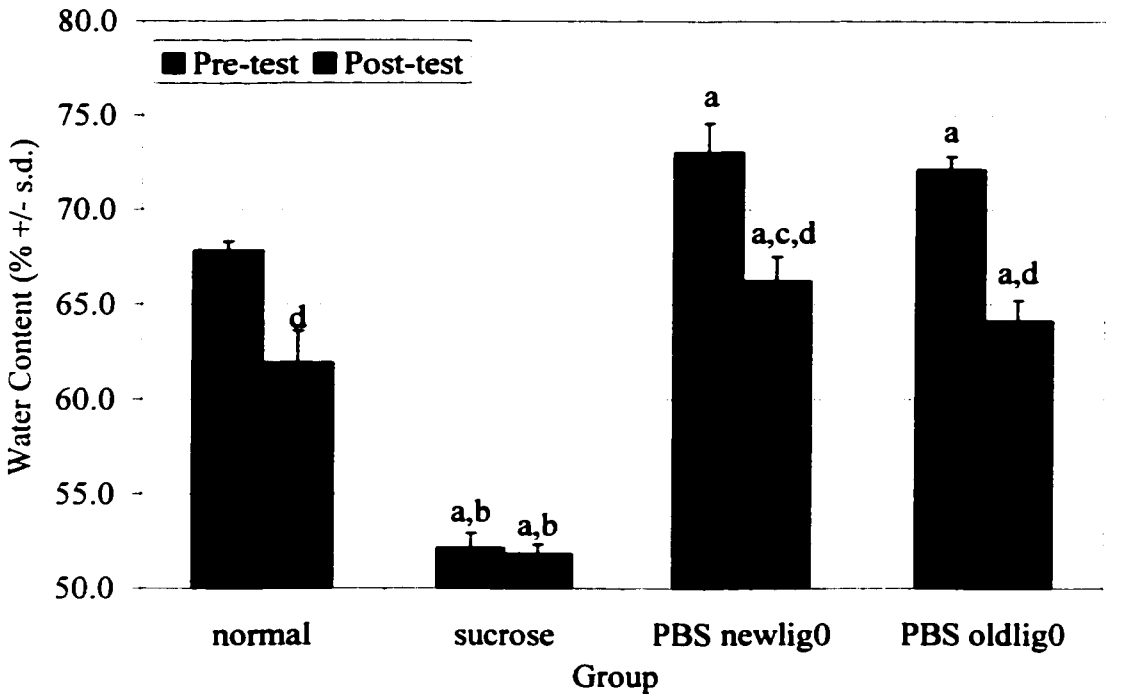

Figure 4.4: Pre-test and Post-test Water Contents of Normal and Soaked MCLs

Pre-test water content was assessed at "ligament zero" appropriate for that group.

Post-test water content was assessed after the creep test.

"s.d." indicates standard deviation

a = different than normal at same test timepoint ($p<0.02$)

b = different than both PBS groups at same test timepoint ($p<0.0001$)

c = different than PBS oldlig0 at same test timepoint ($p=0.02$)

d = different than Pre-test (includes paired data) ($p<0.003$)

Table 4.2: Shift in "ligament zero" and Pre-Stress of Normal and Soaked MCLs

Measurement	Normal	n	Sucrose	n	PBS newlig0	n	PBS oldlig0	n
Lig0 Shift (mm)	n/a		0.00±0.02	4	-0.10±0.03[a]	5	-0.07±0.04[a]	6
Creep Start Point (mm)	0.00±0.01	7	-0.01±0.02	4	-0.10±0.03[b]	5	0.03±0.03	6
Preload at 0 mm (N)	0.11±0.06	7	0.33±0.18	4	1.77±0.84[c]	5	0.92±0.48[c]	6

"Lig0 Shift" is the shift in "ligament zero" as a result of soaking.

For the PBS oldlig0 group the shift in "ligament zero" was manually removed by returning the MCL to approximately 0 mm, that is, the crosshead displacement where "ligament zero" was set prior to soaking in PBS.

Data are shown as mean ± standard deviation and "n/a" indicates measurement is not applicable.

"a" indicates pooled PBS Lig0 Shift (-0.08 ± 0.03 mm; n=11) is different than sucrose ($p=0.0005$)

"b" indicates different than normal, sucrose and PBS oldlig0 ($p<0.0001$)

"c" indicates pooled PBS Preload (1.31 ± 0.77 N; n=11) is different than normal ($p=0.0003$) and sucrose ($p=0.008$)

pre-stress of PBS soaked MCLs were thus greater than for the sucrose soaked MCLs ($p<0.008$). The creep test start point is "ligament zero" after soaking for the PBS newlig0 group but has been manually adjusted to 0.03±0.03 mm from the "ligament zero" prior to soaking for the PBS oldlig0 group. Creep testpoint strains (cyclic initial and static final) were measured relative to the creep test start point to account for this difference between PBS newlig0 and PBS oldlig0.

Sucrose decreased (0.29 % strain) and PBS newlig0 (0.58 % strain) increased total creep strain compared to normal MCLs (Figure 4.5). Total creep strains of the PBS newlig0, normal and SUC groups were all significantly different ($p<0.004$) from each other. The PBS oldlig0 group had total creep strain greater than normal and less than PBS newlig0 ($p<0.02$). For both PBS groups and normal MCLs, the cyclic initial strain (C1) was significantly less ($p<0.002$) than the sucrose group (Figure 4.6). The static final strain (Sf) was significantly greater ($p<0.01$) for the PBS newlig0 group over all groups (Table 4.3). The final strain for all groups relative to their "ligament zero" prior to soaking (oldlig0) were similar.

The cross-sectional area of MCLs was measured before and after soaking in the solutions (Table 4.4). In order to measure cross-sectional area, the soaking solution and water bath had to be removed briefly exposing the MCL to the air to permit access of the area caliper. It is interesting to note that the water content of the MCLs that had this second area measurement were less than the water content of MCLs at the same test time point that did not undergo an additional area measurement. The act of measuring the

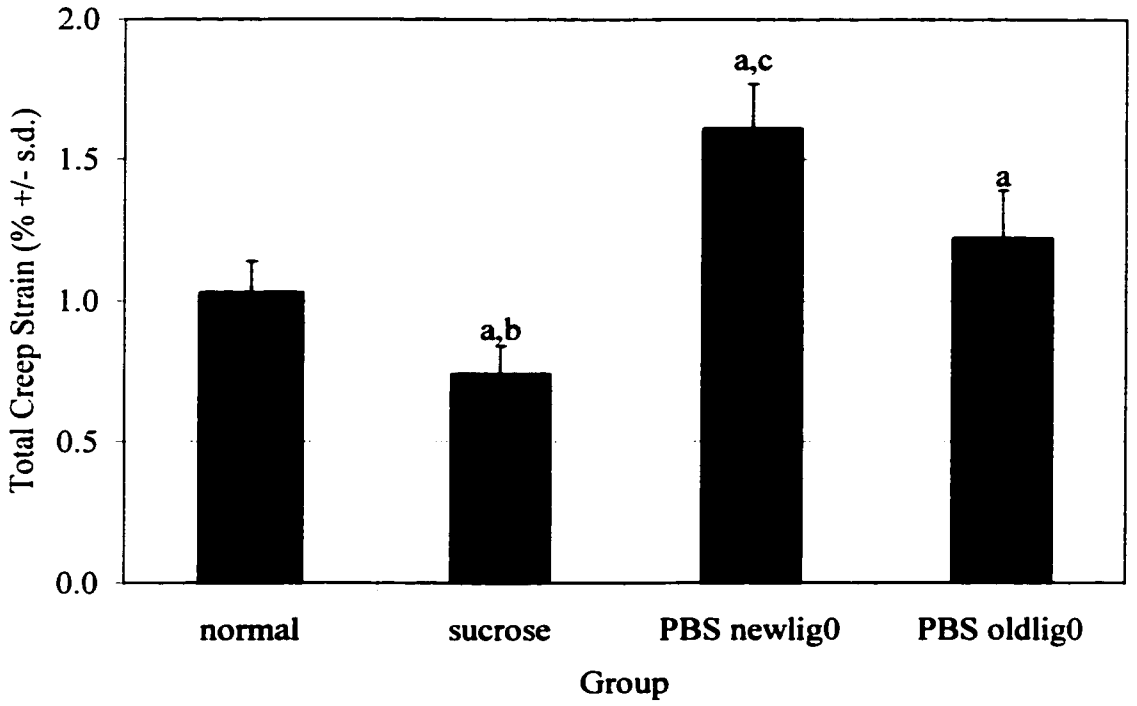

Figure 4.5: Total Creep Strain of Normal and Soaked MCLs

"s.d." indicates standard deviation

a = different than normal ($p<0.02$)

b = different than both PBS groups ($p<0.0001$)

c = different than PBS oldlig0 ($p=0.0002$)

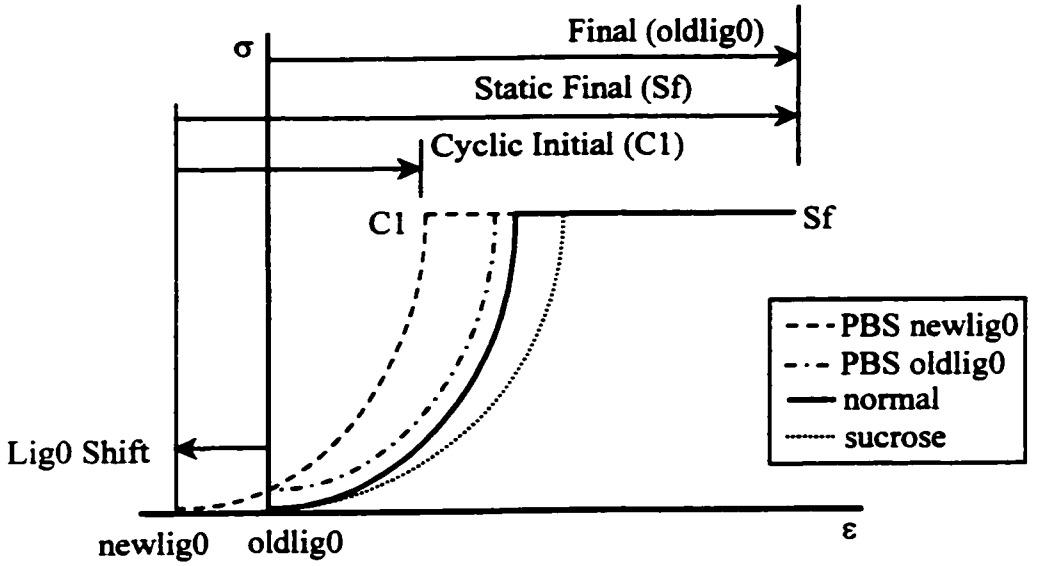

Figure 4.6: Creep Testpoint Strain of Normal and Soaked MCLs

"σ" indicates stress and "ε" indicates strain

"oldlig0" is the "ligament zero" set prior to soaking (set to 0 mm at 0.1 N tension).

"newlig0" corresponds to the crosshead displacement at 0.1 N tension after soaking.

"Lig0 Shift" is the shift in "ligament zero" as a result of soaking.

Cyclic Initial (C1) and Static Final (Sf) are measured relative to the creep test start point.

Final (oldlig0) is measured relative to "ligament zero" set prior to soaking.

Table 4.3: Creep Testpoint Strains for Normal and Soaked MCLs

Testpoint	Normal	n	Sucrose	n	PBS newlig0	n	PBS oldlig0	n
Lig0 Shift (%)	n/a		0.00±0.07	4	-0.41±0.11[a]	5	-0.31±0.15[a]	6
Cyclic Initial (%)	1.60±0.04	7	1.89±0.20[b]	4	1.60±0.15	5	1.44±0.19	6
Static Final (%)	2.63±0.27	7	2.63±0.27	4	3.20±0.13[c]	5	2.66±0.31	6
Final (oldlig0) (%)	2.65±0.10	7	2.61±0.33	4	2.77±0.18	5	2.77±0.33	6

"Lig0 Shift" is the shift in "ligament zero" as a result of soaking. Cyclic Initial and Static Final are measured relative to the creep test start point. Final (oldlig0) is relative to "ligament zero" prior to soaking. All testpoints are shown in Figure 4.5.

Data are shown as mean ± standard deviation and "n/a" indicates measurement is not applicable.

"a" indicates different than sucrose ($p<0.002$)

"b" indicates different than normal, PBS oldlig0 and PBS newlig0 ($p<0.01$)

"c" indicates different than normal, sucrose and PBS oldlig0 ($p<0.001$)

Table 4.4: Cross-sectional Area Change as a Result of Soaking and Water Content Change as a Result of Area Measurement

	Pre-soak Area (mm^2)	**Post-soak Area (mm^2)**	**Mean Area Change ($mm^2 \pm$ s.d.)**	**Post-area Water Content[a] (% ± s.d.)**	**Post-soak Water Content[a] (% ± s.d.)**
PBS			+ 0.22±0.09 [b]	68.7±0.6 [d]	72.1±0.7 (n=4)
1 left	4.85	5.13			
2 right	4.51	4.66			
Sucrose			- 0.36±0.04 [c]	47.1±0.1 [d]	52.1±0.8 (n=4)
1 right	5.07	4.74			
2 left	4.30	3.92			

"a" Post-area water content was measured after the second area measurement (i.e. measured after the first area measurement, one hour soak and second area measurement were completed). Post-soak water contents are the pre-test water contents (i.e. measured after one area measurement and the one hour soak were completed). Normal pre-test water content measured immediately prior to creep testing was 67.8 ± 0.5 % (n=4).

"b" indicates an increase in area ($p=0.09$)

"c" indicates a decrease in area ($p=0.02$)

"d" indicates different from Post-soak water content ($p<0.004$)

cross-sectional area while exposed to air may have caused a decrease in water content. The PBS samples had an increase in area after soaking despite this decrease in water content (n=2; p=0.09). The sucrose samples had a decrease in area after soaking (n=2; p=0.02).

The action of proteases during soaking did not affect the creep behaviour. When protease inhibitors were added to the PBS of one MCL tested from newlig0, the total creep strain (1.80%) was within the range of the PBS test without protease inhibitors (1.44% to 1.85%; n=5). Likewise, when the test of the contralateral limb was started at oldlig0, the total creep strain (1.47%) was within the range of creep tests in PBS without protease inhibitors (0.99% to 1.51%; n=6).

Loading frequency was also eliminated as a factor for the difference in creep. The time to load from 0 mm to the peak of the first cycle was two-fold larger for the PBS oldlig0 group compared to the PBS newlig0 group owing to the different creep test start points (Table 4.5). A pair of MCLs was tested from PBS newlig0 with the loading frequency of one limb greater than the other. The paired samples showed that a two-fold increase in the time to load to the peak of the first cycle did not affect the total creep strain (Table 4.5).

4.3.2 Serial Solution Tests

Serial soaking in PBS for one hour followed by sucrose for 1 hour and 15 minutes decreased the water content to the same value as soaking in sucrose alone (Table 4.6).

Table 4.5: First Cycle Loading Frequency Altered for Pair of PBS newlig0 Samples

Measurement	PBS oldlig0 (n=5)	PBS newlig0 (n=6)	Right MCL (n=1)	Left MCL (n=1)
Start of Cycle to Peak of Cycle				
strain (%)	1.44±0.19	1.60±0.15	1.52	1.80
time (seconds)	0.70±0.02	0.70±0.01	0.54	1.05
Start of Cycle to 0 mm				
strain (%)	0	-0.43±0.11	-0.26	-0.10
time (seconds)	0	0.35±0.03	0.18	0.16
0 mm to Peak of Cycle				
strain (%)	1.44±0.19	1.17±0.26	1.26	1.70
time (seconds)	0.70±0.02	0.35±0.04[a]	0.36	0.89
Total Creep Strain (%)	1.22±0.17	1.61±0.16[a]	1.33	1.33

Data are shown as mean ± standard deviation.

"a" indicates different than PBS oldlig0 ($p<0.004$)

Table 4.6: Pre-test Water Contents of MCLs with Single or Serial Solution Protocols

Protocol	Single Solution	n	Serial Solution	n
Sucrose 1:00	52.1 ± 0.8 %	4		
PBS 1:00 & Sucrose 1:15			53.2 ± 0.3 %	3
PBS 1:00	72.1 ± 0.7 %	4		
Sucrose 1:00 & PBS 1:15			71.7 ± 0.6 %	3

Data are shown as mean ± standard deviation.

The same soaking times produced similar water contents for single and serial soaking in PBS. The shift in "ligament zero" for creep tested MCLs with PBS single and serial solution protocols were similar (Table 4.7). The total creep strain of the PBS serial soaked MCLs (1.34% and 1.52%) were within the range of the single solution creep behaviour (0.99% to 1.51%; n=6) (Table 4.8). Examining only the two samples of paired data would suggest that the total creep strain of the serial soaked MCLs were different than the single soaked MCLs ($p=0.05$). However, when the larger number of samples from the complete single solution data set was used (n=6), no significant difference in the total creep strain of PBS single and serial soaked MCLs was detected ($p=0.2$). The post-test water content of the PBS serial and single soaked MCLs was similar. The total creep strain of normal MCLs soaked in PBS was the same those soaked in sucrose and then PBS.

The creep tested MCLs that were soaked in sucrose alone revealed a negligible shift in "ligament zero" (shown in Table 4.2 in mm and Table 4.9 in % strain). However, when examining the MCLs soaked in sucrose alone that were not creep tested but used only to assess water content, a small shift in "ligament zero" was recorded (-0.13 ± 0.07 %). Thus, soaking in sucrose alone can cause a small shift in "ligament zero". This same observation was made when MCLs were soaked in PBS and then soaked in sucrose. After soaking in PBS, soaking in sucrose created an additional strain shift in "ligament zero" (-0.15 ± 0.06 %). Thus, the shift in "ligament zero" due to soaking in sucrose was similar in the serial and single solution tests (Table 4.9).

Table 4.7: Shift in "ligament zero" for Creep Tested MCLs with Single and Serial Solution Protocols in PBS Manually Returned to "ligament zero" Set Prior to Soaking

Protocol		n	Lig0 Shift PBS (%)
Single Solution	**PBS 1:00**	6	-0.31±0.15
Serial Solution	**Sucrose 1:00 & PBS 1:15**	2	-0.32±0.23

Data are shown as mean ± standard deviation.

"Lig0 Shift" is the shift in "ligament zero" as a result of soaking.

Single solution data set includes paired data of serial solution data set. The shift in "ligament zero" is not statistically different comparing the serial solution data to either the paired (n=2) or complete (n=6) single solution data set ($p>0.8$).

Table 4.8: Total Creep Strain for Creep Tested MCLs with Single and Serial Solution Protocols in PBS Manually Returned to "ligament zero" Set Prior to Soaking

Protocol	**Total Creep Strain (%)**	**Total Creep Strain (%) mean ± s.d.**	**n**	**Water Content (%) mean ± s.d.**	**n**
Single Solution		1.22±0.17	6	64.1±1.1	5
1 right	1.24				
2 left	1.51				
3 right	1.14				
4 left	0.99				
5 right	1.30				
6 left	1.14				
Serial Solution		1.43±0.13[a]	2	65.3±2.1	2
5 left	1.52				
6 right	1.34				

"s.d." indicates standard deviation

"a" paired data set for single solution 1.22 ± 0.11 % (n=2) compared to serial p=0.05

complete data set for single solution 1.22 ± 0.17 % (n=6) compared to serial p=0.2

Table 4.9: Shift in "Ligament Zero" for MCLs with

Single and Serial Solution Protocols in Sucrose

Timepoint	n	Lig0 Shift Sucrose (%)
Single Solution Sucrose 1:00		
Not Creep Tested	4	-0.13±0.07
Creep Tested no manual 0	4	0.00±0.07
Creep Tested manual 0	1	-0.12
mean ± s.d.	9	-0.07±0.09
Serial Solution PBS 1:00 & Sucrose 1:15		
Not Creep Tested	3	-0.14±0.08
Creep Tested manual 0	2	-0.18±0.03
Creep Tested no manual 0	1	-0.14
mean ± s.d.	6	-0.15±0.06

"s.d." indicates standard deviation

"Lig0 Shift" is the shift in "ligament zero" as a result of soaking.

"manual 0" indicates that the MCL was manually returned to 0 mm.

Because the shift in "ligament zero" of the MCLs that were soaked in PBS followed by sucrose was not negligible, the creep test was started at 0 mm requiring a manual zero step. The previous creep tests of sucrose soaked MCLs were performed without a manual zero step. In order to compare the sucrose serial and single solution protocols, two additional tests were performed: (a) one single solution creep test with a manual zero and (b) one serial solution creep test without manual zero (Table 4.10). The total creep strain of MCLs soaked in sucrose had comparable creep behaviour to those soaked in PBS and then sucrose (Table 4.10). The post-test water content of the single and serial soaked groups were similar.

4.4 Discussion

These results show five interesting things. To start, this investigation is, to the author's knowledge, the first to document that increased water content can create a pre-stress in ligament. Before soaking in the PBS solution, "ligament zero" was set as the MCL was unloaded from two compression-tension cycles stopping at 0.1 N tension. At the 0.1 N tension, the displacement was set to 0 mm. The ligament was then buckled and soaked in PBS. Then, when the compression-tension cycles were performed again and the test was stopped at 0.1 N tension, the displacement was no longer 0 mm but had decreased to a negative value. "Ligament zero" was shifted or, rather, the functional length of the ligament decreased as a result of increasing the water content. Soaking shifted the displacement at 0.1 N tension to a negative value (no longer 0 mm) and thus

Table 4.10: Total Creep Strain for MCLs with

Single and Serial Solution Protocols in Sucrose

Protocol	**Total Creep Strain (%)**	**Total Creep Strain (%) mean± s.d.**	**n**	**Water Content (%) mean± s.d.**	**n**
Single Solution		0.72±0.10	5	52.7±2.0	5
no manual 0					
1 right	0.75				
2 left	0.67				
3 right	0.66				
4 left	0.87				
manual 0					
5 left	0.63				
Serial Solution		0.76±0.03	3	52.9±0.5	3
manual 0					
5 right	0.79				
6 left	0.75				
no manual 0					
7 right	0.73				

"s.d." indicates standard deviation

"manual 0" indicates that the MCL was manually returned to 0 mm.

ligament laxity was decreased since ligament laxity was defined as the difference in displacement measured between 0.1 N tension and 0.1 N compression. When the tissue was returned to 0 mm, the stress on the ligament was a larger positive value than recorded before soaking; that is, the ligament had a pre-stress as a result of increasing the water content.

Second, these results showed that the decrease in ligament functional length was accompanied by an increase in cross-sectional area. These changes in geometry were required to satisfy a new stress equilibrium and altered the conditions for collagen fibre recruitment. The cyclic initial deformation for the PBS soaked ligaments (increased water content) was less than for the sucrose soaked ligaments (decreased water content). The interaction between the collagen fibres and the increased amount of water in the PBS soaked ligament allowed the ligament to be recruited into tension faster. Panagiotacopulos et al. (1979) used polymer theory to explain how increased water content caused increased relaxation of intervertebral disc material. The increased presence of water in the tissue increased the freedom with which molecular chain segments could move relative to each other. Apsden (1988) employed a similar theory of molecular rearrangement to model changes of mechanical properties of the cervix due to increased water content. In the sucrose case, the state of interaction between the collagen fibres and water allowed for less freedom for molecular rearrangement and thus slower recruitment into tension than in the PBS case.

The third interesting feature of these results was that these changes in water content affected ligament creep behaviour. The sucrose group had pre-test water content significantly lower than normal, no change in water content post-creep, and significantly lower total creep strain than normal. The PBS groups had pre-test water content significantly greater than normal, had significantly reduced water content post-creep and had significantly greater creep strain than normal. This is in agreement with previous observations of the effect of water content on another viscoelastic property, stress relaxation. Chimich et al. (1992) showed that immature rabbit MCLs immersed in 25% sucrose (50% initial water content) had 15% cyclic relaxation; whereas, those immersed in PBS (74% initial water content) had 45 % cyclic relaxation. Likewise, Haut and Haut (1997) found that human patellar tendon had faster static relaxation in hypotonic solutions (distilled water) than in hypertonic solutions (25% sucrose). The interaction between the water and the fibres suggests a greater freedom for creep in the case where more water is present. The tissue with less water had a corresponding increased resistance to creep.

Fourth, the PBS soaked ligaments loaded from the pre-stressed state had significantly less total creep strain than the PBS soaked ligaments loaded from the unloaded state. The pre-stressed state is the displacement where "ligament zero" was set prior to soaking (0 mm; oldlig0) and the unloaded state is the displacement at "ligament zero" after soaking (0.1 N; newlig0). Of equal importance was that the MCLs loaded from the pre-stressed state had significantly greater water loss during creep testing than

those loaded from the unloaded state. The differences in water content are suggestive of differences in the interaction between the water and fibres in the two cases. Previously, limited fibre recruitment and, correspondingly, increased creep occurred when fibres were straightened at a 28 MPa creep test stress (i.e. there were no more fibres available to recruit). Abnormally increased water content resulted in increased creep and may have created the condition where fibres were already recruited. However, loading these fibres from the pre-stressed state would have further limited the potential fibre recruitment. This would have increased creep, not decreased creep as observed here. Alternatively, what may be the case is that increased water content prevents the fibres from being engaged to resist creep. As suggested by the polymer analogy (117), increased water content may permit greater freedom of movement of collagen fibres relative to each other within the limits of the collagen fibre-ground substance network, facilitating increased creep from the unloaded state. Loading from a pre-stressed state may dissipate some of the viscous component of the response, reducing the freedom of movement of collagen fibres and allowing these fibres to become recruited to resist creep. The fact that more water is exuded during creep from the pre-stressed state could suggest that more fibres are being recruited and less space is available for the water to occupy. Alternatively, increased water loss may have occurred because the water was more mobile (less of the water was bound to the GAGs in the ground substance).

Fifth, reversible changes in mechanical properties were observed in both solutions; therefore, the solutions affected water content alone. The ligaments soaked in

sucrose alone had similar mechanical behaviour of the ligaments soaked in PBS followed by sucrose. The important implication of this result is that whatever mechanism caused increased creep in PBS was completely reversed by soaking in sucrose. The most likely factor is the increased water content. Others have shown that articular cartilage and intervertebral disc material become more deformable with increased hydration (103,109,117). Prolonged exposure to PBS (24 hours) has recently been shown to extract protein fragments related to fibronectin and albumin (35). Small quantities of fibronectin are found in the ligament matrix and albumin is secreted by various cell lines in the body. To date, the mechanical role of these proteins is largely unknown. Given the reversibility of the mechanical changes in the present study, the one hour soaking time may not have been long enough to permit protein extraction, or the mechanical role of these protein are not critical to low-load viscoelastic behaviour.

Reversible mechanical changes were also observed for sucrose comparing PBS soaked ligaments to those soaked in sucrose followed by PBS. The decreased creep response of the sucrose soaked ligaments is likely due to the reduction in hydration. Dehydrated rat tail tendon has increased stiffness and strength (19,47). Because the changes were reversible it is unlikely that the sucrose promoted additional cross-linking such as that observed in *in vitro* models of diabetes in which connective tissues are treated with glucose, resulting in increased tissue stiffness (123). Non-enzymatic glycation is the reaction of the glucose, a reducing sugar, with amino groups of collagen

producing a crosslink (90,124). Because sucrose does not have a reducing group (140), it is unlikely that it made this type of crosslink with collagen.

To conclude, new information about the effect of water content on creep was shown by these results: increased water content increased creep and decreased water content decreased creep. In addition, the fact that increased water content created a pre-stress in ligament was a novel and unexpected result. Essentially, water set the functional length of these ligaments and altered the conditions for fibre recruitment. Clearly, water has an important functional role which influences the stress state of the ligament, the collagen fibres, and likely the cells in the ligament. In addition to this mechanical evidence, morphological evidence of the effect of water on collagen fibre recruitment would be instructive, although its changes to crimp are likely too subtle to apply the methods previously described. These unique observations show that maintenance of physiological water content is thus critical to *in vitro* mechanical testing of soft tissues, as deviation from normal water content changes ligament functional length and creep behaviour. Water appears to have a key role in the creep of ligament that has increased water content by virtue of treatment or injury.

CHAPTER 5

CREEP BEHAVIOUR AND CREEP MECHANISMS OF HEALING LIGAMENTS

5.1 Introduction

Collagen fibre recruitment and increased water content have been shown earlier to be mechanisms of creep in normal ligaments. The mechanisms of creep in healing ligaments are of critical importance considering that some ligament grafts have been shown to "stretch out" with healing (99). This is the first investigation to quantify the creep behaviour of healing ligaments. The material properties of scars are inferior to normal ligament (52), and excessive creep of healing ligaments could contribute to joint dysfunction by causing either temporary or permanent abnormalities in joint kinematics. Therefore, the creep behaviour of control ligaments (normals and contralaterals) was compared to that of ligament gap scars (experimentals) at various stages of healing (144). Based on the evidence that early healing MCLs are much more lax in stress-inducing models of combined ligament instability (25,70,164), the hypothesis was that early ligament scars in isolated MCL injuries would creep more than normal ligament and that this creep would decrease but remain abnormal over time. Also of interest was a description of the water contents of these tissues before and after creep testing as the first step in identifying a potential role of water in this viscoelastic response (31,69). Further,

the effect of the order of cyclic creep and static creep was examined. The hypothesis was that the cumulative creep strain from cyclic and static creep testing would be similar regardless of the order of cyclic and static creep. Finally, drawing on other previously published data regarding biochemical (52,56) and morphological (54,55,135) properties of this specific gap model of scar, it is possible to speculate on mechanisms of scar creep.

Aim 1. To quantify the creep of fresh healed unilateral gap injury MCLs and contralateral MCLs at various healing intervals. MCL scars at 3, 6 and 14 weeks of healing were tested at 2.2, 4.1 and 7.1 MPa, respectively. An additional group of 6 week scars were included to examine the effect of cyclic and static creep test order inversion.

Aim 2. To quantify the water content pre-test and post-recovery to document any relationship between initial water content or water content loss and creep testing.

Aim 3. To use previous quantification of scar properties at these same healing intervals and determine if correlations between these morphological and biochemical indices and creep exist.

5.2 Methods

In this study, a well characterized animal model was used in which a standardized length of bridging ligament scar could be isolated and quantified using multiple techniques. Standardized surgeries (30) were performed on the right MCLs of 32 one-year-old female New Zealand White rabbits. By removing a small (2.0±0.5 mm) segment of the MCL an acute 4.0±0.5 mm gap in the midsubstance was created due to a slight

retraction of the cut ends (Figure 5.1). The four corners of these cut ends were demarcated with 6-0 nylon sutures to identify the ligament ends and intervening scar tissue at sacrifice. The resulting scars were harvested at 3 weeks (n=11), 6 weeks (n=11), and 14 weeks (n=10) of healing (Table 5.1). Three MCLs at each time interval were used to assess pre-test water content. The remaining MCLs were used to assess creep behaviour (cyclic creep followed by static creep) and post-recovery water content.

The failure strengths of scars have been shown to increase with healing time: 7.4±2.3, 13.8±6.7, and 23.7±7.9 MPa at 3, 6 and 14 weeks of healing, respectively (unpublished data in addition to Chimich et al. (1991)). A standardized method for comparing the creep properties of these scars with documented changing mechanical properties was required. The stress at which the creep test was performed was a constant 30 percent of the particular scar failure strength. The resulting creep test stresses for the 3, 6 and 14 week healing intervals were 2.2, 4.1 and 7.1 MPa, respectively. The use of a constant stress-strength ratio to compare creep tests of materials with different failure strengths is common engineering practice (masonry (5), concrete (112), polymer (65), prestressing steel (34)). The 30% stress-strength ratio was based on the limits of the MTS test system (MTS Systems Corporation, Minneapolis, Minnesota, U.S.A.) because we had to ensure that the command load for the weakest scar (3 week) was large enough to be controlled by the system. Each left MCL served as a contralateral control (60) and was tested at the same stress as its scar, allowing for comparison of the tissue behaviour in the same healing interval under similar conditions of stress, regardless of failure strength.

Figure 5.1: **(a) MCL Gap with Sutures Demarcating Cut Ends**

(b) Appearance of MCL Gap Scar at 6 weeks

Table 5.1: Experimental Design for MCL Gap Scars and Normals

Group	Creep Tested	allotted n	revised n*	Water Content	allotted n	revised n*
3 week scar	no			pre-test	3	3
3 week contralateral	no			pre-test	3	3
3 week scar	2.2 MPa standard	8	6	post-recovery	8	6
3 week contralateral	2.2 MPa standard	8	7	post-recovery	8	7
6 week scar	no			pre-test	3	3
6 week contralateral	no			pre-test	3	3
6 week scar	4.1 MPa standard	8	6	post-recovery	8	6
6 week contralateral	4.1 MPa standard	8	7	post-recovery	8	7
6 week scar	4.1 MPa inverted	5	5	post-recovery	5	5
14 week scar	no			pre-test	3	3
14 week contralateral	no			pre-test	3	3
14 week scar	7.1 MPa standard	7	5	post-recovery	7	5
14 week contralateral	7.1 MPa standard	7	7	post-recovery	8	7
normal	no			pre-test	6	6
normal	4.1 MPa standard	7	7	post-creep	7	4
normal	7.1 MPa standard	6	6	post-recovery	6	6
normal	4.1 MPa inverted	5	5	post-creep	5	5

"*" indicates that "revised n" accounts for exclusion of specimens

For comparisons between the healing intervals, the same stress-strength ratio was used; within healing intervals, the same stress was used.

A set of normal MCLs was also employed for comparisons with scars. Six normal MCLs were assessed for pre-test water content. Normal ligaments from the previous work were used for comparison (Chapter 3) that matched the 6 and 14 week intervals: 4.1 MPa (n=7) and 7.1 MPa (n=6).

All animals were weighed weekly and had daily charting of water and food intake. Sick animals were eliminated and replaced as required. Animals were sacrificed with an overdose of pentobarbital (Euthanyl, 1.5 mL/animal, MTC Pharmaceuticals, Cambridge, Ontario, Canada). The hindlimbs were disarticulated at the hip and ankle. All soft tissues including muscle and fascia were removed rapidly from the femur and tibia, leaving the menisci, collateral and cruciate ligaments. All animals had documentation of gross ligament complex appearance. If required for water content analysis, the MCL was excised at this point. If required for creep analysis, bones were transected 3 cm from the MCL insertions. Tissues were kept moist by wrapping the joint with PBS soaked gauze.

The tibia was cemented into the upper grip of the test system with polymethylmethacrylate. The upper grip was attached to the 500 N load cell of the hydraulic actuator of the MTS system and positioned for alignment of the MCL with the load axis of the actuator. Load was zeroed to account for specimen weight. The femur was cemented into the lower grip with the knee at approximately 70° flexion, and

displacement was zeroed. Tissues were then kept moist by intermittent application (every 30 to 60 seconds) of PBS.

The standard order creep test is detailed in Figure 5.2. The knee joint was subjected to two cycles of 5 N compression and 2 N tension at 1 mm/min. Menisci, cruciate and lateral collateral ligaments were dissected away leaving the isolated MCL. Additional compression-tension cycles were then performed. The second cycle ended at a 0.1 N tension load to establish "ligament zero". The MCL length was measured at the transition between periosteal and palpable ligamentous tissue at both femoral and tibial insertions using Vernier calipers (accurate to 0.01 mm). In order to accommodate the area caliper, a small portion of the medial femoral condyle was removed lateral to the MCL and distal to the femoral MCL insertion. Then, 5 N tension was applied and maintained during the measurement of the cross-sectional area of the midsubstance of the MCL using an area caliper (accurate to 0.01 mm^2) as previously described (134). A custom built environment chamber (37°C and 99% relative humidity) was installed around each test specimen (158), and additional compression-tension cycles were performed to re-establish "ligament zero".

In each cyclic creep test, the tissue was loaded for 30 cycles at 1 Hz (30 seconds of testing) from "ligament zero" to the prescribed stress for that particular test. For a static creep test, each MCL was then loaded immediately to the same stress as in cycling and held in load control for 20 minutes. That ligament was allowed to recover at 0 N for 20 minutes. The MCL was then excised for post-test water content assessment.

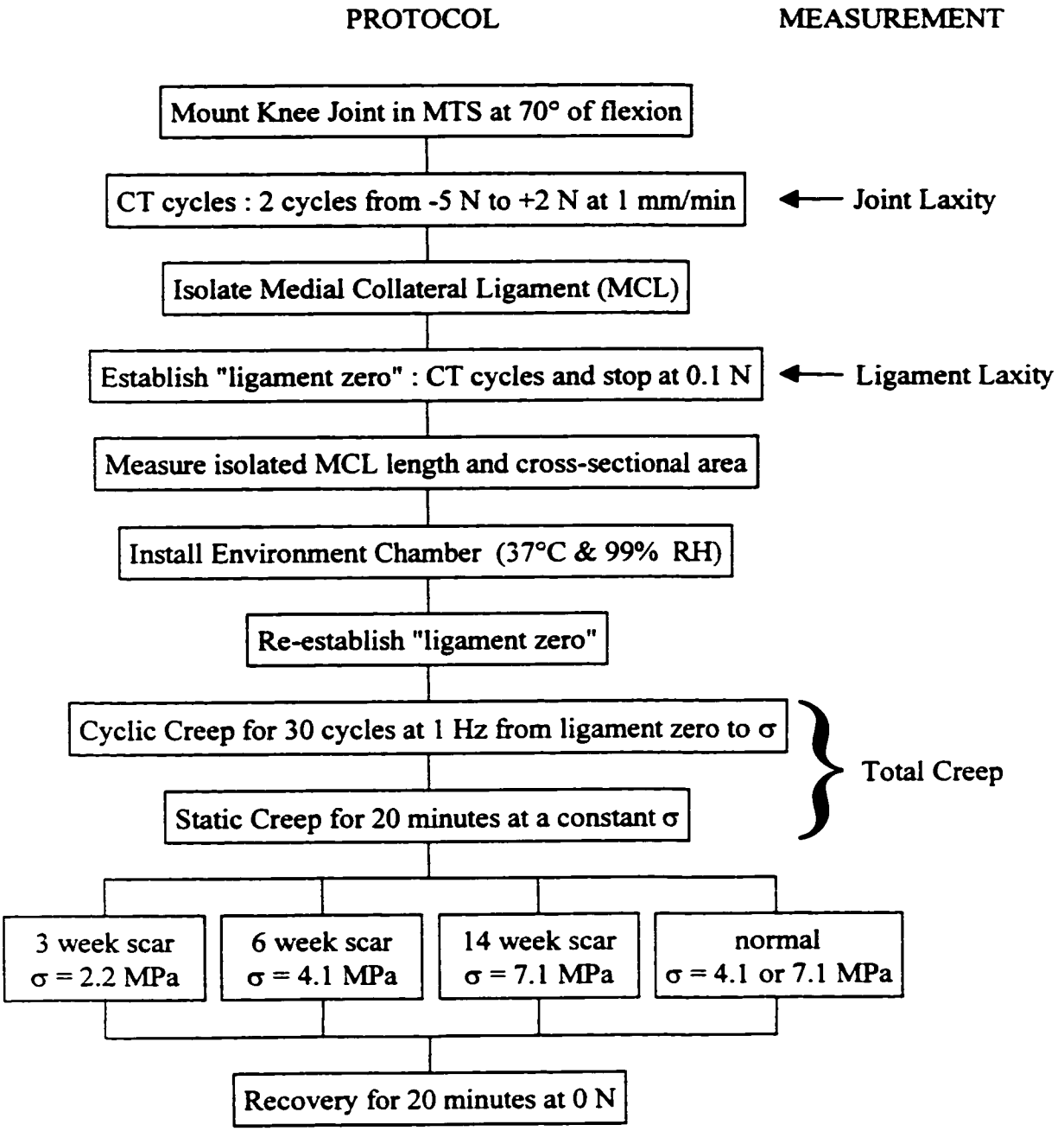

Figure 5.2: Standard Order Test Protocol for MCL Scars and Normals

"CT" is compression-tension and "RH" is relative humidity

Two scars from the 3 week interval were excluded due to ligament failure during static creep testing. Two scars from the 6 week interval were excluded because of discontinuities in the static creep curve. One 14 week scar failed during static creep and one 14 week scar had a discontinuity during static creep; these were also excluded. A discontinuity was deemed to have occurred if, during static creep testing, there was any step increase in the deformation while the force was maintained at the programmed value. In other words, any specimens in which detectable fibre failures occurred, as distinct from creep, were eliminated. Also, one contralateral from each of the 3 and 6 week intervals were excluded due to force control errors of the test system. This resulted in 17 scars (3 weeks (n=6), 6 weeks (n=6) and 14 weeks (n=5)) and 21 contralaterals (3, 6, and 14 weeks (n=7 each)) included in the creep analysis (Table 5.1).

To determine if creep testing altered water content, the pre-test water contents of 9 scars and 9 contralaterals were measured. These were compared to the water contents of the 17 scars and 21 contralaterals that had been creep tested. After the recovery period, these latter 38 MCLs were excised at their insertion sites and divided in half longitudinally. The anterior half was frozen and stored for future biochemical analysis, and the posterior half was weighed for water content analysis. Wet weights were measured immediately on a microbalance (accurate to 0.0001 g). Each sample was then lyophilized until the dry weight ceased to change. Water content was calculated by subtracting the dry weight from the wet weight and dividing by the wet weight to express percentage water content.

The pre-test water content of 6 normal MCLs was assessed for comparison with creep tested normal MCLs. Normal MCLs tested at 4.1 MPa were harvested after the creep test (post-creep; n=4) and after the recovery period (post-recovery; n=4) (66.4±1.7%; n=4). The normal MCLs tested at 7.1 MPa (n=6) were harvested after the recovery period (post-recovery).

Similar to the normals (Chapter 3), an additional group of 6 week scars (n=5) was used to check the effect of creep test order. After establishment of "ligament zero" in the environment chamber, the MCL was immediately loaded to 4.1MPa and held in load control for 20 minutes for the static creep test (Figure 5.3). For the cyclic creep test, the MCL was then immediately loaded for 30 cycles at 1 Hz from "ligament zero" to 4.1 MPa. The scars then had a recovery period of 20 minutes at 0 N and were harvested for post-recovery water content (Table 5.1).

Creep stress was controlled for each ligament by applying a load calculated from the midsubstance (scar or normal) cross-sectional area for that ligament. Strain was defined as the deformation of the MCL divided by the undeformed MCL length. Joint laxity was defined as the displacement recorded when the whole joint was loaded from 5 N compression to 2 N tension. Ligament laxity was defined as the displacement of the MCL between "ligament zero" (+0.1 N) and the point when the tibial and femoral condyles began to transmit compressive load across the joint (-0.1 N). Total creep strain was the increase in strain from the time load was first applied to immediately prior to when the load was removed completely. For the standard order creep tests (cyclic creep

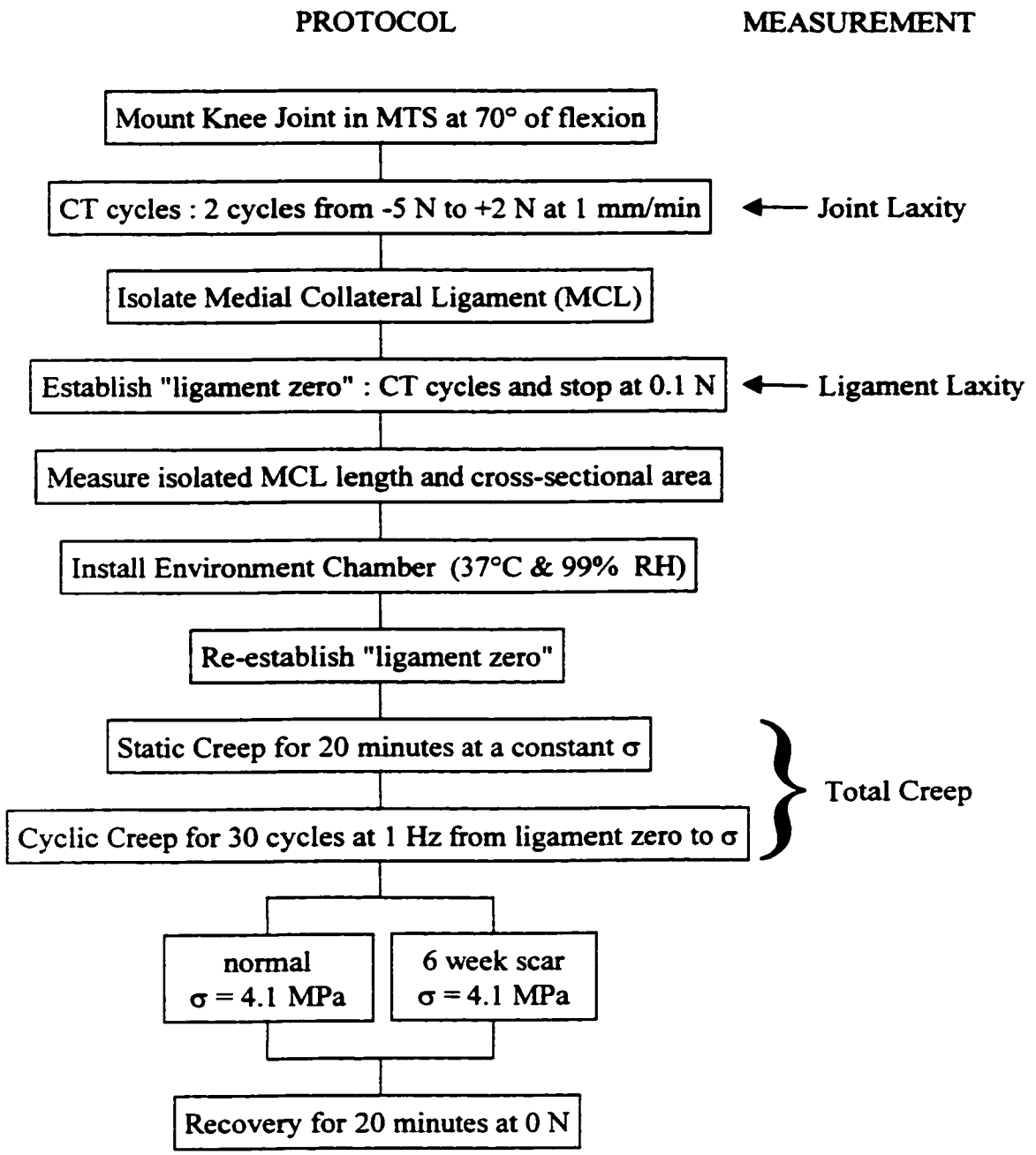

Figure 5.3: Inverted Order Test Protocol for MCL Scars and Normals

"CT" is compression-tension and "RH" is relative humidity

followed by static creep), total creep strain is therefore the increase in strain from the peak of the first loading cycle in the cyclic creep test to the end of the 20 minute static creep test (Figure 5.4a). Cyclic creep strain was defined as the increase in strain from the peak strain of the first cycle to the peak strain of the thirtieth cycle. Static creep strain was defined as the increase in strain from the from the beginning of the constant stress application to the end of the 20 minute constant stress application. The moduli of the cyclic loading curves were calculated fitting a linear regression to the last 60% of the stress range ensuring that the coefficient of determination, r^2, was equal to 0.99.

For the inverted order creep tests (static creep followed by cyclic creep), total creep strain was the difference in the strains at the end of cyclic creep (the peak strain of the thirtieth cycle) and at the beginning of static creep (the beginning of the constant stress application) (Figure 5.4b).

Total creep strain takes into account the complete creep testing protocol because 30 seconds of loading in cyclic creep may be too short to reveal meaningful creep strains, while the cumulative increase in strain (total creep strain) over an additional 1200 seconds of static creep was likely more representative of longer term effects. As well, the use of total creep strain facilitates comparison of the standard order and inverted order creep tests.

Analysis of variance was used to assess the significance of the main effects of interest and the corresponding interactions. Analyses comparing scars and normals at the same creep test stresses required one-way analysis of variance, as did comparing

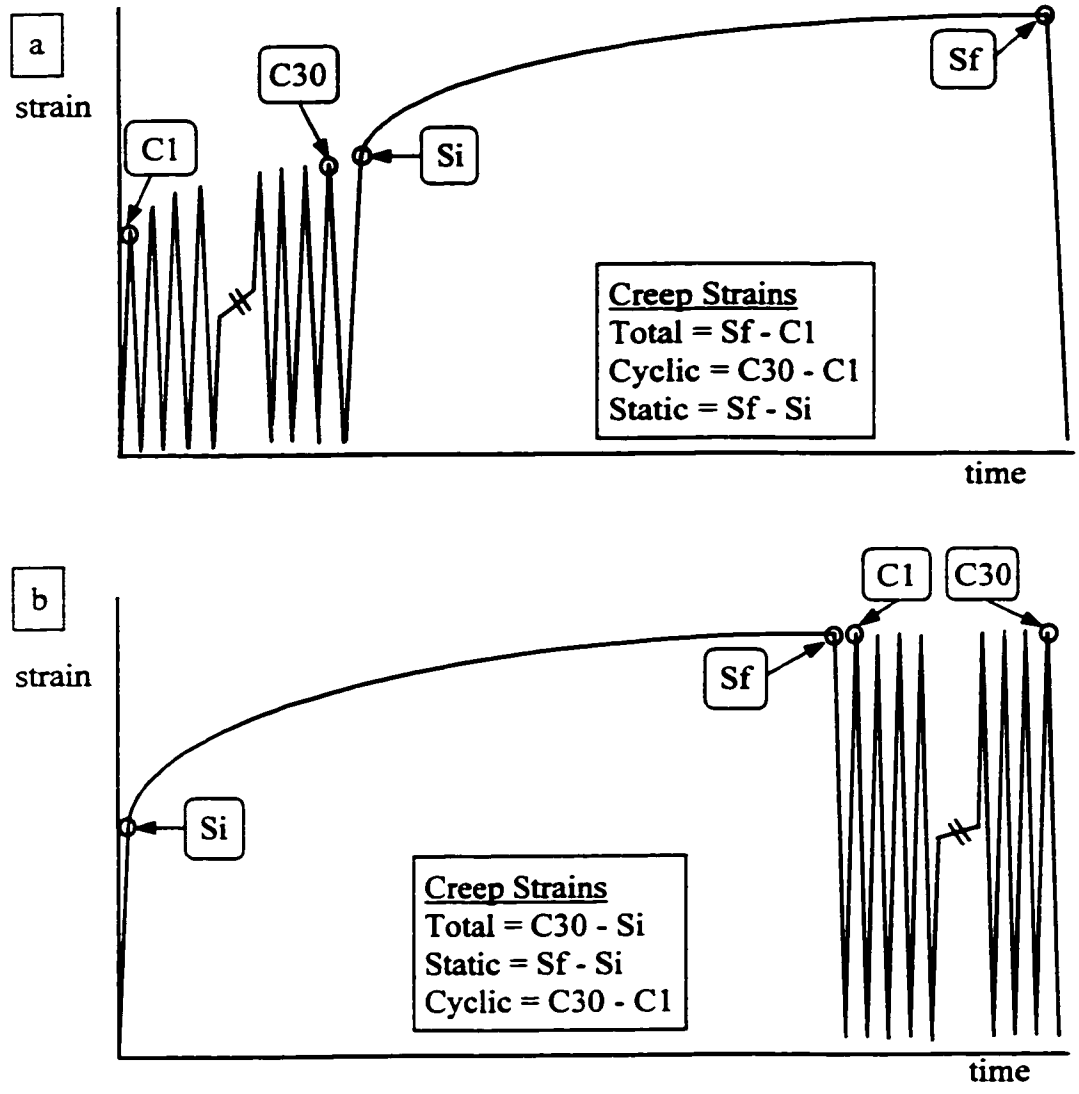

Figure 5.4: (a) Schematic of Standard Order Creep Tests

(b) Schematic of Inverted Order Creep Tests

"C1" equals the peak strain of the first cycle in cyclic creep

"C30" equals the peak strain of the thirtieth cycle in cyclic creep

"Si" equals the strain at the beginning of the constant stress application in static creep

"Sf" equals the strain at the end of 20 minutes constant stress application in static creep

contralaterals and normals. Multiple comparisons were made using linear contrasts (129) which have the advantage of providing an exact p-value for each specially defined comparison of interest. Comparisons between the scars and contralaterals required the use of split-plot analysis of variance due to the nesting in the design (131). Nesting was caused by repeated measures of each rabbit; that is, the measurement of both legs (the scar right leg and the contralateral left leg). The effects included were the within rabbit effect of the treatment (scar/contralateral), the between rabbit effect of healing time (3/6/14 weeks), the treatment and healing interaction, the random rabbit effect (130) and the random error. Again, specially defined linear contrasts were tested to assess differences between the levels of the treatment and healing effects.

5.3 Results

When subjected to the same stress, the total creep strain of the 4 mm gap scars were significantly greater than contralaterals ($p<0.0006$) and normals ($p<0.0001$) at all healing intervals for the standard order creep tests (Figure 5.5). At 3 weeks, the increase was four-fold that of controls and, even at 14 weeks, the increase remained over two-fold that of controls. For the same stress-strength ratio, the total creep strain of 6 and 14 week scars was less than that at 3 weeks ($p<0.004$).

Static creep strain of scars was significantly larger than contralaterals ($p<0.07$) and normals ($p<0.0001$) at all healing intervals (Figure 5.6). When examining the creep

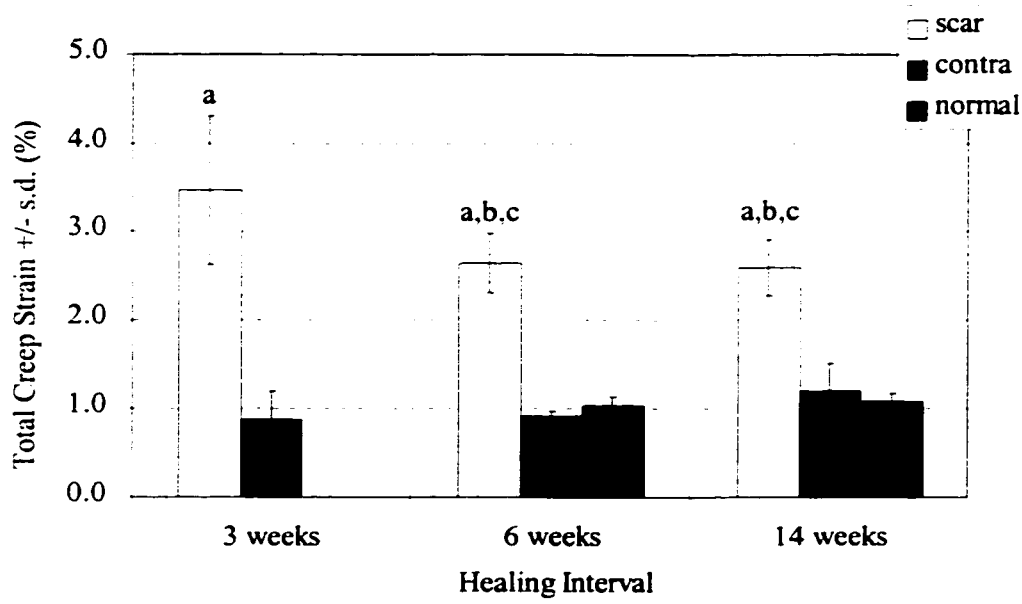

Figure 5.5: Total Creep Strain of MCL Scars and Controls

at 30% Ultimate Tensile Strength of Scars

"contra" indicates contralateral control and "s.d." indicates standard deviation

significantly different than: a = contralateral ($p<0.0006$)

b = normal ($p<0.0001$)

c = 3 week scar ($p<0.004$)

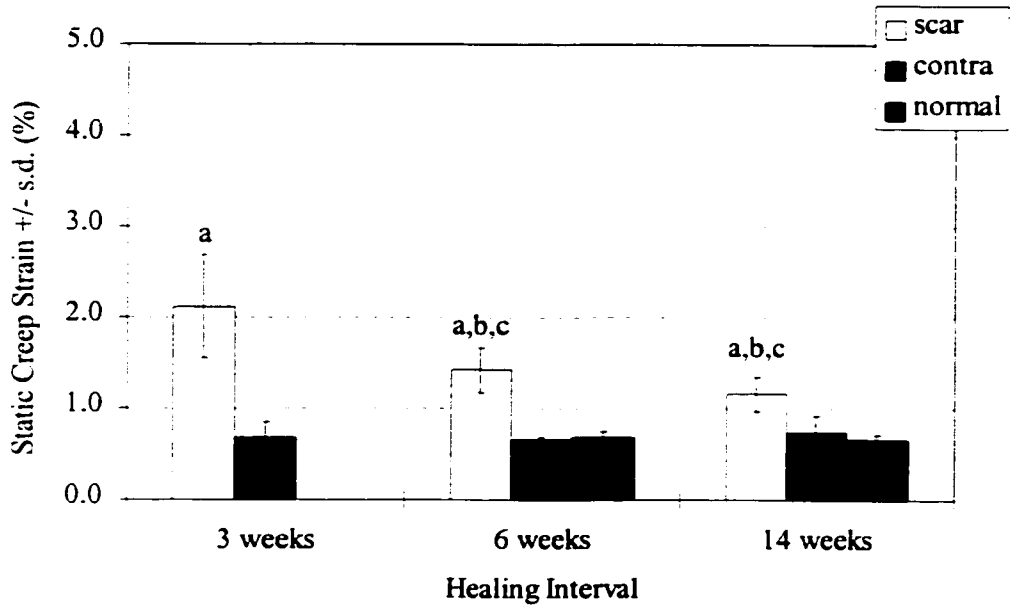

Figure 5.6: Static Creep Strain of MCL Scars and Controls

at 30% Ultimate Tensile Strength of Scars

"contra" indicates contralateral control and "s.d." indicates standard deviation

significantly different than: a = contralateral ($p<0.07$)

b = normal ($p<0.0001$)

c = 3 week scar ($p<0.0002$)

of scars alone (at the same stress-strength ratio), the static creep strain of 6 and 14 week scars were significantly lower than that at 3 weeks ($p<0.0002$).

Cyclic creep strains of scars were over three-fold greater than their corresponding contralaterals and normals at all healing intervals ($p<0.0001$) (Figure 5.7). The cyclic creep strains of scars were not significantly different between the healing intervals. The cyclic modulus at the thirtieth cycle was greater than the cyclic modulus at the first cycle for all groups (Table 5.2). It is important to note that none of the scars had discontinuities in the cyclic creep curves (Figures 5.8 and 5.9). The modulus of the scars was significantly lower than of the corresponding normal MCLs tested at the same stress. Even though the modulus increased from 6 weeks to 14 weeks of healing, the scar modulus remained only 40% of the normal value.

Ligament laxity of scars was significantly greater than contralaterals and normals at 3 and 6 weeks (Figure 5.10). By 14 weeks, scar laxity returned to normal values. Joint laxity measurements were not able to reveal differences between scars, contralateral and normals at the early intervals (Figure 5.11). At 14 weeks, the joint laxity of the contralateral was less than normal values and the scar was not different than the contralateral.

Water contents (pre-test and post-recovery) of scars were significantly greater than contralaterals ($p<0.0001$) and normals ($p<0.0007$) at 3 and 6 weeks of healing (Figure 5.12). In addition, water content (pre-test and post-recovery) of scars at 3 and 6 weeks of healing were significantly greater than at 14 weeks ($p<0.05$). At the end of the recovery

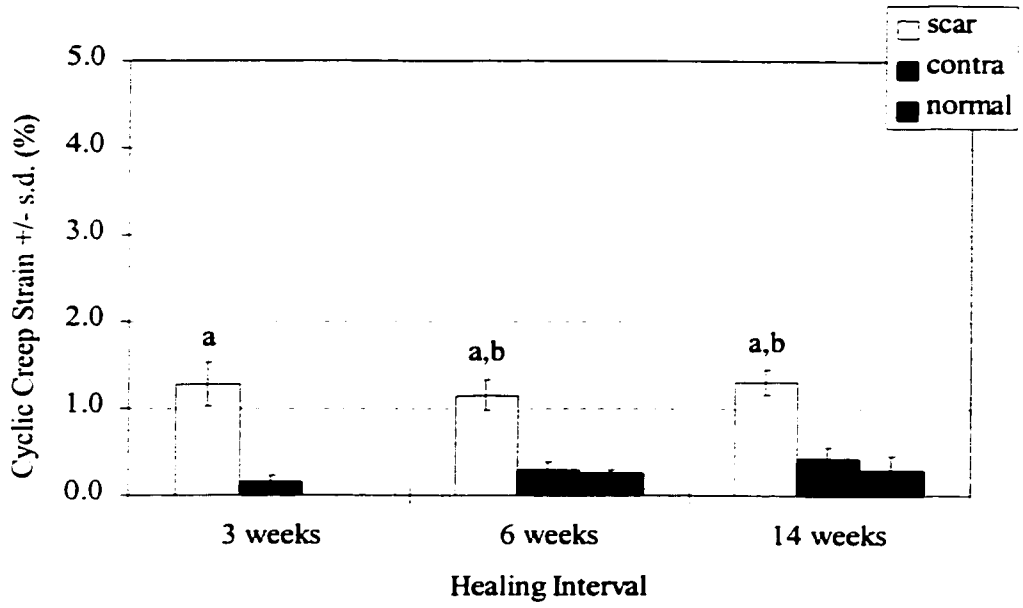

Figure 5.7: Cyclic Creep Strain of MCL Scars and Controls

at 30% Ultimate Tensile Strength of Scars

"contra" indicates contralateral control and "s.d." indicates standard deviation

significantly different than: a = contralateral ($p<0.0001$)

b = normal ($p<0.0001$)

Table 5.2: Cyclic Modulus of MCL Scars and Normals

Group	Cyclic Modulus Cycle 1 (MPa)	Cyclic Modulus Cycle 30 (MPa) [a]	Modulus Increase (C30-C1:MPa)
3 week scar	87.4 ± 14.6	103.3 ± 17.1	15.9 ± 3.7
6 week scar	158.3 ± 25.0 [c,d]	185.0 ± 28.6 [c,d]	26.7 ± 4.5 [c]
4.1 MPa normal	362.6 ± 35.3 [b]	399.0 ± 37.1 [b]	36.4 ± 11.7
14 week scar	200.0 ± 47.3 [c]	233.7 ± 58.4 [c]	33.7 ± 12.9 [c]
7.1 MPa normal	511.5 ± 38.2 [b]	550.2 ± 48.6 [b]	38.7 ± 11.1

"C1" indicates cycle 1 and "C30" indicates cycle 30

"a" indicates that the cyclic modulus at the cycle 30 was greater than at cycle 1 for all groups ($p<0.004$; paired t-test)

"b" indicates that scar is different than normal MCL creep tested at the same stress ($p<0.0001$)

"c" indicates that 6 week and 14 week scars are different than 3 week scar tested at same stress-strength ratio ($p<0.03$)

"d" indicates that 6 week scar is different than 14 week scar tested at same stress-strength ratio ($p<0.04$)

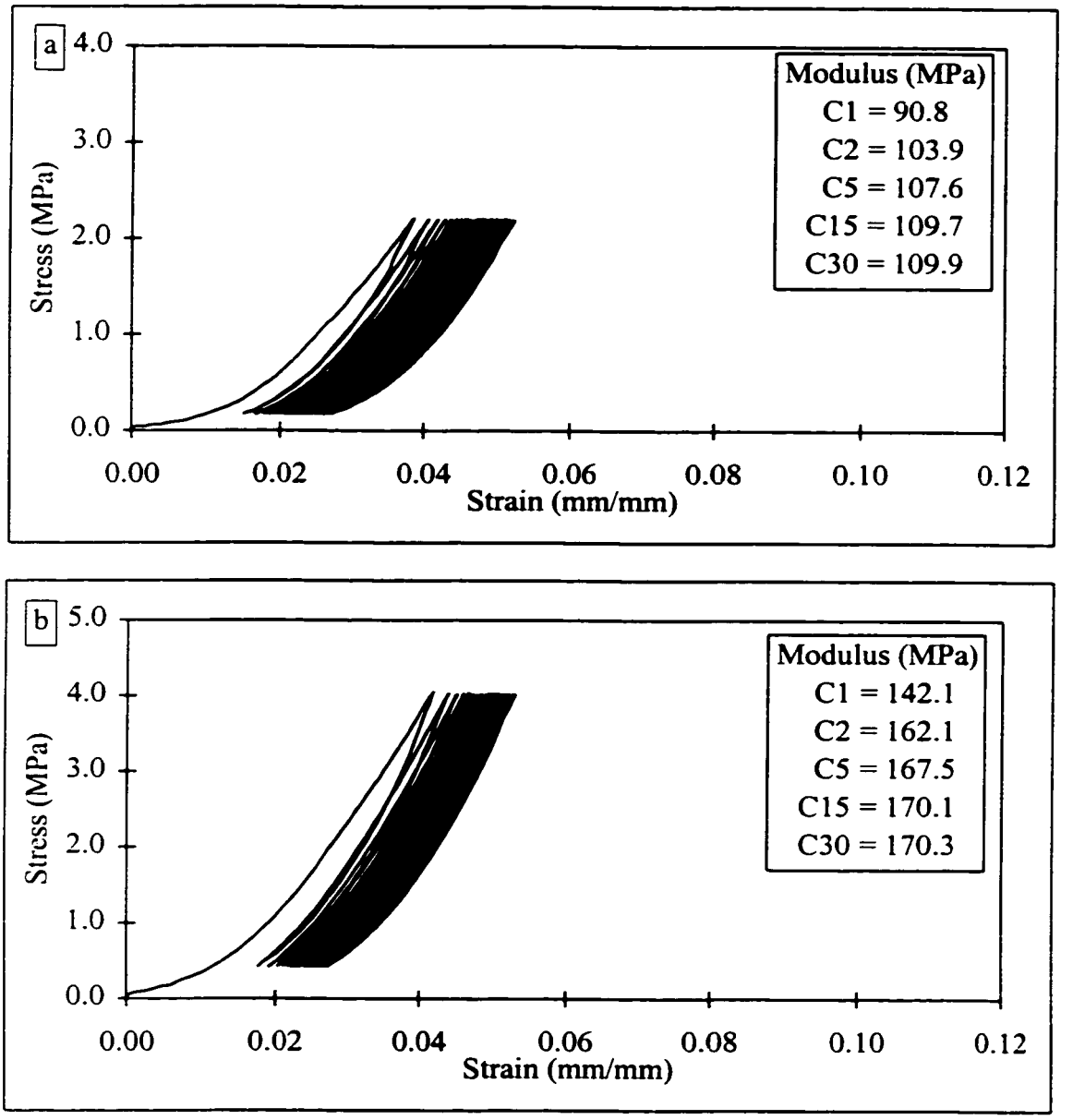

Figure 5.8: (a) Cyclic Plot of a Representative 3 week Scar Creep Tested at 2.2 MPa

(b) Cyclic Plot of a Representative 6 week Scar Creep Tested at 4.1 MPa

"C1" indicates Cycle 1

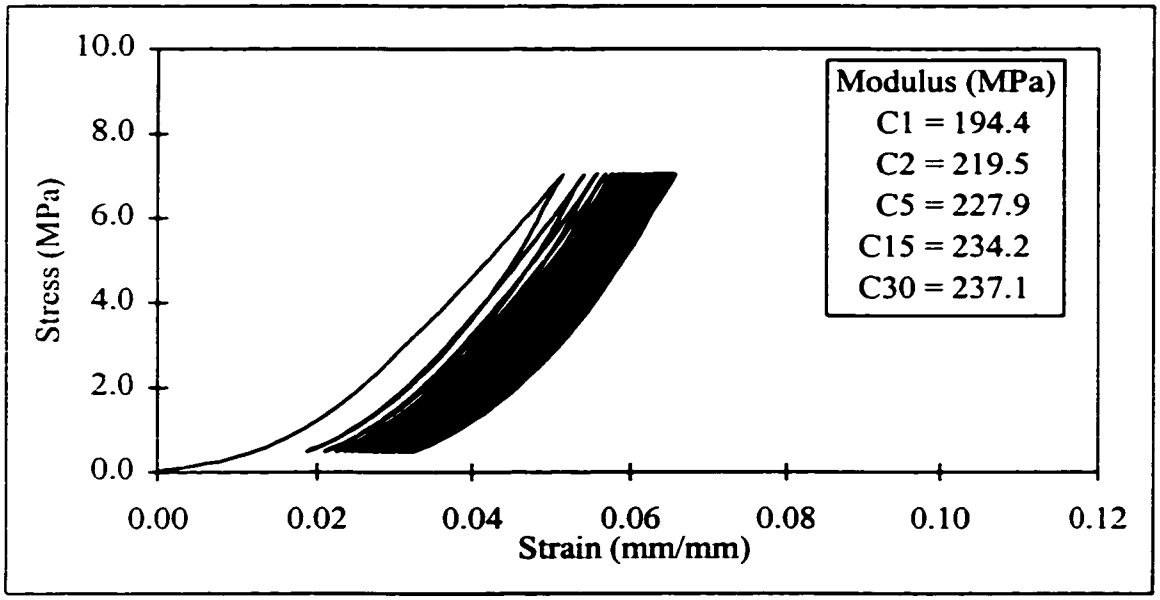

Figure 5.9: Cyclic Plot of a Representative 14 week Scar Creep Tested at 7.1 MPa

"C1" indicates Cycle 1

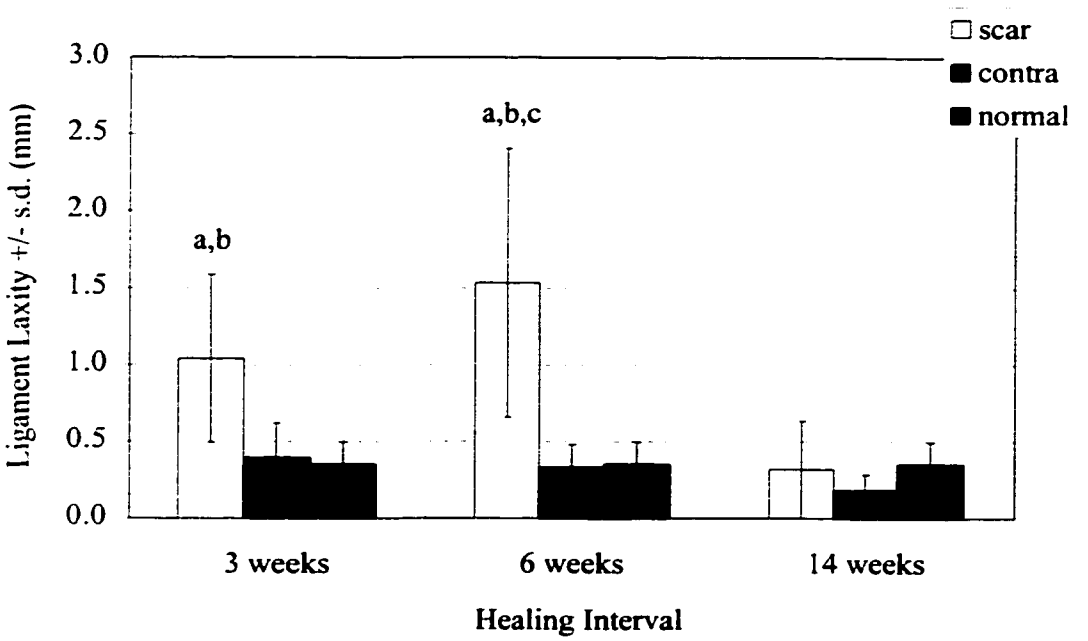

Figure 5.10: Ligament Laxity of MCL Scars and Normals

Pooled normal values are shown (creep tested at 4.1 and 7.1 MPa).

"contra" indicates contralateral control and "s.d." indicates standard deviation

significantly different than: a = contralateral ($p<0.0007$)

b = normal ($p<0.0001$)

c = 14 week scar ($p<0.007$)

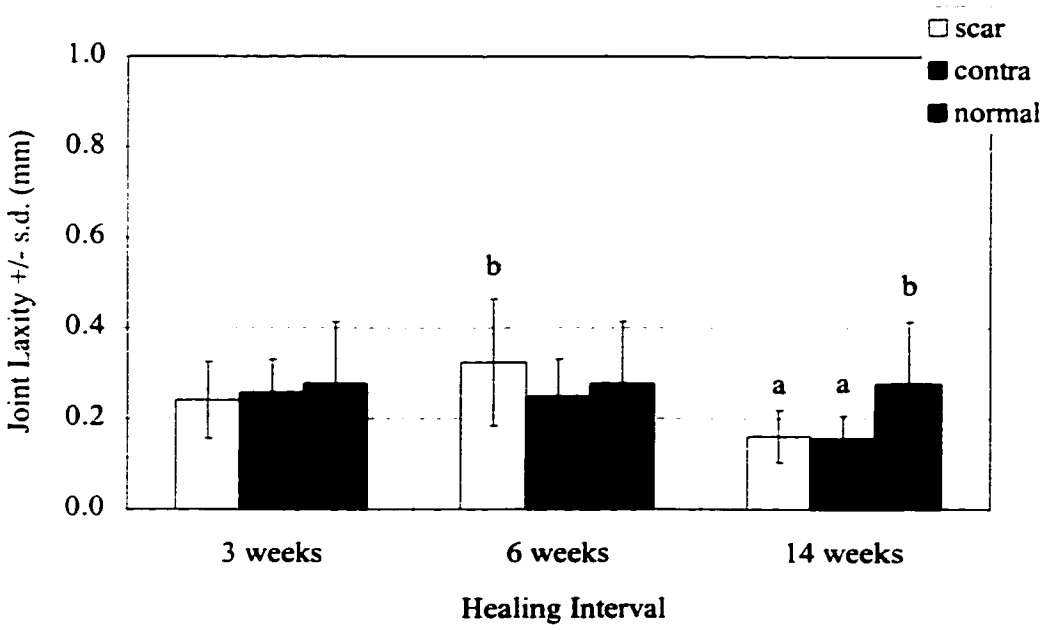

Figure 5.11: Joint Laxity of MCL Scars and Normals

Pooled normal values are shown (creep tested at 4.1 and 7.1 MPa).

"contra" indicates contralateral control and "s.d." indicates standard deviation

significantly different than: a = normal ($p<0.05$)

b = 14 week scar ($p<0.02$)

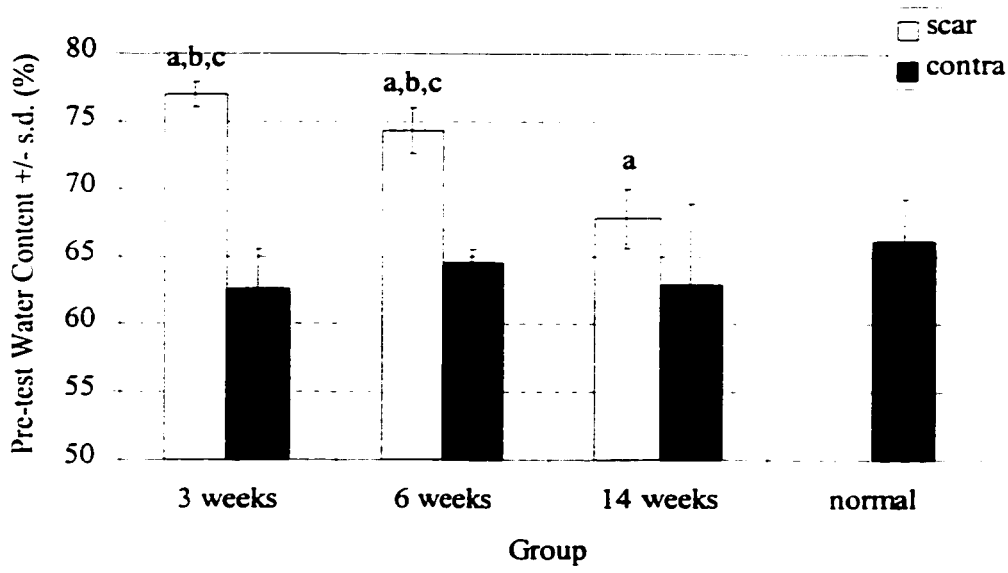

Figure 5.12: Pre-test Water Content of MCL Scars and Controls

"contra" indicates contralateral control and "s.d." indicates standard deviation

significantly different than: a = contralateral ($p<0.01$)

b = normal ($p<0.0007$)

c = 14 week scar ($p<0.05$)

period after creep testing, tissue water content was not different than pre-test values within each group of scars and contralaterals.

No significant differences in total creep strain were found comparing the standard order and inverted order creep tests for 6 week MCL scars (Table 5.3). Whichever component of creep was tested first had larger creep strain than when that component was tested second. The post-test water contents of the inverted order tests were slightly (but significantly) elevated compared to the standard order tests. Finally, the total creep strain of 6 week scars was significantly greater than that of normals (tested at 4.1 MPa) comparing within standard order creep tests and inverted order creep tests ($p<0.0001$).

The scars were tested at the same stress as the controls. The cross-sectional areas of these scars were larger than normal (Table 5.4). Given the observation that creep behaviour of normal ligament was similar at the lower stresses (see Chapter 3), there would be no differences in the conclusions from these results if the scars were compared to normal MCLs based on creep test force instead of creep test stress.

5.4 Discussion

These results show that despite some improvement with healing, ligament gap scars clearly remained inferior to controls in terms of their ability to resist creep at comparable stresses. For all parameters of creep (total, cyclic and static), the creep strain of scars was significantly greater than contralaterals and normals. Cyclic modulus of scars increased with healing but was less than half of normal values. Total creep strains

Table 5.3: Creep Strains and Water Contents for Standard and Inverted Order Creep Tests of 6 week Scars and Normal MCLs

Standard order (4.1 MPa)	Total Creep Sf - C1 (% +/- s.d.)	Cyclic Creep C30 - C1 (% +/- s.d.)	Static Creep Sf - Si (% +/- s.d.)	n	Water Content (%+/- s.d.)*	n
6 week scar	2.64±0.34[b]	1.15±0.18[a,b]	1.42±0.25[a,b]	6	72.7±1.8[a]	6
normal	1.03±0.11	0.25±0.04[a]	0.68±0.07[a]	7	61.9±1.7	4
Inverted order (4.1 MPa)	**Total Creep C30 - Si (% +/- s.d.)**	**Static Creep Sf - Si (% +/- s.d.)**	**Cyclic Creep C30 - C1 (% +/- s.d.)**	**n**	**Water Content (% +/- s.d.)***	**n**
6 week scar	2.52±0.37[b]	2.77±0.40[b]	-0.06±0.08	5	75.1±1.4	5
normal	1.13±0.10	1.18±0.10	-0.03±0.02	5	63.4±1.8	5

"C1", "C30, "Si" and "Sf" are defined on Figure 5.3 and "s.d." is standard deviation.

"*" indicates that the water content of 6 week scars was measured post-recovery and water content of normals was measured post-creep; thus, no comparisons were made between the groups

"a" indicates significantly different compared to the same parameter measured in the inverted order creep test within the same group (scar or normal; $p<0.03$)

"b" indicates significantly different compared to normal creep strain within the same order creep test ($p<0.0001$)

Table 5.4: Cross-sectional Area and Creep Test Force for MCL Scars and Normals

Group	n	Cross-sectional Area (mm^2)	Creep Test Stress (MPa)	Creep Test Force (N)
3 week scar	6	9.65 ± 2.98 [a]	2.2	21.2 ± 6.6 [c]
6 week scar	6	5.79 ± 1.72 [a,b]	4.1	23.8 ± 7.1 [d]
14 week scar	5	7.84 ± 2.74 [a]	7.1	55.7 ± 19.5 [e]
4.1 MPa normal	7	4.33 ± 0.63	4.1	17.8 ± 2.6
7.1 MPa normal	6	4.10 ± 0.68	7.1	29.1 ± 4.8
14 MPa normal	9	3.97 ± 0.37	14	55.6 ± 5.2

"a" indicates different than pooled normal MCL cross-sectional area (4.22 ± 0.55 mm^2; $n=22$; $p<0.0004$)

"b" indicates cross-sectional area of 6 week scar different than 3 week scar ($p=0.02$)

"c" indicates similar to 4.1 MPa normal creep test force ($p=0.2$)

"d" indicates similar to 7.1 MPa normal creep test force ($p=0.2$)

"e" indicates similar to 14 MPa normal creep test force ($p=0.9$)

were equal comparing the standard and inverted order tests even though the cyclic and static creep strain magnitudes varied with test order. Thus, total scar creep changed over time but remained abnormal after 14 weeks of healing.

For the scar groups, only pre-test and post-recovery water contents were measured. Post-recovery water contents were not different than pre-test values. As described previously, the water content of normal MCLs tested at 4.1 MPa was significantly decreased post-creep but returned to pre-test values post-recovery. For the scars as well, it is likely that water return to the scar during the recovery period balanced the water loss during creep testing. The gradient for water return would be enhanced by the elevated levels of GAG in scars (52).

The fact that pre-test water content of scars was elevated early and decreased over time may have contributed to the scar creep response. Increasing the water content of normal MCLs using PBS soaking solution caused an increased creep response. Nonetheless, this magnitude of increased water content could only account for about half of the creep strain observed here. Additionally, because the water content of scars returned to normal values at 14 weeks and creep remained abnormal, water content alone cannot account for the measured creep behaviour.

The laboratory where this research was undertaken has established previously an extensive database of biochemical and morphological property changes of this same MCL gap scar model over time. The logic proposed is that if one of these previously published property changes was found to change over the 14 week interval and to remain abnormal

after 14 weeks of healing (as did the total scar creep in the current study), that property change may be established as a potential mechanistic factor involved in creep.

For example, in a study by Frank et al. (1995), MCL gap scar collagen (hydroxyproline) concentration was observed to increase with healing back to normal levels by 14 weeks. In a different study by Frank et al. (1991), MCL gap scar collagen fibre alignment towards the long axis of the ligament improved with healing and equaled normal values by 14 weeks. These two properties improved with healing, changing over time, like creep. However, they returned to normal values by 14 weeks and are thus unlikely to account for the persistently abnormal creep behaviour on their own.

In another study, Frank et al. (1992) found that MCL gap scar collagen fibril diameters were significantly smaller than in control MCLs at all healing intervals (3, 6, and 14 weeks) and fibril diameters did not change over the 14 week healing interval. Although the fibril diameters remained abnormal (similar to creep), they did not change over the 14 weeks which cannot explain the fact that scar creep improved over the same interval.

If collagen fibres are considered as a whole (concentration, alignment, fibril diameter), the combination matches the characteristics of scar creep, changing over time and remaining abnormal at 14 weeks. Thus, while the individual properties of collagen fibres do not match scar creep characteristics, collagen fibres, in total, do. These initially poorly aligned fibres never increase in diameter and may never make the spatial connections required to restore normal fibre architecture. These abnormalities would

cause poorer collagen fibre recruitment. As documented previously, collagen recruitment is an important mechanism for minimizing creep in normal ligaments. Inferior fibre recruitment would lead to ineffective stress redistribution over the available fibres and scar collagen fibres that were recruited would be carrying more creep stress. This is further complicated by the fact that the scar collagen fibres are not as large as normal ligament fibres and may have altered creep response.

Frank et al. (1995) documented that MCL gap scar collagen crosslink (hydroxylysylpyridinoline) density increased with healing but reached only 55% of normal values by 14 weeks. If there is a reduction in the crosslinks between the collagen fibres, there will be easier movement of one fibre relative to another. Thus, loaded fibres could straighten faster and potentially not recruit their neighbours which would reduce the ability of the tissue to resist creep. Despite some improvement with healing, crosslinks remained abnormal and thus seems to be a reasonable candidate as a mechanism of scar creep.

Frank et al. (1983a) also observed that GAG (hexosamine) content of MCL gap scars decreased with healing but remained elevated compared to normals at 14 weeks. With GAG content elevated, the ratio of bound to free water may be changed which may increase creep. In Shrive et al. (1995), the mean total area of flaws (blood vessels, fat cells, hypercellular areas, loose matrix and/or disorganized matrix) as a percentage of total section of MCL gap scar was found to decrease with healing but was still larger than

control values at 14 weeks. Flaws create stress concentrations, and thus the tissue may creep more because the concentrated stress causes higher creep local to the flaws.

To date, only collagen properties of normal tissue that may relate to fibre recruitment (like collagen alignment and crosslinking) have been investigated with respect to creep. Fibre recruitment (through altered crimp patterns) is heavily implicated as a mechanism to minimize creep of normal rabbit MCL at low stresses. A working hypothesis of Cohen et al. (1976) was that the activation energy for creep of collagenous tissue was less than the activation energy for collagen fibril creep and greater than the activation energy for the interfibrillar sliding from straightening out of the wavy fibrils. Even more fundamental, Jenkins and Little (1974) confirmed that the viscoelastic properties of bovine ligamentum nuchae were dependent on the presence of collagen.

Ligament laxity was elevated early but returned to normal values by 14 weeks. This may be due to the return of collagen fibre alignment by 14 weeks. The whole joint laxity of scars did not show differences compared to contralaterals which may have occurred because of compensatory changes in other structures of the whole joint; for example, bone or cartilage.

These unique results showed that sustained and repetitive stress can cause creep of rabbit MCL scars. Ligament scars are still more susceptible to creep than normal MCLs even after 14 weeks of healing. Combined with previous results in this same model of scar, it is proposed that there are several possible mechanisms implicated for this inferiority: increased water content, deficiencies in collagen fibre properties that affect

fibre recruitment, elevated GAG content and flaws in the scar tissue involved in ligament repair. Treatments aimed at altering these abnormalities may improve ligament scar creep and thus prevent the "stretching out" of healing ligaments.

CHAPTER 6

EFFECT OF IMMOBILIZATION ON LAXITY AND CREEP

6.1 Introduction

6.1.1 Bilateral Gap Scars with Immobilization

In the past, injured ligaments had been treated with immobilization to prevent the healing tissue from experiencing damaging stresses (163). However, recent studies have shown detrimental effects of immobilization on normal ligaments. In addition to decreased tissue strength (161), immobilization causes increased collagen turnover with a tendency towards more degradation than synthesis (6,7) and increased glycosaminoglycan degradation (64).

Mechanical loading therefore is important to the mechanical properties of healing ligaments. Immobilization decreased the failure strength of immobilized ligaments compared to non-immobilized healing ligaments (162) and control ligaments (67,162). Similarly, others have documented decreased failure loads of immobilized healing ligaments compared to non-immobilized healing ligaments (70) and control ligaments (70,148). Woo et al. (1987b) found that after immobilization varus-valgus laxity of the joint was increased for medial collateral ligaments (MCLs) post-transection in immobilized and moved joints compared to controls. Hart and Dahners (1987) observed increased ligament laxity of immobilized healing MCLs compared to moved

experimentals and normal controls. In cases where joint instability has been created with injury to both the MCL and anterior cruciate ligament (ACL), immobilization was beneficial in reducing MCL laxity as compared to the laxity of the MCL that was allowed motion (25,70). In one study, the laxity of the immobilized scar was similar to normal values (25). Even though immobilization reduced laxity, the failure load of immobilized healing MCLs was less than MCLs that were not immobilized and less than controls (25,70).

The effect of immobilization on the creep behaviour of healing ligament was yet unknown. The purpose of this section of this thesis was to quantify the creep behaviour of MCL scars with and without immobilization. Joint and ligament laxity were quantified in addition to the energy absorption during creep of immobilized and moved (non-immobilized) healing ligaments. The hypothesis was that immobilization would increase laxity, increase cyclic creep and increase cyclic energy absorption as compared to moved contralateral scars.

Aim 1. To quantify the creep behaviour of fresh healed bilateral gap injury MCL (pin-immobilized healed gap injury MCL and contralateral healed gap injury MCL) at various healing intervals. MCL scars at 3, 6 and 14 weeks of healing were tested at 2.2, 4.1 and 7.1 MPa, respectively.

6.1.2 Long-Term Autografts with Remobilization

Knee joints with ligament injury and chronic laxity are often reconstructed using soft tissue autografts. Most autografts produce a clinical improvement; however, recent evidence has shown that some of these autografts can "stretch out" (creep) over time (99). If, during a period of recovery after creep loading, the graft is not able to return to its original length, a permanent elongation (unrecovered creep) could result. Few studies have documented the experimental creep and creep recovery of autografts at different healing intervals with any type of rehabilitation. Boorman et al. (1998) recently documented the increased creep response and increased unrecovered creep of rabbit medial collateral ligament (MCL) autografts compared to normal MCLs after short-term healing. In this section of the thesis, the creep response and creep recovery of MCL autografts over the first two years of healing with or without 6 weeks of early post-operative immobilization was quantified. Boorman et al. (1998), showed that immobilization increased graft creep response short-term. Thus, the current hypothesis was that long-term grafts would have a reduced ability to recover from creep. In addition, joint and ligament laxity may be related to creep recovery.

Aim 2. To quantify the creep of long-term unilateral MCL autografts at 2 years (moved) and 1 year (moved and remobilized after 6 weeks) post-operatively in order to determine the effects of early immobilization on long-term healing. Grafts were tested at 4.1 MPa with normal controls at 4.1 MPa (stress-matched) and 7.1 MPa (force-matched).

6.2 Methods

6.2.1 Bilateral Gap Scars with Immobilization

The rabbit MCL gap model of healing was used; in this case, bilateral surgeries were performed on the MCLs of 17 one-year-old rabbits. A segment of the midsubstance of the MCL was removed to leave an acute 4.0 ± 0.5 mm gap between the opposing ligament ends (30). The four corners of the ends were marked with single 6-0 nylon sutures. The immobilization technique pinned the knee in full flexion (approximately 150-160°) using an extra-articular 1.6mm diameter stainless steel transfixing pin (3,25) (Figure 6.1). The right leg was pin-immobilized; the left leg remained non-immobilized (moved). MCLs were allowed to heal for 3, 6, or 14 weeks. For creep tests of unilateral scars described earlier, a 30% stress-strength ratio was used. The resulting creep test stresses were 2.2, 4.1 and 7.1 MPa, for the 3, 6 and 14 week healing intervals, respectively. For the study of bilateral scars, the same creep test stresses were used because unilateral MCL gap scars and bilateral MCL gap scars have similar failure strengths (from the laboratory database, Table 6.1). The 30% stress-strength ratio was chosen based on the minimum controllable force for the MTS system: 2.2 MPa for the 3 week scar. Given evidence in different animal models of MCL healing (70,162) it was expected that the failure strength of the immobilized bilateral scars would be less than that of the non-immobilized bilateral scars; however, the test was limited to the 2.2 MPa stress, giving a load controllable with the test equipment. Scars were assigned to groups according to the schedule shown in Table 6.2. Normal MCLs were tested at 4.1 (n=7)

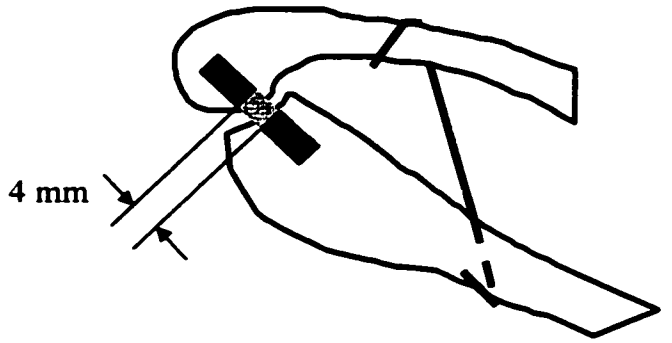

Figure 6.1: Diagram of MCL Gap Scar with Joint Pin-Immobilized

Table 6.1: Failure Strength of Unilateral and Bilateral MCL Gap Scars

Healing Interval	Failure Strength Unilateral MCL Gap (MPa)	n	Failure Strength Bilateral MCL Gap (MPa)	n	Creep Test Stress (MPa)
3 week	7.4 ± 2.3	9	5.1 ± 1.3	5	2.2
6 week	13.8 ± 6.7	8	15.9 ± 6.0	6	4.1
14 week	23.7 ± 7.9	9	21.1 ± 7.8	5	7.1

Data are shown as mean ± standard deviation.

Table 6.2: Experimental Groups for Bilateral MCL Gap Scars with Immobilization

Group	assigned n	actual n	reason for lost samples
3 week immob	5	4	tested at lower stress *
3 week moved	5	4	not enough tissue to test
6 week immob	6	3	tested at lower stress *
6 week moved	6	6	
14 week immob	6	6	
14 week moved	6	5	not enough tissue to test

* Some immobilized scars failed during creep testing at the prescribed stresses (Table 6.1). Selected samples were tested at lower stresses if the test load was within a controllable range; however, that data is not reported here.

and 7.1 MPa (n=6) (detailed in Chapter 3), stresses that match those used for the 6 and 14 week scars, respectively.

After sacrifice and dissection of all surrounding tissues except ligaments and menisci, the knee joint was mounted at 70° flexion in an MTS system for testing (Figure 6.2). After undergoing 2 cycles of 5 N compression and 2 N tension at 1 mm/min, the remaining tissues were dissected to isolate the MCL. The MCL was then subjected to 2 cycles of 5 N compression and 2 N tension at 1mm/min ending at 0.1 N tension to establish "ligament zero". Cross-sectional area was measured and a custom built environment (37°C and 99% relative humidity) chamber installed. "Ligament zero" was re-established in that test environment. The MCL was then loaded for 30 cycles at 1 Hz from "ligament zero" to the prescribed stress for the healing interval. If the tissue did not fail, the MCL underwent static creep testing being held at the prescribed stress for 20 minutes and recovery being held at 0 N for 20 minutes while the change in ligament length was recorded by the test system.

Joint laxity was defined as the displacement recorded when the whole joint was loaded from 5 N compression to 2 N tension. Ligament laxity was defined as the displacement of the MCL between "ligament zero" (+0.1 N) and the point when the tibial and femoral condyles began to transmit compressive load across the joint (-0.1 N). Stress was defined as the recorded force divided by the MCL cross-sectional area and strain was defined as the recorded deformation divided by the undeformed MCL length. Energy (per unit volume) was calculated as the area under the cyclic stress-strain curve. For a

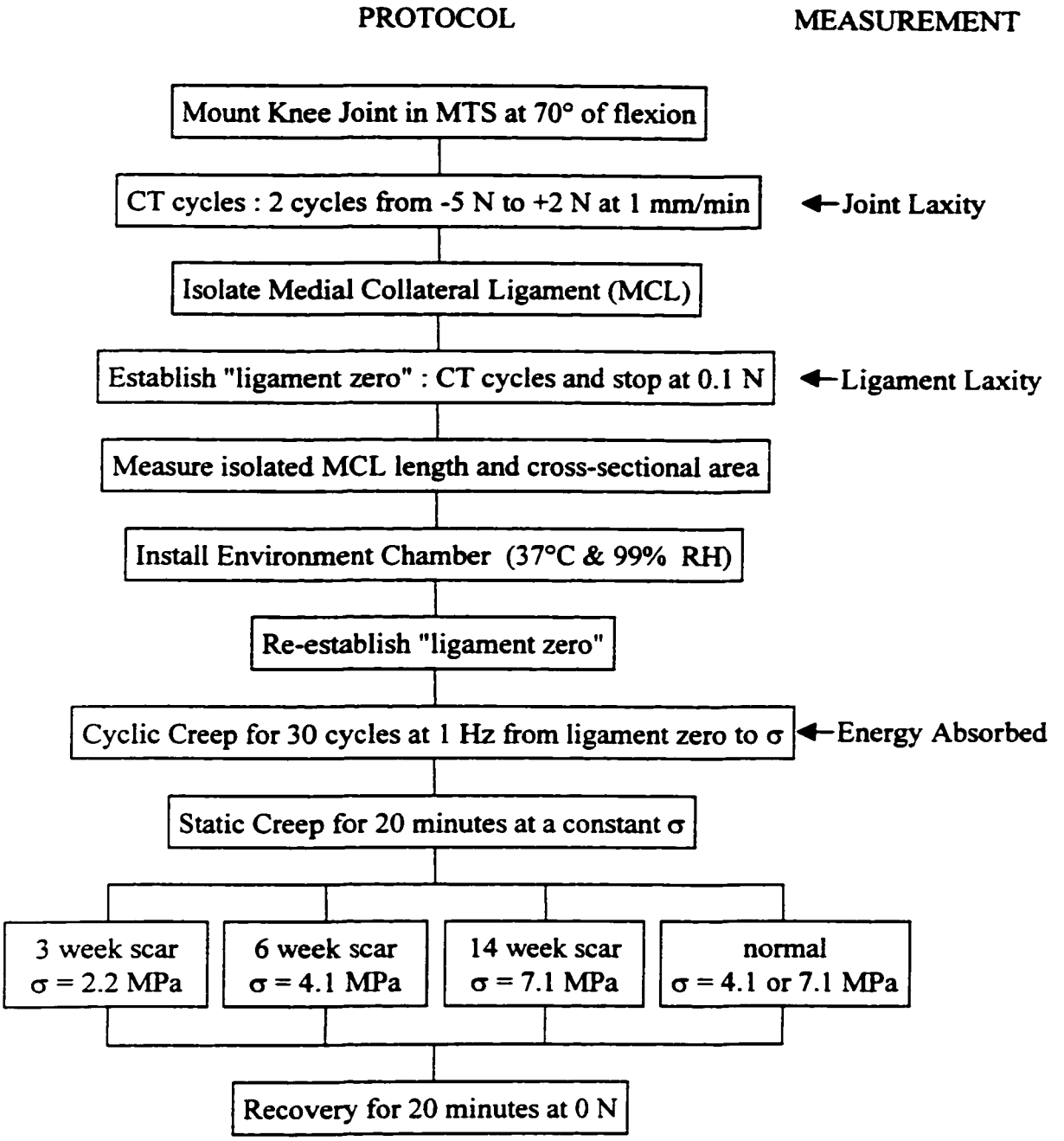

Figure 6.2: Creep Test Protocol for Bilateral MCL Gap Scar with Immobilization

"CT" is compression-tension and "RH" is relative humidity

completed cycle, energy absorbed was the difference in the area under the loading curve and the area under the unloading curve: hysteresis energy. For a cycle in which failure occurred, the energy absorbed was the area under the curve up to the peak (failure) stress. The total energy absorbed by the MCL was the sum of the hysteresis and failure energies. Tissues that failed in the first cycle have a hysteresis component equal to zero and tissues that did not fail during cycling have no failure energy component. Cumulative energy absorption calculations were performed over the course of the cyclic test. Cyclic modulus was calculated taking the slope of the stress-strain plots of the loading cycles over the last 60% of the stress range (linear regression; r^2=0.99). The number of samples that failed during the course of testing was also recorded. Analysis of variance with linear contrasts (significance at p=0.05) was used to compare all the data except the number of failures in the groups were compared using Fisher's test (142).

6.2.2 Long-Term Autografts with Remobilization

A standardized orthotopic bone-MCL-bone autograft procedure was performed on the right hind limbs of 16 rabbits (128) (Figure 6.3 and 6.4a). The autografts were designated to the following healing groups: 2 year moved (n=5), 1 year moved (n=5) and 1 year remobilized (n=6). The moved groups were permitted unrestricted cage activity. The remobilized group had the right hind limb pin-immobilized in full flexion (~150-160°; Figure 6.4b) (3,25) for the first 6 weeks post-operatively followed by pin removal,

Figure 6.3: MCL Autograft at time zero

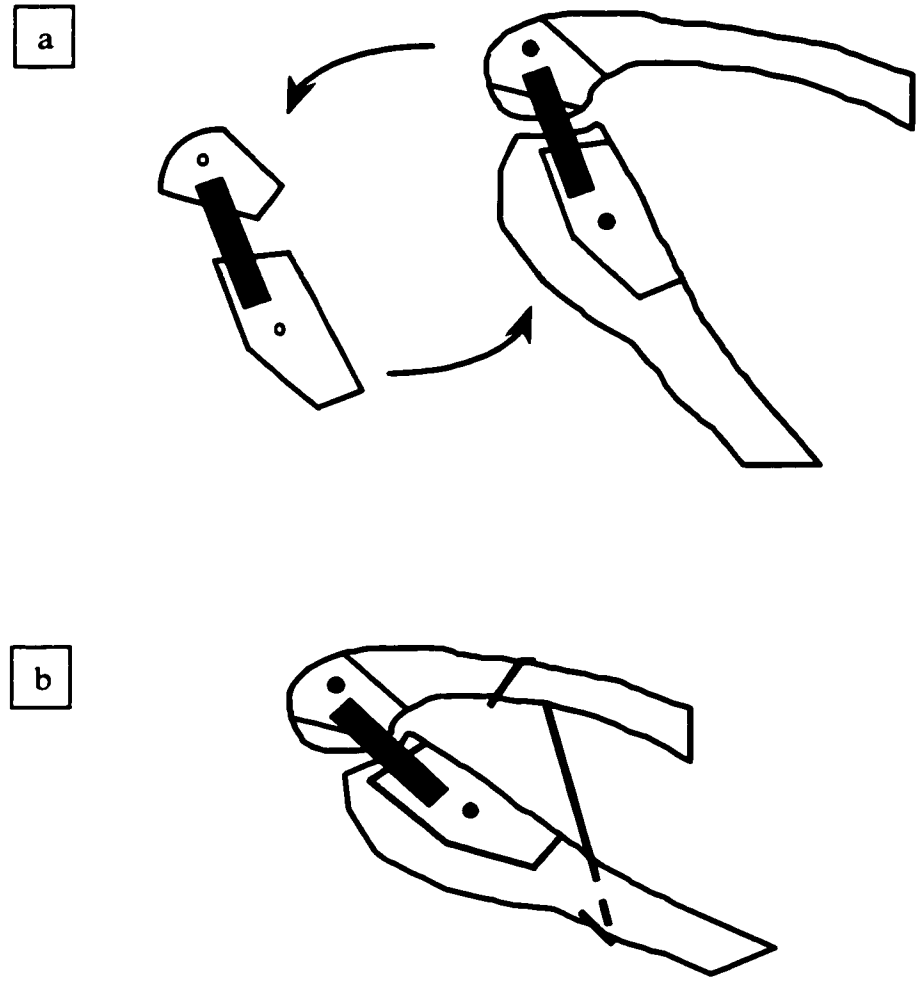

Figure 6.4: (a) Diagram of MCL Autograft Procedure

(b) Diagram of MCL Autograft with Joint Pin-Immobilized

remobilization of the joint and unrestricted cage activity for the remainder of the 1 year healing period.

Stress was controlled during *in vitro* testing of each ligament by applying a force calculated from the midsubstance cross-sectional area for that ligament. All autografts were creep tested at 4.1 MPa. The mean area of grafts was 7.73 ± 1.25 mm^2 requiring an average test force of 31.7 ± 5.1 N to achieve a 4.1 MPa creep test stress. Two normal control groups were also tested to span this range of loading. The first group tested at 4.1 MPa (n=7) had a mean creep test force of 16.2 ± 1.9 N (stress-matched). The second group tested at 7.1 MPa required at mean creep test force of 29.1 ± 4.8 N (force-matched). The normal MCL data for tests at 4.1 MPa included both creep and creep recovery (identified as the 4.1 MPa recovery group in Chapter 3).

After sacrifice and dissection of all surrounding tissues except ligaments and menisci, the knee joint was mounted at 70° flexion in the laboratory MTS system for testing. The whole joint was subjected to 2 cycles of 5 N compression and 2 N tension at 1 mm/min (Figure 6.5). After isolating the MCL, the compression-tension cycles were repeated and stopped at 0.1 N tension to establish "ligament zero". MCL length and cross-sectional area were measured. After a custom built environment (37°C and 99% relative humidity) chamber was installed, "ligament zero" was re-established. In each cyclic creep test, the tissue was loaded for 30 cycles at 1 Hz from "ligament zero" to the desired stress. For a static creep test, each MCL was then loaded immediately to the same

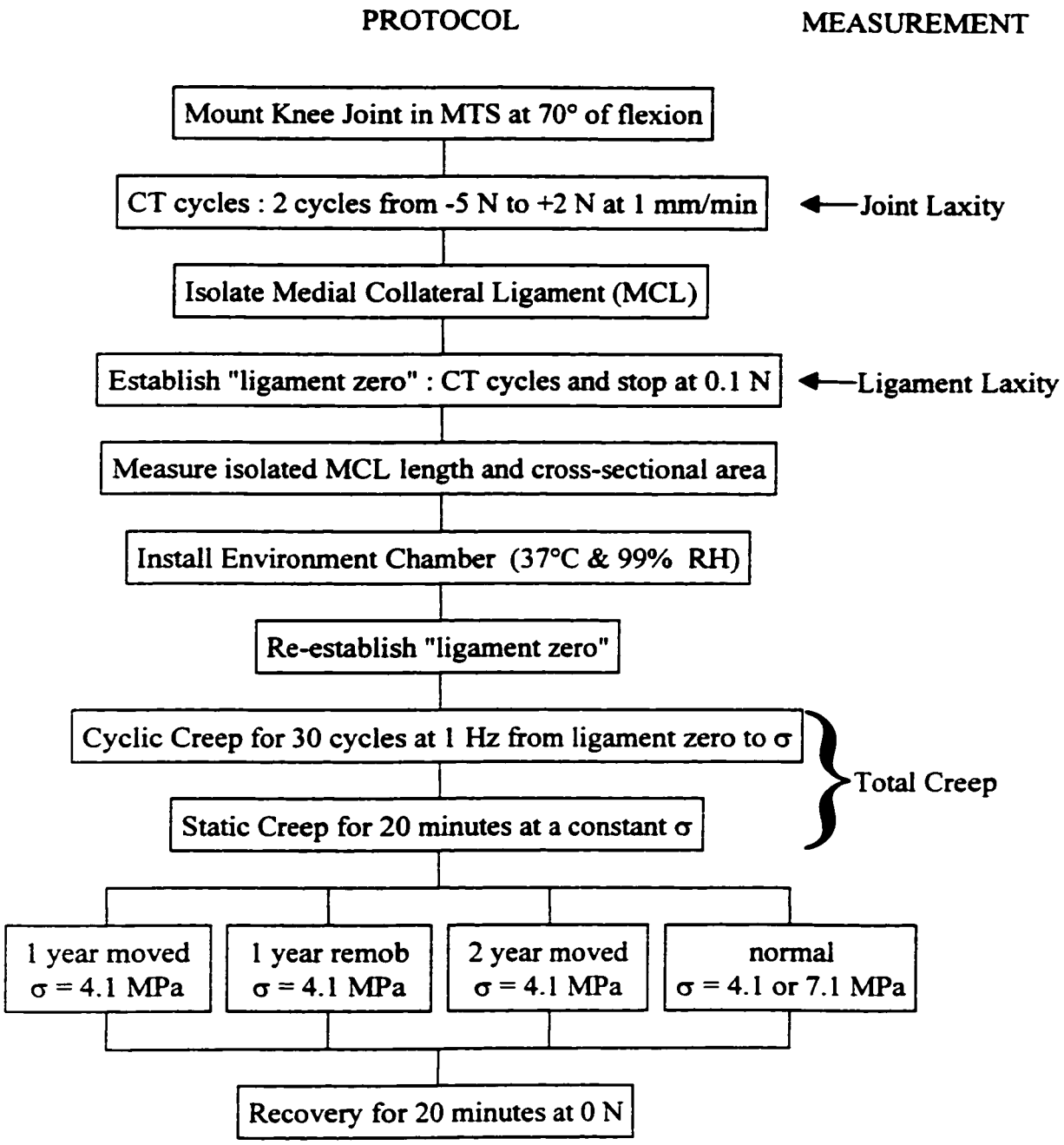

Figure 6.5: Creep Test Protocol for MCL Autografts

"CT" is compression-tension and "RH" is relative humidity

stress as in cycling and held in load control for 20 minutes. The creep test was followed by a recovery period. The MCL was unloaded to 0 N and held at 0 N for 20 minutes.

Joint laxity was defined as the displacement recorded when the whole joint was loaded from 5 N compression to 2 N tension. Ligament laxity was defined as the displacement of the MCL between "ligament zero" (+0.1 N) and the point when the tibial and femoral condyles began to transmit compressive load across the joint (-0.1 N). Creep test and recovery period components are shown in Figure 6.6. Strain was defined as the deformation of the MCL divided by the undeformed MCL length. Total creep is the behaviour that results from the complete creep testing protocol. Total creep strain was defined as the increase in strain from the peak of the first cycle in cyclic creep to the end of the static creep. The "elastic" recovery ratio was defined as the ratio of the "elastic" unloading over the "elastic" loading. "Elastic" loading is the change in strain caused by monotonic loading at the prescribed loading rate. "Elastic" unloading is the change in strain caused by monotonic unloading at the prescribed loading rate. The term "elastic" is used here in lieu of "initial" and would therefore contain a viscous as well as the true elastic response. A ratio of 1 would indicate complete "elastic" recovery. Viscoelastic recovery was the difference between the strain at the beginning of the 20 minute recovery period and the strain at the end of recovery. The unrecovered creep strain was the residual strain in the MCL at the end of the period of recovery used. Statistical analysis was performed using analysis of variance with linear contrasts (significance defined by $p<0.05$).

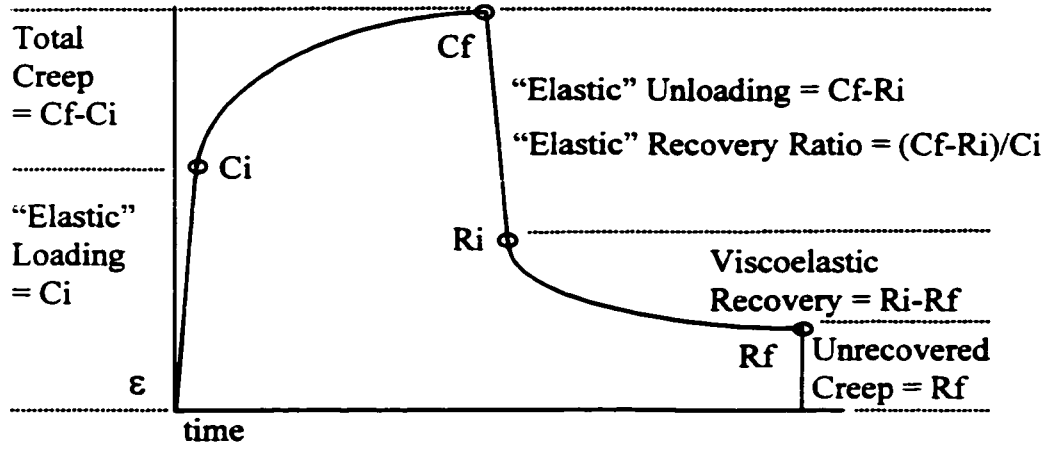

Figure 6.6: Creep Test Components for MCL Autografts

"Elastic" is used instead of "initial"; thus, includes a viscous in addition to the true elastic response.

"Cf" is the strain at the end of the static creep test

"Ci" is the peak strain of the first cycle in the cyclic creep test

"Ri" is the strain at the beginning of the recovery period

"Rf" is the strain at the end of the recovery period

6.3 Results

6.3.1 Bilateral Gap Scars with Immobilization

The ligament laxity of immobilized scar returned to normal values after 6 weeks of healing; however, the ligament laxity of moved scars did not return to normal values even after 14 weeks ($p<0.05$; Figure 6.7). In fact, the ligament laxity for 14 week immobilized scars was negligible (0.00 mm). The joint laxity of 14 week immobilized scars was also less than normal ($p=0.001$; Figure 6.8).

All of the immobilized 6 week scars failed at the first cycle in cyclic creep, whereas only two of the six of the moved 6 week scars failed during cyclic creep ($p=0.1$; Table 6.3). The total energy absorbed was similar regardless of treatment (Figure 6.9). Five of the six immobilized 14 week scars failed during cyclic creep and the one remaining sample from that group failed during static creep (Table 6.3). None of the moved 14 week scars failed during cyclic creep which was significantly less than the number of immobilized 14 week scars that failed ($p=0.01$). The energy absorbed by the 14 week immobilized scars was not significantly different than 14 week moved scars. The majority of immobilized scars failed during cycling whereas the majority of the scars that were never immobilized survived the cyclic creep test (6 and 14 week scars). The energy absorbed by 6 and 14 week scars was significantly greater than that absorbed by normal ligaments tested at the same stress. None of the normal MCLs failed during cyclic testing and this was significantly different than the number of failures experienced by the immobilized scars ($p<0.008$).

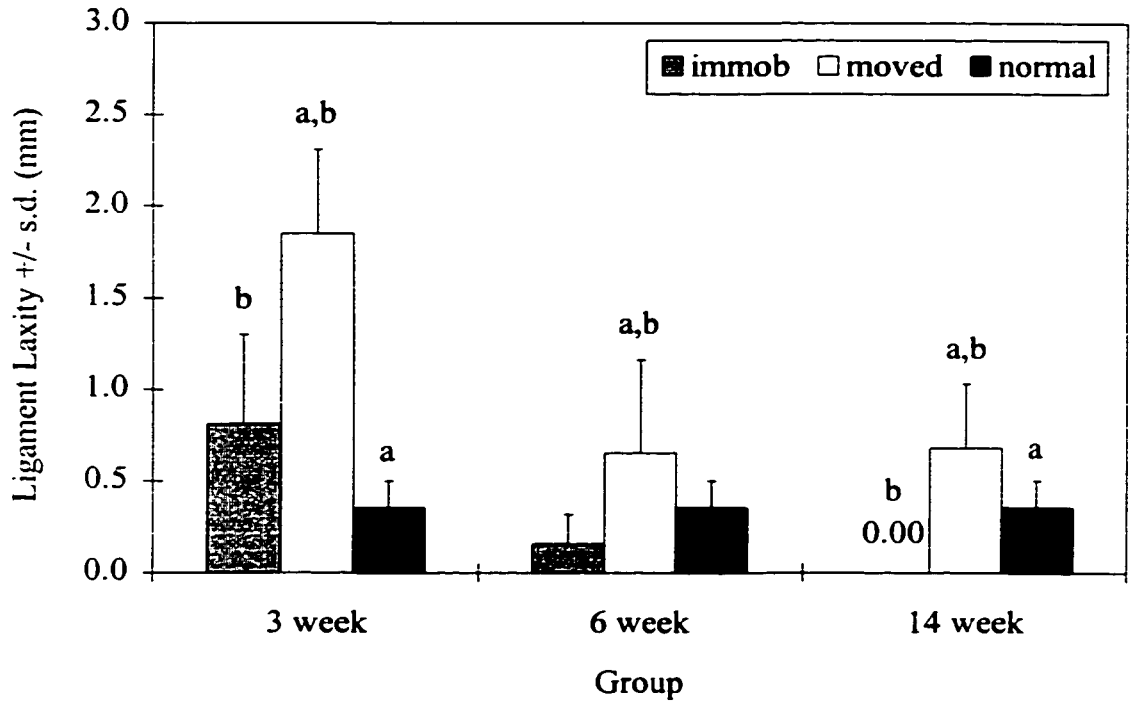

Figure 6.7: Ligament Laxity of Bilateral MCL Gap Scars and Normals

Pooled normal values are shown (creep tested at 4.1 and 7.1 MPa).

"immob" indicates immobilization and "s.d" is standard deviation

a = different than immobilized scar ($p<0.03$)

b = different than normal ($p<0.05$)

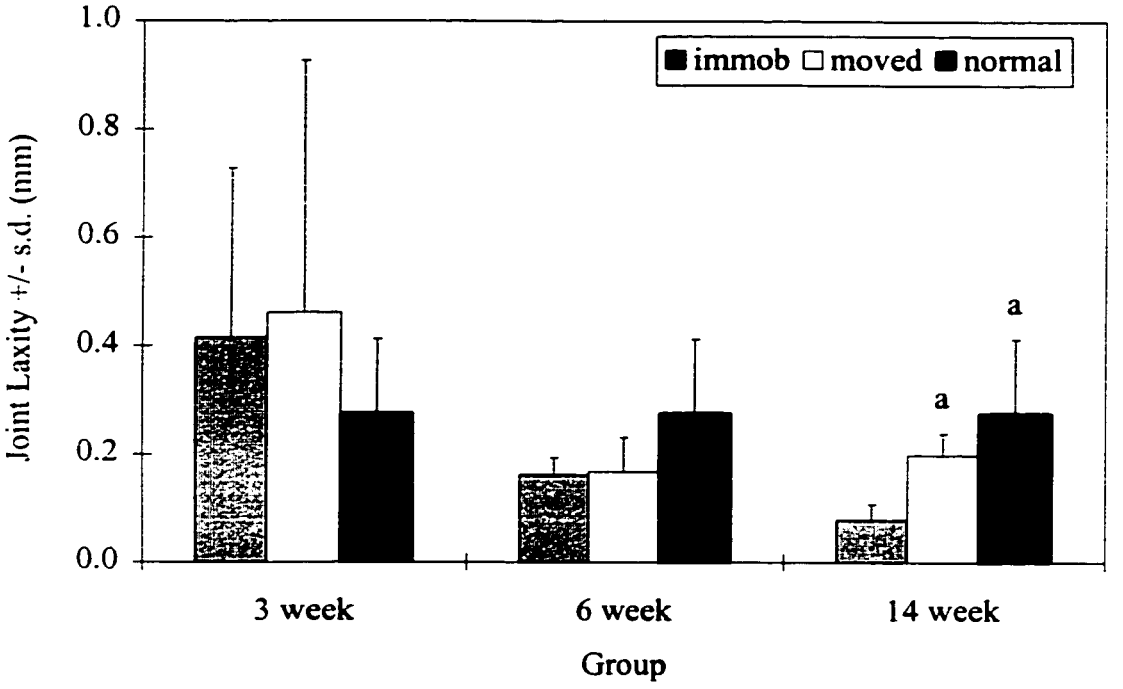

Figure 6.8: Joint Laxity of Bilateral MCL Gap Scars and Normals

Pooled normal values are shown (creep tested at 4.1 and 7.1 MPa).

"immob" indicates immobilization and "s.d" is standard deviation

a = different than immobilized scar ($p<0.001$)

Table 6.3: Timepoints of Failures and Completions of Creep Testing for Bilateral MCL Gap Scars and Normals

Group	**Total** total tested	# fail during area	# fail during first cycle	# fail during cyclic creep (cycle)	**Failures** # failed / total tested	# completed cyclic creep	**Completions** # completed cyclic creep / total tested
3 week immob	4	2	0	1 (12)	3/4	1	1/4
3 week moved	4	0	2	2 (2 & 21)	4/4	0	0/4
6 week immob	3	0	3	0	3/3 [a]	0	0/3 [a]
6 week moved	6	0	2	0	2/6	4	4/6
normal 4.1MPa	7	0	0	0	0/7	7	7/7
14 week immob	6	0	4	1 (17)	5/6 [b]	1	1/6 [b,c]
14 week moved	5	0	0	0	0/5	5	5/5
normal 7.1MPa	6	0	0	0	0/6	6	6/6

"immob" indicates immobilization

"a" indicates different from 6 week moved ($p=0.1$) and normal 4.1 MPa ($p=0.008$)

"b" indicates different from 14 week moved ($p=0.01$) and normal 7.1 MPa ($p=0.001$)

"c" indicates that the remaining sample failed during static creep

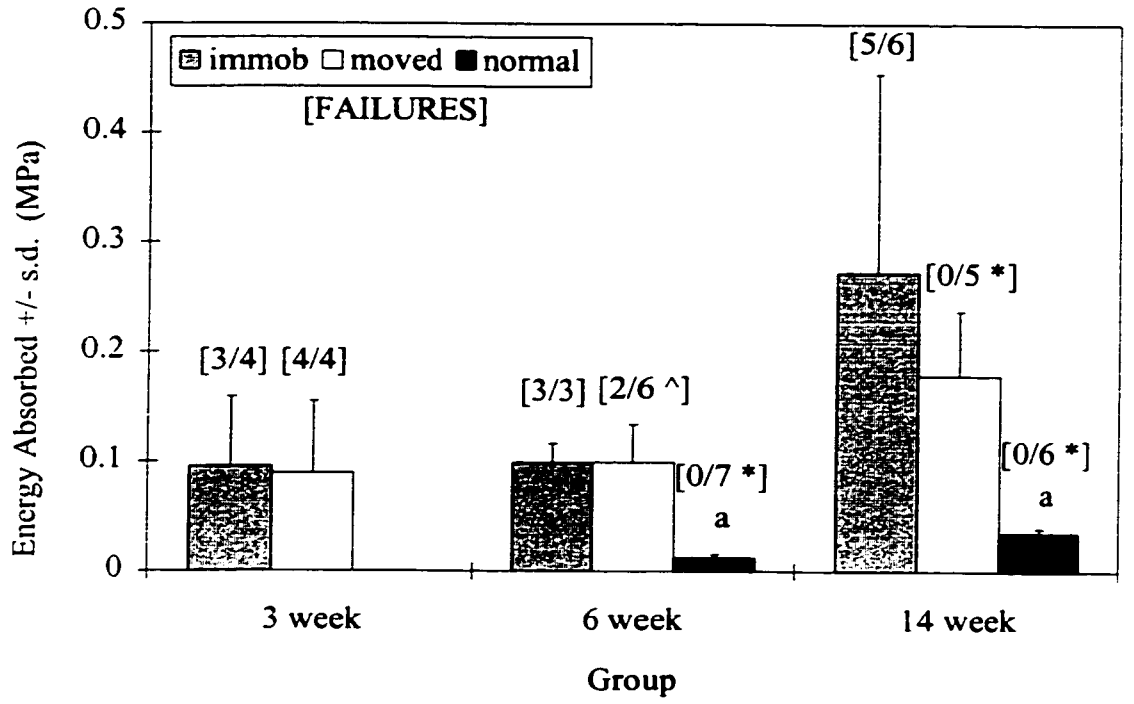

Figure 6.9: Energy Absorbed during Cycling of Bilateral MCL Gap Scars and Normals

Normal MCLs are shown with groups tested at the same stress.

Energy absorbed is hysteresis energy plus failure energy.

"immob" indicates immobilization and "s.d" is standard deviation

"[FAILURES: numbers in brackets]" indicate the number of samples that failed during the course of the test / total tested in that group

a = energy absorbed is different than scars ($p<0.05$)

[*] = number of failures are different than immobilized scar ($p<0.008$)

[^] = number of failures are different than immobilized scar ($p=0.1$)

Only four scars survived the first cycle of cyclic creep to fail at a later timepoint in the cyclic creep test and one of these four failed at the second cycle (Table 6.3). The three remaining scars (one 14 week immobilized, one 3 week immobilized and one 3 week moved) that failed during cycling were used to examine the change in modulus during cycling. The modulus of the representative 14 week moved scar (non-failure) increased over the first few cycles (cycle 1 to cycle 4 shown in Figure 6.10a) and maintained a relatively constant value over the remainder of the test without failure (similar to the trend in modulus change shown for normal MCLs). The modulus of the 14 week immobilized scar (failed at cycle 17) increased over the first few cycles (cycle 1 to cycle 4 shown in Figure 6.10b) to attain a constant modulus from cycle 4 to cycle 16 upon which there was a 17% reduction in modulus and subsequent failure of the MCL scar. For one 3 week moved scar, the first 16 cycles had a trend similar to the 14 week moved scar (Figure 6.11a). After cycle 16 there was a disruption in the cyclic pattern and when cycling resumed there was a 39% reduction in modulus. The pattern continued for a few additional cycles until failure at cycle 21. One 3 week immobilized scar had a similar pattern to the 14 week immobilized scar, failing at cycle 12 with a corresponding 20% reduction in modulus (Figure 6.11b).

6.3.2 Long-Term Autografts with Remobilization

The total creep strain of long-term autografts was consistently greater than normal values. Even after 2 years of healing, the MCL autografts had total creep strain 1.7 times

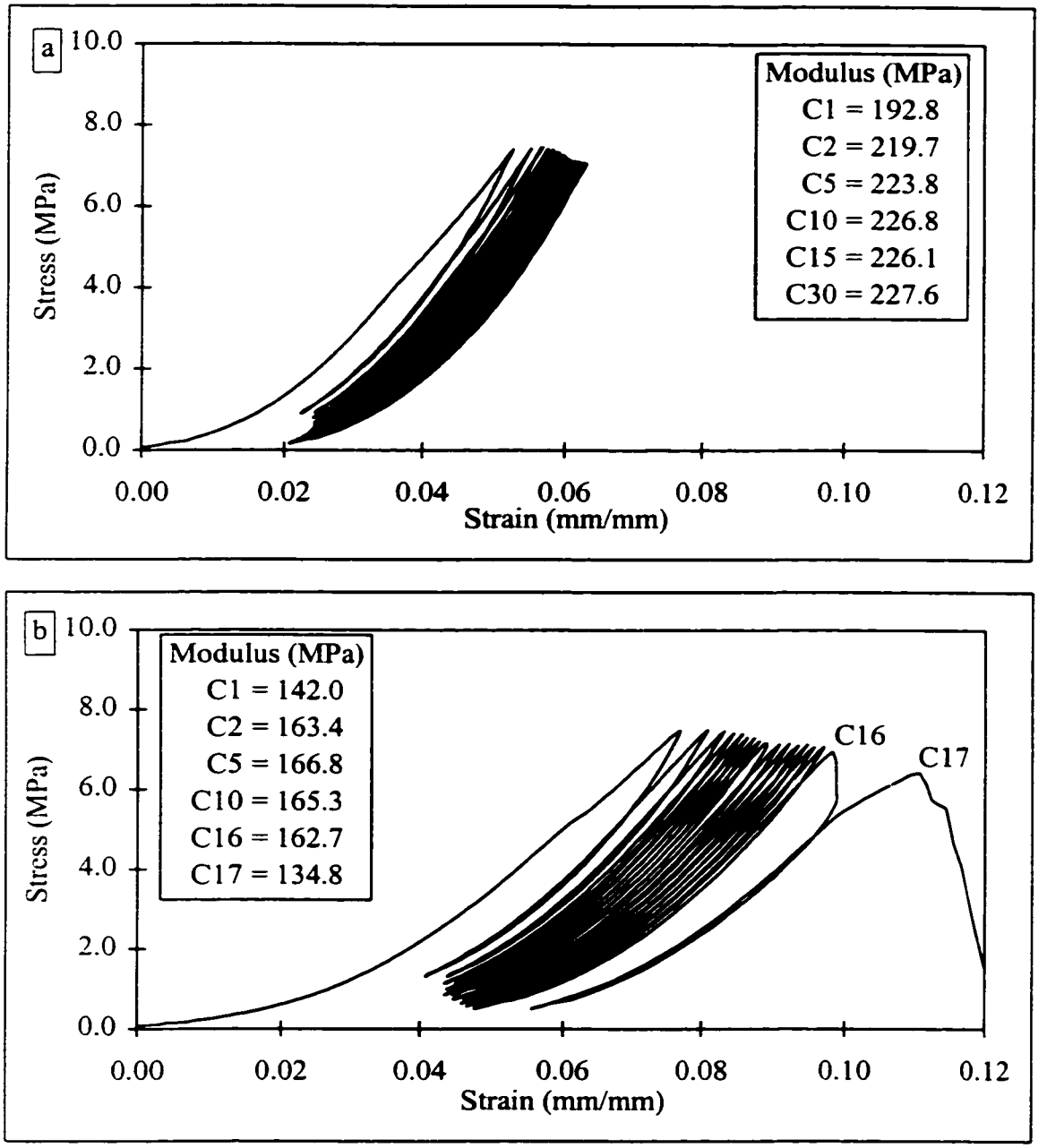

Figure 6.10: (a) Cyclic Plot of a Representative 14 week Moved Scar

(b) Cyclic Plot of the 14 week Immobilized Scar with Failure at Cycle 17

"C1" indicates Cycle 1

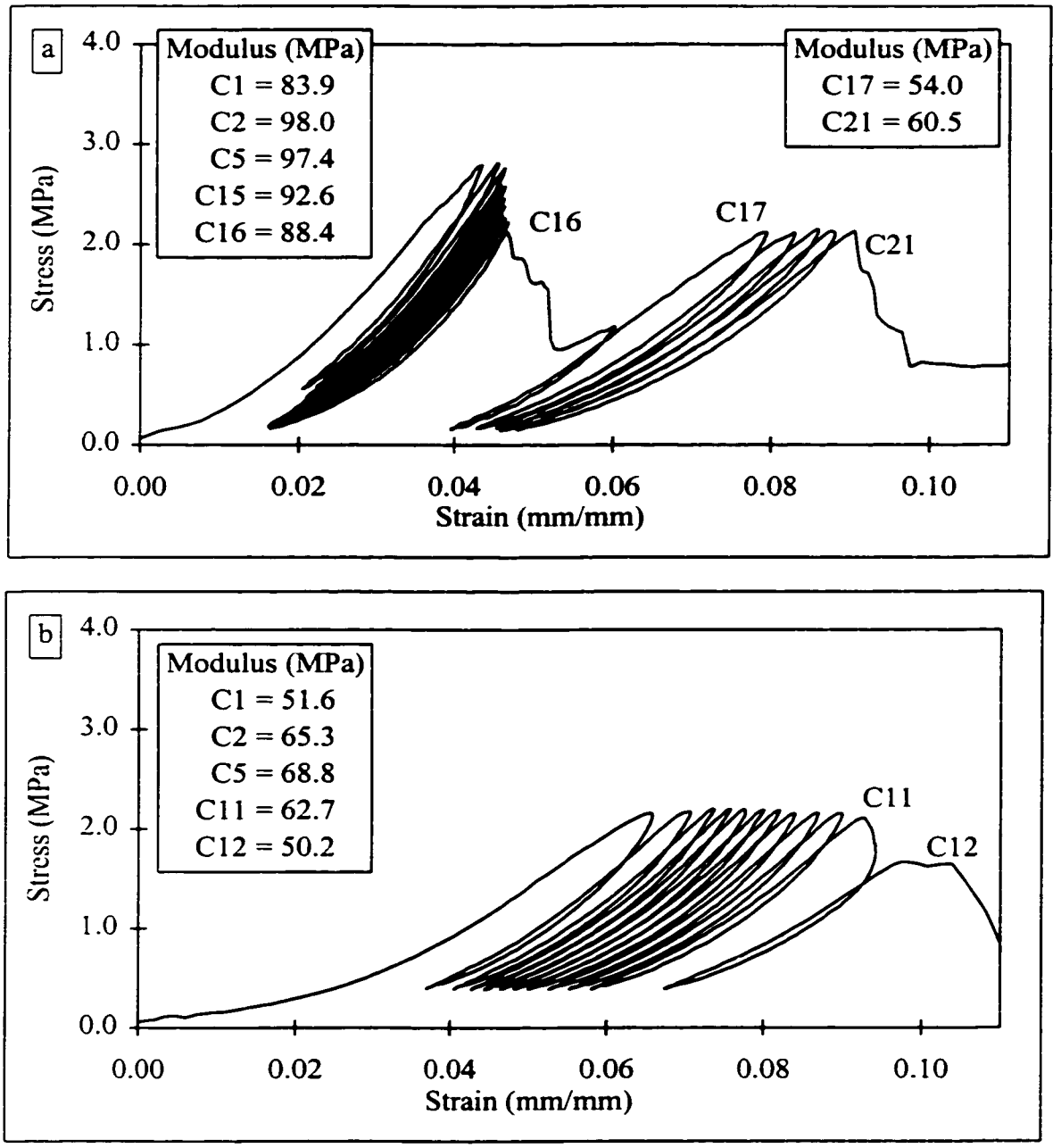

Figure 6.11: (a) Cyclic Plot of the 3 week Moved Scar with Failure at Cycle 21

(b) Cyclic Plot of the 3 week Immobilized Scar with Failure at Cycle 12

"C1" indicates Cycle 1

greater than normals ($p<0.0001$) (Figure 6.12). No statistical difference was found between the two normal control groups which spanned the range of loading required for 4.1 MPa graft stress. Recall that the mean graft cross-sectional area for all grafts (no significant difference in area between groups) was 7.73 ± 1.25 mm^2 and thus two normal groups were required: stress matched (4 MPa) and force matched (29 N as shown on Figure 6.12). The total creep strain of the moved 1 year MCL autografts was 1.8 times greater than normals ($p<0.0001$). No statistical difference was found between the 1 year and 2 year moved MCL autografts. The 1 year MCL autografts that were remobilized after immobilization for the first 6 weeks of treatment had total creep strain 2.2 times greater than normals ($p<0.0001$). As well, the total creep strain of the remobilized 1 year autografts was 1.2 times greater than those that were never immobilized ($p<0.05$). The difference in the 1 year grafts was in the static creep component ($p=0.01$).

In addition, the creep recovery of grafts was consistently inferior to normal. The viscoelastic creep and unrecovered creep of the 2 year moved grafts were greater than normal ($p<0.002$) (Figure 6.13). There was no difference in the unrecovered creep comparing 2 year moved, 1 year moved and 1 year remobilized grafts (Table 6.4). To explain this substantially increased amount of unrecovered creep, the components of recovery were examined. The "elastic" recovery ratio was significantly less than normal for only the 2 year moved group ($p=0.03$) (Table 6.4). The "elastic" recovery is complete if the ratio is 1 (not different than normal). Thus, for the other two cases (1 year moved and 1 year remobilized), the viscoelastic recovery is the only other factor to explain the

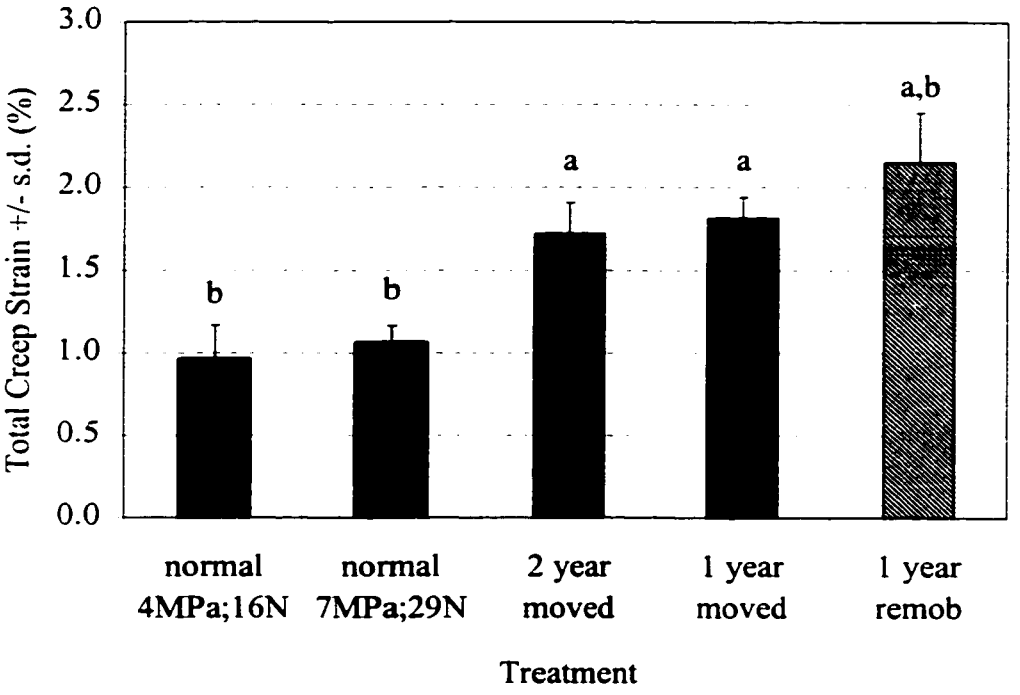

Figure 6.12: Total Creep Strain of MCL Autografts and Normals

"remob" indicates remobilization and "s.d." is standard deviation

a = different than normal ($p<0.0001$)

b = different than 1 year moved autograft ($p<0.05$)

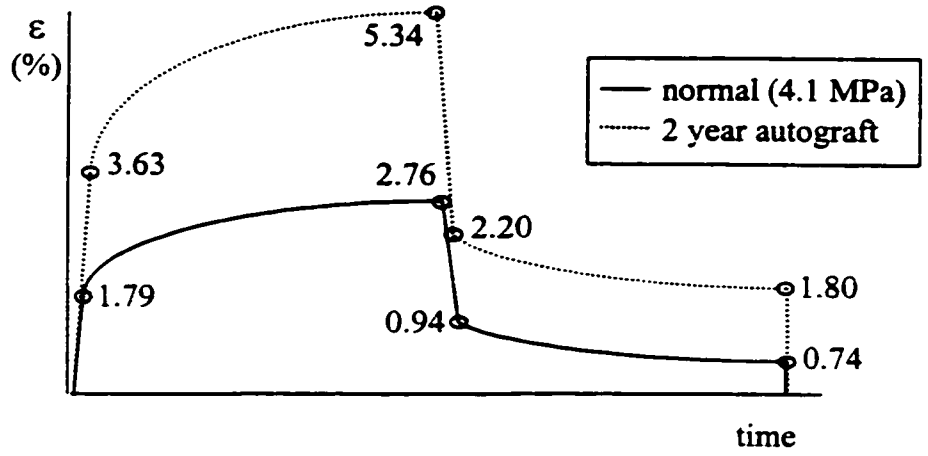

Figure 6.13: Creep and Creep Recovery of 2 year MCL Autografts and Normal MCLs

"ε" indicates strain and mean strains are shown.

Table 6.4: Laxity and Recovery of MCL Grafts and Normals

Group	Joint Laxity (mm)	Ligament Laxity (mm)	Elastic Recovery Ratio	Viscoelastic Recovery (% strain)	Unrecovered Creep (% strain)
normal	0.18±0.04	0.19±0.13	1.02±0.09	0.20±0.12	0.74±0.22
1 year remob	0.30±0.15	0.23±0.09	0.99±0.08	0.39±0.11[a]	1.82±0.34[a]
1 year moved	0.38±0.18[a]	0.37±0.18	0.92±0.13	0.30±0.09[b]	1.86±0.59[a]
2 year moved	0.22±0.08	0.31±0.27	0.88±0.09[a]	0.41±0.04[a]	1.80±0.53[a]

Data are shown as mean ± standard deviation.

"remob" indicates remobilization

"a" indicates different than normal ($p<0.05$)

"b" indicates different than 2 year moved grafts ($p<0.04$)

amount of unrecovered creep. The viscoelastic recovery was significantly greater than normal for the 2 year moved and 1 year remobilized groups ($p<0.002$). However, these grafts were attempting to recover from a viscoelastic creep that was greater than normal. For the viscoelastic recovery to reduce effectively the unrecovered creep to normal values, it would have to be 7 times greater than normal recovery, not 2 times greater, as documented here. Normal joint laxity was observed for grafts that had increased viscoelastic recovery (2 year moved and 1 year remobilized). The abnormal joint laxity observed in the moved grafts after 1 year of healing had returned to normal values by 2 years post-operatively. Ligament laxities were within normal limits for all of the long-term grafts.

6.4 Discussion

6.4.1 Bilateral Gap Scars with Immobilization

Interestingly, the joint and ligament laxities of the 6 and 14 week immobilized scar were comparable or less than normal values; in fact, immobilized 14 week scars had negligible ligament laxity. Previous studies have documented increased joint and ligament laxity after immobilization of healing ligaments (70,162). The very low laxity of the immobilized scars in this study may be a result of the position of immobilization with legs in full flexion. In MCL scars of knee joints that were immobilized in full flexion (~150° to 160°), Frank et al. (1991) documented a more rapid realignment of collagen fibres towards the long axis of the ligament with the joint positioned at 70°

flexion. The new collagen laid down in the immobilized scar may be stretched out when positioned at 70° flexion; thus, recruiting the fibres and promoting alignment. This "short scar" produced while the knee was immobilized in full flexion would be highly recruited once extended to 70° flexion and, in the current investigation, had definite impact on reducing the laxity of the ligament. Concurrent with better alignment than moved scars, immobilized scars had less ligament laxity than moved scars. This same immobilization method was used by Bray et al. (1992) on rabbit knees with MCL/ACL injury and in that study the ligament laxity of the injured MCL was similar to normal values. Fibre recruitment is acting to minimize the laxity of the immobilized scar.

Of equal interest, cyclic energy absorption of scars was greater than normal. Immobilized scars failed during cyclic creep more frequently than moved scars; with very high proportions failing after 6 or more weeks of immobilization (when tested cyclically at 30% of the failure strength of the non-immobilized MCL gap scar). In fact, all of the 6 week immobilized scars failed during cyclic creep and all but one of the 14 week immobilized scars failed during cyclic creep (and that one failed during static creep). The changes in the viscoelastic response of the immobilized ligaments (just like the reduction in laxity) is related apparently to fibre recruitment. The large amount of recruitment at the start of the test was advantageous for laxity but too advanced to aid in resisting creep. Six of the twelve normal MCLs tested at 28 MPa had an increased creep response because limited fibre recruitment was available to resist creep as evidenced by an almost extinguished crimp pattern. The other 6 of the 12 MCLs tested at 28 MPa had

discontinuities in the creep curves, half occurring in cyclic creep where there was a reduction in modulus in consecutive cycles similar to that of the one 14 week immobilized scar. Although the normal MCLs did not have the discontinuity followed by a complete ligament failure, the reduction in modulus has previously been used as an indicator of damage to tendon (156,157) and fibre composites (18). These results suggest that fibre recruitment acts to minimize creep and to prevent failure but is limited based on the amount of recruitment available (or remaining) under specific conditions. The poorer resistance to failure of immobilized scar as compared to moved scar was in agreement with previous observations of reduced failure strength of scars with immobilization (162). Additionally, these results suggest that an immobilized scar when remobilized, is likely to fail very quickly under repeated cycling, likely promoting a new injury response. This could help explain the long-term inferiority of remobilized scars shown by Inoue et al. (1990).

Moved scars were less likely to experience a failure than immobilized scars (2/6 at 6 weeks and 0/5 at 14 weeks). The moved scars better survived the cyclic creep test even though ligament laxity was abnormally increased. The reduced laxity in the immobilized scars may be attributed to the altered fibre recruitment in the "short scar"; perhaps, fibre recruitment in the moved scar was able to resist creep and failure better but permitted increased laxity.

Returning to the concept that reduction in loading cycle modulus is an indicator of tissue damage, the three cases available from this study support the concept (Figures 6.9b,

6.10a and 6.10b). A reduction in modulus always preceded failure of the ligament scar. In two of the cases, the scar failed immediately after the loading cycle for which the reduced modulus was measured. In the remaining case, there was a discontinuity in the cyclic creep curve after which the scar was able to complete 5 more cycles (with reduced modulus) before failing. Recall that for the normal MCLs tested at 28 MPa, discontinuities in cyclic creep were followed by reductions in modulus and discontinuities in static creep were related to fibre ruptures. All of these findings support the fact that reduction in modulus of loading cycles can be used as a indicator of damage in normal and healing ligaments.

Even though some scars failed at the first cycle in the cyclic creep test, the test protocol exposes the ligament to increases and decreases in stress prior to the cyclic creep test (laxity and area measurements). In addition, other scars failed during cyclic loading (which was preceded by a reduction in modulus). These results in combination suggest that there is a relationship between creep and fatigue failure. In fact, the preceding discussion of fibre recruitment indicated a relationship between resisting creep and resisting failure. Conventional definitions for creep and fatigue were developed studying engineering metals where the two could be easily separated: creep resulting from sustained loading and fatigue resulting from fluctuating loading (with no mean load). For viscoelastic materials; these definitions are not as easily applied. Compressive testing of ligaments which are structures that resist tension is not practical. Thus, based on the above definitions, the cyclic creep test used here would combine both creep and fatigue.

In tendon, Wang et al. (1995) found through similar cyclic tests that tendon failure was not the result of creep alone nor of fatigue alone. Clearly, the new evidence presented here suggests that there is a complex interplay between creep and fatigue failure in healing ligament.

6.4.2 Long-Term Autografts with Remobilization

The most interesting feature of these results was that even after 2 years of healing the creep properties of the MCL autografts remained inferior to normals. No improvement occurred between the first and second years of healing. In fact, when Boorman et al. (1998) investigated the short-term healing of this same autograft model, they observed a critical increase in creep in the first three weeks of healing, but no subsequent increase from 3 weeks to 8 weeks. The results from the 1 year and 2 year time points continue to show no significant change (Figure 6.14). These findings together suggest that the creep behaviour of grafts plateaus in the short-term and has a limited capability to change in the long-term. The lack of long-term improvement may be due in part to two possible mechanisms. First, inflammation or increased water content may have an effect. It was shown previously that a 5% increase in water content from normal (using PBS) can create a pre-stress in the rabbit MCL. If this shift was not taken into account, the apparent measured creep behaviour was comparable to the moved grafts. Thus, *in vivo* increases in water content could increase creep. Second, the creep behaviour of the moved grafts was greater than normal ligaments but less than ligament

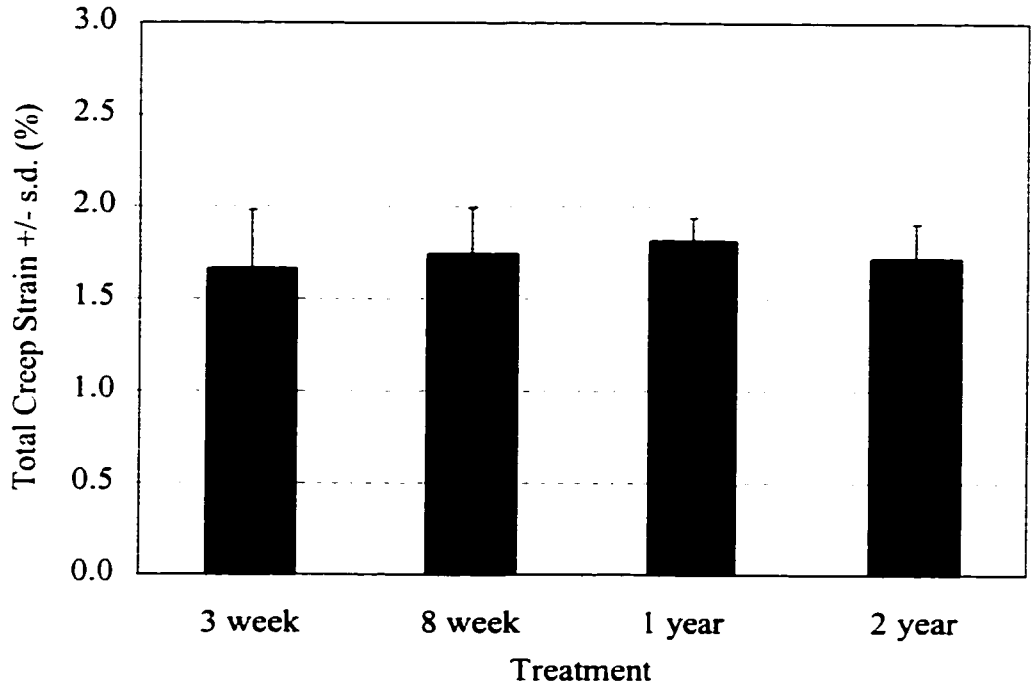

Figure 6.14: Total Creep Strain of MCL Autografts (Short and Long-Term Healing)

3 week and 8 week MCL autograft data from Boorman et al. (1998)

"s.d." is standard deviation

scars (Figure 6.15). Mechanically, the structure is behaving like a composite of ligament and scar. So there is a clear mechanical benefit to having the graft structure in place for the scar to infiltrate rather than having scar alone. However, several structural factors of MCL scars were identified previously that do not return to normal with healing. Of principal importance is that the scars never have the same fibre organization and fibre interconnections as normal MCLs; thus, fibre recruitment in scars is less able to resist creep. These same types of fibre recruitment abnormalities may prevent grafts from attaining normal creep behaviour.

One year MCL autografts remobilized after 6 weeks of immobilization had greater total creep strain than 1 year grafts that had no post-operative immobilization. Boorman et al. (1998) studied the creep behaviour of MCL autografts that had been immobilized or moved for the total time of the post-operative treatment (3 weeks or 8 weeks). The immobilized MCL autografts had greater total creep strain than the moved grafts. Interestingly, the MCL autografts that had 6 weeks of immobilization followed by remobilization totaling 1 year of treatment had total creep strains comparable to the grafts that were immobilized for the total treatment period of 3 or 8 weeks (Figure 6.16). There are three possible mechanistic explanations. First, altered water content in an immobilized graft could be a mechanistic factor. Second, immobilization may create the condition for increased scar infiltration and matrix degradation as compared to moved grafts. Valias et al. (1981) speculated that immobilization of healing MCLs allowed for increased collagen degradation without a balanced increase in collagen synthesis.

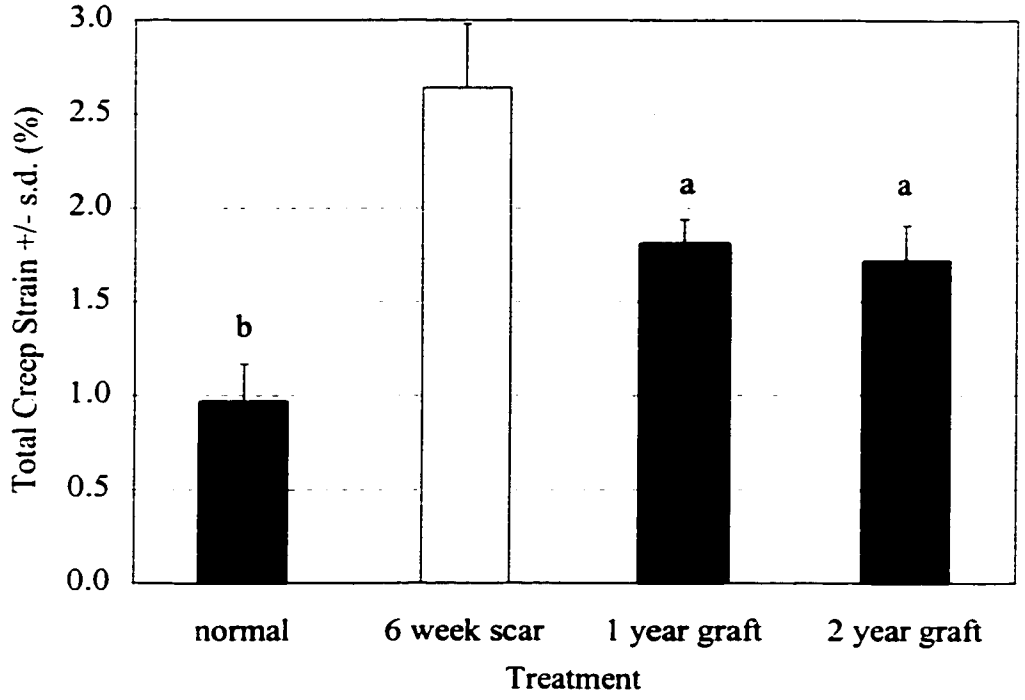

Figure 6.15: Total Creep Strain of MCL Autografts, Gap Scars and Normals Tested at 4.1 MPa

"s.d." is standard deviation

a = different than 6 week scar and normal ($p<0.0001$)

b = different than 6 week scar and autografts ($p<0.0001$)

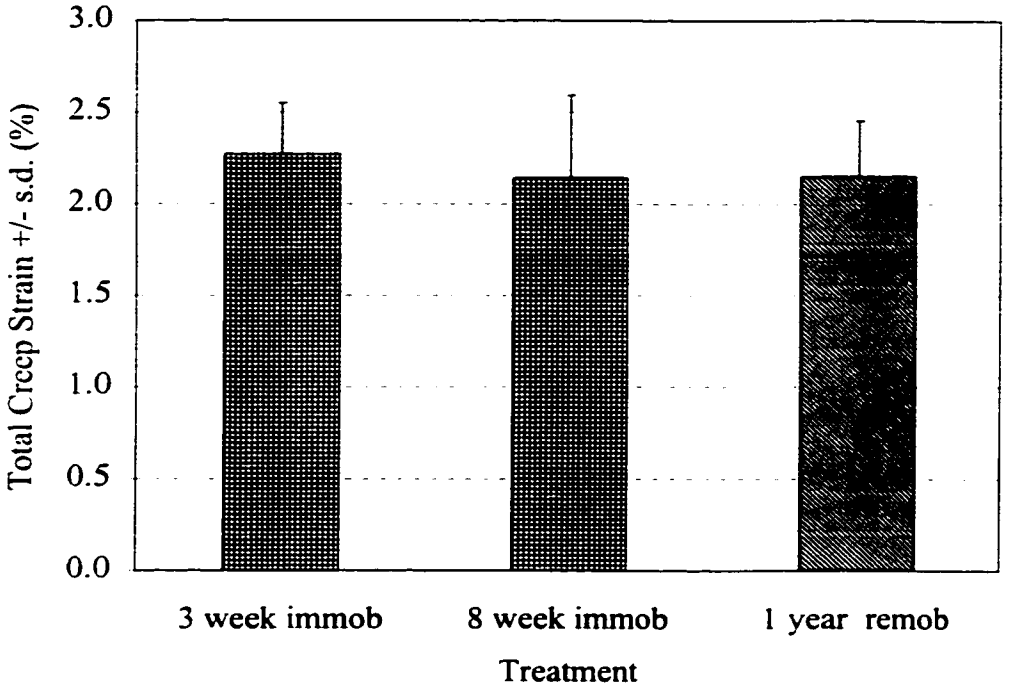

Figure 6.16: Total Creep Strain of MCL Autografts (Immobilization and Remobilization)

Immobilized 3 week and 8 week autograft data from Boorman et al. (1998)

"immob" indicates immobilization, "remob" indicates remobilization

and "s.d." is standard deviation

Amiel et al. (1983) documented an increase in collagen degradation in immobilized normal MCLs. In MCL scar, GAG content was persistently elevated even at 14 week of healing (52). Gamble et al. (1984) documented that immobilization increases GAG degradation in normal ligaments. These factors may account for differences between the immobilized and moved grafts and perhaps none of these changes are reversed by subsequent remobilization. Third, similar to the 14 week immobilized scars (Section 6.3.1), the 3 and 8 week grafts that were immobilized had negligible ligaments laxities (unpublished data from Boorman (24)). The grafts in the current study experienced a loading environment change when the graft (stiffened by 6 weeks of immobilization) was remobilized for the remainder of 1 year. The change in loading environment from immobilized to remobilized may have promoted a new injury response and encouraged additional scar infiltration and matrix degradation. Short-term immobilization of these grafts had long-term detrimental consequences.

The creep recovery results show that even after 2 years of healing MCL autografts have substantially larger unrecovered creep than normal MCLs. The unrecovered creep of the long-term moved grafts was 1.5 times larger than that of these same grafts quantified after 3 to 8 weeks of healing (24). Thus, long-term MCL autografts still have reduced ability to recover from creep compared to both normal ligaments and short-term MCL autografts. Regardless of the early rehabilitation protocol (moved or immobilized), grafts had similar abnormally increased susceptibility to creep. Therefore, early post-operative immobilization was not an advantage when examining unrecovered creep strain. The

process of creep recovery may be slower than the process of creep. In a pilot study on normal MCLs creep tested at 4.1 MPa or 14 MPa, recovery was performed with the ligament in a buckled position (-1 mm deformation from "ligament zero") and, at hourly intervals, the ligament underwent two compression-tension cycles to determine if the deformation at 0.1 N tension had returned to 0 mm. For both the 4.1 MPa or 14 MPa creep test stresses, three hours was required for the MCL to recover from 20 minutes of creep. The recovery in grafts may be even slower. The lack of recovery in the grafts may be due to those matrix abnormalities caused by scar infiltration. The inferior fibre architecture may have undergone a conformational change and was not able to return to its original configuration and deformation.

These data suggest that despite grafts having a pronounced *in vitro* susceptibility to creep, this susceptibility was not revealed in the test of whole joint laxity. A possible explanation is that the MCL may only have a limited contribution to whole joint laxity when the joint has all ligaments and menisci intact; however, even changes in MCL laxity were not detected. The first possible reasons is that the unrecovered creep caused a change in laxity but it was not detected. The maximum tensile load for tests of joint laxity (2 N) and ligament laxity (0.1 N) are possibly not large enough to detect difference between the grafts and the normal MCLs. The second possible reason is that the grafts were eventually able to recover from creep due to *in vivo* loading. *In vivo* loading may be lower than that used in the *in vitro* tests due to neuromuscular protection or adaptive changes in other structures of the joint *in vivo*. The whole joint is capable of remodeling

and these other structures, such as cartilage and bone, have a role in the assessment of whole joint laxity but clearly do not have a role in the creep behaviour of the isolated graft. If the graft was not exposed to *in vivo* stresses that would cause creep, the reduced joint and ligament laxity may be analogous to the reduction of laxity in immobilized scar produced by conditions of fibre recruitment that reduced laxity but were not effective at resisting creep. In the current tests, laxity was assessed before creep testing. In order to gain an understanding of how laxity changes with recent activity, it would be instructive to measure laxity after creep testing *in vitro*. A further understanding of the compensatory mechanisms could be gained by assessing the changes in unrecovered creep and laxity in an unstable joint. Others have shown the benefit of limiting excess stresses in an unstable joint which resulted in reduced ligament laxity of the immobilized joint compared to the moved joint (25,70).

In summary, immobilized scars had reduced laxity and increased susceptibility to failure during cyclic creep. These unique results suggest that fibre recruitment in these "short scars" was at a high level owing to differences in the joint position during immobilization and during mechanical testing. The results from these immobilized scars (in addition to normal ligaments creep tested at a linear region stress) provide a new understanding of how limited potential for fibre recruitment is related to increased creep response. In addition, reduction of cyclic modulus was confirmed to be an acceptable marker for tissue damage in normal and healing ligament which further suggests the importance of examining the complex relationship between creep and fatigue. This was

the first investigation to show that long-term autografts had inferior creep behaviour than normal MCLs. This persistent inferiority was likely due to changes in water content and fibre recruitment caused by scar infiltration. These results may have important implications for post-operative treatment given that remobilized autografts had even poorer creep behaviour that non-immobilized grafts. This inferior creep response may be due to increased scar infiltration upon re-injury of the highly recruited graft after remobilization. In the tests presented here, laxity measurement did not reveal the susceptibility of grafts to unrecovered creep either because of limitations of the laxity test, adaptive compensation in the joint or recovery of the graft *in vivo*.

CHAPTER 7

OVERALL DISCUSSION OF RESULTS AND METHODS

7.1 Discussion of Results

The critical path for the investigations in this thesis addressed five major questions.

1. Can ligament creep behaviour be predicted from previously measured stress relaxation behaviour?
2. Can fibre recruitment account for the difference between creep and stress relaxation behaviour in normal ligament?
3. How are creep and water content related in normal ligament (both water content initial conditions and water content changes due to creep)?
4. Are ligament scars more susceptible to creep than normal ligaments and which of the biochemical and morphological changes in scar (including fibre recruitment and water content) could account for such behaviour?
5. Does immobilization of ligament scars and ligament grafts minimize or exacerbate creep?

The purpose of this overall discussion is to restate the results briefly as they relate to the above five questions and to expand on the implications of these results.

7.1.1 Fibre Recruitment and Creep (Question 1 and Question 2)

This was the first investigation to measure experimentally both the creep and stress relaxation of rabbit MCL. The results showed that ligament creep behaviour was not predicted by the inverse stress relaxation behaviour. A novel yet simple structural model of ligament creep accounted for this difference by incorporating fibre recruitment with fibre creep. The assumptions in the model were that the creep test allowed fibre recruitment and the stress relaxation test did not, such that the inverse stress relaxation function could be used to model the creep of a particular group of fibres. These model assumptions were then confirmed using a unique approach for quantifying the crimp patterns before and after creep and relaxation testing: creep caused fibre recruitment and stress relaxation did not.

The analysis of crimp patterns led to a new understanding of the mechanisms of creep in normal ligaments. Collagen fibres were recruited during creep at lower, toe region stresses which was apparent because the modulus increase during cyclic creep and the strain increase during static creep were similar over 4.1 MPa to 14 MPa. The creep strain increased significantly when the ligament was tested at a creep stress in the linear region where fibre recruitment was limited (predominance of straightened fibres post-creep). These results suggest that a spectrum of fibre recruitment potential exists: varying amounts of recruitment are available to maintain creep at an equally small amount over the range of stresses in the toe region and limited fibre recruitment is available at stresses in the linear region. These exciting observations suggest that fibre recruitment is an ideal system to reduce fatigue and maintain joint stability during activities within a permitted

functional range of stresses (defined here by the toe region of the stress-strain curve). Given that crimp is a feature of both ligaments and tendons, these principles of fibre recruitment during creep are applicable to human ligaments and tendons. Any repair or reconstruction of an injured ligament should seek to replicate some type of fibre recruitment that can act to minimize creep over a range of stresses. Fibre recruitment is obviously a key factor for any theoretical models of ligament behaviour.

7.1.2 Water Content and Creep (Question 3)

The results confirmed previous observations that water content was decreased as a result of creep testing. A new finding was that the process of water loss during creep was faster than the process of water return during recovery in this environment. These general principles apply *in vivo* recognizing that the magnitude of water exchanged may be different *in vivo* compared to the *in vitro* tests given the absence of epiligament in these latter tests. These results imply that water is exuded from the ligament during activity and the time scale for water to return to the ligament is longer that the activity itself. If activities are performed in succession with less time in between activities than the activity itself, the ligament would be loaded in any subsequent activity under conditions of reduced water content. It is interesting to note that ligaments soaked in sucrose to reduce their water content had less creep than ligaments with normal hydration. These unique observations taken together reveal another way that ligaments may act to minimize creep during long-term, repetitive activities.

This was the first investigation to show that ligament creep behaviour was clearly affected by the initial state of hydration: decreased creep with decreased hydration and increased creep with increased hydration. Another unique finding was that ligaments with increased hydration had decreased ligament functional length and/or increased ligament pre-stress. The creep behaviour was decreased if the ligament was loaded from the pre-stressed state compared to the unloaded state. The increased creep of the abnormally hydrated ligaments loaded from the unloaded state might suggest that increased water content created limited fibre recruitment, which was shown previously to be related to increased creep. However, loading such a ligament from a pre-stressed state would further limit the fibre recruitment and increase the creep response which was not the behaviour observed. If the polymer analogy applies (117), increased water content permits greater freedom of movement of collagen fibres. Because of the reversible mechanical behaviour observed in the serial solution tests, the freedom of movement would be confined to the limits of the collagen fibre-ground substance network. Perhaps in the pre-stressed state some of the viscous component of the stress/strain response was dissipated, restricting this freedom of movement and recruiting the fibres to resist creep. The increased water loss in ligaments loaded from the pre-stressed state (compared to the unloaded state) further supports this concept.

Obviously, to obtain meaningful *in vitro* mechanical data, tissue hydration must be maintained. These data also have some important clinical implications. Any naturally occurring change in water content *in vivo*, such as inflammation, could significantly change ligament creep behaviour. Ligament being infiltrated with water *in vivo* would

likely result in a pre-stress on the ligament in lieu of a decrease in ligament length which would require bones to move closer together. This is a well-designed functional response because the pre-stress occurs to ensure active fibre recruitment even though tissue water content is increased. If during a surgical procedure such as ligament harvesting and grafting, a ligament is buckled and exposed to saline solution, the creep response of that tissue would be increased. Precautions must be taken to ensure that the tissue is implanted under enough pre-stress to ensure fibre recruitment. Another interesting consideration is whether reducing the water content of the tissue before grafting (through a controlled dehydration) would allow the subsequent increase in water content due to inflammation and scar infiltration to be maintained within normal limits. Clearly, the method of controlled dehydration could not have a negative effect on cell viability pre-implantation or on the collagen turnover process post-implantation.

7.1.3 Creep of Ligament Scars (Question 4)

This was the first study to document the creep properties of healing ligament scars. Results showed that scar creep was abnormally increased even after 14 weeks of healing. Scars had increased water content but this could not account completely for the increase in creep. Collagen crosslinks and collagen fibre alignment were deficient and caused inferior fibre recruitment in scars, which is an important potential mechanism for the observed increased creep. Increased GAG content and flaws in the scar tissue were also implicated as having a mechanistic role in scar creep. More information about the mechanisms of scar creep could be obtained by using this same MCL gap model of scar

formation by varying the size of the gap created surgically for the scars to repair. The principle of increased creep of scar tissue compared to normal tissue is probably also applicable to human ligaments that repair with scar tissue and grafts that are infiltrated by scar tissue. Any surgical intervention to a healing ligament should seek to establish improved fibre recruitment and control ligament water content. Nakamura et al. (1999) made some advances in this regard demonstrating that MCL scars treated with decorin antisense gene therapy had increased numbers of large fibrils and better creep resistance than scars that received no gene therapy. The fact that creep is not being resisted by scar tissue has detrimental implications for stability of joints with repaired or reconstructed ligaments and thus may result in altered joint kinematics in long-term, repetitive activities.

7.1.4 Immobilization of Healing Ligaments (Question 5)

These unique results showed that immobilization exacerbated creep susceptibility whether the immobilization was for the full rehabilitation period of ligament scars or for a short time in the long-term rehabilitation period of ligament grafts. Immobilization of ligament scars in full flexion created a "short scar" that was well-aligned at 70° flexion, had reduced laxity, but was ill-equipped to resist creep. The advanced fibre recruitment in this new joint position further supports the new perspective of fibre recruitment given by these investigations: there is a spectrum of recruitment available in normal and healing ligaments where limited potential for recruitment means poor resistance to creep.

The results of these tests showed that ligament grafts had persistently increased creep even at 2 years of healing. Short-term immobilization of grafts had the long-term consequence of increased creep compared to moved grafts at 1 year of total healing. When these grafts were remobilized, the new loading conditions likely caused a re-injury and furthered the process of scar infiltration. In general, immobilization was not beneficial at improving creep behaviour of healing ligaments.

The creep of grafts was less than scars suggesting the benefit of the ligament scaffold for the scar to infiltrate rather than bridging a gap with scar alone. The graft provided some improvement to the fibre architecture in the ligament repair. These novel findings suggest that establishing fibre organization that permits fibre recruitment to aid in resisting creep is critical for successful *in vivo* ligament repairs and reconstructions.

Although this study made advances in quantifying creep recovery of long-term autografts, our understanding of the *in vivo* implications of unrecovered creep are still limited. First, future work needs to establish the time scale of recovery to determine if or when the grafts can recover from creep. Second, "Does unrecovered creep have implications for ligament laxity?" Future studies should assess ligament laxity immediately after creep testing and at various intervals during recovery in attempts to recreate the conditions that would exist after an activity *in vivo*. Third, this model of ligament grafting may not have been an appropriate choice to reveal changes in laxity with creep *in vivo*. The ligament / joint / neuromuscular system may be capable of compensating for deficiencies in an MCL graft which is not likely the case for an ACL graft given the clinical evidence of abnormal laxity in joints with ACL reconstructions.

The current model was advantageous because the onset of creep was measurable. Any future model should attempt not only to measure the onset of creep but the *in vivo* consequence of the changes it creates.

7.1.5 Stress Distribution (Further Implications from Question 2 and Question 5)

Several of the unique observations from this thesis suggest that using total ligament cross-sectional area to calculate stress oversimplifies the stress distribution in ligament. Discontinuities in the creep test of normal MCLs tested at 28 MPa were apparently caused by fibre ruptures suggesting that some fibres in the cross-section were loaded much higher than 28 MPa - on the order of 90 MPa. In addition, under conditions of partial recruitment, the model of ligament creep would not produce accurate predictions if the fibre modulus was estimated using a value averaged over the cross-section, rather than a value for only the loaded fibres. A non-homogeneous stress redistribution is key to minimization of creep because as more fibres are recruited, the stress is redistributed over the increased number of fibres now bearing load and the stress on the initially loaded fibres gets decreased. The clear and significant implication from these results is that conventional measurement of area cannot provide meaningful representations of stress in ligaments.

Another important finding in this thesis was that cyclic modulus reduction appears to be a useful indicator of damage. In addition to the results of 3 normal ligaments creep tested at 28 MPa, 3 bilateral ligament scars also had reduction in cyclic modulus with discontinuity in the cyclic creep curve. In these scars, the reduction in modulus was

followed quickly by total scar failure. This is important new morphological and mechanical evidence that reduction in modulus is an appropriate marker of tissue damage in normal and healing ligament. It is also important to note that although some of the creep curves at 28 MPa had discontinuities, none resulted in total ligament failure. In fact, when the discontinuity occurred in the cyclic creep test, the modulus increased back to the value that was obtained before the discontinuity. Such "microfailures" must induce some repair *in vivo*. This evidence gives an exciting new perspective on the ability of a normal ligament to regain normal creep behaviour after a fibre rupture. After the rupture of one fibre, stress on the other fibres would be increased causing increased deformation and recruitment of additional fibres to carry the load; thus, effectively reducing the stress on all the fibres.

7.1.6 Future Directions

First, future creep experiments, whether performed on normal ligament, ligament scars and ligament grafts, should examine a succession of creep tests that represent a series of active and resting periods *in vivo*. First, a creep test would be performed. Second, water content, laxity and unrecovered creep would be measured immediately after creep and at set time intervals after creep. Specifically this would address: "How does laxity change after creep in ligament grafts?" The hypothesis is that laxity would be increased due to the large amount of unrecovered creep. Third, select one of these time intervals after which to start the second creep test. Thus, the initial conditions for the second test would be different than for the first test, but would represent resumed activity

after an potentially insufficient rest period. This would address: "How does unrecovered creep affect subsequent viscoelastic creep response?" The effect of decreased water content after creep and complete water return after creep on the subsequent creep behaviour could also be examined.

Second, although clear mechanical evidence of the relationship between water and fibre recruitment was presented here, a method of documenting morphologically the interaction between water and fibres would be an asset. The changes are likely too subtle for detection using the methods of crimp analysis described here. As well, given the issues about cross-sectional area, ideally a combination of optical and modeling techniques could be used to assess the number of fibres and the cross-sectional area of fibres carrying load.

Third, creep and fatigue interact in a complex way in ligament. Some definitions isolate creep and fatigue in the following way: creep results from sustained constant stress and fatigue results from fluctuating stress about a mean stress of zero. If these definitions were applied to the cyclic creep test used here, cyclic creep loading was a fluctuating stress about a sustained mean stress (i.e. fatigue superimposed on creep). Wang et al. (1995b) attempted to use similar cyclic tests but at various frequencies over a given stress range to isolate creep and fatigue. Their hypothesis was that creep failure would be time dependent (regardless of frequency) and that fatigue failure would be cycle dependent (regardless of time elapsed). However, they found that failure was the result of neither isolated creep nor fatigue. Creep and fatigue can interact in engineering materials (45). As well, Caler and Carter (1989) studied the interaction between creep and fatigue in

bone. Failure resulting from both compressive and tensile loading occurred earlier than was predicted by the addition of cycle dependent and time dependent damage. Perhaps, for ligament an understanding of the interaction between creep and fatigue could be gained using an approach similar to that Smith and Weitsman (1998) used for randomly reinforced polymer composites (structural reaction injection molded glass-urethane composites). These authors incorporated damage as a function of load cycle into a coupled viscoelastic-damage model of creep.

Fourth, the most ambitious future direction would be to find an approach to ligament repair that establishes fibre recruitment to resist creep. Could this be done with a modification to current grafting techniques? Although extremes of graft tensioning (too tight or too loose) lead to poor healing, the graft tension required for optimal remodeling is yet unknown (11). Can scar infiltration be stopped and, if so, can the graft be positioned and loaded to achieve the desired fibre recruitment? Is there a way of creating functional fibre recruitment in graft tissue (inducing increased crimp or creating increased crosslinks)? Given that gene therapy was able to increase the number of large diameter fibrils in scar, perhaps a similar technique could be used to reproduce the collagen-interfibrillar interactions thought to produce crimp (153). Perhaps the question is how to design fibre recruitment into an artificial scaffold that would serve as a ligament replacement. Even if any of the above could be done, the challenge that remains is to define the range of stress over which fibre recruitment needs to act *in vivo* and to keep recruitment active over that range after implantation.

7.2 Discussion of Methods

7.2.1 Cross-sectional Area

Cross-sectional area of the rabbit MCL was measured using a specially designed area caliper described previously (134). The caliper traversed the surface of the tissue measuring the thickness as a function of position along the width; thus, measuring the area of the total ligament cross-section. Several results presented in this thesis suggest that using the total ligament cross-sectional area to calculate stress underestimated the stress distribution in ligament. Clearly, conventional cross-sectional area measurements do not provide information on the actual number of fibres carrying load. This has a few important implications. First, fibre recruitment should not be overlooked as a factor in any experimental or theoretical investigation of ligament mechanical behaviour. Second, both stress-based and force-based comparisons of experimental and control specimens are important for *in vitro* tests. Third, morphological data could be used to develop a model to predict the number of fibres (or percent of total cross-section) under load. For example, the percent crimp area measured here could be combined with information on the distribution of fibres across the cross-section to more accurately estimate the number of loaded fibres. Fourth, any technique that could record real-time changes in fibre recruitment would be an asset for understanding the dynamic compensation of the fibres to minimize creep.

7.2.2 Creep Recovery

During the 20 minute recovery period that was used in these tests, the MTS was commanded to hold the ligament at 0 N while the change in deformation was recorded. The tuning of the MTS feedback system was optimized for the creep test. As mentioned before there were small loads at which the MTS, using these tuning parameters, did not have optimum performance. In fact, during the recovery program, the force occasionally drifted but was maintained between ± 1 N. Thus, at the end of the recovery period, the MCL was manually returned to 0 N and the corresponding deformation was recorded. This approach was used to be consistent with previous study on short-term autograft creep recovery (24). Modification can now be made to the test protocol such that different tuning parameters are used for the recovery test than for the creep test. Although the tuning for the recovery test has some early transient force adjustment which was not acceptable for the creep test, it had minimal effect on recovery.

In the present study, the time of the recovery period was equal to the time of the creep test, 20 minutes. Normal ligament recovery was assessed using an additional method. During recovery, the ligament was buckled to -1 mm from "ligament zero". Every hour, compression-tension cycles were used to determine if the deformation at 0.1 N tension had returned to 0 mm. After 3 hours of recovery, the MCL had fully recovered (after creep testing at 4.1 and 14 MPa). These test were also useful for determining the time scale for water return to the ligament after creep testing. Clearly, a 20 minute recovery period (equal in time to the creep test) was not long enough. Accurate

description of creep recovery and the effect of incomplete creep recovery on subsequent creep behaviour is critical to understanding creep after repetitive activity *in vivo*.

7.2.3 Crimp Analysis

The methods of crimp analysis used in this study were unique. The MCL was snap-frozen with liquid nitrogen while the ligament was held in the MTS system. This facilitated rapid freezing of the ligament in the loaded state to obtain a "snapshot" of crimp at the desired test timepoint. Since the creep test was performed in force control, the MTS was switched into length control immediately prior to freezing. Freezing took 20 seconds. Once the ligament was frozen, the midsubstance was harvested and immediately embedded into chilled O.C.T. compound and the compound was frozen around the frozen MCL using liquid nitrogen. All samples underwent the same freezing protocol and the rapid freezing had no adverse effect on the crimp analysis.

This study took a novel approach to quantifying crimp by identifying crimp categories. The three categories were defined based on easily distinguishable visual characteristics. Type I and Type II Crimp could be further classified using measurable features of crimp. Crimp angle was measured identifying the point of band extinction using the calibrated rotating stage on the polarized light microscope (43). Crimp period was measured using a distance measurement feature of the VIDAS system (VIDAS 2.1, Kontron Electronik GmbH, Eching, Germany). Type I Crimp had an angle range of 35° to 20° and a period range from 70 to 20 μm. Type II Crimp had crimp angle less than 20° and period less than 30 μm. For the rabbit MCL, Amiel and Kleiner (1988) reported the

crimp period was around 45 μm and the amplitude was around 10 μm. These crimp characteristics are comparable to the crimp measured here.

In this thesis, crimp after fibre rupture has been documented. The rupture was indicated by a mechanically detectable discontinuity in the static creep curve i.e. a catastrophic event. The crimp after rupture was documented while the tissue was in the loaded state at the end of static creep. This crimp after rupture was different than functional crimp: more superficial (less evident banding), irregular banding with somewhat increased period, and separation between the fibres. These distinctions are similar to those seen in tendon fibres after rupture (152). An interesting future direction of this thesis work could involve defining a new category of crimp based on these observations (Type IV). Furthermore, these features of crimp after rupture could be used in a future study of damage causing rupture due the creep and fatigue in normal ligament.

7.3 Generalizability of Principles

This thesis has established several general principles of creep behaviour that are not exclusive to the rabbit MCL. Although it is important to recognize the boundary conditions of this experimental work (for example, animal model, specimen age, test environment, joint position), the general principles of creep behaviour documented here should also apply to human MCL, ACL and ACL grafts *in vivo*. This work has these broader implications because of the structural and functional properties that these tissues have in common (even though magnitudes may differ).

In normal ligaments, creep was increased under conditions of limited fibre recruitment and abnormally elevated water content, revealing that both are mechanisms of creep. Ligament scars and grafts were more susceptible to creep than normal ligaments. In addition to limited fibre recruitment and elevated water content, ligament scars also had increased GAG content and soft tissue flaws. Restoration of normal values to mechanistic factors in order to control creep would improve joint healing by restoring joint kinematics and maintaining normal joint loading. This work suggests that any successful repair or reconstruction of a ligament requires fibre recruitment in order to minimize creep within the desired functional range of stresses. Control of tissue water content is also important to replicate normal behaviour. Immobilization was not an effective intervention to prevent creep.

REFERENCES

1. Aglietti P, Buzzi R, D'Andria S, Zaccherotti G: Long-term study of anterior cruciate ligament reconstruction for chronic instability using the central one-third patellar tendon and a lateral extraarticular tenodesis. *Am J Sports Med* 20:38-45, 1992

2. Aglietti P, Buzzi R, Zaccherotti G, De Biase P: Patellar tendon versus doubled semitendinosus and gracilis tendons for anterior cruciate ligament reconstruction. *Am J Sports Med* 22:211-7, 1994.

3. Akeson WH, Woo SL-Y, Amiel D, Coutts RD, Daniel D: The connective tissue response to immobility: Biochemical changes in periarticular connective tissue of the immobilized rabbit knee. *Clin Orthop* 3:356-362 1973

4. Akeson WH, Amiel D, Abel MF, Garfin SR, Woo SL: Effects of immobilization on joints. *Clin Orthop* 219:28-37, 1987

5. Ameny P, Jessop EL, Loov RE: Strength, elastic and creep properties of concrete masonry. *The International Journal of Masonry Construction* 1:33-39, 1980

6. Amiel D, Woo SL, Harwood FL, Akeson WH: The effect of immobilization on collagen turnover in connective tissue: a biochemical-biomechanical correlation. *Acta Orthop Scand* 53:325-332, 1982

7. Amiel D, Akeson WH, Harwood FL, Frank CB: Stress deprivation effect on metabolic turnover of the medial collateral ligament collagen. A comparison between nine- and 12-week immobilization. *Clin Orthop* 172:265-270, 1983

8. Amiel D, Kleiner JB: Biochemistry of tendon and ligament. In: *Collagen Biotechnology*, vol 3, pp 223-251. Ed by ME Nimi. Boca Raton, CRC Press, 1988

9. Amiel D, Kuiper S: Experimental studies on anterior cruciate ligament grafts: Histology and biochemistry. In: *Knee Ligaments: Structure, Function, Injury, and Repair*, pp 379-388. Ed by DM Daniel, WH Akeson, JJ O'Connor. New York, Raven Press, 1990

10. Amiel D, Billings Jr E, Akeson WH: Ligament structure, chemistry and physiology. In *Knee Ligaments: Structure, Function, Injury and Repair*, pp 77-91. Ed by DM Daniel, WH Akeson, JJ O'Connor. Raven Press, New York, 1990

11. Andersen HN, Amis AA: Review on tension in the natural and reconstructed anterior cruciate ligament. *Knee Surg Sports Traumatol Arthrosc* 2:192-202, 1994

12. Andriacchi TP, Mikosz RP: Musculoskeletal dynamics, locomotion and clinical applications. In: *Basic Orthopaedic Biomechanics*, pp 51-92. Ed by VC Mow, WC Hayes. New York, Raven Press, 1991

13. Arnoczky SP, Warren RF: Anatomy of the cruciate ligaments. In: *The Crucial Ligaments: Diagnosis and Treatment of Ligamentous Injuries About the Knee*, pp 179-195. Ed by JA Feagin Jr. New York, Churchill Livingstone, 1988

14. Aspden RM: The theory of fibre-reinforced composite materials applied to the mechanical properties of the cervix during pregnancy. *J Theor Biol* 130:213-221, 1988

15. Ateshian GA, Warden WH, Kim JJ, Grelsamer RP, Mow VC: Finite deformation biphasic material properties of bovine articular cartilage from confined compression experiments. *J Biomech* 30:1157-1164, 1997

16. Bach Jr BR, Jones GT, Hager CA Sweet FA, Luergans S: Arthrometric results of arthroscopically assisted anterior cruciate ligament reconstruction using autograft patellar tendon substitution. *Am J Sports Med* 23:179-185, 1995

17. Ballock RT, Woo SL-Y, Lyon RM, Hollis JM, Akeson WH: Use of patellar tendon autograft for anterior cruciate ligament reconstruction in the rabbit: A long-term histologic and biomechanical study. *J Orthop Res* 7:474-485, 1989

18. Beaumont PWR: The failure of fibre composites: An overview. *Journal of Strain Analysis* 24:189-205, 1989

19. Betsch DF, Baer E: Structure and mechanical properties of rat tail tendon. *Biorheology* 17:83-94, 1980

20. Beynnon BD, Johnson RJ, Fleming BC, Renstrom PA, Nichols CE, Pope MH, Haugh, LD: The measurement of elongation of anterior cruciate-ligament grafts *in vivo*. *J Bone Joint Surg [Am]* 76:520-531, 1994a

21. Beynnon, BD, Johnson RJ, Toyama H, Renstrom PA, Arms SW, Fischer RA: The relationship between anterior-posterior knee laxity and the structural properties of the patellar tendon graft. A study in canines. *Am J Sports Med* 22:812-820, 1994b

22. Beynnon BD, Risberg MA, Tjomsland O, Ekeland A, Fleming BC, Peura GD, Johnson RJ: Evaluation of knee joint laxity and the structural properties of the anterior cruciate ligament graft in the human. *Am J Sports Med* 25:203-206, 1997

23. Bishop PB, Bray RC: Abnormal joint mechanics and the proteoglycan composition of normal and healing rabbit medial collateral ligament. *J Manipulative Physiol Ther* 16:300-305, 1993

24. Boorman RS, Shrive NG, Frank CB: Immobilization increases the vulnerability of rabbit medial collateral ligament autografts to creep. *J Orthop Res* 16:682-689, 1998

25. Bray RC, Shrive NG, Frank CB, Chimich DD: The early effects of joint immobilization on medial collateral ligament healing in an ACL-deficient knee: A gross anatomic and biomechanical investigation in the adult rabbit model. *J Orthop Res* 10:157-166, 1992

26. Buss DD, Warren RF, Wickiewicz TL, Galinat BJ, Panariello R: Arthroscopically assisted reconstruction of the anterior cruciate ligament with use of autogenous patellar ligament grafts: Results after twenty-four to forty-two months. *J Bone Joint Surg [AM]* 75:1346-1355, 1993

27. Butler DL, Malaviya P, Awad H, Boivin GP, Smith F: A multi-disciplinary approach to analyzing tendon fibrocartilage mechanics, structure and chemistry. *Abstracts of the Third World Congress of Biomechanics* 213a, 1998

28. Caler, WE, Carter DR: Bone creep-fatigue damage accumulation. *J Biomech* 22:625-635, 1989

29. Chen D, McCabe RP, Vanderby R: Two electrokinetic phenomena in rabbit patellar tendon: Pressure and voltage. *Proceedings of the 1995 Bioengineering Conference (ASME)* 29:31-32, 1995

30. Chimich D, Frank C, Shrive N, Dougall H, Bray R: The effects of initial end contact on medial collateral ligament healing: A morphological and biomechanical study in a rabbit model. *J Orthop Res* 9:37-47, 1991

31. Chimich D, Shrive N, Frank C, Marchuk L, Bray R: Water content alters viscoelastic behaviour of the normal adolescent rabbit medial collateral ligament. *J Biomech* 25:831-837, 1992

32. Cohen RE, Hooley CJ, McCrum NG: Viscoelastic creep of collagenous tissue. *J Biomech* 9:175-184, 1976

33. Collins JJ, O'Connor JJ: Muscle-ligament interactions at the knee during walking. *Proc Instn Mech Engrs [H]* 205:11-18, 1991

34. *Concrete Design Handbook*, p 10-5. Ottawa, Canadian Portland Cement Association, 1995

35. Cunningham KD: The structure-function relationship of the extracellular matrix in the rabbit medial collateral ligament. *MSc Thesis* University of Calgary, 1998

36. Daly CH, Nicholls JL, Kydd WL, Nansen PD: The response of the human peridontal ligament to torsional loading – I. Experimental Methods. *J Biomech* 7:517-522, 1974

37. Daniel DM, Stone ML: KT-1000 anterior-posterior displacement measurements. In: *Knee Ligaments: Structure, Function, Injury, and Repair,* pp 427-447. Ed by DM Daniel, WH Akeson, JJ O'Connor. New York, Raven Press, 1990a

38. Daniel DM, Stone ML Reihl B: Ligament surgery. The evaluation of results. In: *Knee Ligaments: Structure, Function, Injury, and Repair,* pp 521-534. Ed by DM Daniel, WH Akeson, JJ O'Connor. New York, Raven Press, 1990b

39. Daniel DM, Stone ML, Dobson BE, Fithian DC, Rossman DJ Kaufman KR: Fate of the ACL-injured patient. A prospective outcome study. *Am J Sports Med* 22:632-644, 1994

40. Decraemer WF, Maes MA, Vanhuyse VJ: An elastic stress-strain relation for soft biological tissues based on a structural model. *J Biomech* 13:463-468, 1980

41. Decraemer WF, Maes MA, Vanhuyse VJ, Vanpeperstraete P: A non-linear viscoelastic constitutive equation for soft biological tissues based upon a structural model. *J Biomech* 13:559-564, 1980

42. DeVita P, Lassiter T, Hortobagyi T, Torry M: Functional knee brace effects during walking in patients with anterior cruciate ligament reconstruction. *Am J Sports Med* 26:778-784, 1998

43. Diamant J, Keller A, Baer E, Litt M, Arridge RGC: Collagen ultrastructure and its relation to mechanical properties as a function of ageing. *Proc R Soc Lond B* 180:293-315, 1972

44. *Dorland's Pocket Medical Dictionary*, 24th ed, Philadelphia, WB Saunders, 1989

45. Dowling NE: *Mechanical Behaviour of Materials,* pp 705-708. New Jersey, Prentice-Hall, 1993

46. Duquette JJ, Grigg P, Hoffman AH. The effect of diabetes on the viscoelastic properties of rat knee ligaments. *J Biomech Eng* 118:557-564, 1996

47. Elden HR: Hydration of connective tissue and tendon elasticity. *Biochim Biophys Acta* 79:592-599, 1964

48. Ferretti A, Conteduca F, De Carli A, Fontana M, Mariani PP: Osteoarthritis of the knee after ACL reconstruction. *Int Orthop* 15:367-371, 1991

49. Findley WN, Lai JS, Onoron K: *Creep and Relaxation of Nonlinear Viscoelastic Materials*, pp 81-87. Amsterdam, North-Holland, 1976

50. Fleming BC, Good L, Peura GD, Beynnon BD: Calibration and application of an intra-articular force transducer for the measurement of patellar tendon graft forces: an *in situ* evaluation. *J Biomech Eng* 121:393-398, 1999

51. Frank C, Amiel D, Akeson WH: Healing of the medial collateral ligament of the knee: A morphological and biochemical assessment in rabbits. *Acta Orthop Scand* 54:917-923, 1983a

52. Frank C, Woo SL-Y, Amiel D, Harwood F, Gomez M, Akeson W: Medial collateral ligament healing: A multidisciplinary assessment in rabbits. *Am J Sports Med* 11:379-389, 1983b

53. Frank C, McDonald D, Lieber R, Sabiston P: Biochemical heterogeneity within the maturing rabbit medial collateral ligament. *Clin Orthop* 236:279-285, 1988

54. Frank C, MacFarlane B, Edwards P, Rangayyan R, Liu Z-Q, Walsh S, Bray R: A quantitative analysis of matrix alignment in ligament scars: A comparison of movement versus immobilization in an immature rabbit model. *J Orthop Res* 9:219-227, 1991

55. Frank C, McDonald D, Bray D, Bray R, Rangayyan R, Chimich D, Shrive N: Collagen fibril diameters in the healing adult rabbit medial collateral ligament. *Connect Tissue Res* 27:251-263, 1992

56. Frank C, McDonald D, Wilson J, Eyre D, Shrive N: Rabbit medial collateral ligament scar weakness is associated with decreased collagen pyridinoline crosslink density. *J Orthop Res* 13:157-165, 1995

57. Frank C, Shrive N: Ligament biology, repair, and transplantation. *Curr Opin Orthop* 7:50-56, 1996

58. Frank CB: Ligament healing: Current knowledge and clinical applications. *J Am Acad Orthop Surg* 4:74-83, 1996

59. Frank CB: Ligament injuries: Pathophysiology and healing. In: *Athletic Injuries and Rehabilitation*, pp 9-25. Ed by JE Zachazewski, DJ Magee, WS Quillen. Philadelphia, WB Saunders Company, 1996

60. Frank CB, Loitz B, Bray R, Chimich D, King G, Shrive N: Abnormality of the contralateral ligament after injuries of the medial collateral ligament: An experimental study in rabbits. *J Bone Joint Surg [Am]* 76:403-412, 1994

61. Frank CB, Shrive NG: Ligament. In: *Biomechanics of the Musculo-Skeletal System*, pp 106-132. Ed by BM Nigg, W Herzog. Chichester, John Wiley and Sons, 1994

62. Fu FH, Bennett CH, Lattermann C, Ma CB: Current trends in anterior cruciate ligament reconstruction. Part 1: Biology and biomechanics of reconstruction. *Am J Sports Med* 27:821-830, 1999

63. Fung YC: *Biomechanics: Mechanical Properties of Living Tissues*, pp 41-48, 50-52, 277-287. New York, Springer-Verlag, 1993

64. Gamble JG, Edwards CC, Max SR: Enzymatic adaptation in ligaments during immobilization. *Am J Sports Med* 12:221-228, 1984

65. Gerritse A: Aramid-based pretensioning tendons. In: *Alternative Materials for the Reinforcement and Pretensioning of Concrete*, pp 172-201. Ed by JL Clarke. London, Blackie Academic & Professional, 1993

66. Goldstein SA, Armstrong TJ, Chaffin DB, Matthews LS. Analysis of cumulative strain in tendons and tendon sheaths. *J Biomech* 20:1-6, 1987

67. Gomez MA, Woo S L-Y, Inoue M, Amiel D, Harwood FL, Kitabayashi L: Medial collateral ligament healing subsequent to different treatment regimens. *J Appl Physiol* 66:245-252, 1989

68. Grana WR, Hines R: Arthroscopic-assisted semitendinosus reconstruction of the anterior cruciate ligament. *Am J Knee Surg* 5:17-22, 1992

69. Hannafin JA, Arnoczky SP: Effect of cyclic and static tensile loading on water content and solute diffusion in canine flexor tendons: An *in vitro* study. *J Orthop Res* 12:350-356, 1994

70. Hart DP, Dahners LE: Healing of the medial collateral ligament in rats: The effect of repair, motion, and secondary stabilizing ligaments. *J Bone Joint Surg [Am]* 69:1194-1199, 1987

71. Haut RC: The mechanical and viscoelastic properties of the anterior cruciate ligament and of ACL fascicles. In: *The Anterior Cruciate Ligament: Current and Future Concepts*, pp 63-73. Ed by DW Jackson, SP Arnoczky, SL-Y Woo, CB Frank, TM Simon. New York, Raven Press, 1993

72. Haut RC, Little RW: A constitutive equation for collagen fibers. *J Biomech* 5:423-430, 1972

73. Haut TL, Haut RC: The state of tissue hydration determines the strain-rate-sensitive stiffness of human patellar tendon. *J Biomech* 30:79-81, 1997

74. Hildebrand KA, Frank CB: Ligaments: Structure, function, and response to injury and repair. In: *Principles of Orthopaedic Practice,* 2nd ed, pp 109-117,. Ed by R Dee, LC Hurst, MA Gruber, SA Kottmeier. New York, McGraw-Hill, 1997

75. Hildebrand KA, Frank CB: Biology of ligament injury and repair. In: *Current Review of Sports Medicine,* 2nd ed, pp 121-132. Ed by RJ Johnson, J Lombardo. Philidelphia, Butterworth Heinemann, 1998

76. Holden JP, Grood ES, Butler DL, Noyes FR, Mendenhall HV, Van Kampen CL, Neidich RL: Biomechanics of fascia lata ligament replacements: Early postoperative changes in the goat. *J Orthop Res* 6:639-647, 1988

77. Holden JP, Grood ES, Korvick DL, Cummings JF, Bulter DL, Bylski-Austrow DI: *In vivo* forces in the anterior cruciate ligament: Direct measurement during walking and trotting in a quadruped. *J Biomech* 27:517-526, 1994

78. Hooley CJ, Cohen RE: A model for the creep behaviour of tendon. *Int J Macromol* 1:123-132, 1979

79. Hooley CJ, McCrum NG, Cohen RE. The viscoelastic deformation of tendon. *J Biomech* 13:521-528, 1980

80. Howard ME, Cawley PW, Losse GM, Johnston III, RB: Bone-patellar tendon-bone grafts for anterior cruciate ligament reconstruction: The effects of graft pretensioning. *Arthroscopy* 12:287-292, 1996

81. Howe, JG, Johnson RJ, Kaplan MJ, Fleming B, Jarvinen M: Anterior cruciate ligament reconstruction using quadriceps patellar tendon graft. Part I. Long-term followup. *Am J Sports Med* 19:447-457, 1991

82. Hurschler C, Loitz-Ramage B, Vanderby R: A structurally based stress-stretch relationship for tendon and ligament. *J Biomech Eng* 119:392-399, 1997

83. Indelicato PA: Injury to the medial capsuloligamentous complex. In: *The Crucial Ligaments: Diagnosis and Treatment of Ligamentous Injuries about the Knee*, pp 197-206. Ed by JA Feagin Jr. New York, Churchill Livingstone, 1988

84. Inoue M, Woo SL-Y, Gomez MA, Amiel D, Ohland KJ, Kitabayashi LR: Effects of surgical treatment and immobilization on the healing of the medial collateral ligament: A long-term multidisciplinary study. *Conn Tiss Res* 25:13-26, 1990

85. Jackson DW, Grood ES, Goldstein JD, Rosen MA, Kurzweil PR, Cummings JF, Simon TM: A comparison of patellar tendon autograft and allograft used for anterior cruciate ligament reconstruction in the goat model. *Am J Sports Med* 21:176-185, 1993

86. Jenkins RB, Little RW: A constitutive equation for parallel-fibered elastic tissue. *J Biomech* 7:397-402, 1974

87. Johnson RJ, Ericksson E, Haggmark T, Pope MH: Five to ten-year follow-up evaluation after reconstruction of the anterior cruciate ligament. *Clin Orthop* 183:122-140, 1984

88. Kapit W, Elson LM: *The Anatomy Coloring Book*, plate 1. New York, Harper Collins, 1977

89. Kastelic J, Palley I, Baer E: A structural mechanical model for tendon crimping. *J Biomech* 13:887-893, 1980

90. Kennedy L, Baynes JW: Non-enzymatic glycosylation and the chronic complications of diabetes: An overview. *Diabetologia* 26:93-98, 1984

91. Kerboull L, Christel P, Meunier A: Étude *in vitro* de l'influence de différents moyens de conservation sur les propriétés mécaniques d'allogreffes de tendon rotulien. [In vitro study of the influence of various conservation methods on the mechanical properties of patellar tendon allografts] *Chirurgie* 117:751-762, 1991

92. Kwan MK, Lin TH-C, Woo SL-Y: On the viscoelastic properties of the anteromedial bundle of the anterior cruciate ligament. *J Biomech* 26:447-452, 1993

93. Lakes RS, Vanderby R: Interrelation of creep and relaxation: A modeling approach for ligaments. *J Biomech Eng* 121:612-615, 1999

94. Lam T: The mechanical properties of the maturing medial collateral ligament. *PhD Thesis* University of Calgary, 1988

95. Lam T, Frank C, Shrive N: Ligament viscoelastic behaviour changes with maturation. *Trans Orthop Res Soc* 14:187, 1989

96. Lanir Y: A microstructure model for the rheology of mammalian tendon. *J Biomech Eng* 102:332-339, 1980

97. Lanir Y: Constitutive equations for fibrous connective tissues. *J Biomech* 16:1-12, 1983

98. Lanir Y, Salant EL, Foux A: Physico-chemical and microstructural changes in collagen fiber bundles following stretch *in vitro*. *Biorheology* 25:591-603, 1988

99. Lerat JL, Moyen B, Mandrino A, Besse JL, Brunet-Guedj E: Étude prospective de l'évolution de la laxité antérieure du genou après reconstruction du ligament croisé antérieur par deux procédés utilisant différemment le tendon rotulien [Prospective study of postoperative anterior knee laxity after anterior cruciate ligament reconstruction using two different patellar tendon grafts] *Rev Chir Orthop Reparatrice Appar Mot* 83:217-228, 1997

100. Liao H, Belkoff SM: A failure model for ligaments. *J Biomech* 32:183-188, 1999

101. Lyon RM, Lin HC, Kwan MK-W, Hollis JM, Akeson WH, Woo SL-Y: Stress relaxation of the anterior cruciate ligament (ACL) and the patellar tendon (PT). *Trans Orthop Res Soc* 13:81, 1988

102. Marcacci M, Zaffagnini S, Iacono F, Neri MP, Petitto A: Early versus late reconstruction for anterior cruciate ligament rupture. Results after five years of followup. *Am J Sports Med* 23:690-693, 1995

103. Maroudas A, Ziv I, Weisman N, Venn M: Studies of hydration and swelling pressure in normal and osteoarthritic cartilage *Biorheology* 22:159-169, 1985

104. Matyas JR, Chowdhury P, Frank CB: Crimp as an index of ligament strain. *23rd Annual Canadian Orthopaedic Research Society* Ottawa, Ontario, June 1988

105. Mittlmeier T, Weliler A, Sohn T, Kleinhaus L, Mollbach S, Duda G, Sudkamp NP: Functional monitoring during rehabilitation following anterior cruciate ligament reconstruction. *Clin Biomech* 14:576-584, 1999

106. Monleon Pradas M, Diaz Calleja R: Nonlinear viscoelastic behaviour of the flexor tendon of the human hand. *J Biomech* 23:773-781, 1990

107. Morchio R, Ciferri A: The role of calcium and of *in vitro* aging on the creep behavior of collagen tendons. *Biophysik* 5:327-330, 1969

108. Mosler E, Folkhard W, Knorzer E, Nemetschek-Gansler H, Nemetschek Th, Koch MHJ: Stress-induced molecular rearrangement in tendon collagen. *J Mol Biol* 182:589-596, 1985

109. Mow VC, Kuei SC, Lai WM, Armstrong CG: Biphasic creep and stress relaxation of articular cartilage in compression? Theory and experiments. *J Biomech Eng* 102:73-84, 1980

110. Mow VC, Homes MH, Lai WM: Fluid transport and mechanical properties of articular cartilage: a review. *J Biomech* 17:377-394 1984

111. Nakamura N, Boorman RS, Hart DA, Shrive NG, Kaneda Y, Frank CB: Decorin antisense gene therapy decreases elongation (creep) behaviour of early ligament scar. *Trans Orthop Res Soc* 24:111, 1999

112. Neville AM: *Properties of Concrete,* 3rd ed, pp 402-403. London, Pitman, 1981

113. Ng GY, Oakes BW, Deacon OW, McLean ID, Lampard D: Biomechanics of patellar tendon autograft for reconstruction of the anterior cruciate ligament in the goat: Three year study. *J Orthop Res* 13:602-608, 1995

114. Noyes FR, Barber SD: The effect of a ligament-augmentation device on allograft reconstruction for chronic ruptures of the anterior cruciate ligament. *J Bone Joint Surg [Am]* 74:960-973, 1992

115. O'Connor JJ and Zavatsky A: Anterior cruciate ligament forces in activity. In: *The Anterior Cruciate Ligament: Current and Future Concepts*, pp 131-140. Ed by DW Jackson, SP Arnoczky, SL-Y Woo, CB Frank, TM Simon. New York, Raven Press, 1993

116. Oakes BW: Collagen ultrastructure in the normal ACL and in ACL graft. In: *The Anterior Cruciate Ligament: Current and Future Concepts*, pp 209-217. Ed by DW Jackson, SP Arnoczky, SL-Y Woo, CB Frank, TM Simon. New York, Raven Press, 1993

117. Panagiotacopulos ND, Knauss WG, Bloch R: On the mechanical properties of human intervertebral disc material. *Biorheology* 16:317-330, 1979

118. Panjabi MM, Yoldas E, Oxland TR, Crisco III JJ: Subfailure injury of the rabbit anterior cruciate ligament. *J Orthop Res* 14:216-222, 1996

119. Petermann J, von Garrel T, Gotzen L: Non-operative treatment of acute medial collateral ligament lesions of the knee joint. *Knee Surg Sports Traumatol Arthrosc* 1:93-96, 1993

120. Purslow PP, Wess TJ, Hukins DWL: Collagen orientation and molecular spacing during creep and stress-relaxation in soft connective tissues. *J Exp Biol* 201:135-142, 1998

121. Radin EL, Yang KH, Riegger C, Kish VL, O'Connor JJ: Relationship between lower limb dynamics and knee joint pain. *J Orthop Res* 9:398-405, 1991

122. Rasmussen TJ, Feder SM, Bulter DL, Noyes FR: The effects of 4 Mrad of γ irradiation on the initial mechanical properties of bone-patellar tendon-bone grafts. *Arthroscopy* 10:188-197, 1994

123. Reihsner R, Menzel EJ: Two-dimensional stress-relaxation behavior of human skin as influenced by non-enzymatic glycation and the inhibitory agent aminoguanidine. *J Biomech* 31:985-993, 1998

124. Reiser KM: Nonenzymatic glycation of collagen in aging and diabetes. *Proc Soc Exp Biol Med* 196:17-29, 1991

125. Rigby BJ, Hirai N, Spikes, JD, Eyring H: The mechanical properties of rat tail tendon. *J Gen Physiol* 43:265-283, 1959

126. Roy CS: The elastic properties of the arterial wall. *J Physiol (Lond)* 3:125-159, 1880

127. Sabiston P, Frank C, Lam T, Shrive N: Allograft ligament transplantation. A morphological and biochemical evaluation of a medial collateral ligament complex in a rabbit model. *Am J Sports Med* 18:160-168, 1990a

128. Sabiston P, Frank C, Lam T, Shrive N: Transplantation of the rabbit medial collateral ligament. I. Biomechanical evaluation of fresh autografts. *J Orthop Res* 8:35-45 1990b

129. *SAS/STAT User's Guide,* Version 6, ed 4, vol 2, pp 905-906. Cary, SAS Institute Inc., 1990

130. *SAS/STAT User's Guide,* Version 6, ed 4, vol 2, pp 922-923. Cary, SAS Institute Inc., 1990

131. *SAS/STAT User's Guide,* Version 6, ed 4, vol 2, pp 926-931. Cary, SAS Institute Inc., 1990

132. Schatzmann L, Brunner P, Staubli HU: Effect of cyclic preconditioning on the tensile properties of human quadriceps tendons and patellar ligaments. *Knee Surg Sports Traumatol Arthrosc* 6:S56-S61, 1998

133. Shino K, Nakata K, Horibe S, Inoue M, Nakagawa S: Quantitative evaluation after arthroscopic anterior cruciate ligament reconstruction. Allograft versus autograft. *Am J Sports Med* 21:609-616, 1993

134. Shrive NG, Lam TC, Damson E, Frank CB: A new method of measuring the cross-sectional area of connective tissue structures. *J Biomech Eng* 110:104-109, 1988

135. Shrive N, Chimich D, Marchuk L, Wilson J, Brant R, Frank C: Soft-tissue "flaws" are associated with the material properties of the healing rabbit medial collateral ligament. *J Orthop Res* 13:923-929, 1995

136. Simon BR, Coats RS, Woo SL-Y: Relaxation and creep quasilinear viscoelastic models for normal articular cartilage. *J Biomech Eng* 106:159-164, 1984

137. Smith LV, Weitsman YJ: Inelastic behavior of randomly reinforced polymeric composites under cyclic loading. *Mechanics of Time-Dependent Materials* 1:293-305, 1998

138. Stouffer DC, Butler DL, Hosny D: The relationship between crimp pattern and mechanical response of human patellar tendon-bone units. *J Biomech Eng* 107:158-165, 1985

139. Stromberg DD, Wiederhielm CA: Viscoelastic description of a collagenous tissue in simple elongation. *J Appl Physiol* 26:857-862, 1969

140. Stryer L: *Biochemistry,* 3rd ed, p 339. WH Freeman and Company, New York, 1988

141. Swenson TM, Harner CD: Knee ligament and meniscal injuries: Current concepts. *Orthop Clin North Am* 26:529-546, 1995

142. *The Statistics Problem Solver*, pp 823-827. New York, Research and Education Association, 1978

143. Thornton GM, Oliynyk A, Frank CB, Shrive NG: Ligament creep cannot be predicted from stress relaxation at low stress: A biomechanical study of the rabbit medial collateral ligament. *J Orthop Res* 15:652-656, 1997

144. Thornton GM, Leask GP, Shrive NG, Frank CB: Early medial collateral ligament scars have inferior creep behaviour. *J Orthop Res* (Accepted for publication August 30, 1999)

145. Timoney JM, Inman WS, Quesada PM, Sharkey PF, Barrack RL, Skinner HB, Alexander AH: Return of normal gait patterns after anterior cruciate reconstruction. *Am J Sports Med* 21:887-889, 1993

146. Tohyama H, Beynnon BD, Johnson RJ, Renstrom PA Arms SW: The effect of anterior cruciate ligament graft elongation at the time of implantation on the biomechanical behavior of the graft and knee. *Am J Sports Med* 24:608-614, 1996

147. Tyler TF, McHugh MP, Gleim GW, Nicholas SJ: Association of KT-1000 measurements with clinical tests of knee stability 1 year following anterior cruciate ligament reconstruction. *J Orthop Sports Phys Ther* 29:540-545, 1999

148. Valias AC, Tipton CM, Matthes RD, Gart M: Physical activity and its influence on the repair process of medial collateral ligaments. *Connective Tissue Research* 9:25-31, 1981

149. Ventura CP, Wolchok J, Hull ML, Howell SM: An implantable transducer for measuring tension in an anterior cruciate ligament graft. *J Biomech Eng* 120:327-333, 1998

150. Viidik A: Biomechanics and functional adaptations of tendons and joint ligaments. In: *Studies on the Anatomy and Function of Bone and Joints*, pp 17-39. Ed by FG Evans. Springer-Verlag, Berlin, 1966

151. Viidik A: Elasticity and tensile strength of the anterior cruciate ligament in rabbits as influenced by training. *Acta Physiol Scand* 74:372-380, 1968

152. Viidik A: Simultaneous mechanical and light microscopic studies of collagen fibers. *Z Anat Entwicklungsgesch* 136:204-212, 1972

153. Viidik A: Properties of tendons and ligaments. In: *Handbook of Bioengineering,* pp 6.1-6.19. Ed by R Skalak, S Chien. New York, McGraw-Hill, 1987

154. Viidik A: Structure and function of normal and healing tendons and ligaments. In: *Biomechanics of Diarthrodial Joints,* vol 1, pp 3-38. Ed by VC Mow, A Ratcliffe, SL-Y Woo. New York, Springer Verlag, 1990

155. Viidik A, Ekholm R: Light and electron microscopic studies of collagen fibers under strain. *Z Anat Entwicklungsgesch* 127:154-164, 1968

156. Wang XT, Ker RF: Creep rupture of wallaby tail tendons. *J Exp Biol* 198:831-845, 1995a

157. Wang XT, Ker RF, Alexander RM: Fatigue rupture of wallaby tail tendons. *J Exp Biol* 198:847-852, 1995b

158. Wilson A, Shrive N, Damson E, Frank C, Leask G, Mikalson I, Kraus V: An environment chamber for soft tissue testing. *Proceedings of the 1995 Bioengineering Conference (ASME)* 29:255-256, 1995

159. Woo SL-Y: Mechanical properties of tendons and ligaments. I. Quasi-static and nonlinear viscoelastic properties. *Biorheology* 19:385-396, 1982

160. Woo SL-Y, Gomez MA, Akeson WH: The time and history-dependent viscoelastic properties of the canine medial collateral ligament. *J Biomech Eng* 103:293-298, 1981

161. Woo SL-Y, Gomez MA, Sites TJ, Newton PO, Orlando CA, Akeson WH: The biomechanical and morphological changes in the medial collateral ligament after immobilization and remobilization. *J Bone Joint Surg* 69A:1200-1211, 1987

162. Woo SL-Y, Inoue M, McGurk-Burleson E, Gomez MA: Treatment of the medial collateral ligament injury II: Structure and function of canine knees in response to differing treatment regimens. *Am J Sports Med* 15:22-29, 1987

163. Woo SL-Y, Horibe S, Ohland KJ, Amiel D: The response of ligaments of injury: Healing of collateral ligaments. In *Knee Ligaments: Structure, Function, Injury and Repair*, pp 351-364 Ed by DM Daniel, WH Akeson, JJ O'Connor. Raven Press, New York, 1990

164. Woo SL-Y, Young EP, Ohland KJ, Marcin JP, Horibe S, Lin H-C: The effects of transection of the anterior cruciate ligament on healing of the medial collateral ligament. *J Bone Joint Surg* 72:382-392, 1990

165. Woo SL-Y, Johnson GA, Smith BA: Mathematical modelling of ligaments and tendons. *J Biomech Eng* 115:468-473, 1993

166. Woo SL-Y, Chan SS, Yamaji T: Biomechanics of knee ligament healing, repair and reconstruction. *J Biomech* 30:431-439, 1997

167. Woo SL-Y, Debski RE, Withrow JD, Janaushek MA: Biomechanics of knee ligaments. *Am J Sports Med* 27:533-543, 1999

168. Yahia L-H, Drouin G. Microscopical investigation of canine anterior cruciate ligament and patellar tendon: Collagen fascicle morphology and architecture. *J Orthop Res* 7:243-251, 1989

169. Yahia L-H, Brunet J, Labelle S, Rivard C-H: A scanning electron microscopic study of rabbit ligaments under strain *Matrix* 10:58-64, 1990

170. Yamamoto N and Takauchi M: *In vivo* measurement of patellar tendon force in rat during running on a treadmill. *Abstracts of the Third World Congress of Biomechanics* 461b, 1998

171. Yoshiya S, Andrish JT, Manley MT, Bauer TW: Graft tension in anterior cruciate ligament reconstruction. An *in vivo* study in dogs. *Am J Sports Med* 15:464-470, 1987

APPENDIX 1

LABORATORY DATABASE

Table A1.1: Ultimate Failure Strengths of Normal and Healing Rabbit MCLs from Laboratory Database

Group	Ultimate Failure Strength (MPa)	n
normal	95.2 ± 12.4	12
3 week Unilateral MCL Gap	7.4 ± 2.3	9
6 week Unilateral MCL Gap	13.8 ± 6.7	8
14 week Unilateral MCL Gap	23.7 ± 7.9	9
3 week Bilateral MCL Gap	5.1 ± 1.3	5
6 week Bilateral MCL Gap	15.9 ± 6.0	6
14 week Bilateral MCL Gap	21.1 ± 7.8	5

Data are shown as mean ± standard deviation.

Failure strength was evaluated from the failure stress-strain curve recorded when the MCL was elongated to failure at 20 mm/min.

APPENDIX 2

FITTED AND PREDICTED FUNCTIONS

Table A2.1: Values of Constants for Fitted and Predicted Functions at 14 MPa

The function form is $c(t) = C_1 e^{-C_2 t} + C_3 e^{-C_4 t} + C_5$; where j(t) is the fitted creep function, g(t) is the fitted relaxation function, $\hat{g}(t)$ is the predicted relaxation function from the fitted creep function and $\hat{j}(t)$ is the predicted creep function from the fitted relaxation function. "exp" indicates experimental, "pred" indicates predicted, and "n/a" indicates data not available because of a fault in the test procedure.

Specimen	Function	C_1	C_2	C_3	C_4	C_5
1 left exp	g(t)	0.15	0.038	0.13	0.002	0.72
1 right pred	$\hat{g}(t)$	0.06	0.046	0.06	0.004	0.88
1 right exp	j(t)	-0.06	0.043	-0.08	0.004	1.14
1 left pred	$\hat{j}(t)$	-0.17	0.032	-0.21	0.002	1.38
2 right exp	g(t)	0.21	0.036	0.17	0.003	0.62
2 left pred	$\hat{g}(t)$	0.08	0.033	0.06	0.003	0.86
2 left exp	j(t)	-0.09	0.030	-0.07	0.003	1.16
2 right pred	$\hat{j}(t)$	-0.26	0.028	-0.36	0.002	1.62
3 left exp	g(t)	0.17	0.034	0.15	0.002	0.68
3 right pred	$\hat{g}(t)$	0.07	0.028	0.05	0.003	0.88
3 right exp	j(t)	-0.07	0.026	-0.07	0.003	1.14
3 left pred	$\hat{j}(t)$	-0.19	0.028	-0.28	0.002	1.47
4 right exp	g(t)	0.18	0.038	0.17	0.002	0.65
4 left pred	$\hat{g}(t)$	0.07	0.038	0.07	0.003	0.86
4 left exp	j(t)	-0.08	0.035	-0.08	0.003	1.16
4 right pred	$\hat{j}(t)$	-0.21	0.031	-0.33	0.002	1.54
5 left exp	g(t)	0.21	0.037	0.19	0.003	0.60
5 right pred	$\hat{g}(t)$	0.10	0.025	0.06	0.002	0.84
5 right exp	j(t)	-0.11	0.023	-0.09	0.002	1.20
5 left pred	$\hat{j}(t)$	-0.25	0.029	-0.41	0.002	1.66
6 right exp	g(t)	0.19	0.034	0.17	0.002	0.64
6 left pred	$\hat{g}(t)$	0.08	0.033	0.06	0.003	0.86
6 left exp	j(t)	-0.09	0.031	-0.08	0.002	1.17
6 right pred	$\hat{j}(t)$	-0.23	0.028	-0.33	0.002	1.56
7 right exp	g(t)	0.26	0.054	0.19	0.003	0.55
7 left pred	$\hat{g}(t)$	0.08	0.034	0.07	0.003	0.85
7 left exp	j(t)	-0.09	0.031	-0.09	0.002	1.18
7 right pred	$\hat{j}(t)$	-0.35	0.040	-0.48	0.002	1.83
8 left exp	g(t)	0.17	0.041	0.13	0.002	0.70
	$\hat{g}(t)$	n/a				
	j(t)	n/a				
8 left pred	$\hat{j}(t)$	-0.20	0.034	-0.22	0.002	1.42

Table A2.2: Values of Constants for Fitted and Predicted Functions at 4.1 MPa

The function form is $c(t) = C_1 e^{-C_2 t} + C_3 e^{-C_4 t} + C_5$; where j(t) is the fitted creep function, g(t) is the fitted relaxation function, $\hat{g}(t)$ is the predicted relaxation function from the fitted creep function and $\hat{j}(t)$ is the predicted creep function from the fitted relaxation function. "exp" indicates experimental and "pred" indicates predicted.

Specimen	Function	C_1	C_2	C_3	C_4	C_5
1 left exp	g(t)	0.38	0.026	0.32	0.003	0.30
1 right pred	$\hat{g}(t)$	0.18	0.020	0.14	0.002	0.68
1 right exp	j(t)	-0.21	0.016	-0.27	0.002	1.48
1 left pred	$\hat{j}(t)$	-0.50	0.017	-1.81	0.001	3.31
2 right exp	g(t)	0.33	0.028	0.31	0.003	0.36
2 left pred	$\hat{g}(t)$	0.18	0.025	0.12	0.003	0.70
2 left exp	j(t)	-0.20	0.021	-0.23	0.003	1.43
2 right pred	$\hat{j}(t)$	-0.41	0.019	-1.37	0.002	2.78
3 right exp	g(t)	0.35	0.027	0.31	0.003	0.34
3 left pred	$\hat{g}(t)$	0.17	0.022	0.14	0.002	0.69
3 left exp	j(t)	-0.20	0.018	-0.25	0.002	1.45
3 right pred	$\hat{j}(t)$	-0.46	0.018	-1.46	0.001	2.92

APPENDIX 3

MODULUS VALUES FOR MODEL

(a) initial modulus for the creep test

14 MPa = 609.0 MPa and 4.1 MPa = 393.0 MPa

The initial modulus for the creep test was calculated as the tangent modulus of the loading curve over the last 80% of the stress range ensuring that the linear regression coefficient of determination (square of correlation coefficient), r^2, was equal to 0.99.

(b) failure modulus of the MCL

774.2 ± 111.4 MPa, n=5

Failure modulus of the MCL was calculated as the tangent modulus to the failure stress-strain curve over the range of 35 MPa to 40 MPa ensuring that there were no discontinuities and that r^2=0.99. The MCLs used to calculate failure modulus were those described in Chapter 2 as being tested at 14 MPa and elongated to failure at 20 mm/min (standard failure protocol used in the laboratory).

(c) modulus range quoted in the literature

400-1000 MPa

This modulus range was taken from reference 100.